MECHANICAL, THERMAL AND ACOUSTIC PROPERTIES OF RUBBERISED CONCRETE INCORPORATING NANO SILICA

Amal Mohamed Naji EL-KHOJA

Submitted for the Degree of
Doctor of Philosophy

Faculty of Engineering and Informatics
University of Bradford

2019

In the Name of Allah the Most Merciful

ABSTRACT

MECHANICAL, THERMAL AND ACOUSTIC PROPERTIES OF RUBBERISED CONCRETE INCORPORATING NANO SILICA

Amal Mohamed Naji El-khoja

University of Bradford, UK, 2019

Keywords: rubberised concrete, nano silica, mechanical properties, thermal conductivity, acoustic properties, prediction, artificial neural networks.

Very limited research studies have been conducted to examine the behaviour of rubberised concrete (RuC) with nano silica (NS) and addressed the acoustic benefits of rubberised concrete. The current research investigates the effect of incorporating colloidal nano silica on the mechanical, thermal and acoustic properties of Rubberised concrete and compares them with normal concrete (NC).

Two sizes of rubber were used R_A (0.5 – 1.5 mm) and R_B (1.5 – 3 mm). Fine aggregate was replaced with rubber at a ratio of 0%, 10%, 20% and 30% by volume, and NS is used as partial cement replacement by 0%, 1.5% and 3%. A constant water to cement ratio of 0.45 was used in all concrete mixes. Various properties of rubberised concrete, including the density, water absorption, the compressive strength, the flexural strength, splitting tensile strength and the drying shrinkage of samples was studied as well as thermal and acoustic properties.

Experimental results of compressive strength obtained from this study together with collected comprehensive database from different sources available in the literature were compared to five existing models, namely Khatib and Bayomy-

99 model, Guneyisi-04 model, Khaloo-08 model, Youssf-16 model, and Bompa-17 model. To assess the quality of predictive models, influence of rubber content on the compressive strength is studied. An artificial neural network (ANN) models were developed to predict compressive strength of RuC using the same data used in the existing models. Three ANN sets namely ANN1, ANN2 and ANN3 with different numbers of hidden layer neurons were constructed. Comparison between the results given by the ANN2 model and the results obtained by the five existing predicted models were presented. A finite element approach is proposed for calculating the transmission loss of concrete, the displacement in the solid phase and the pressure in the fluid phase is investigated. The transmission loss of the 50mm concrete samples is calculated via the COMSOL environment, the results from the simulation show good agreement with the measured data.

The results showed that, using up to 20% of rubber as fine aggregate with the addition of 3% NS can produce a higher compressive strength than the NC. Experimental results of this research indicate that incorporating nano silica into RuC mixes enhance sound absorption and thermal conductivity compared to normal concrete (NC) and rubberised concrete without nano silica. This work suggests that it is possible to design and manufacture concrete which can provide an improvement to conventional concrete in terms of the attained vibro-acoustic and thermal performance.

PUBLICATIONS

Journals papers

1- El-Khoja, A. ; Ashour, A. ; Abdalhmid, J. ; Dai, X. ; Khan, A. (2018), **'Prediction of Rubberised Concrete Strength by Using Artificial Neural Networks** ', World Academy of Science, Engineering and Technology, International Science Index 143, International Journal of Civil, Environmental, Structural, Construction and Architectural Engineering, 12(11), 1068 - 1073.

2- Musab Alhawat, Ashraf Ashour, Amal El-khoja,' **Properties of concrete incorporating different nano silica particles**', Materials Research Innovations.

3- Amal El-khoja, Ashraf Ashour "Experimental study on the properties of rubberised concrete incorporating colloidal nano silica" submitted to ICE Journal construction materials.

4- Amal El-khoja, Amir Khan, and Ashraf Ashour "Vibro acoustic properties of rubberised concrete incorporating nano silica" submitted to Construction and building materials Journal.

Conference papers

1- Amal El-khoja, Amir Khan, and Ashraf Ashour, 1th prize (the best paper) titled 'Acoustic **Properties of Rubberised Concrete Containing Nano Silica**' in the Faculty of Engineering and Informatics, 2nd Annual Innovative Engineering Research Conference, AIERC '18, held at University of Bradford 17 October 2018.

2- Amal El-khoja, Ashraf Ashour, Jamila abdalhmid, X. Dai and Amir Khan, 4st prize (the best paper) titled ' **Using Artificial Neural Networks to Predict the Compressive Strength of Rubberised Concrete**' in the Faculty of Engineering and Informatics, 2nd Annual Innovative Engineering Research Conference, AIERC ' 18, held at University of Bradford 17 October 2018.

DEDICATION

To

- *My Father and Mother for their endless support and encouragement during my study, without them, I would not have been able to study and succeed.*
- *My Sisters and Brothers*
- *My Niece (Elaf) and my Nephews (Nagi & Hamoudi)*

ACKNOWLEDGMENTS

Praise be to Allah the cherisher and sustainer of the world.

First and foremost, I would like to thank Allah; our Lord, the Almighty, the most Merciful and the most Compassionate.

I would like to express my special appreciation and thanks to my supervisors **Prof. Ashraf Ashour, Dr. Khan and Dr. Dai** for their support, encouragement and supervision throughout the period of this work. I deeply appreciate **Prof. Ashour** for his great support, patience and help, especially throughout the difficult time and critical circumstances in my country, Libya.

My thanks go to the laboratory member who were always ready to help in times of needs. I would like to particularly thank **Steve Robinson** and **Joanna Wood** for their expert help and advice during my experimental investigation.

Special thanks to my family for their endless support and patience during my study. Your constant prayer for me was what sustained me thus far.

I would also like to express my appreciation to all my friends, especially my office members who supported me to strive towards my goal.

Finally, my personal involvement with the study would not have been possible without the grant financial support provided by the Ministry of Higher Education the Libyan Ministry of Higher Education.

TABLE OF CONTENTS

ABSTRACT ..... **II**

DEDICATION ..... **VI**

ACKNOWLEDGMENTS ..... **VII**

TABLE OF CONTENTS ..... **VIII**

LIST OF FIGURES ..... **XVI**

LIST OF TABLES ..... **XXIII**

ABBREVIATIONS ..... **XXV**

NOTATION ..... **XXVII**

1 CHAPTER ONE- INTRODUCTION **1**

1.1 Background 1

1.2 Research significance 2

1.3 Research aim and objectives 4

1.4 Research methodology 5

1.5 Thesis layout 7

2 CHAPTER TWO- LITERATURE REVIEW **10**

2.1 Introduction 10

2.2 Background of Rubberised Concrete 10

2.3 Advantages and Disadvantages of Rubberised Concrete 13

2.4 Classification of waste tyre rubber 14
2.4.1 Mix Design and Mixing Approach 16
2.5 Properties of Rubberised Concrete 17
2.5.1 Fresh Concrete Properties 17
2.5.1.1 Workability 17
2.5.1.2 Air Content (Porosity) 20
2.5.2 Properties of Hardened Concrete 21
2.5.2.1 Unit Weight 21
2.5.2.2 Compressive Strength 22
2.5.2.3 Splitting tensile strength 26
2.5.2.4 Flexural Strength 27
2.5.2.5 Shrinkage 28
2.5.2.6 Impact resistance 28
2.5.2.7 Thermal Conductivity 29
2.5.2.8 Sound absorption 31
2.6 Applications of rubberised concrete: 33
2.7 Nano Silica 34
2.7.1 The significance of nano silica in concrete 34
2.7.2 Production method of NS 35
2.7.3 Effect of nano silica on properties of concrete 37
2.7.3.1 Mechanical properties 37
2.7.3.2 Durability properties 40
2.8 Prediction of compressive strength of rubberised concrete 40

2.9 Concluding Remarks 41

3 CHAPTER THREE- MATERIALS AND EXPERIMENTAL METHODOLOGY 44

3.1 Introduction 44

3.2 Materials 44

3.3 Design of Experiments 50

3.3.1 Trial mix phase 50

3.3.2 Main experimental phase 51

3.3.3 Mixing procedure 54

3.3.4 Preparation of test specimens 55

3.4 Experimental tests 56

3.4.1 Fresh properties tests 56

3.4.1.1 Slump test 56

3.4.1.2 Mechanical properties tests 57

3.4.1.3 Dry Density 57

3.4.1.4 Water absorption 57

3.4.1.5 Porosity 58

3.4.1.6 Compressive strength 59

3.4.1.7 Splitting tensile strength 60

3.4.1.8 Flexural strength 61

3.4.1.9 Drying shrinkage test 62

3.4.1.10 Impact resistance under drop weight test 64

3.4.2 Thermal and Acoustic Properties tests 65

3.4.2.1 Thermal conductivity 65

3.4.2.1.1 Principle and set-up 65
3.4.2.1.2 Measurement procedure and calibration 67
3.4.2.2 Acoustic properties 69
3.4.2.2.1 Sound absorption and Transmission loss 70
3.4.2.2.2 Impact Sound Insulation Equipment Set-up 72
3.4.2.3 Dynamic stiffness 74
3.4.2.3.1 Experiment BS29052 74
3.4.2.3.2 Experimental setup 74
3.4.2.4 Damping performance 76

3.5 Concluding remarks 79

4 CHAPTER FOUR- WORKABILITY AND MECHANICAL PROPERTIES - RESULTS AND DISCUSSION 80

4.1 Introduction 80

4.2 Trial experimental test results 80
4.2.1 Workability 80
4.2.2 Compressive strength 81

4.3 Main experimental test results 85
4.3.1 Workability 85
4.3.2 Dry Density 87
4.3.3 Water absorption 89
4.3.4 Porosity 90
4.3.5 Compressive strength 92
4.3.5.1 Effect of rubber content 92
4.3.5.2 Effect of NS replacement 94
4.3.6 Splitting tensile strength 98
4.3.7 Flexural strength 100

4.3.8 Drying shrinkage strain. 102

4.3.9 Impact resistance under drop weight 105

4.3.9.1 Failure patterns under impact 111

4.4 Conclusions 112

4.4.1 Trial experimental investigations 112

4.4.2 Main experimental investigations 113

5 CHAPTER FIVE – THERMAL AND ACOUSTIC PROPERTIES OF RUBBERISED CONCRETE WITH AND WITHOUT NANO SILICA 115

5.1 Introduction 115

5.2 Thermal Properties 115

5.2.1 Thermal Conductivity 115

5.2.2 The relationship between density and thermal conductivity of concrete 118

5.3 Acoustic Properties of Rubberised Concrete 119

5.3.1 Sound Absorption 119

5.3.2 Dynamic modulus of elasticity 126

5.3.3 Acoustic Transmission Loss 127

5.4 Prediction of transmission loss 132

5.4.1 Comparison with experimental measurement 140

5.4.2 Parametric study 142

5.5 Impact sound insulation 145

5.6 Conclusions 148

6 CHAPTER SIX - PREDICTION OF COMPRESSIVE STRENGTH OF RUBBERISED CONCRETE USING ARTIFICIAL NEURAL NETWORK 150

6.1 Introduction 150

6.2 Background and Basic principle of ANN 150

6.3 Advantages and Disadvantages of ANN 152

6.4 Architecture of ANN 153

6.4.1 Number of Layers and Neurons 153

6.4.2 Transfer Function 154

6.4.3 Weights and Biases 155

6.4.4 NN Learning 155

6.5 Training and testing process of NNs 155

6.6 Experimental database 157

6.6.1 Data normalisation 161

6.7 Construction of ANN model 161

6.7.1 Performance of the developed neural network 163

6.8 Parametric study 170

6.8.1 Influence of W/C Ratio 170

6.8.2 Influence of fine rubber content 171

6.8.3 Effect of nano silica content on compressive strength 171

6.9 Concluding remarks 172

7 CHAPTER SEVEN – PREDICTION OF COMPRESSIVE STRENGTH OF RUBBERISED CONCRETE USING EXISTING MODELS 175

7.1 Introduction 175

7.2 Comparison of rubberised concrete compressive strength prediction models 175

7.3 Assessment of rubberised concrete compressive strength prediction models 177

7.3.1 Effect of rubber content on compressive strength using various models 177

7.4 Database for compressive strength 178

7.5 Results and discussions 180

7.5.1 Experimental and predicted compressive strength comparison. 180

7.5.2 Evaluation of existing models to predict the compressive strength of rubberised concrete 184

7.5.3 Comparison between the prediction using different existing models and ANN model. 188

7.6 Conclusions 190

8 CHAPTER EIGHT – CONCUSIONS AND RECOMMENDATIONS FOR FUTUTRE RESEARCH 192

8.1 Summary 192

8.2 Conclusions 193

8.2.1 Experimental findings 193

8.2.2 Analytical findings 195

8.3 Recommendations for future research 196

9 REFERENCES 198

10 APPENDIX A- DATABASE OF RUBBERISED CONCRETE 211

11 APPENDIX B- STATISTICAL ANALYSIS OF ANN MODELS 234

LIST OF FIGURES

Figure 1-1 Research methodology diagram 7

Figure 2-1 Rubber size 16

Figure 2-2 Effect of rubber particles on workability (Author) 19

Figure 2-3 Trapped air bubbles at rubber particles submerged in water (Sukontasukkul, 2012) 20

Figure 2-4 Relationship between the ratio of RuC density to control concrete density and rubber% (Author) 21

Figure 2-5 Relationship between the reduction of compressive strength and the rubber content (Author) 23

Figure 2-6 Thermal conductivity versus crumb rubber replacement (Mohammed et al., 2012). 30

Figure 2-7 Particle size range and specific surface area (SSA) of concrete components, adapted from Sobolev and Ferrara (2005) 35

Figure 2-8 A Schematic and general flow chart for Sol-gel process (Rahman and Padavettan, 2012) 36

Figure 3-1 Gradation curves for both coarse and fine aggregate. 47

Figure 3-2 Gradation curves for FA, rubber A and rubber B 48

Figure 3-3 XRD analysis for (a) NS-50, (b) NS-250 and (c) NS-500. 49

Figure 3-4 Sequence of constituent mixing flowchart 55

Figure 3-5 Preparing, casting and curing procedure. 56

Figure 3-6 Slump test for normal concrete mix 57

Figure 3-7 The vacuum saturated machine used for porous measurements 58

Figure 3-8 Compressive test machine 60

Figure 3-9 Splitting tensile strength test 61

Figure 3-10 Flexural strength test 62
Figure 3-11 Free drying shrinkage specimens. 63
Figure 3-12 Free drying shrinkage strain measurement 64
Figure 3-13 Drop weight test 65
Figure 3-14 Illustration of thermal conductivity apparatus 69
Figure 3-15 Photograph of sound impedance tube 71
Figure 3-16 Schematic diagram of the sound impedance tube 71
Figure 3-17 Schematic diagram of impact transmission rig 73
Figure 3-18 an accelerometer attached on the upper surface of concrete ... 73
Figure 3-19 Experimental setup for BS29052 measurement 75
Figure 3-20 An accelerometer output of the recorded impact with WinMLS software. 76
Figure 3-21 Frequency response of the recorded impact. 77
Figure 3-22 Amplitude of Vibration with Frequency 78
Figure 4-1 Effect of NS on the compressive strength of concrete (a) at 7 days and (b) at 28days. 84
Figure 4-2 Slump of rubberised concrete with and without NS, R_A 86
Figure 4-3 Slump of rubberised concrete with and without NS, R_B 87
Figure 4-4 Density of rubberised concrete 88
Figure 4-5 Density of rubberised concrete with different NS% 89
Figure 4-6 water absorption of concrete with two different size of rubber 90
Figure 4-7 Porosity of different mixes of rubberised concrete mixes 91
Figure 4-8 Effect of rubber replacement on compressive strength of the tested mixtures at 7 and 28 day (a) R_A, and (b) R_B 93
Figure 4-9 7days compressive strength of rubberised concrete 94

Figure 4-10 28 days compressive strength of rubberised concrete..... 95
Figure 4-11 90 days compressive strength of rubberised concrete..... 95
Figure 4-12 Compressive strength versus nano silica addition for rubberised concrete mixture with 20% of rubber..... 96
Figure 4-13 The relationship between Density and compressive strength of rubberised concrete 97
Figure 4-14 The relationship between porosity and compressive strength of rubberised concrete 98
Figure 4-15 Variation in the splitting tensile strength of rubberised concrete with nano silica, (a) R_A and (b) R_B..... 99
Figure 4-16 Flexural strength for varying percent of rubber, (a) R_A and (b) R_B. 101
Figure 4-17 Effect of R_A content and NS addition on drying shrinkage of concrete 103
Figure 4-18 Effect of R_B content and NS addition on drying shrinkage of concrete 103
Figure 4-19 Relation between rubber content and drying shrinkage at 90 days for different two different size of rubber..... 104
Figure 4-20 Relation between nano silica content and drying shrinkage at 90 days for different two different size of rubber. 105
Figure 4-21 Number of blows for first crack (N1) (a) 0% NS, (b) 1.5% NS and (c) 3% NS 109
Figure 4-22 Number of blows for ultimate failure (N1) : (a) 0% NS, (b) 1.5% NS and (c) 3% Ns 111

Figure 4-23 Failure patterns: (a) plain specimen, (b) specimen with R and (c) specimen with R and NS 112
Figure 5-1 Thermal conductivity vs rubber % for different mixes with (a) R_A and (b) R_B 117
Figure 5-2 Thermal conductivity of rubberised concrete with various percentage of Ns compared with control concrete 117
Figure 5-3 Variation of the thermal conductivity with the density 118
Figure 5-4 (a) damping ratio and (b) single number rating (SNR) for various mixes 121
Figure 5-5 Acoustic absorption of RuC mixtures with (a) R_A, and (b) R_B ... 122
Figure 5-6 Acoustic absorption of RuC mixtures with 1.5 % NS for (a) R_A and (b) R_B 124
Figure 5-7 Acoustic absorption of RuC mixtures with 3 % NS for (a) R_A and (b) R_B 125
Figure 5-8 Relationship between dynamic modulus of elasticity and rubber content (a) R_A and (b) R_B 127
Figure 5-9 Transmission loss of rubberised concrete mixtures with (a) R_A, (b) and R_B 128
Figure 5-10 Transmission loss of rubberised concrete mixtures with (a) 10 %R_A, (b) 20% R_A and (c) 30%R_A 130
Figure 5-11 Transmission loss of rubberised concrete mixtures with (a) 10%R_B, (b) 20%R_B and (c) 30%R_B 132
Figure 5-12 The model geometry adopted in COMSOL, (a) standing pressure waves in tube, (b) pressure profile in sample, (c) mesh of whole impedance tube, (d) finer mesh used for concrete specimens 139

Figure 5-13 Comparison of experimental and predictive results of transmission loss (a) Control mix, (b) R30-0NS, (c) R30-1.5NS and (d) R30-3NS 142
Figure 5-14 Effect of thickness on the transmission loss of concrete..... 143
Figure 5-15 Effect of Young's modulus on the transmission loss..... 144
Figure 5-16 Effect of density of concrete on transmission loss 144
Figure 5-17 Effect of loss factor on the transmission loss..... 145
Figure 5-18 Acoustic insulation comparison between normal concrete and various rubberised concrete mixtures (a) With R_A and (b) with R_B..... 147
Figure 5.19 Effect of incorprating 1.5% NS on impact sound insulation of RuC 147
Figure 5-20 Effect of incorprating 3% NS on impact sound insulation of RuC 148
Figure 6-1 Artificial neuron model 152
Figure 6-2 Frequency distribution of water/cement ratio 158
Figure 6-3 Frequency distribution of fine aggregate content..... 159
Figure 6-4 Frequency distribution of coarse aggregate content..... 159
Figure 6-5 Frequency distribution of rubber aggregate content 160
Figure 6-6 Frequency distribution of nano silica content..... 160
Figure 6.7 Typical artificial neural network model architecture 163
Figure 6-8 Comparison of experimental and predicted compressive strength for ANN1 (a) training data set and (b) testing data set. 167
Figure 6-9 Comparison of experimental and predicted compressive strength for ANN2 (a) training data set and (b) testing data set. 168
Figure 6-10 Comparison of experimental and predicted compressive strength for ANN3 (a) training data set and (b) testing data set. 169

Figure 6-11 Effect of water- cement ratio on compressive strength using ANNs models 170
Figure 6-12 Effect of fine rubber content on compressive strength using ANNs models. 171
Figure 6-13 Effect of nano silica content on compressive strength using ANN2 and ANN3 172
Figure 7-1 Effect of rubber content on predictive compressive strength with different models 178
Figure 7-2 Comparison between experimental and predicted compressive strength of RuC using various prediction models: (a) Khatib and Bayomy model, (b) Khaloo model (c) Guneyisi model, (d) Youssf model and (e) Bompa model. 184
Figure 7-3 Residual error Versus Compressive Strength for Khatib and Bayommy model 185
Figure 7-4 Residual error Versus Compressive Strength for Khaloo model186
Figure 7-5 Residual error Versus Compressive Strength for Guneyisi model 186
Figure 7-6 Residual error Versus Compressive Strength for Youssf model187
Figure 7-7 Residual error Versus Compressive Strength for Youssf model187
Figure 7-8 Comparison between experimental and predicted compressive strength of RuC using the existing models and the ANN2model. 189
Figure B-1 Screenshot of best validation performance of ANN2..... 234
Figure B-2 Screenshot of best validation performance of ANN3..... 235
Figure B-3 Screenshot of error histogram of ANN1 235
Figure B-4 Screenshot of error histogram of ANN2 236

Figure B-5 Screenshot of error histogram of ANN3 236

Figure B-6 Screenshot of Training Regression of ANN1..... 237

Figure B-7 Screenshot of Training Regression of ANN2..... 238

Figure B-8 Screenshot of Training Regression of ANN3..... 239

LIST OF TABLES

Table 2-1 Methods to introduce rubber to concrete used by several researchers 12

Table 2-2 List of studies focusing on the effect of NS on concrete strength 39

Table 3-1Physical properties of cement 45

Table 3-2 Chemical analysis of the cement 45

Table 3-3 Physical properties of coarse aggregate, fine aggregate and rubber 46

Table 3-4 Physical properties of Nano silica 49

Table 3-5 Chemical composition (%) of NS 49

Table 3-6 Trial mix proportions of concrete 51

Table 3-7 Mix proportions of concrete 53

Table 4-1 Impact resistance results for rubberised concrete with and without NS 107

Table 5-1 Range of the input parameter values used in the model 136

Table 6-1Range of input and output parameters in database 158

Table 6-2 Artificial neural network selection 162

Table 6-3 Comparison of different training algorithms 165

Table 6-4 Performance of ANNMs models for different hidden layers neurones developed 166

Table 7-1 Compressive strength prediction models of rubberised concrete176

Table 7-2 Summary of rubberised concrete experimental database used in all models 179

Table 7-3 Statistical indicators for compressive strength predicted by the five models 181

Table 7-4 Comparison of statistical indicators between the predictions of compressive strength of rubberised concrete by different models and ANN model 188
Table A-1 Details of database 211

ABBREVIATIONS

The following abbreviations are used in this research:

AEA	Air-entraining admixture
ANN	Artificial Neural Network
ANNs	Artificial neural networks
BPNN	Back Propagation Neural Network
BR	Bayesian regularization
CA	Coarse aggregate
CCl4	Carbon tetrachloride
COV	Coefficient of variation
C-S-H	Calcium - Silicate - Hydrate
E_d	Dynamic modulus of elasticity
EPR	Evolutionary Polynomial Regression
FA	Fine aggregate
FEM	Finite element method
FFT	Fast Fourier transform
FL	Fuzzy logic
GP	Genetic Programming
HRWR	High range water reducer
ITZ	Interfacial transition zone
LF	Loss factor
LM	Levenberg-Marquardt
LVQ	Learning Vector Quantisation
MSE	Mean square error

N_1	Numbers of blows required for causing first visible crack
N_2	Numbers of blows required for causing ultimate failure
NaOH	Sodium hydroxide solution
NC	Normal concrete
NS	Nano silica
P	Porosity
R_A	Rubber size (0.5 -1.5 mm)
R_B	Rubber size (1.5 - 3 mm)
RuC	Rubberised concrete
SCA	Silane coupling agent
SCG	Scaled conjugate gradient
SCMs	Supplementary cementitious materials
SD	Standard deviation
SF	Silica fume
SNR	Single number rating
SP	Superplasticiser
SSA	Specific surface area
SSD	Saturated surface dry state

NOTATION

The following symbols are used in the present thesis:

f'_{cr}	Compressive strength of rubberised concrete
ΔT_m	Mean temperature difference between thermocouples
M_d	Mass of dried sample
M_s	Mass of saturated sample
R_t	Flexural strength
R_t	Rubber as a volumetric ratio by total aggregate volume
$S_b(\omega)$	Acceleration spectrum for the signal detected using the accelerometer attached to the loading plate
$S_t(\omega)$	Reference acceleration spectrum detected using the accelerometer attached to the top of the armature disk.
V_W	Volume of water inside sample
V_d	Volume of dry sample
f_1	Frequency value, 3 dB down from peak value
f_2	Frequency value, 3 dB down from peak value
f'_c	Compressive strength of control concrete
f_o	Frequency of resonant peak
f_t	Splitting tensile strength
λ_{alu}	Thermal conductivity of aluminium
ρ_d	Density of dried sample
ρ_w	Density of water
Δd	Compressed thickness under the loading during the measurement
A	Cross sectional area of the aluminium cylindrical column

CRD	Difference between the comparator reading of the Specimen and the reference bar at any age
g	gravity acceleration
h	Drop height
m	Mass of drop hammer
N	Number of blows at crack level
q	Heat flux
ΔT	Temperature difference between thermal sensors 3 and 4
D	Cross sectional diameter of the specimen
F	Dynamic force acting perpendicularly on the test specimen
G	Gauge length
L	Length of specimen
P	Maximum split load
S	Area of the test specimen
$T(\omega)$	Frequency dependent transfer function for the two measured accelerations
d	Distance between the thermocouple junctions
s'	Dynamic stiffness per unit area
ζ	Damping ratio
λ	Thermal conductivity

CHAPTER ONE- INTRODUCTION

1.1 Background

The accumulation of waste tyres becomes one of the worst problems for environmental pollution across the world. The municipal authorities in many countries have already prohibited dumping of waste tyres into the landfills due chiefly to the resistance of rubbers to biodegradation. In the United Kingdom alone, there are approximately 48,000 tonnes of used tyres disposed each year, of which only a small fraction about 5% of the waste is recycled.

One of the possible solutions to tackle this problem is to incorporate the waste tyre into concrete, to partially replace natural fine aggregates (El-Gammal et al., 2010; Ling et al., 2010; Pierre, 2013). This would not only solve the problem of accumulation of tyres but will also preserve natural resources.

However, the results obtained from several researchers (Khatib and Bayomy 1999; Güneyisi et al. 2004; Papakonstantinou and Tobolski 2006; Balaha et al. 2007; Gesoğlu and Güneyisi 2007; Zheng et al. 2007; Khaloo et al. 2008; Taha et al. 2008; Zheng et al. 2008; Topçu and Bilir 2009; Güneyisi 2010; Pelisser et al. 2011; Najim and Hall 2012; Güneyisi et al. 2014) revealed that the use of waste tyre in concrete mixtures reduced strength and modulus of elasticity of rubberised concrete mixtures. On the other hand, ductility, impact resistance, thermal conductivity, and acoustic properties were significantly improved.

Generally, previous researches suggested various methods to modified the surface of rubber particles, such as the immersion of rubber particles in sodium hydroxide solution (NaOH) to excess its adhesion to the surrounding cement paste (Balaha et al. 2007, Mohammadi et al. 2014) and others found that coating

rubber particles with various materials like silane coupling agents (SCA) (Dong et al., 2013), mortar, or cement paste (Youssf et al., 2014) can increase the strength of rubberised concrete. However, researchers observed that the pre-treatment of rubber particles has led a slight enhancement in the compressive strength of rubberised concrete (Shu and Huang, 2014). Moreover, other researcher suggested that the strengths of rubberised concrete can be enhanced by using supplementary cementitious materials (SCMs) such as silica fume (SF) and nano silica (NS). Güneyisi et al. 2004, Onuaguluchi et al. 2014, Elchalakani, 2015) showed that the addition of SF can improves the compressive strength of rubberised concrete due to the enhancement of the interfacial transition zone (ITZ) bonding and the reduction of the pore size in the cement paste. Recently, Mohammed et al. 2016) observed that incorporating nano silica to rubberised concrete showed a reasonable improvement in the compressive strength.

Very scarce literature is available on the effect of incorporating nano silica on the mechanical properties of rubberised concrete. Because of this limited number of studies, an experimental study was conducted to investigate and confirm the effect of incorporating nano silica on various properties of rubberised concrete.

Prediction models proposed by several researches have been used to assess the prediction of compressive strength of rubberised concrete and compared with experimental results.

1.2 Research significance

A number of researchers have focused on the use of waste tyre rubber as a replacement of fine and coarse aggregates in concrete mixtures. Using waste rubber in concrete will make it more sustainable and generally enhances several properties such as ductility, toughness behaviour, thermal insulation and impact

resistance, but there is a vital need to enhance the strength of rubberised concrete. In recent years, using nanotechnology has gained considerable attention in concrete industry, due to its nanoparticle size, to enhance the mechanical properties of concrete. Therefore, the negative effect of using waste rubber in concrete can be tackled by adding nano silica due its pore filling ability and its pozzolanic reactivity. According to the literature review which has been done in chapter 2 and to the author's best knowledge, there is scarce research on the addition of NS to the rubberised concrete. However, there is a few investigations that have been conducted on roller compacting rubberised concrete incorporating with nano silica. Based on previous studies, the inclusion of NS in conventional concrete mixtures enhances the strength and it suggested that the optimal percentage of nano silica is 3%. One of the goals of this research is to explore the effect of various levels of nano silica and elastomeric polymer content on the mechanical, thermal, and vibro-acoustic properties of rubberised concrete. This research will present an extensive experimental programme aiming at furthering the understanding of the behaviour and properties of rubberised concrete incorporating nano-sized particles. The scientific significance of this research results from a contribution that provide a further knowledge and understanding of the properties of rubberised concrete with nano silica. Computational models using COMSOL Multiphysics package to predict transmission loss (TL) of RuC and evaluate the influence of several parameters on the TL have not been used to date on concrete samples.

1.3 Research aim and objectives

The aim of this research is to investigate the effect of nano silica on the properties of rubberised concrete. As mentioned above, very few studies have been carried out to address these effects. The essential objectives included:

1. To explore the feasibility of using nano silica with various rubber content and investigate its effect on workability and mechanical properties of concrete compared with NC and RuC without NS.
2. To investigate the effect of nano silica on the thermal conductivity of the rubberised concrete samples.
3. To study the acoustical properties of rubberised concrete samples with and without nano silica by experimental analysis and via theoretical modelling.
4. To evaluate the accuracy of compressive strength prediction models of rubberised concrete proposed by several researchers, including Khatib and Bayomy-99 Model, Khaloo-08 Model, Guneyisi-04 Model, Youssf et al-16 Model and Bompa et al -17 Model against the present and previous results.
5. To develop an artificial neural network (ANN) model using MATLAB to predict compressive strength of rubberised concrete with and without nano silica, using extensive database collected from different sources in the literature together with the current experimental results and conduct a series of parametric studies.
6. To compare between the results given by the ANN model and the results obtained by the five existing predicted models mentioned above.

7. To develop a FEM model using COMSOL Multiphysics software to estimate the transmission loss of rubberised concrete with and without nano silica and carry out a parametric study.
8. To explore the damping performance of rubberised concrete with the addition of nano silica.

1.4 Research methodology

To achieve the above aim and objectives, the research methodology is divided into three tasks, as shown in Figure 1-1:

Task 1: Review of literature

A comprehensive literature review was conducted. The main purpose of this review is to identify the gap in rubberised concrete. In addition, to validate the results of this investigation by comparing them with previous findings of other researchers.

Task 2: Experimental Work

The experimental work in this research was divided into two stages, trial mixing stage and main experimental stage.

❖ **Trial mixing stage**

It is important to conduct trial mixing of control mixing to achieve the compressive strength target and to see the effect of adding three different sizes of nano silica on rubberised concrete mixes. The aim of this stage to establish the effective size and percentage of nano silica.

❖ **Main experimental stage**

A series of experiments have been designed and carried out with cement replacement by three different percentage (0%, 1.5% and 3%) of nano silica and different level (10%, 20% and 30%) replacement of fine aggregate by two different sizes of rubber, the w/c ratio was 0.45 for all mixes . It includes the property tests of concrete samples such as workability and mechanical tests. Besides, the thermal and acoustic properties were also tested.

Task 3: Analytical Work

The following analytical investigations have been developed:

- An artificial neural network model has been developed to predict a compressive strength of RuC, using collected comprehensive database from different sources in the literature and conduct the parametric study to investigate the generalization ability of the developed neural network model within the range of inputs considered in the current study and examine the influence of the main input parameters on the compressive strength.
- Existing models, including Khatib and Bayomy-99 Model, Khaloo-08 Model, Guneyisi-04 Model, Youssf et al-16 Model and Bompa et al -17 Model have been used to predict the compressive strength of RuC.
- COMSOL Multiphysics software based on Finite Element Method (FEM) has been used to predict the transmission loss of concrete samples.

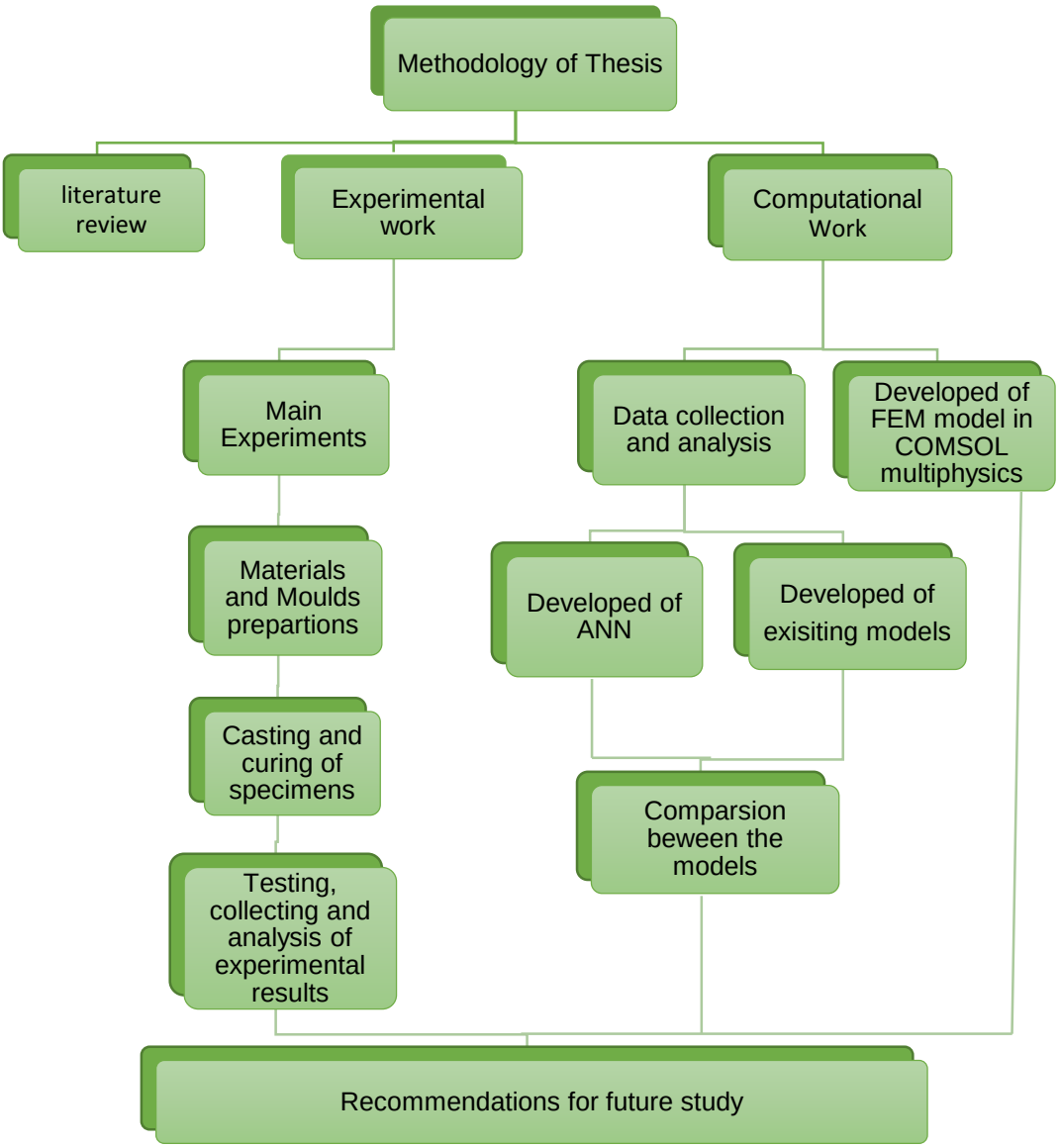

Figure 1-1 Research methodology diagram

1.5 Thesis layout

This thesis is organized in eight chapters, which are divided into sections and subsections, followed by references and appendices.

Chapter one outlines general background of rubberised concrete, discusses the significance as well as the aim and objectives of this research. Moreover, the

research methodology and the brief review of thesis work flow are provided in this chapter.

Chapter two provides a comprehensive review of the previous researches on rubberised concrete, specifically effect of use of crumb rubber aggregates on the fresh and mechanical properties as well as the thermal and acoustic properties, also involves the use of nano silica in concrete and its effect on mechanical properties.

Chapter three introduces the details of experimental programme, mix design procedure for trial and main mixes, specimen preparation, curing and casting of concrete. Also it presents the testing procedure for measuring the fresh, mechanical, thermal and acoustic properties of rubberised concrete have been illustrated in this chapter.

Chapter four provides the first part of experimental test results, which includes the results of workability and compressive strength of trials experiments as well as the workability and the mechanical properties of the main experimental results.

Chapter five presents the second part of experimental results, which deals with thermal and acoustical properties of rubberised concrete. As well as the prediction model of transmission loss using COMSOL Multiphysics software are proposed in this chapter.

Chapter Six in this chapter, prediction of compressive strength of RuC using ANN model, providing background knowledge about ANNs, and data collected from previous research. A parametric study using developed ANN models is also presented in this chapter.

Chapter Seven aims to predict the compressive strength of rubberised concrete using various computational existing models namely, Khatib and Bayommy-99, Khaloo-08, Gunisiyi-04, Youssf et al-16 and Bompa-17 models. Comparison between the different models predicted and calculated of rubberised concrete compressive strength. Based on the experimental results collected from this work as well as from the literature, predictability of the existing models has been confirmed. Finally, a comparison between existing models presented in current chapter with previous computational models (ANN) have been covered.

Finally, **chapter eight** summarise the main conclusions involved in Chapters 3 to 7 and provides recommendation and suggestions for future research.

CHAPTER TWO- LITERATURE REVIEW

2.1 Introduction

This chapter provides a comprehensive review on the work conducted by various researchers in the field of rubberised concrete. The first part of this chapter shows a brief background on rubberised concrete and a review of the fresh, mechanical, thermal and acoustic properties of rubberised concrete. The second part explains characteristics of nano silica (NS) and its effect on concrete when it is used as cement replacement. The main findings from previous studies are then reported at the end of the chapter.

2.2 Background of Rubberised Concrete

Recent studies have shown that the accumulation of waste tyre becomes one of the most vital problems as a source of the environmental pollution across the world due to the large increase in number of vehicles. One of the possible solutions to tackle this problem is to incorporate the waste tyre into concrete, to totally or partially replace natural aggregates.

The first publication on the usage of waste tyre rubber in concrete was by Eldin and Senouci (1993) in the early 1990s. Their aim was to study the effect of incorporating tyre rubber on mechanical properties of concrete. It has been found that the addition of tyre rubber to concrete leads to low strength and this limits its use in structural applications (Mohammadi, 2014) but helps to improve the ductility. Studies have continued by many researchers on rubberised concrete to explore various properties. The results indicated that the utilisation of rubber as an alternative to aggregates present lower density, increased ductility and toughness, higher impact resistance and sound insulation and severe reduction in compressive strength particularly with 100% replacement of aggregate with

rubber (Toutanji, 1996, Hernandez-Olivares et al., 2002, Benazzouk et al., 2007, Mohammed et al., 2011, Xu et al., 2014, Liu et al., 2016). Adding rubber particles also offers an attractive solution to counteract the shrinkage cracking and strain failure of concrete through incorporating waste rubber particles which lead to more deformability under pre-failure loads (Najim and Hall, 2010).

A Systematic review of published papers related to the properties of rubberised concrete by databases of Google Scholar, Science Direct, and Web of Science up to March 2019 was carried out. To focus on our study, Papers written in languages other than English language have been excluded. Broad keywords have been used such as rubber, concrete, rubberised concrete, rubbercrete, crumb rubber to ensure there is no omission, then many unrelated studies were deleted.

From an extensive review, three methods were found to introduce rubber to concrete, namely direct addition of rubber by percentage of weight or volume of concrete, the replacement of aggregates by weight and by volume. Table 2-1 shows that eight researches adopted the method of adding directly, around 19 researches adopted replacing aggregates by weight and about 71 researches by volume using absolute volume method. The addition of extra rubber or replace the aggregate with rubber by weight causes a large problem of mixture ratio due to variation of the densities of different materials.

Table 2-1 Methods to introduce rubber to concrete used by several researchers

Method		
Direct addition of rubber	Replacement of aggregates by weight	replacement of aggregates by volume
Hernandez-Olivares et al. (2002) Hernández-Olivares and Barluenga (2004) Hernández-Olivares et al. (2007) Li et al. (2009) Yesilata et al. (2009) Son et al. (2011) Yang et al. (2011) Richardson et al. (2012)	Fattuhi and Clark (1996) Topcu (1997) Lee et al. (1998) Albano et al. (2005) Sukontasukkul and Chaikaew (2006) Skripkiūnas et al. (2007) Ganjian et al. (2009) Skripkiūnas et al. (2009) Snelson et al. (2009) Sukontasukkul (2009) Mavroulidou and Figueiredo (2010) Mohammed et al. (2011) Pelisser et al. (2011) Azevedo et al. (2012) Najim and Hall (2012) Najim and Hall (2013) Holmes et al. (2014) Hall and Najim (2014) Elchalakani (2015)	Eldin and Senouci (1993) Ahmed and Neil (1993) Eldin and Senouci (1994) (Topcu, 1995) (Khatib and Bayomy, 1999) (Güneyisi et al., 2004) (Huang et al., 2004) (Li et al., 2004a) Bignozzi and Sandrolini (2006) (Gesoğlu and Güneyisi, 2007) (Topçu and Demir, 2007) (Reda Taha et al., 2008) (Khaloo et al., 2008a) Turatsinze and Garros (2008) Atahan and Sevim (2008) Batayneh et al. (2008b) Wong and Ting (2009) Jingfu et al. (2009) Aiello and Leuzzi (2010) Al-Mutairi et al. (2010) Güneyisi (2010) Mohammed (2010) Gesoğlu (2011) Li et al. (2011) Ling (2011) (Ozbay et al., 2011) Rahman et al. (2012) Bravo and de Brito (2012) Atahan and Yücel (2012) Mohammed et al. (2012) Ho et al. (2012) Ling (2012) (Sukontasukkul, 2012) Liu et al. (2012) Ganesan et al. (2013b) Yung et al. (2013)

		Shen et al. (2013) Issa and Salem (2013) Al-Tayeb et al. (2013) Dong et al. (2013) Liu et al. (2013) Meddah et al. (2014) (Thomas et al., 2014) Gesoğlu et al. (2014a) Gesoğlu et al. (2014b) Guo et al. (2014) Gupta et al. (2014) Li et al. (2014b) Mohammadi et al. (2014) Onuaguluchi and Panesar (2014) Su et al. (2015a) Su et al. (2015b)

2.3 Advantages and Disadvantages of Rubberised Concrete

In spite of concrete is the most popular engineering materials, it does have shortage that limit its use in specific applications. Concrete is known as a brittle material with very low tensile strength compared to metals. To improve the tensile strength of concrete, the addition of rubber was suggested as partial replacement of aggregate. Several successful achievements were reported by researchers around the world and they found that there are some benefits and drawbacks of using rubber waste. One of the most vital benefits of using rubber waste is to reduce the unit weight of concrete. Moreover, it was found an improvement in non-structure crack resistance, and resistance to acid, offering lower heat conductivity and noise level reduction when concrete incorporated with rubber up to 30% of the cement weight. In addition, rubberised concrete proved to be lighter in weight with its density reduced compared with NC (Topcu, 1995, Rostami et al., 2000, Najim and Hall, 2013).

Generally, when comparing rubberised concrete with conventional concrete it shows many advantageous such as lower unit weight (Demir et al., 2015), improvement in ductility (Shu and Huang, 2014), higher toughness (Mohammed et al., 2011), higher impact resistance (Ganjian et al., 2009), better resistance to chloride penetration (Bravo and de Brito, 2012), lower thermal conductivity (Mohammed et al., 2012) and higher noise reduction factor (Li et al., 2004b) as well as an improvement in electrical resistivity (Onuaguluchi and Panesar, 2014). However, the main drawbacks of rubberised concrete are the significant reduction in compressive strength, splitting tensile strength, flexural strength and Young's modulus as the partial replacement of rubber to aggregate increased. This reduction in strength has been attributed to a lack of bonding between the rubber particles and cement matrix. This decline was found to be directly proportional to the rubber content. As well as the rubber size (Eldin and Senouci, 1993). Therefore, in this work we will focus on how to improve the mechanical properties.

2.4 Classification of waste tyre rubber

Generally, the waste tyre rubber added to concrete is classified by size rather than composition. The utilisation of waste rubber most often requires reduction of particle size by means of a grinding. The grinding process is mechanical and usually occurs either at ambient or cryogenic (Goulias and Ali, 1997).

Ambient temperature mechanical grinding is generally used in the industry. By using cracker mills and granulator techniques, the waste tyre is cut into small sizes ranging between several centimetres and fraction of centimetre. Then, the steel wires and the textile part would be separated from the rubber particles

magnetically in different stages of granulation. To sort rubber particles into several gradations the mechanical sieve analysis is performed (Owen, 1998).

In the case of cryogenic grinding, the temperature is below glass transition temperature. At this temperature a liquid nitrogen is used to frozen the waste tyre rubber shreds. The frozen rubber shreds become extremely fragile. Then, they are crushed into smaller sizes through the closed loop of the hammer-mill (Karger-Kocsis et al., 2013). The steel wires are magnetically removed as in the mechanical grinding process. This process is performed in a deoxygenated environment to avoid surface oxidation (Owen, 1998).

There are various sizes of rubber obtained after grinding as shown in Figure 2-1. Different sizes of rubber particles will leads to different effects on concrete.

In most of the investigation performed, three categories of waste tyre rubber which mainly utilised as concrete component as following (Ganjian et al., 2009):

- Shredded or chipped rubber commonly used to replace coarse aggregates (CA). This rubber is produced by shredded tyres in three stages. At the first stage, the size of rubber pieces would be shredded to 300–430 mm in length and 100–230 mm in width. In the second stage of shredding, the length would be reduced to 100–150 mm, and then in the final stage it would be reduced to 13–76 mm.
- Crumb rubber which replaces fine aggregates (FA) is manufactured in particular mills that grind the tyre rubber to granules of size ranging from 0.425mm to 4.75 mm.
- Ground rubber can partially replace cement and it depends on the equipment used for size reduction. If the micro-milling process is adopted, the size of rubber particles could be made into 0.075–0.475 mm.

Shredded/chipped-tyre Crumb rubber Ground rubber

Figure 2-1 Rubber size

2.4.1 Mix Design and Mixing Approach

Up to date, there is no standardised mixture procedure is documented for rubberised concrete (RuC). Research is still searching for the best mix approaches for structural purposes.

Many researchers have suggested different approaches in terms of substitution type, whether coarse, fine, or a combination. Most of the presented studies used traditional mix design methods to design a control mix and then using the trial and error method to modify a rubberised concrete mix based on the targeted fresh and hardened properties and rubber particles size and replacement content. Rubberised concrete is usually produced by partially substituting fine aggregate and/or coarse aggregate with rubber. Generally, this replacement increases segregation and bleeding tendency, and that is the main issue facing the use of conventional mix design methods (Najim and Hall, 2010). It is not easy to produce rubberised concrete mix due to many factors that need to be taken into account. The first and the most important factor is the rubber itself, which can be used in a wide range of sizes and replacement amount, from very fine particles to large

pieces and up to 100% replacement. There is an agreement among many studies about mixing all dry constituents together first before adding the mixing water gradually. However, there is a debate around mixing time: (Turgut and Yesilata, 2008) suggested 1 min, while (Sukontasukkul, 2009) proposed 5 min for solid constituents plus superplasticizer (SP) and styrene butadiene rubber (SBR) admixtures adding if specified (Al-Mashhadani, 2001), then, the mixing process is continued for between 3 and 5 min or until a homogenous state is achieved (Al-Sakini, 1998). Ganjian et al. (2009) have proposed mixing the coarse aggregate (CA) with cement, followed by the gradual addition of rubber, fine aggregate (FA) and water containing 75% of the SP and 25% of the SP is added during the last 3 min of mixing. While, Al-Khamisi (1999) suggested mixing coarse and fine aggregate with half of the rubber particles with 25% of the mixing water , after that, adding the cement to the wet mix plus half of the mixing water, before gradually adding the remaining water and mixing for a further 3 to 5 min to obtain homogenous fresh concrete.

2.5 Properties of Rubberised Concrete

2.5.1 Fresh Concrete Properties

Although the fresh state of mixed concrete is just a temporary stage, it highly affects the hardened properties due to the degree of compaction, segregation, bleeding, etc. Therefore, concrete consistency is a critical factor that needs to be carefully judged.

2.5.1.1 Workability

In general, the vast majority of studies have been conducted on the rubberised concrete to evaluate the workability by using the slump test of the mixture. Many researchers have observed that the slump of concrete decreased as the amount

of rubber particles increased (Ozbay et al., 2011, Holmes et al., 2014, Youssf et al., 2014). Several studies have revealed that the slump reduction can be attributed to the overall reduction in the unit weight of the plastic mix in addition to the high friction which usually occurs among the rubber aggregate particles and the other ingredients because of the rough surface texture of the rubber particles (Batayneh et al., 2008b, Reda Taha et al., 2008).

The above findings are in general agreement with several other studies (Zheng et al., 2008a, Cairns and Kenny, 2004, Hernández-Olivares and Barluenga, 2004), but their interpretation of the reduction value relies upon the replacement proportion of rubber aggregate and its size. In contrast, results from other researchers (Aiello and Leuzzi, 2010, Huang et al., 2004, Onuaguluchi and Panesar, 2014) are show that the addition of rubber aggregate increase the workability of concrete (Figure 2-2). Li et al. (2004b) found that there is slight effect of rubber aggregate on the workability of concrete. Furthermore, Khaloo et al. (2008b) showed that rubberised concrete has acceptable workability in terms of ease of handling, placement, and finishing.

Despite the wide range of sizes of rubber particles that have been used as a partial replacement of aggregate, earlier research has shown that using rubber replacement as high as 15% of coarse aggregate by weight appears to have a slight effect on the original slump value regardless of size and shape (Khaloo et al., 2008b). Other studies have found that a sharp decrease in slump, from values of between 80 and 180 mm down to zero slump, occurs when natural aggregate is replaced by rubber aggregate by between 40% (Khatib and Bayomy, 1999) and 50% (Güneyisi et al., 2004) volume replacement of total aggregate, depending upon mix parameters.

On the contrary, some studies have reported that when crumb rubber aggregate was used as a fine aggregate replacement by volume, the slump increases with crumb rubber content up to a maximum value at around 15% (Khaloo et al., 2008b), while another study (Aiello and Leuzzi, 2010) showed that there was a slight improvement in slump when coarse or fine aggregates were replaced by rubber shreds, which the rubber size was between 10 and 25 mm, for up to 75% vol. Yilmaz and Degirmenci (2009) found that replacing 40% of fine aggregate volume with crumb rubber appears to still maintain viability of concrete workability compared with control mixes and this finding was confirmed by (Batayneh et al., 2008a).

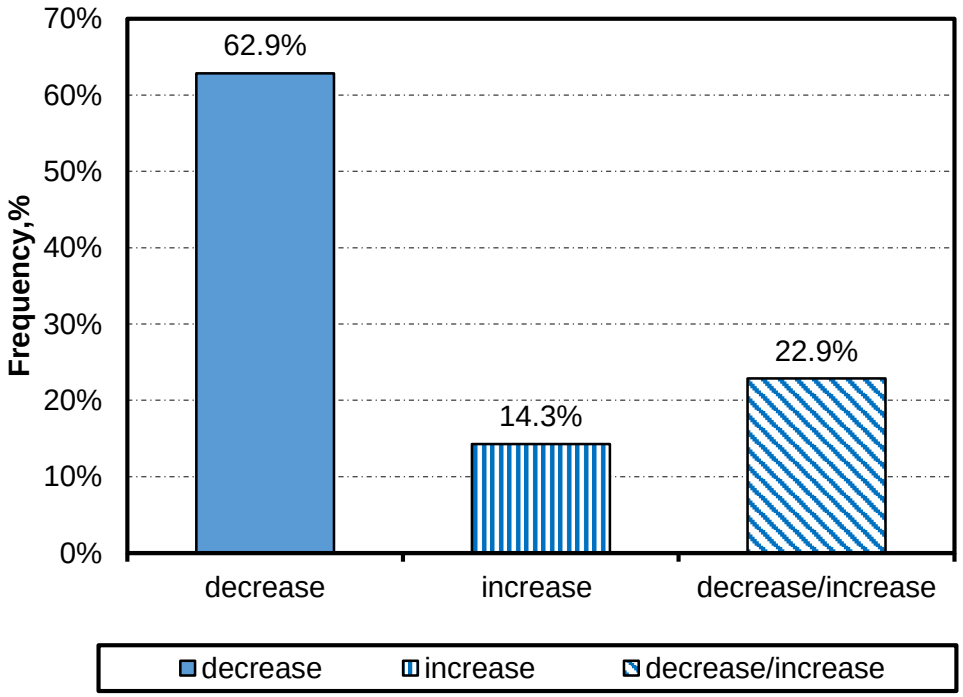

Figure 2-2 Effect of rubber particles on workability (Author)

Many researchers have reported comparative studies on the feasibility of using crumb, chipped or combined chipped/crumb rubber replacement in terms of workability. According to the results, it has been concluded that concrete made with crumb rubber replacement alone has significantly higher workability than that

made with other replacements (Khatib and Bayomy, 1999, Reda Taha et al., 2008, Khaloo et al., 2008b). To enhance the workability of rubberized concrete (Kumar et al., 2014) have recommended to add a required quantity of superplasticizer.

2.5.1.2 Air Content (Porosity)

Many researchers have found that adding rubber aggregates will increase air content in concrete even without using air-entraining admixture (AEA) (Fedroff et al., 1996, Khatib and Bayomy, 1999, Li et al., 2004b, Huang et al., 2004, Mohammadi et al., 2014, Dong et al., 2013). This increase in the air content of rubberised concrete could be attributed to the non-polar nature, roughness of rubber particles and their tendency to entrap air bubbles on their rough surfaces (Savas et al., 1997). Figure 2-3 shows obvious air bubbles around the surface of rubber particle. This phenomenon causes the interface between the rubber particles and cement matrix to be porous and highly absorptive (Sukontasukkul, 2012).

Figure 2-3 Trapped air bubbles at rubber particles submerged in water (Sukontasukkul, 2012)

2.5.2 Properties of Hardened Concrete

2.5.2.1 Unit Weight

Figure 2-4 shows the relationship between the ratio of RuC density to density of control concrete (ρ_{cr}/ρ) and the percentage of rubber. The results were collected from several studies (Reda Taha et al., 2008, Aiello and Leuzzi, 2010, Sukontasukkul, 2012, Kumar et al., 2014, Thomas et al., 2014, Mohammed and Azmi, 2014, Onuaguluchi and Panesar, 2014, Marie, 2016b, Hassanli et al., 2017, Mohammed et al., 2018). As expected, the replacement of normal aggregates by rubber particles tends to reduce the density of concrete based on the amount of replacement, regardless of the size of rubber. This reduction can be attributed to the low specific gravity of rubber particles. Most researchers mentioned above stated that density of concrete decreased uniformly with the increase of rubber percentage in the mixture. Sukontasukkul (2012) reported that the effect of rubber particles on density was clearer when smaller size of rubber particles was used.

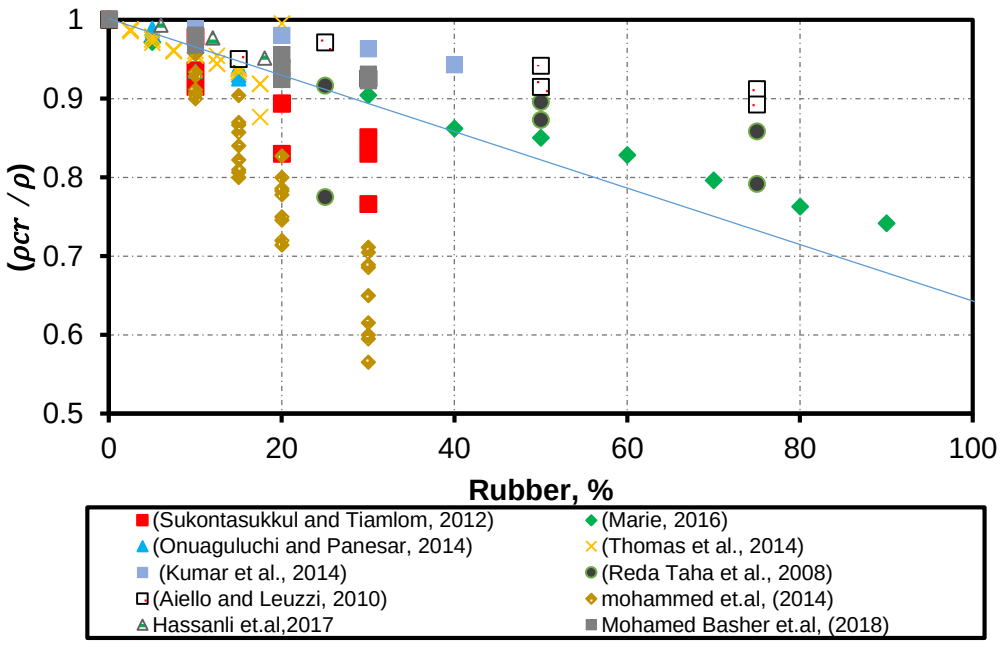

Figure 2-4 Relationship between the ratio of RuC density to control concrete density and rubber% (Author)

2.5.2.2 Compressive Strength

Compressive strength of rubberised concrete has been investigated by several authors (Aiello and Leuzzi, 2010, Batayneh et al., 2008a, Su et al., 2015b, Dong et al., 2013, Youssf et al., 2014, Eldin and Senouci, 1993). Most of the previous research has agreed that the addition of rubber, regardless of its size, leads to a reduction in compressive strength of concrete. This reduction may be attributed to the following possible reasons. First of all, due to the hydrophobic nature of rubber particles, the bond between the rubber particles and the cement matrix is weak (Topcu, 1995, Huang et al., 2004), besides its low stiffness compared to natural aggregate. Moreover, rubber particles has a tendency to move upwards during vibration which lead to higher rubber concentration at the top layer (Ganjian et al., 2009).

Also, there is a consensus among aforementioned researchers that the compressive strength of rubberised concrete mixtures is greatly affected by several factors such as the size and the rubber content, the texture of rubber particles, and the type of cement used in such mixtures. The first study by Eldin and Senouci (1993) found that concrete mixtures with introducing tyre chips and crumb rubber particles showed dramatically reduction in compressive strength compared to conventional concrete. The reduction reaches approximately 85% when coarse aggregate was fully replaced by tyre chips whereas when fine aggregate was fully replaced by crumb rubber the reduction was about 65%. Similar results were obtained by (Kaloush et al., 2005), however they explained part of the strength reduction was due to entrapped air, which increases as the rubber content increases. Further work showed that the strength reduction could be considerably reduced by adding a de-airing agent into the mixing just prior to the placement of the concrete (Kaloush et al., 2005).

The relationship between the percentage of rubber (chip and crumb rubber) and the reduction of compressive strength based on the results of different studies (Khatib and Bayomy, 1999, Topçu and Bilir, 2009, Zheng et al., 2008b, Onuaguluchi and Panesar, 2014, Atahan and Yücel, 2012, Li et al., 2016b, Hassanli et al., 2017, Fan et al., 2017) was illustrated in Figure 2-5. It can be seen that the reduction in compressive strength is higher when using chip rubber than using crumb rubber. Najim and Hall (2010) recommended avoiding the use of chipped rubber particles due to the significant reduction in the compressive strength and preferably use crumb rubber which has relatively low implications for strength reduction. In this study, two sizes of crumb rubber was used as a substitution of fine aggregate.

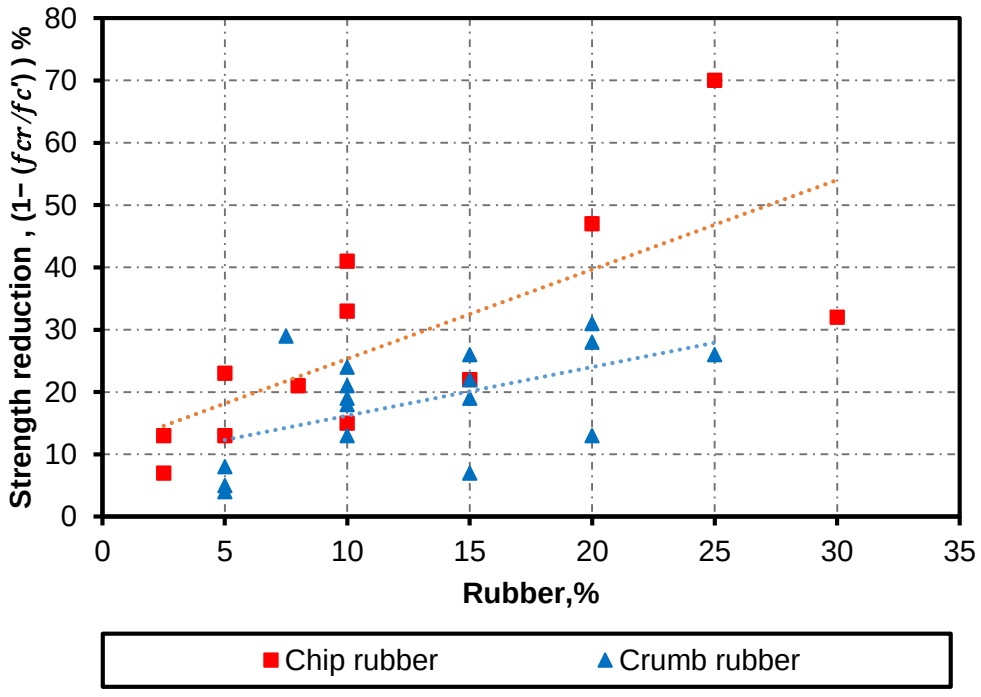

Figure 2-5 Relationship between the reduction of compressive strength and the rubber content (Author)

In contrast, the study by (Ali et al., 2000, Fattuhi and Clark, 1996) indicated that rubberised concrete mixtures with fine grading of rubber particles had higher reduction in compressive strength than that with coarse rubber grading.

One of essential reason of the reduction of rubberised concrete mixtures is the weak bond between rubber particles and the cement matrix. Several methods were examined to reduce the deficiencies of using rubber in concrete, such as pre-treating the rubber particles prior incorporating in concrete, and addition of some external additives to enhance the mechanical properties of concrete. However, experimental results on the effectiveness of these methods have been inconsistent and in some cases conflicting in the current literature.

There are various ways of pre-treatments to enhance the strength of RuC such as washing rubber particles with water or sodium hydroxide (NaOH) to remove carboxyl group and the acidic on the surface of rubber particles (Chou et al., 2007, Najim and Hall, 2012, Youssf et al., 2014) or coating rubber particles with various materials like silane coupling agents (SCA) (Dong et al., 2013), mortar, or cement paste (Youssf et al., 2014). The results showed that the pre-treatment of rubber aggregate with water washing have marginally improvement in strength (Najim and Hall, 2012, Raffoul et al., 2016), whereas using NaOH showed better results. Balaha et al. (2007) reported that using NaOH as a pre-treatment of rubber particles increased compressive strength and tensile strength by 15% and 6% respectively. Danko et al. (2006) also were conducted a pre-treatment of rubber surface with using a (NaOH), affecting the interfacial transition zone (ITZ) and allowing the rubber to has better adhere with the cement paste. Utilisation of treated rubber to concrete shows varying degrees of success.

Su et al. (2015a) have carried out surface treatment on rubber using SCA to enhance the bond strength between rubber particles and cement matrix. Rubber particles were submerged in SCA until all surface was saturated by the agent before being added into the mixture. The results showed that using the SCA as a pre-treatment method leads to an enhancement in the compressive strength of rubberised concrete by 19.3% at 1 day, 9.3% at 7days, and 6.8% at 28 days, respectively. Huang et al. (2013) found that using SCA followed by coating with cement paste could increase the compressive strength by up to 110%. A similar method was used by Dong et al. (2013), but their results exhibited only 10-20% enhancement in compressive strength.

Cairns and Kenny (2004) also conducted another method for pre-treatment of rubber particles by using Carbon tetrachloride (CCl4). A results showed a significant improvement in compressive strength (about 57%).

The utilisation of several additives such as silica fume (SF), steel fibre and nano silica (NS) was also used to enhance the mechanical properties of rubberised concrete. Elchalakani (2015) observed an enhancement in the flexural strength of rubberised concrete with the addition of SF and reduction in water to cement ratio. As the effect of SF enhanced the bonding of interfacial transition zone (ITZ), the loss in strength of high strength rubberised concrete was lower than that of the conventional concrete. The same finding was observed by Onuaguluchi and Panesar (2014) in the concrete containing coated rubber and silica fume.

The addition of steel fibres to rubberised concrete mixtures resulting in a strength increase of 3% to 16% as stated by (Ganesan et al., 2013a, Ganesan et al., 2013b). Recently, nano silica has been added to roller compacting concrete and the results showed a successful improvement (Mohammed et al., 2016a), Yet,

there is a lack of research in rubberised concrete incorporating nano silica due to these limited studies, further investigations are needed.

In general, using the appropriate pre-treatment method for rubber particle surface is a promising technique, which produces high performance material suitable for many engineering applications.

2.5.2.3 Splitting tensile strength

One of the major disadvantages of conventional concrete is its low tensile strength. Therefore, it is important to understand the influence of rubber particles on the tensile strength of concrete. A huge number of previous studies have reported that the splitting tensile strength for RuC hugely reduced as the rubber replacement increased (Benazzouk et al., 2003, Atahan and Sevim, 2008, Zheng et al., 2008a, Snelson et al., 2009, Ganjian et al., 2009, Thomas and Gupta, 2015, Aslani et al., 2018). The reasons of the reduction of splitting tensile strength are similar to those affecting the compressive strength. However, Youssf et al. (2014) found that there were some improvements when rubber content was less than 3.5%, but no reason was provided for this.

The addition of 20% silica fume to RuC, with up to 50% rubber replacement, has been shown to have a beneficial effect in terms of splitting tensile strength, where the improvement were 27%. On the other hand, the results of a different study showed that with 50% vol. total aggregate replacement, the reduction in splitting tensile strength can achieve 80% (Güneyisi et al., 2004).

Generally, to avoid significant reductions in mechanical properties, several researchers have recommended the maximum rubber aggregate content should not exceed between 20% (Khatib and Bayomy, 1999), 25% (Khaloo et al., 2008b), and up to 30% total aggregate volume (Zheng et al., 2008b).

2.5.2.4 Flexural Strength

The flexural strength results of rubberised concrete has shown similar trend to the compressive strength and splitting tensile strength results. There is a reduction in flexural strength can reach 37% when chip rubber particles were partially replaced by coarse aggregates and 29% loss when powder rubber was partially replaced by cement Ganjian et al. (2009). In addition, Su et al. (2015b) observed a decrease of 12.8% in the flexural strength when 20% fine aggregate was replaced with rubber particles. It was found that the specimens with smaller size of rubber particles show less reduction in flexural strength compared with those that have larger particles.

Less reduction in strength was obtained when the size of rubber particles were smaller. This is because of the filler effect of small rubber particles that increase the compactness of concrete, reduce the stress singularity at internal voids, and hence reduce the probability of fracture. This is supported by (Aiello and Leuzzi, 2010) study which reveal that higher loss in flexural strength when the coarse aggregate was substituted by rubber particles rather than fine aggregate.

However, Elchalakani (2015) noticed that the addition of silica fume with a reduction in water/cement ratio has enhanced the flexural strength of rubberised concrete. As the effect of silica fume enhanced the interfacial transition zone (ITZ) bonding, the reduction in strength of high strength rubberised concrete was lower than that of the normal strength concrete.

The control specimens exhibited brittle failure and split into two pieces immediately after cracking, while the specimens containing rubber fibres showed deformation without complete shattering (Yilmaz and Degirmenci, 2009). Another study by (Segre and Joekes, 2000) examined the flexural strength of concrete

with treated rubber with NaOH and untreated rubber. In both cases, the flexural strength was higher than the control specimens. Toutanji (1996) also stated a decrease in flexural strength up to 35 %, depending on the rubber content, compared with conventional concrete.

2.5.2.5 Shrinkage

Shrinkage is defined as the contraction occurred due to the loss of the gel water caused by evaporation or by hydration of cement (Neville and Brooks, 1987). Shrinkage in rubberised concrete is relatively higher than those of normal concrete. Bravo and de Brito (2012) found that the shrinkage of rubberised concrete increases as the amount of rubber particles increase. The variation was smaller when coarse aggregate was replaced with chipped rubber. The shrinkage of conventional concrete and rubberised concrete was more intense in the first 15 days after casting and has decreased by the end of 90 days.

Based on the investigation done by (Sukontasukkul, 2012), the shrinkage of rubberised concrete depends on the size of the rubber used as well as the rubber content. The concrete specimen with ground rubber (passing 26 sieve) showed more shrinkage than those with crumb rubber (passing 6 sieve). This can be due to the flaky particle size of the rubber particle that allows them to act like a spring. The combined effect of reducing the water–cement ratio and adding silica fume in high strength concrete mix reduced the 28 days shrinkage by about 50%. The behavior of rubberised concrete against shrinkage can be improved by reducing the water–cement ratio and adding mineral admixtures (Sukontasukkul, 2012).

2.5.2.6 Impact resistance

High-impact resistance and greater energy absorption capacity is require for many structural applications, such as foundation pads of machinery, airport

runways, bridge deck and highway pavement. Adding rubber particles to concrete can contribute to improving the impact resistance and energy absorption due to their lower stiffness.

Energy absorption capability of rubberised concrete based on the impact resistance test has been investigated by various researchers (Dong et al., 2013, Liu et al., 2012, Ozbay et al., 2011, Al-Tayeb et al., 2013). The results indicated that the addition of rubber particles to concrete enhanced energy absorption compared to normal concrete. Also, it showed that the average of dissipated energy increases as the rubber content increase in concrete. Besides, the energy absorption capability of rubberised concrete is better than that of conventional concrete. The duration of impact increased more than 6 times between normal concrete and 100% rubber replacement samples (Atahan and Yücel, 2012). This is mainly because of the natural property of rubber material which has a much lower stiffness than concrete. Therefore, when rubber particles are used to replace natural aggregate, concrete becomes more ductile.

The research study by Ozbay et al. (2011) also found that the greater the percentage of rubber aggregate, the higher energy absorption capability of rubberised concrete. Based on these conclusions, rubberised concrete has a high potential for applications such as safety barriers because they lead to smaller deceleration forces and hence less damage (Atahan and Yücel, 2012). The improvement of the energy absorption with the inclusion of rubber aggregate is one advantage of using this recycled material.

2.5.2.7 Thermal Conductivity

Thermal conductivity is defined as quantity of heat transmitted through a unit thickness in a direction normal to a surface of unit area due to a unit temperature

gradient under steady state conditions. Mohammed et al. (2012) have investigated the thermal conductivity of crumb rubber hollow concrete block. Their results showed that thermal conductivity decreases with the increase of rubber content (Figure 2-6). Sukontasukkul (2009) has noted that the thermal conductivity of rubberised concrete in general is less than that of conventional concrete by 20–50% whilst another study has indicated the figure to be closer to 60% (Yesilata et al., 2009), and this difference is significantly dependent on the content and the size of rubber replacement. Mohammed et al. (2012) also mentioned that the combination of silica fume and fly ash as a replacement of cement content in rubberised concrete causes a reduction in thermal conductivity. This may be due to the lower thermal conductivity of silica fume and fly ash when compared to cement. Sukontasukkul (2009) also indicated that the thermal conductivity of a material has an inverse relation with its density; hence the addition of rubber particles greatly improves the thermal conductivity of concrete mixture.

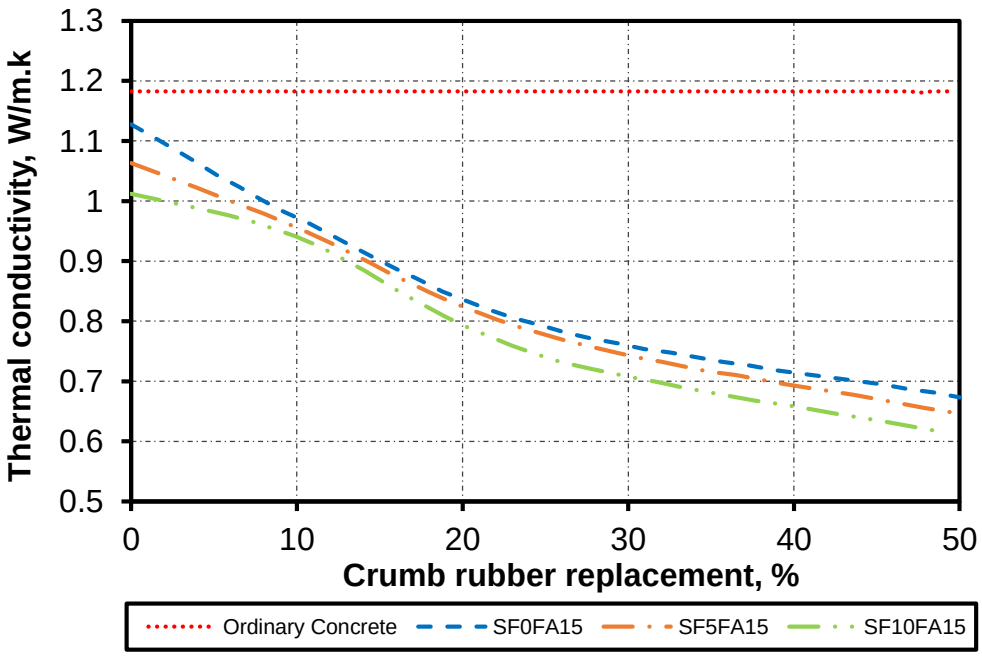

Figure 2-6 Thermal conductivity versus crumb rubber replacement (Mohammed et al., 2012).

2.5.2.8 Sound absorption

Sound absorption is defined, as the incident sound that strikes a material and is not reflected back. Rubberised concrete has better sound absorption properties compared to the conventional concrete. The sound absorption coefficient increases as the amount of rubber increases. With the amount of rubber aggregate increasing air content increases due to the entrapped air on rubber surface, leading to a higher porosity (P) of rubber concrete. Consequently, sound energy is absorbed more easily during the process of reduced reflection from the pores (Khaloo et al., 2008b). The use of silica fume in rubberised concrete reduces the sound absorption properties due to the micro filling abilities (Mohammed et al., 2012). Holmes et al. (2014) conducted experimental investigations on the sound absorption properties of rubberised concrete. They explained that the crumb rubber concrete was found to be more effective than plain concrete in absorbing sound in low, normal, and high temperature environments. Better absorption coefficients were observed at crumb rubber 2–6 mm and 10–19 mm, used for 15% substitution of fine aggregates. Crumb rubber concrete showed better performance as an insulator for high frequency sounds due to the wider surface affected. Pacheco-Torgal et al. (2012) noted that the rubberised concrete is an effective absorber of sound and vibration energy. A large reduction in the ultrasonic modulus with increasing rubber concentration demonstrates a porous composition for rubberised concrete.

Holmes et al. (2014) found that the absorption coefficient of the RuC ranges from 0.013 to 0.2 compared with 0.018 in the plain concrete which is similar to previous work in this area (Fedroff et al., 1996). The results indicated that the level of absorption was greater for those concretes with higher volumes and larger grades of rubber. For instance, the 7.5% replacement of fine aggregate by dust yielded

an absorption co-efficient of 0.013 compared to 0.018 from the control. However, as the size and volume of particles increase, the opposite is true as the larger surface area and heavier graded rubber is capable of absorbing more sound. For instance, there was an increase in absorption coefficient of 623%, 107%, 33% and 21% between the 7.5% and 15% replacement levels for the dust, 1–3 mm, 2–6 mm and 10–19 mm crumb rubber particles respectively. This increased absorption demonstrates that both volume and grading of rubber affect RuC acoustic absorbance properties.

Holmes et al. (2014) also observed that similar sound insulation properties with the control sample particularly at 63 and 125 Hz where the level of sound retained both was approximately 15 and 11 dB respectively. However, the control sample appears to be a slightly better insulator that the RuC at the higher frequencies (250 and 500 Hz) with a 3–4 dB improvement throughout due to the longer wavelengths allowing it to penetrate a larger surface area. Previous research(Khaloo et al., 2008b, Sukontasukkul, 2009) has shown that higher density materials have improved insulation properties with the lower densities for all RC's than the control. Moreover, a minor decrease in the insulation performance of RuC in the elevated temperature was observed on the largest rubber grade (10–19 mm) due to some minor cracking on the surface. None of the previous researchers have examined acoustic properties of rubberised concrete with nano silica. Thus, as a part of this study, the acoustic properties of rubberised concrete with the addition of nano silica compared to NC and RuC will be highlighted.

2.6 Applications of rubberised concrete:

The use of rubberised concrete in civil engineering applications is expected to become more common if the compressive strength of the rubberised concrete has been enhanced. The low density of rubber particles compared to a natural aggregate can be significantly involved in the development of lightweight concrete, which helps to reach a more economical design. It is noted that the rubberised concrete has many advantages such as, high impact resistance, excellent thermal and sound insulation. Yet, it is very weak in both compressive and tensile strength.

Recently, rubberised concrete is used in different applications such as the precast sidewalk panel, precast roof for green buildings, and non-load bearing walls in buildings (Tomosawa et al., 2005). It also can be used in the road intersections, entertainment courts, and pathways, and skid resistant ramps (Kaloush et al., 2005). Rubberised concrete can be suitable for architectural applications, which require low density and do not need high strength, such as wall panels, building facades and nailing concrete, or other light architectural units. It can be used in vital application which exposed to repeated freezing and thawing cycles.

In addition, it can be used in building as an earthquake absorber, where vibration damping is required such as in foundation pads for machinery railway station, where resistance to impact or explosion is required, such as in railway buffers, bunkers and for trench filling.

To widen the practical application of rubberised concrete and increasing its acceptability in the construction industry, it is essential to enhance the strength of rubberised concrete.

2.7 Nano Silica

2.7.1 The significance of nano silica in concrete

Extensive experimental research have been carried out to improve the durability and sustainability of concrete. In recent years, using nanotechnology has gained particular attention in concrete industry due to its nanoparticle size which ranging between 1 to 100 nm and its high surface area to enhance the mechanical properties of concrete. The most common nanomaterial is Nano silica. The particles size of nano silica and concrete ingredients are described in Figure 2-7. The utilization of nano silica in construction industry still limited due to relativity high cost of it in the commercial market compared with other cementitious replacement such as fly ash and GGBS. However, NS is used in very small percentages comparing with other materials. Nano silica has introduced many amazing benefits to concrete due to nano size of its particles. It has the ability to fill the voids between cement grains (Aleem et al., 2014). The addition of nano silica increased the density of concrete and that may lead to reducing the amount of water demand for mixing. Therefore, the strength of concrete can be improved due to the reduced capillary porosity. In addition to the physical properties enhancement, the possibility of improving the bond between aggregate and cement matrix is expected as well as durability properties.

Nano silica also acts as an activator to pozzolanic reaction, which further produces more C–S–H gel leading to enhancing the microstructure of concrete (Nili and Ehsani, 2015, Mukharjee and Barai, 2014b).

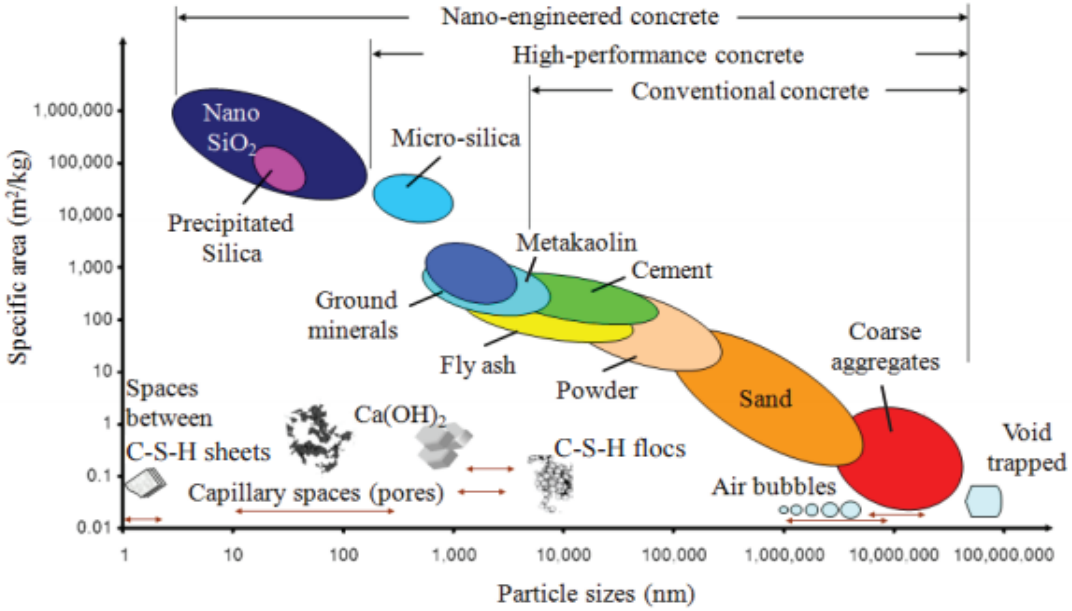

Figure 2-7 Particle size range and specific surface area (SSA) of concrete components, adapted from Sobolev and Ferrara (2005)

2.7.2 Production method of NS

Nano-silica is an amorphous SiO_2 nano particles; it can be available in two forms, a compacted dry form or in a colloidal dispersion form. Both types of nano-silica have been used as a partial replacement of cement (Nazari and Riahi, 2011, Rupasinghe et al., 2017). There are several methods to synthesis of nano silica such as: sol-gel method (Pinto et al., 2006), precipitation (Jal et al., 2004) plasma (Wu et al., 1997), microwave heating (Rungrodnimitchai et al., 2009), and it can be directly prepared from bio waste like Rice, ash, Husk, however, Sol-gel method is still the main method used because of the possibility through this method to control the size of particles and monitoring the size distribution at mild conditions (Björnström et al., 2004). The production of NS by Sol-gel method can be explained as (water or organic route) is applied in room temperature when materials as sodium silicon (Na_2Sio_4) and organometallic such as tetraethylorthosilicate (TMOS, $Si(OC_2H_5)_4$) are attached in a solvent of the

solution, following by changing in pH leading to the precipitation of silica gel. Then, the gel goes through mixing and filtering process to form Xerogel which can be dried and burned or dispersed again with stabilized agents (Na, K, NH3) to introduce nano silica with (20 to 40%) solid content . Alternatively, it can be manufactured by the vaporization of silica in high temperature ranging between 1500 to 2000°C by decreasing quartz (SiO_2) in an electric arc furnace (Rahman and Padavettan, 2012). A general flow chart and schematic for Sol-gel process are shown in figure 2-8.

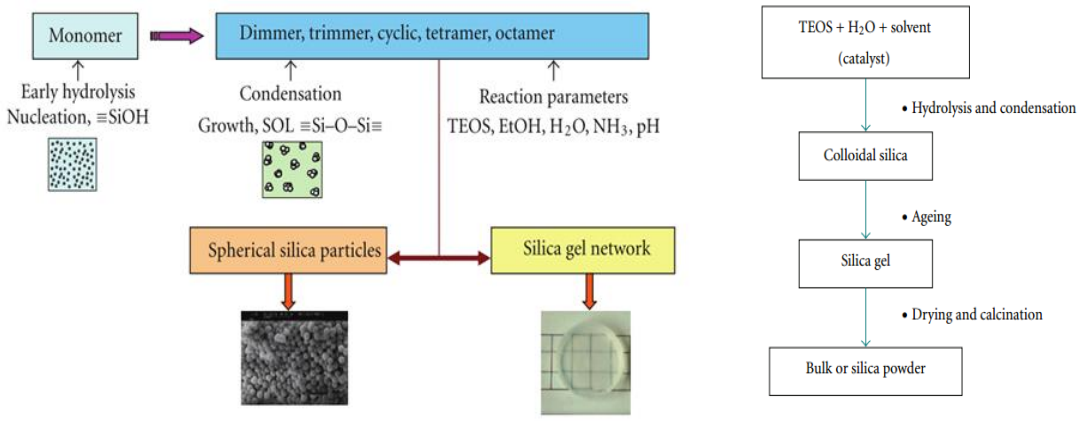

Figure 2-8 A Schematic and general flow chart for Sol-gel process (Rahman and Padavettan, 2012)

Particles of nano silica could contribute in the acceleration of cement hydration due to the pozzolanic activity. After Silicic acid ($H_2SiO^{2-}_4$) is formed from cement grains and nano silica particles, it reacts with Calcium to form an additional calcium–silicate–hydrate (C–S–H) which in turn would spread in the water that located between cement particles making concrete more compact. This formation leads to the acceleration of hydration process, at the same time consuming free calcium hydroxide Ca $(OH)_2$. As a result, compressive strength can be enhanced especially in the first days (Singh et al. 2013). These reactions are described in the following equations.

$$SiO_2 + H_2O \rightarrow H_2SiO^{2-}_4 \quad (2.1)$$

$$Ca(OH)_2 + H_2O \rightarrow Ca^{2+} + OH^- \quad (2.2)$$

$$H_2SiO^{2-}_4 + Ca2 \rightarrow C\text{-}S\text{-}H \text{ (additional C-S-H)} \quad (2.3)$$

2.7.3 Effect of nano silica on properties of concrete

Studies have shown that adding nano silica in small dosage has the ability to enhance the mechanical and durability of concrete. This enhancement is demonstrated in the following sections.

2.7.3.1 Mechanical properties

Recently, many investigations have been done in order to evaluate the feasibility of utilizing NS in normal concrete (Lin et al., 2011, Mukharjee and Barai, 2014a, Rupasinghe et al., 2017) . Mukharjee and Barai (2014a) found that the addition of NS resulted in 20% enhancement in compressive strength, similarly, a significant improvement is recorded in splitting tensile strength and flexural tensile strength. This enhancement could attributed to the ability of NS to densify the ITZ between aggregates and cement matrix which leads to better bond and thus improving the strengths of the concrete

The same impact was also reported by Ghosal and Chakraborty (2015). However, other investigations found that the improvement in compressive strength could reach around 70% compared to conventional concrete (Nazari and Riahi, 2011). However, these results depend on the conditions of synthesis and production of SiO_2 nanoparticles and that dispersion of SiO_2 nanoparticles in the paste play a significance role. The influence of nano silica particle size on mechanical properties of concrete were also studied (Givi et al., 2010). The

results demonstrated that the compressive strength of samples with smaller size was better than those containing larger particle size at early days.

Nano silica has been recently added to rubberised concrete to enhance the mechanical properties (Mohammed et al., 2016b). The inclusion of nano silica would refine the size of the pores and densify the interfacial transition zone between cement matrix and aggregate in rubberised concrete. Table 2.1 shows the variation of findings of several investigations from the literature regarding the effect of nano silica on compressive strength of concrete.

Table 2-2 List of studies focusing on the effect of NS on concrete strength

Author	NS			W/b ratio	Dosage usage (%)	Optimum ratio (%)	Improvement %	
	Type	Size(nm)	SSA (m^2/g)				7 days	28 days
Esmaeili & Andalibi (2008)	P	20	220	0.45	3, 5 and 7	7	53.2	57.2
Najigivi et al., (2010)	C	15 80	160 560	0.4	0.5, 1, 1.5 and 2	1	21.2	18.5
Nazari & Riahi (2011)	P	15	165	0.4	1,2,3,4 and 5	4	-	74.3
Zhang & Li (2011)	P	10	640	0.42	1 and 3	1	-	12.3
Najigivi et al., (2013)	P	15	640	0.4	0.5, 1, 1.5 and 2	1	21.2	21.5
Beigi et al., (2013)	P	15	160	0.39	2,4 and6	4	-	19
Du et al., (2014)	P	13	200	0.48	0.3 and0.9	0.9	12	12
Ghafari et al., (2014)	P	15	160	0.2	1,2,3 and 4	3	40	8
Bolhassani & Samani, (2015)	C	25 5	80 500	0.53 0.53	1.5, 4and 7 1.5 and 4	7 4	28 36	30 34
Mujkharjee & Barai, (2015)	C	8, 20	-	0.4	0.5, 1.5 and 3	3	14	25
Alam Shah et al., (2016)	P	5, 40	-	0.35	1, 2, 3, 4, 5, 6, 7 and 8	4	47.9	29.6
Isfahani et al.,(2016)	C	20	- -	0.65 0.5	0.5,1 and 1.5	1.5 1	30.3 -	41 10.6
Khaloo et al., (2016)	P	12	200	0.35	0.75 and 1.5	1.5	25	12
Serag et al., (2017)	P	20, 80	-	0.42	1.5, 3 and 4.5	3	4.5	43.5
Palla et al., (2017)	C	-	116	0.25	0.5 and 2	2	39	30

Note: P:powder and C: colloidal

So far, only a few investigations on the effects of nano-silica on mechanical properties of roller compacting concrete are available (Mohammed and Adamu, 2018, Mohammed et al., 2018, Adamu et al., 2018b). Therefore, the current study aims to further investigate and understand the influence of nano silica on mechanical properties of rubberised concrete.

2.7.3.2 Durability properties

Durability properties of concrete containing NS showed a distinct improvement compared to normal concrete. It was found that the addition of 3% nano silica caused a reduction in water penetration depth, diffusion coefficient and chloride migration coefficient by 45%, 31% and 28.7%, respectively compared to normal concrete (Du et al., 2014). In addition, due to the blockage effect of nano silica, it leads to reduce the permeability and reduction of capillary porosity of concrete.

2.8 Prediction of compressive strength of rubberised concrete

There are many empirical models associated with the accuracy of compressive strength prediction of rubberised concrete. According to a review of the literature there are five existing models namely, Khatib and Bayomy-99 Model, Khaloo-08 Model, Guneyisi-04 Model, Youssf et al-16 Model and Bompa et al -17 Model. Moreover, there is an increasing interest in applying artificial intelligent (AI) techniques research to problems related to rubberised concrete. Many studies have proposed approaches for modelling rubberised concrete strength and mechanical properties. Eldin and Senouci (1993) first used Artificial Neural Network (ANN) to estimate the strength of rubberised concrete. Topcu and Sarıdemir (2008) recently applied ANN and fuzzy logic (FL) to predict the properties of rubberised concrete. They modelled rubberised concrete properties using input variables including cement, sand, water, fine crushed stone, coarse

crushed stone, fine rubber, coarse rubber and output variables including the unit weight and flow table of fresh concrete. Gesoğlu et al. (2010) established a mathematical formula using ANN and Genetic Programming (GP) to model rubberised concrete properties and measure the influence of silica fume on rubberised concrete properties. More recently, Abdollahzadeh et al. (2011) used ANN to predict the compressive strength of rubberised concrete. However, their dataset of only 20 instances is likely inadequate to accurately assess model performance. (Ahangar-Asr et al., 2010) used a new data mining technique, named Evolutionary Polynomial Regression (EPR), to predict the mechanical behaviour of rubber concrete. Data used in training and testing of the EPR models were obtained from results of an experimental study involving a total of 70 rubber concrete samples. None of previous studies were developed ANN model to predicted compressive strength of RuC with extensive database. More details about the existing models and ANN model to predict compressive strength of RuC has been presented in chapters six and seven.

2.9 Concluding Remarks

Rubberised concrete has a great possibility to be used in practice because it is environmentally beneficial, commercially competitive, and supportive of a more sustainable society.

Although many researchers have tried to reduce the loss of strength of rubberised concrete, more studies are still needed to significantly improve the performance of rubberised concrete. There are many advantages of using rubberised concrete, the most significant advantage of rubberised concrete is its excellent energy absorbing characteristics. It also can effectively improve the ductility, reduce density, higher impact resistance, and prevent brittle failures. However, the strength reduction

is one of the most significant disadvantages of rubberised concrete, which prohibits its applications to structural components.

To summarise the main findings that are relevant to rubber concrete, based on the extensive literature that has been reviewed, the following points can be listed:

- ✓ The reduction of size of rubber particles will effectively reduce the loss of strength of rubberised concrete. Meanwhile, the cost of producing fine rubber aggregates should be considered along with the benefit of improved performance of rubber concrete.
- ✓ Incorporating rubber aggregates in concrete leads to a decrease in the unit weight, workability, and strength, whilst increasing the ductility and air content.
- ✓ The strength of concrete depends greatly on the density, size, and hardness of coarse aggregate. The use of soft rubber material as coarse aggregate will inevitably reduce much of concrete strength.
- ✓ In order to avoid considerable reduction in mechanical properties, several studies have recommended that the maximum content of rubber aggregate should not exceed 30%. Other researchers have concluded that the use of crumb rubber aggregate (sand replacement) gives less reduction in mechanical properties than chipped rubber aggregate (gravel replacement).
- ✓ Results of various studies indicate that the mechanical strength of rubberised mixtures is greatly affected by the size, proportion, and surface texture of rubber particles and the type of cement used in such mixtures.

- ✓ Rubberised concrete shows a significant improvement in terms of thermal and Acoustic insulation. However, there is no available data in the literature regarding thermal and acoustic of rubberised concrete with nano silica.
- ✓ It should be noted from the above literature review, that very limited studies are available on using nano silica with rubberised concrete and this has motivated the present study.

CHAPTER THREE- MATERIALS AND EXPERIMENTAL METHODOLOGY

3.1 Introduction

The third chapter is concerned with the methodology used for this study. The design of experimental programme can be broken down into two parts: The trial experimental phase and the main experimental phase. The purpose of the trial experimental phase was to determine the optimum size of nano silica particles and optimum replacement content of colloidal nano silica in the concrete mixtures. However, the main experimental phase was to study and further understanding the effects of colloidal nano silica on various characteristic such as, mechanical, thermal and acoustic properties of rubberised concrete mixtures.

This chapter shows in detail the materials used and the testing procedure in this study.

3.2 Materials

The materials used in this study included ordinary Portland cement, fine and coarse aggregate, rubber particles, colloidal nano silica and superplasticiser (SP). The properties of these materials are presented below.

Cement: Portland cement (CEM I/ 52.5N), which complying with the standard specification of BS EN 197-1 was used in this study. The cement was obtained from Hanson Company. The physical and chemical properties of cement are shown in Table 3-1Physical properties of cement

and 3-2, respectively as provided by supplier.

Table 3-1Physical properties of cement

Property	Value
Specific gravity	3.15
Blaine fineness(m^2/kg)	400
Initial setting time (Mins)	150
28 compressive strength, MPa	60

Table 3-2 Chemical analysis of the cement

Oxides	Value (concentration %)
SiO_2	20.10
AL_2O_3	5.04
Fe_2O_3	2.28
CaO	36.24
MgO	2.50
SO_3	3.39
Na_2O	0.28
K_2O	0.62
CI	0.05
loss of ignition	2.87

Superplasticiser: An aqueous solution containing polycarboxylic ether, Glenium 51 from BASF, was used as high range water reducer (HRWR) in the experiment to obtain the desired workability of the concrete mixture, in accordance with BS EN 934-2.

Aggregates: The fine aggregate (FA) used throughout this study was river sand with a maximum size of 5 mm, whereas the maximum particle size of coarse aggregate (CA), uncrushed gravel, was 10 mm. All the aggregates used were from the same source. The primary tests for both types of aggregate were

conducted to determine the specific gravity, water absorption and bulk density were determined in accordance with ASTM C29, (2009) as shown in Table 3-3. The moisture contents of fine and coarse aggregates were measured each time before mixing and the free water was adjusted according to these moisture contents.

Table 3-3 Physical properties of coarse aggregate, fine aggregate and rubber

Property	Coarse aggregate	Fine aggregate	Rubber A	Rubber B
Relative density (SSD)	2.63	2.6	1.19	1.26
Relative density (Dry)	2.65	2.63	1.52	1.65
SSD water absorption (%)	0.98	3.5	4.56	5.95
Water content (kg/m^3)	0.3	2.76	-	-
Bulk density (kg/m^3)	1686	1592	726.5	776

Particle size distribution for natural aggregate is performed in accordance with ASTM C33 by sieve analysis through a set of sieves placed on a mechanical shaker. The grading curve of the Fine aggregate and the coarse aggregate used are given with the standard curves in Figure 3-1. The figure shows clearly the difference in grain size distribution between the two types. However, both types are well-graded.

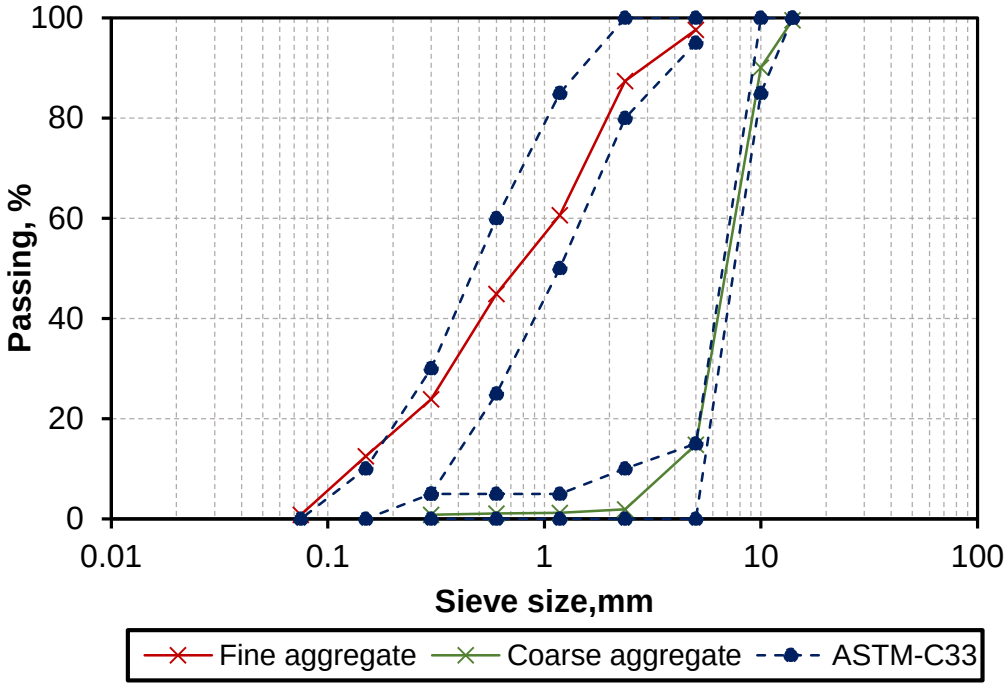

Figure 3-1 Gradation curves for both coarse and fine aggregate.

Crumb rubber: Two different sizes of crumb rubber R_A (0.5 – 1.5 mm) and R_B (1.5 – 3.0 mm) were used as a partial replacement for fine aggregate. The reason behind choosing these sizes is due to the economic point of view, this size is cheaper and commonly available as compared with finer ones, and the sieve analysis showed that the gradation of rubber is close to the size of natural aggregate fraction Figure 3-2.

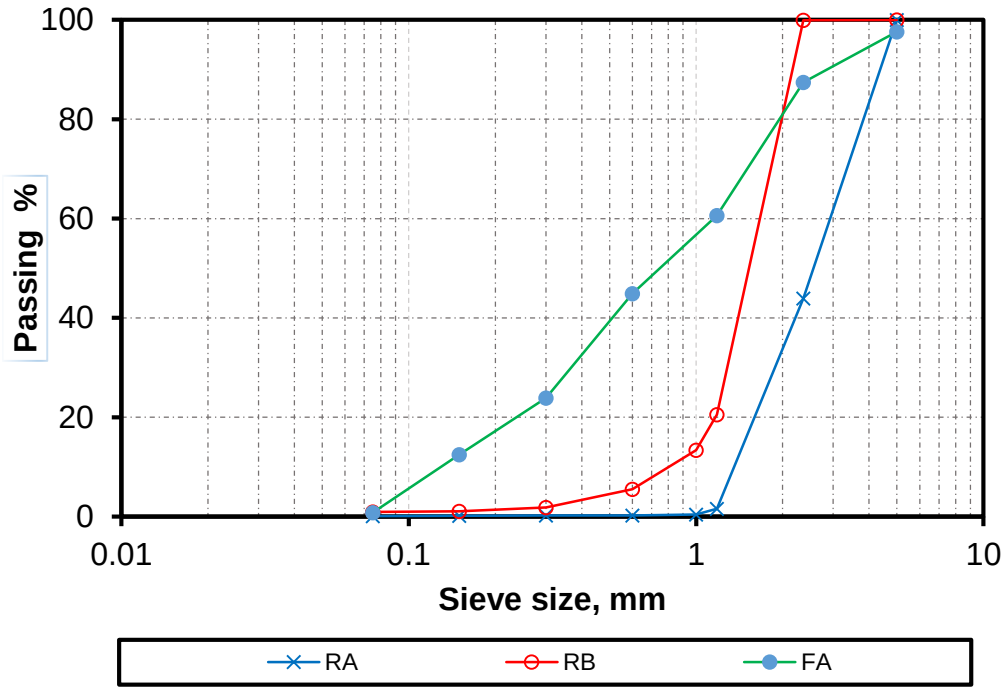

Figure 3-2 Gradation curves for FA, rubber A and rubber B

Nano silica: Three different commercial colloidal nano silica having different specific surface area (SSA) and different particle size were used in the trial experimental phase. The first type was supplied from BASF Company with a relatively small SSA (51.40 m^2/g), while the other two types were produced by Akzonobel Company with larger SSA 250 and 500 m^2/g. These products were named; NS-50, NS-250, and NS-500, respectively based on their specific surface area. The physical and chemical properties of these types of nano silica are shown in Table 3.4 and Table 3.5, respectively. Further, X-ray diffraction analysis (XRD) was conducted using 2Theta for the three types of NS and presented in Figure 3-3. On the X-ray scale, the three types of NS particles appear to be amorphous and had a very low of crystallinity with high purity of silica. Numerous trials were made in the preliminary stage of the research in order to choose the appropriate type of nano silica.

Table 3-4 Physical properties of Nano silica

	Particle size (nm)	SSA (m^2/g)	Colour	Bulk density (Kg/m^3)	Relative density	pH	SiO_2 (%)
NS-50	98.7	51.4	Milky	-	1.2	9.4	40
NS-250	11	250	translucent	1200	1.2	6.8	30
NS-500	5	500	Clear cloudy	1050	1.1	10	15

Table 3-5 Chemical composition (%) of NS

Oxides, %	NS-50	NS-250	NS-500
SiO_2	99.99	99.99	99.99
AL_2O_3	-	-	-
Fe_2O_3	-	-	-
C_aO	-	-	-
M_gO	-	-	-
SO_3	-	-	-
Na_2O	-	-	-
K_2O	-	-	-
CI	-	-	-
loss of ignition	0.01	0.01	0.01

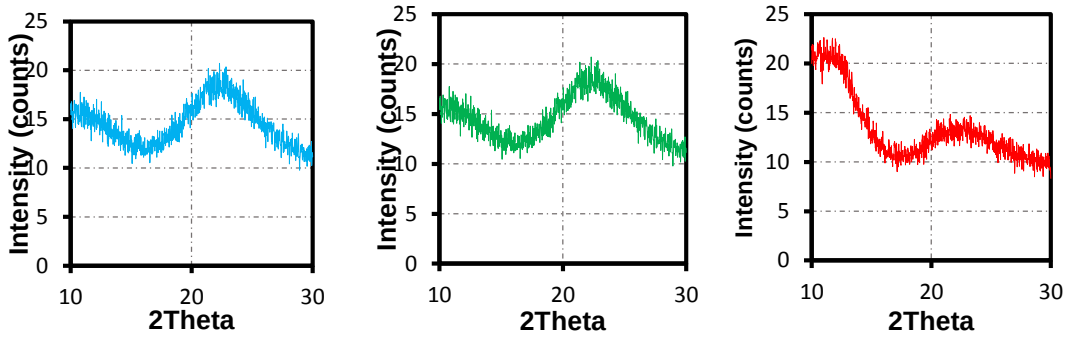

(a) (b) (c)

Figure 3-3 XRD analysis for (a) NS-50, (b) NS-250 and (c) NS-500.

Added water: The tap water was used as the mixing water. It is drinkable, clear and apparently clean, and does not contain any substances at excessive amounts that can be harmful for making concrete.

3.3 Design of Experiments

In this section, the mix design, mixing procedure, casting and curing for trial and main experimental phase are described in addition to the specified fresh and hardened properties tests.

3.3.1 Trial mix phase

The trial experimental phase was designed to determine the optimum dosage and size of nano-silica for normal concretes. To achieve this, various nano silica contents 0%, 0.25%, 0.5%. 0.75%, 1%, 1.25%, 1.5%, 2% and 3% for NS-250 and NS-500, continued with 5% and 10 % for NS-50 were examined in this phase. It was very difficult even with SP to mix concrete with NS dosages higher than 3%, due to the high surface area of NS-250 and NS- 500. It is worth mentioning that the amount of SP was amended for different mixes to achieve the same slump. All of mixtures were designed at a constant water – binder ratio of 0.45. Details of concrete mix proportions are given in Table 3-6.

All mixing and curing procedures were kept the same for all mixes except replacing cement by the desired quantity of NS. It is important to mention that the mixing water was adjusted based on the amount of water existing in the solution and the content of silica for each NS type.

Table 3-6 Trial mix proportions of concrete

NS type	NS, %	Cement	CA	FA	Water	SP, %
		Kg/m^3				
NS - 50	0, 0.25, 0.5, 0.75, 1, 1.25, 1.5, 2, 3, 5 and10	500	732	675	225	0,0.125, 0.375 and 0.5
NS - 250	0, 0.25, 0.5, 0.75, 1, 1.25, 1.5, 2 and 3	500			225	0,0.125, 0.375, 0.5, 0.75, 1, 1.25, 1.5 and 2
NS - 500	0, 0.25, 0.5, 0.75, 1, 1.25, 1.5, 2 and 3	500			225	0,0.125, 0.375, 0.5, 0.75, 1, 1.25, 1.5 and 2

The mixing procedure started with mixing NS separately with the mixing water for 2 min to avoid any possibility of agglomeration of nano silica particles, and to assure the particles of nano silica are uniformly dispersed. Then, the amount required of SP was mixed for another 1 min with the solution in order to maintain the workability. Meanwhile, coarse aggregate, cement and fine aggregate were mixed in a rotary mixer for 1 min, then, the solution was immediately added to concrete constituents and mixed for another 2 mins. After casting, all specimens were covered with plastic sheets and left at room temperature for 24 hours before they were de-moulded. Finally, all specimens were cured in water tank until the day of test.

3.3.2 Main experimental phase

Based on the results obtained from the trial experimental tests described in Chapter 4, It is observed that amongst the three NS types used, NS-250 achieved

the highest enhancement rate for 7 days and 28 days. Due to this results, the NS-250 was used to enhance the strength of rubberised concrete. The dosage of nano silica used in this study is 0%, 1.5% and 3%.

According to the previous studies (Khaloo et al., 2008a, Reda Taha et al., 2008, Liu et al., 2016, Gupta et al., 2016), it was recognised that the increasing of the rubber content leads to the reduction in compressive strength. To keep the strength of the rubberised concrete within the acceptable range of structural applications, a compressive strength of 40 MPa was designed for the control mix. All the concrete mixes were designed at a constant water/binder ratio of 0.45. The mix proportions presented in Table 3-7 are reported as mass per cubic meter. The variables were rubber content as a replacement of 0%, 10%, 20% and 30% of fine aggregate by volume for two different sizes and colloidal nano silica content as a replacement of 0%, 1.5% and 3% of cement.

Table 3-7 Mix proportions of concrete

Mixture number	Mixture designation	R (%)	NS (%)	Mix proportions (Kg/m^3)						
				C	CA	FA	W	R	NS	SP
M1	NC	0	0	500	731.9	675.6	225	0	0	0
M2	NC-NS1.5	0	1.5	492.5	731.9	675.6	225	0	7.5	0
M3	NC-NS3	0	3	485	731.9	675.6	225	0	15	0
M4	RA10-NS0	10	0	500	731.9	608.04	225	30.81	0	0
M5	RA20-NS0	20	0	500	731.9	540.48	225	61.62	0	0
M6	RA30-NS0	30	0	500	731.9	472.92	225	92.42	0	0
M7	RA10-NS1.5	10	1.5	492.5	731.9	608.04	225	30.81	7.5	0
M8	RA20-NS1.5	20	1.5	492.5	731.9	540.48	225	61.62	7.5	2.5
M9	RA30-NS1.5	30	1.5	492.5	731.9	472.92	225	92.42	7.5	3.75
M10	RA10-NS3	10	3	485	731.9	608.04	225	30.81	15	2.5
M11	RA20-NS3	20	3	485	731.9	540.48	225	61.62	15	3.75
M12	RA30-NS3	30	3	485	731.9	472.92	225	92.42	15	2.5
M13	RB10-NS0	10	0	500	731.9	608.04	225	32.9	0	3.75
M14	RB20-NS0	20	0	500	731.9	540.48	225	65.8	0	2.5
M15	RB30-NS0	30	0	500	731.9	472.92	225	98.71	0	3.75
M16	RB10-NS1.5	10	1.5	492.5	731.9	608.04	225	32.9	7.5	2.5
M17	RB20-NS1.5	20	1.5	492.5	731.9	540.48	225	65.8	7.5	3.75
M18	RB30-NS1.5	30	1.5	492.5	731.9	472.92	225	98.71	7.5	2.5
M19	RB10-NS3	10	3	485	731.9	608.04	225	32.9	15	3.75
M20	RB20-NS3	20	3	485	731.9	540.48	225	65.8	15	2.5
M21	RB30-NS3	30	3	485	731.9	472.92	225	98.71	15	3.75

Note: NC: normal concrete, R: rubber, NS: nano silica, C: cement, CA: coarse aggregate, FA: fine aggregate W: water, SP: superplastisiser.

3.3.3 Mixing procedure

A drum mixer of 0.08 m^3 capacity was used to mix all the assessed mixes, the interior surface of the mixer was cleaned and wetted prior to placing the raw materials. Most of previous studies have used the same sequence of concrete mixing in rubberized concrete which is mixing the dry constituents: sand, gravel, cement, and rubber particles were blended first for about 2 min. Thereafter, the mixing water was gradually added along with continuous mixing for about 3 min to obtain a homogenous consistency. However, in this study, after many trials of different sequence of mixing order of the constituent the following sequence shown in Figure 3-4 was selected in order to improve the quality of rubberised concrete.

The addition of cement to water is called slurry, by adding sand to the rubber covered with slurry leads to roughness surface of rubber and that enhances the bond between the rubber and cement paste.

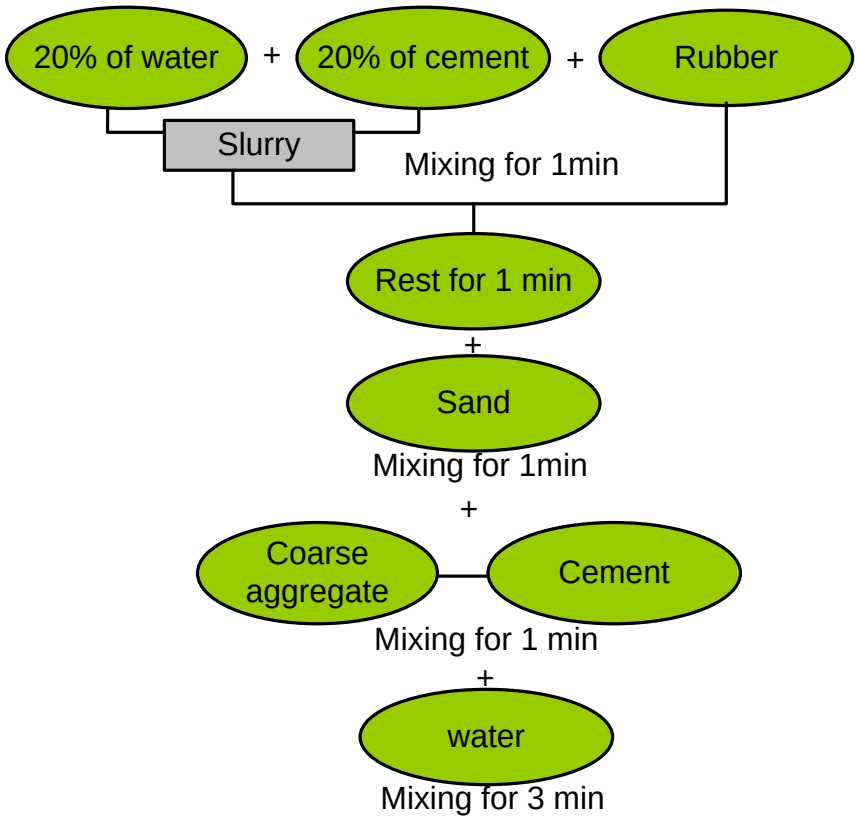

Figure 3-4 Sequence of constituent mixing flowchart

3.3.4 Preparation of test specimens

For all tested samples, the moulds were pre-coated with a thin layer of mineral oil release agent before filling with concrete according to (ASTM/C192/C192M, 2015). The specimens were cast in two almost-equal layers; each one compacted using a vibrating table for around 30 s. Afterwards, the top layer was levelled and the mould covered with a plastic sheet to prevent moisture loss and kept in the laboratory for 24 ± 2 h until demoulding. Then the samples were marked and immersed in curing water tanks until the test age which was 28 days. Figure 3-5 shows preparing, casting and curing of specimens.

Figure 3-5 Preparing, casting and curing procedure.

3.4 Experimental tests

3.4.1 Fresh properties tests

3.4.1.1 Slump test

The standard slump test according to (ASTM/C143/C143M, 2015) was conducted to measure the workability of concrete in fresh state for all mixes (Figure 3-6). The Abrams cone is filled with three fresh concrete layers. Each layer is tamped 25 times using a steel rod of 16 mm Ø. The drop of the fresh concrete after the vertical removal of Abram's cone represents the slump of the mix.

Figure 3-6 Slump test for normal concrete mix

3.4.1.2 Mechanical properties tests

3.4.1.3 Dry Density

The hardened concrete density was determined in accordance to BS 1881-114:1983. Three samples per mixture were assessed. The density was calculated by dividing the weight of the samples after 28 days by their volumes.

3.4.1.4 Water absorption

After 28 days of curing, three cubes of each mix were taken out from water tank for water absorption test according to BS 1881-122. Samples were placed in a dry oven at 100±5 °C for 24 h. After removing each sample from the oven, it was allowed to cool in dry air to a temperature of 20 to 25°C and the average weight of the oven dry samples was recorded (A). Immediately after drying and cooling, the samples were completely immersed in water for 24 h at 21°C. By removing water from the surface with a moist cloth, the samples then were become in saturated surface dry state (SSD). Then the weight of the three samples for each mix was taken (B). The water absorption was calculated as the ratio of water

mass absorbed to that of the dry mass of the specimen. Water absorption was calculated by the formula given below;

$$\text{Water absorption (\%)} = \frac{B-A}{A} * 100 \quad (3.1)$$

3.4.1.5 Porosity

Porosity (P) can be identified as the ratio of the volume of pores to the total volume of the sample. A vacuum-saturation method is one of the simple methods that used to evaluate the porosity of concrete mixtures. In this study, three disc samples with a dimension of 100 mm diameter and 50 mm height were used for each mix. The specimens were dried at 100 ±5°C until constant weight was achieved then their weight was recorded. Then, the dried samples were submerged underwater in a vacuum vessel below a perforated plate see Figure 3-7.

Figure 3-7 The vacuum saturated machine used for porous measurements

A sample is normally put on the top of the plate to ensure that it is totally immersed underwater. The tube connection between the vacuum vessel and the pump should be greased with Vaseline to deter any possible air leakage. The air-pump machine is switched on for 1 to 2 hours to generate vacuum in the vessel. Typically the sample becomes fully saturated with water when no more bubble are released from its surface. At this point the pump can be switched off and the vacuum can be released into the atmosphere. The sample is then taken off carefully from the vessel to be weighed. The difference between the dry and wet weights relates directly to the amount of water occupying the material pore space so that the porosity was computed using expression (3.2) given below.

$$P = \frac{V_w}{V_d} = \frac{\left(\frac{M_s - M_d}{\rho_w}\right)}{\left(\frac{M_d}{\rho_d}\right)} \tag{3.2}$$

Where, P is the porosity, V_W is the volume of water inside sample, V_d is the volume of dry sample, M_s is the mass of saturated sample, M_d is the mass of dried sample, ρ_w is the density of water and ρ_d is the density of dried sample.

3.4.1.6 Compressive strength

For all concrete mixes, nine 100 mm cubes were prepared, water-cured at 20 ± 2°C, and tested at an age of 7, 28 and 90 days, and the average of three samples was taken as the final result of the compressive strength. A 3000-kN maximum loads capacity testing machine (see Figure 3-8), was used to test the samples at

a loading rate of 0.2 MPa/s, and the test procedure was carried out in accordance with ASTM C39/C39M-17b.

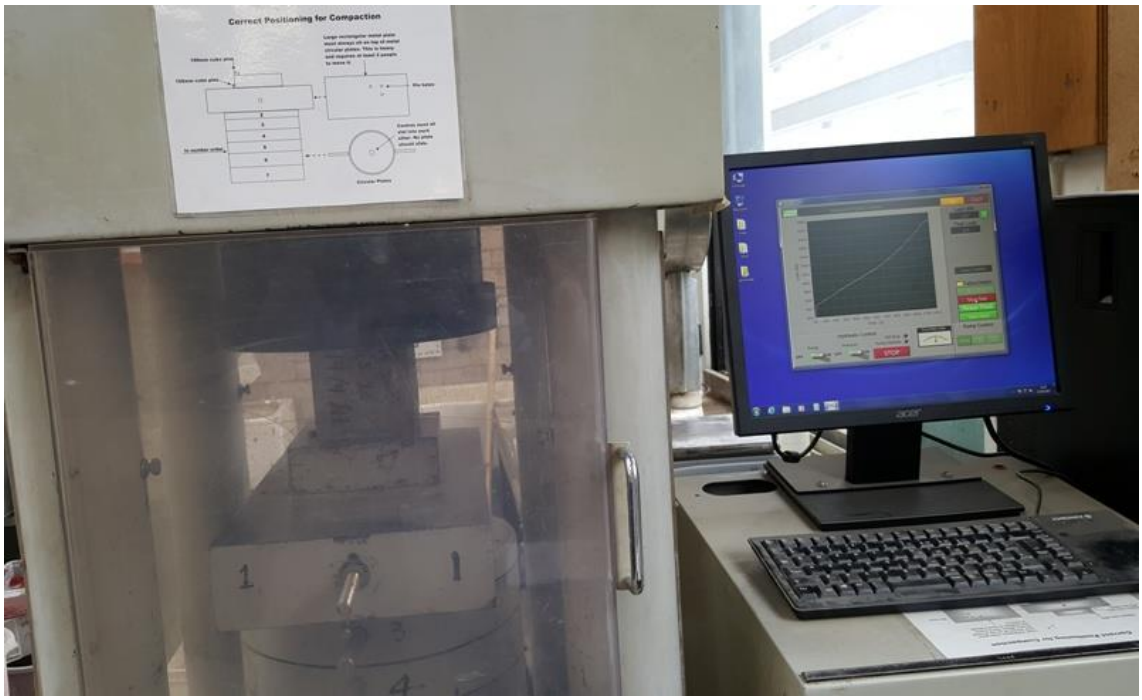

Figure 3-8 Compressive test machine

3.4.1.7 Splitting tensile strength

The splitting tensile strength of 150 mm x 300 cylinders was determined in accordance with BS 1881-117 (Figure 3-9). Prior to conducting the splitting tensile test, all samples were moist-cured by immersion in water tank until the day of testing, and the same machine that was used to test the compressive strength was used at a loading rate of 0.2 MPa/s Figure 3-9, the concrete cylinder specimen was placed horizontally in a frame and load applied. When the sample failed, the loading value was recorded and the average value was recorded. The splitting tensile strength (f_t) was calculated using the following equation:

$$f_t = \frac{2P}{\pi DL} \quad (3.3)$$

where, P is the maximum split load (N), L is the length of specimen (300 mm), D is the cross sectional diameter of the specimen (150 mm).

Figure 3-9 Splitting tensile strength test

3.4.1.8 Flexural strength

Flexural strength testing was carried out to determine the Modulus of Rupture, R_t, flexural toughness indices, flexural stiffness K using a 500 × 100 × 100 mm prism sample. R_t was calculated using equation (3.5). A 2000-kN maximum loads capacity testing machine. Four-point flexure over a span of 300 mm was used in accordance with ASTM C 1018 as shown in Figure 3-10.

Two prisms for each mix were prepared, water-cured at 20 ± 2°C and tested at the age of 28 days, and the average value was recorded.

$$R_t = \frac{PL}{bd^2} \quad (3.4)$$

Where, R_t the flexural strength in MPa, P is an ultimate load in N, L is the prism span in mm, b and d are the width and height of the prism in mm.

Figure 3-10 Flexural strength test

3.4.1.9 Drying shrinkage test

Drying shrinkage can be defined as a reduction of concrete volume due to an overall loss of water from cement paste to the environment through evaporation. Drying shrinkage was experimentally investigated over 90 days based on ASTM C157/08 (ASTM/C157, 2008), using prisms with dimensions of 100 x 100 x 300 mm (Figure 3-11). All specimens were cast in three layers and covered with a plastic sheet to prevent moisture loss and then demoulded after 24 ± 2 hrs. Demec points were fixed on the top surface of the specimens by using super glue.

Prisms were placed in a room at a temperature of 20°C $\pm$2°C and a relative humidity of 50% $\pm$ 10%. The change in length was measured on a regular time intervals using a digital dial gauge. The average reading of two specimens (6 sides) was recorded to the nearest 0.01μstrain.

After an initial reading, the length measurements were taken at 7, 14, 21, 28, 56 and 90 days. In order to reduce the error in drying shrinkage readings at each age, drying shrinkage of the specimen was calculated for the same side and direction (Figure 3-12). The drying shrinkage strains were calculated using the formula below;

$$\varepsilon_{sh} = \frac{\mathrm{CRD} - \mathrm{initial\ CRD}}{\mathrm{G}} \tag{3.5}$$

where ε_{sh} is the drying shrinkage strain of the specimen (mm/mm), CRD is the difference between the comparator reading of the specimen (mm) and the reference bar at any age, $\mathrm{initial\ CRD}$ is the difference between the comparator reading of the specimen and the reference bar at first reading and G is the gauge length which is equal to 220 mm.

Figure 3-11 Free drying shrinkage specimens.

Figure 3-12 Free drying shrinkage strain measurement

3.4.1.10 Impact resistance under drop weight test

The test was performed on cylindrical specimen (discs), 100 mm in diameter and 50 mm in height, three specimens for each mix to estimate the energy absorption of concrete specimens. A repeated loading was applied through a 45.4 N hammer falling from 450 mm height onto a 50.6 mm steel ball. The steel ball was placed on the top of the centre of a cylindrical concrete specimen as shown in Figure 3-13. The number of blows needed to cause the initial crack (N_1) and to produce ultimate failure (N_2) was recorded to indicate the initial crack and the ultimate crack resistance. Generally, the impact energy (IE) was calculated by the equation given below:

$$\mathrm{IE} = \mathrm{Nmgh} \qquad (3.6)$$

where N is the number of blows at crack level, m is the mass of drop hammer (4.54kg), g is gravity acceleration (9.81 m/s^2) and h is the drop height (450 mm).

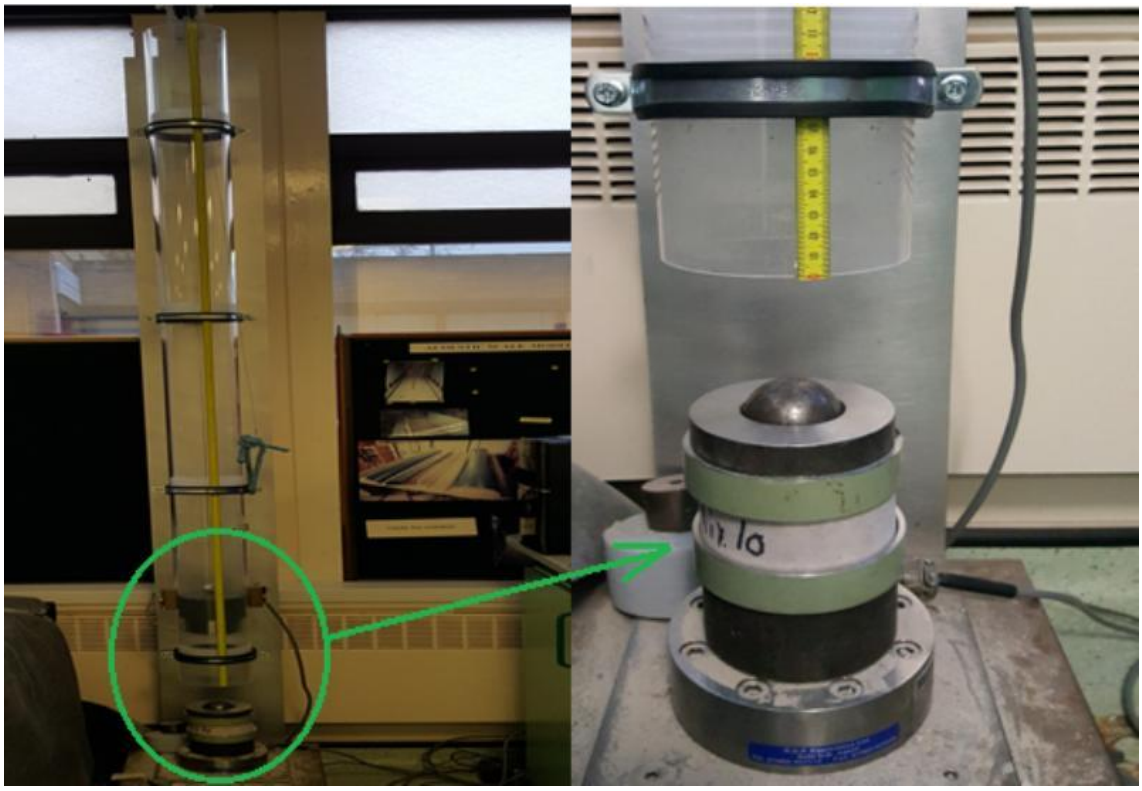

Figure 3-13 Drop weight test

3.4.2 Thermal and Acoustic Properties tests

3.4.2.1 Thermal conductivity

Thermal conductivity (λ) represents the ability of a material to transfer heat. In this investigation, the determination of the thermal conductivity for the concrete samples with variable level of rubber and nano silica was conducted according to BS 1902-5.8(1992). The thermal conductivity principle and measurement is described in the following subsections:

3.4.2.1.1 Principle and set-up

The principle and the procedure for determining the thermal conductivity is based on the split column which is recommended for testing shaped refractory materials with thermal conductivities in the range 3 to 80 W/m.K and for mean temperature in the range 300 to 850^{o}C. BS 1902-5.8(1992) was modified to measure thermal

conductivities above that of vermiculite (30 mW/mK) at temperatures in the range of 75 to 150^{o}C. So, the steel blocks suggested in the standard were replaced with two aluminium cylinders to boost the thermal conductivity and the resultant heat flux to and from the sample. Since the thickness of the concrete samples used in this test (50 mm), it was impractical to insert a thermocouple pair in the sample. Instead, the difference in temperature was determined using a pair of thermocouples installed at the bottom and upper blocks in the general vicinity of the sample surface. The distance from the centres of these thermocouples to the surface of the sample was 10 mm. This method provides a relatively good estimate of the thermal conductivity of the prepared samples.

According to the split column method, the thermal conductivity of the tested sample is calculated in two steps.

First of all, the heat flux, q (Watts), through the aluminium cylinders is calculated from:

$$\mathrm{q} = \frac{\lambda_{\mathrm{alu}}(\Delta \mathrm{T_m})\mathrm{A}}{\mathrm{d}} \qquad (3.7)$$

where, λ_{alu} is the thermal conductivity of aluminium (172Watts/(mK)), $\Delta T_m$is the mean temperature difference between thermocouples (K), A is the cross sectional area of the aluminium cylindrical column (m^2), d is the distance between the thermocouple junctions (m).

Second, the thermal conductivity of the sample was then found from

$$\lambda = \frac{\mathrm{qt}}{\mathrm{A}\Delta \mathrm{T}} \qquad (3.8)$$

where, λ is the thermal conductivity of the test sample at the mean temperature (Watts/(m.K), t is the thickness of test sample (in m), A is the cross sectional area of the test sample (in m^2) and ΔT is temperature difference between thermal sensors 3 and 4 (in K).

Figure 3-14 shows the experimental setup used in this investigation. The equipment consists of an aluminium cylindrical column split into three parts. The bottom aluminium cylindrical column is 100mm in diameter and 150mm in length. Four 125mm long heaters are permanently installed in the aluminium column in the direction perpendicular to the top surface.

The diameter of the heating element is about 12.5 mm and the power rating of each heating element is 500 W. These heaters are electronically controlled and supplied with 230Volt AC.

The middle part of aluminium cylinder is attached to the bottom part to transfer the heat. This aluminium cylinder is 150mm long and it has the diameter of 100mm. The top aluminium cylinder has the same dimension as the middle part. Three thermal sensors are installed inside each of the two cylinders between which a 50mm thick material sample is placed to control the temperature of the heater through the electronic control unit (see Figure 3-14).

3.4.2.1.2 Measurement procedure and calibration

Before the measurement started, the heater which is positioned at the bottom of the apparatus was required to preheat to the required maximum temperature. The top aluminium cylinder is placed directly on the top surface of the middle cylinder and left in this position until the temperature of thermal sensor no. 4 in

the top cylinder is the range between 40 to 45^{o}C. At this point the concrete sample can be inserted between the middle and top cylindrical columns which means between thermal sensors 3 and 4 as shown in Figure 3-14**.** At the same time, the cooling water supply is turned on so that the temperature of the upper part of the top cylinder is controlled within 10-18^{o}C. Finally, vermiculite is placed around the cylindrical column to reduce the heat loss and to obtain accurate results for measuring thermal conductivity.

Calibration and accuracy of thermal conductivity apparatus can be found by measuring some commercial products (wool, wooden and PVC samples) with known value of thermal conductivity.

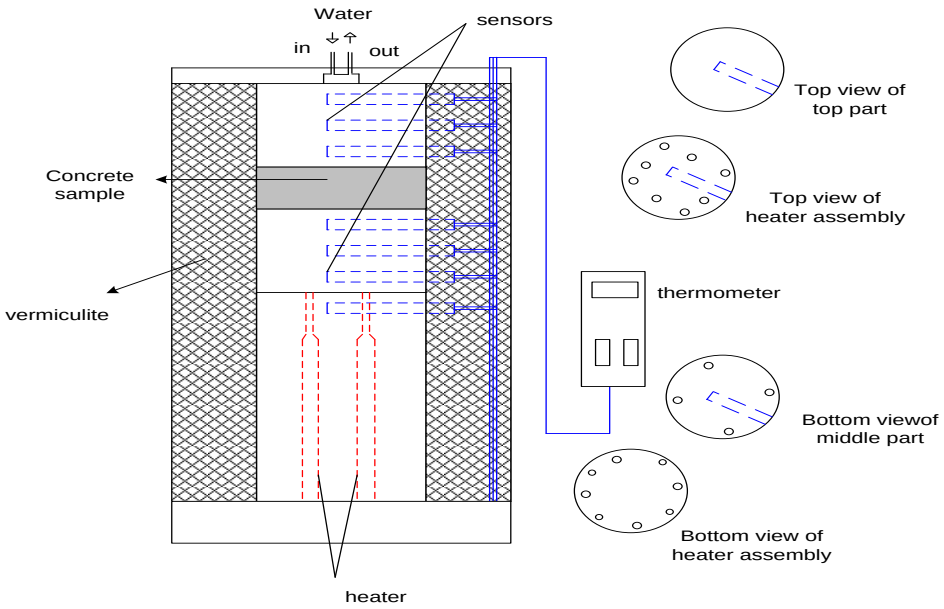

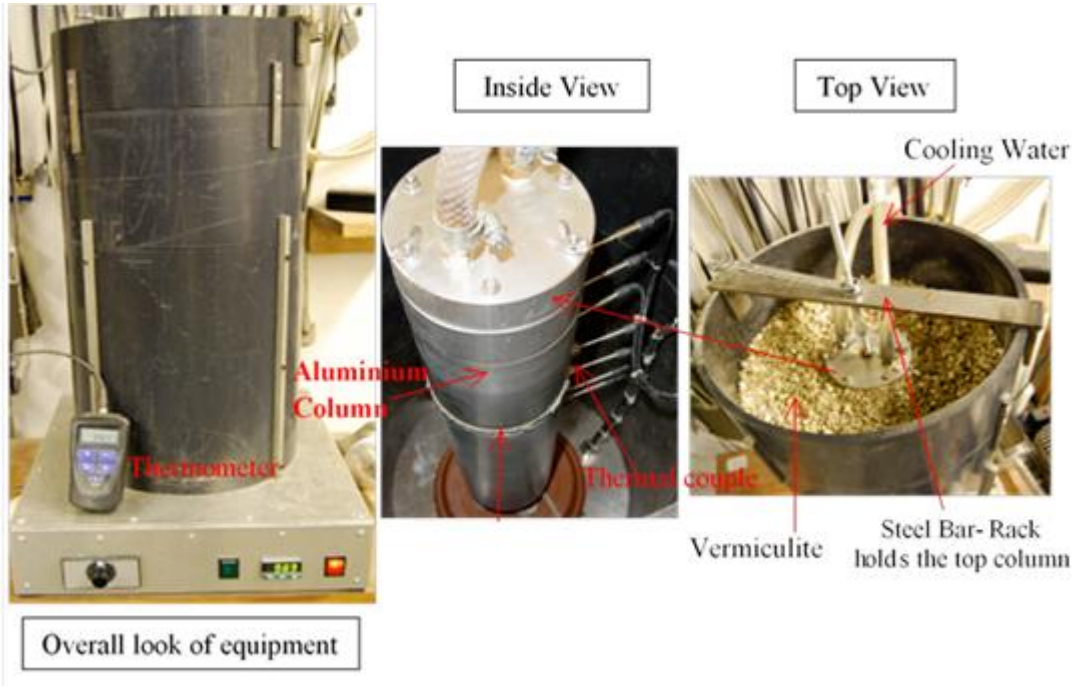

Figure 3-14 Illustration of thermal conductivity apparatus

3.4.2.2 Acoustic properties

Frequency-domain analysis is a tool of utmost importance in signal processing applications. While time-domain analysis shows how a signal changes over time, frequency-domain analysis shows how the signal's energy is distributed over a range of frequencies. A frequency-domain representation also includes information on the phase shift that must be applied to each frequency component in order to recover the original time signal with a combination of all the individual frequency components. A signal can be converted between the time and frequency domains with a pair of mathematical operators called a transform. An example is the Fast Fourier transform (FFT), which decomposes a function into the sum of a (potentially infinite) number of sine wave frequency components. The 'spectrum' of frequency components is the frequency domain representation of the signal. The inverse FFT converts the frequency domain function back to a time function.

FFT has traditionally been used to obtain the frequency content (or Fourier spectrum) of a signal. The spectrum gives the distribution of energy of the signal among its constituent frequency components. However, Fourier coefficients are the averaged spectral amplitudes over the entire duration of the signal. Therefore, FFT is an ideal tool for spectral analysis of periodic and stationary signals for which the distribution of energy is uniform throughout the signal. Time-frequency analysis will be used here as a complementary tool for studying complex impact signals. Using this technique, the impacts from the various concrete formulations that are separable from the target impacts in time and/or frequency domains can be determined.

In terms of acoustic properties, sound absorption, transmission loss and impact sound insulation are the initial properties, measured as described below.

3.4.2.2.1 Sound absorption and Transmission loss

The impedance tube is a method to measure acoustical properties such as sound absorption coefficient and transmission loss. It also determines non acoustical parameters such as porosity, tortuosity, flow resistivity, viscous and thermal characteristic lengths (Niresh et al., 2015). The measurement was carried out using Standard Bruel and Kjear type 4206 impedance tube of 100 mm. The impedance tube speaker is driven by the Bruel and Kjear power amplifier of type 2706 as shown in the Figure 3-15.

To carry out the impedance tube method, two conditions were applied at the end of the impedance tube which involves an open ended tube condition and a hard closed ended tube condition. For open ended tube condition, the cap was removed and the broadband signal was applied to measure the absorption coefficient of the concrete samples. A single microphone method was employed

to measure the broadband signal at each microphone port. This eliminated the need for calibration of the microphone at each location on the tube. Four microphone ports were utilised during this experiment and the same microphone probe was used to measure the signal at each location sequentially. Two pairs of microphone ports were located at both sides of the sample; P1 and P2 at one side and P3 and P4 at the other side. Signals recorded at these channels were then analysed to determine the absorption coefficient of the sample tested.

Figure 3-15 Photograph of sound impedance tube

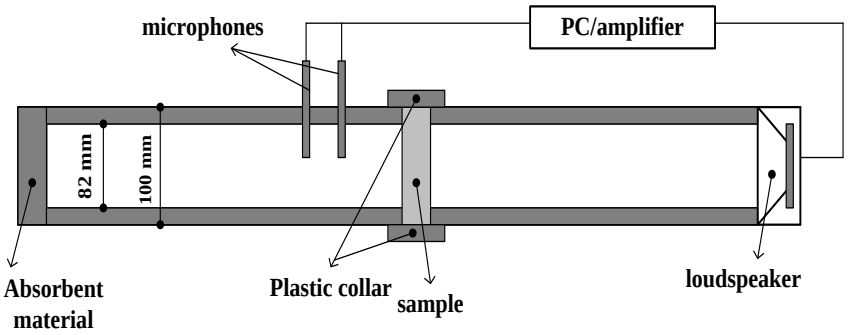

Figure 3-16 Schematic diagram of the sound impedance tube

For each condition, i.e. open and closed ended, the signal at each microphone port was recorded to determine its absorption coefficient for every sample. Since there were four channels, there were eight readings in total. Four readings for the open ended condition and four readings for closed ended condition for each

sample were attained from this experiment and saved as wmb. File. The absorption coefficient was processed and presented in the results section for each concrete sample.

3.4.2.2.2 Impact Sound Insulation Equipment Set-up

The design of the equipment for the impact sound insulation experiment is based on the requirement in the ISO 140 Part 8 and Building Regulation Approved Document E. A test rig was constructed for testing small material specimens to simulate the standard ISO140-8 tests but in a smaller scale and using only one impact hammer dropped two times manually at four positions distributed uniformly across the specimen. This experimental setup allowed the specimen to be quickly installed and replaced so that indicative data on the impact sound insulation of a large number of small samples could be measured in short time. In this experiment the presumption was made that the sound pressure level which would result from the cylinder impact would be directly proportional to the corresponding level of the floor acceleration so that the need for an expensive reverberation chamber and large area of material surface was avoided. The concrete samples were clamped as shown in Figure 3-17. The impact sound was measured in the form of the vibration acceleration which was caused by dropping a mass onto the concrete sample.

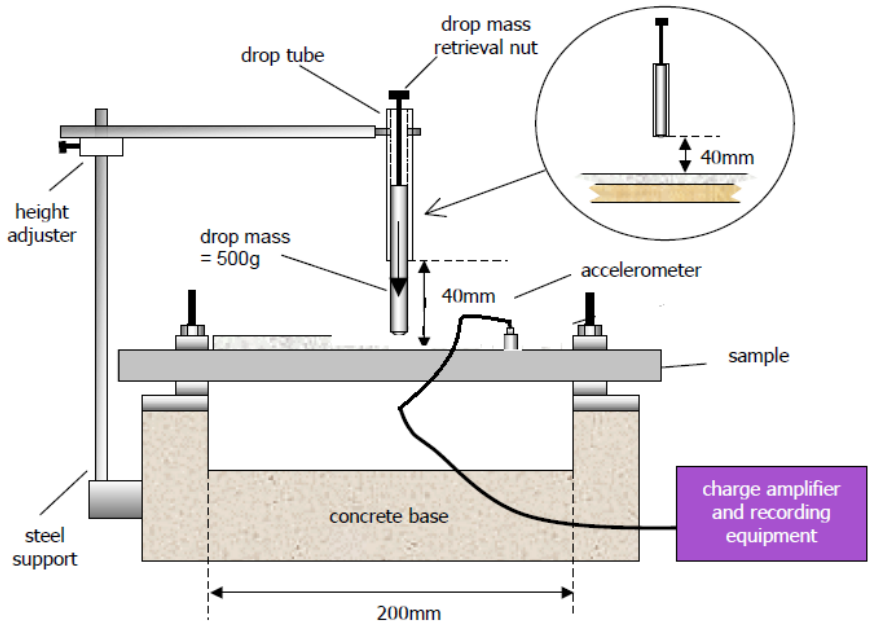

Figure 3-17 Schematic diagram of impact transmission rig

An accelerometer was attached to the highest flat surface of concrete sample (Figure 3-18)**.** The signal from the accelerometer was conditioned using a BK 2635 charge amplifier and recorded on a PC. The drop mass was a 500 g brass cylinder which was released from a 40 mm height to fall onto the surface of the material specimen.

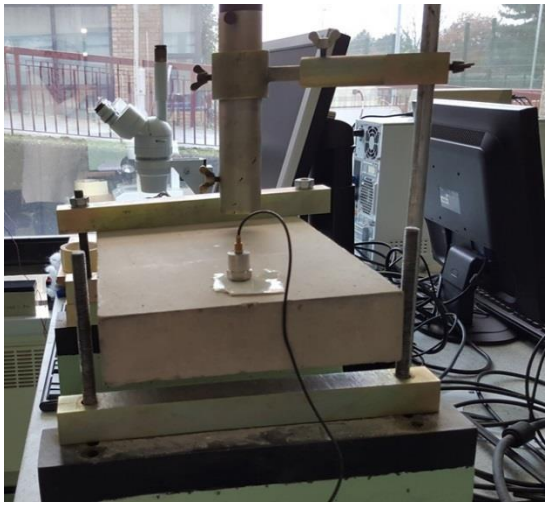

Figure 3-18 an accelerometer attached on the upper surface of concrete

The accelerometer had to be calibrated prior to the experiment using a standard calibrator. The mass of the accelerometer. Type (4368) was 36.7 g. The accelerometer was connected to the calibrator (Bruel & Kjaer Type 4291), and then the acceleration level of 1g was set taking into account the fixed mass of the calibrate accelerometer. The sensitivity of the charge amplifier was set to 31.6 mV/unit during the calibration for the 35 g accelerometer.

3.4.2.3 Dynamic stiffness

3.4.2.3.1 Experiment BS29052

The purpose of this experiment was to determine the dynamic stiffness per unit area of the insulation material used under floating floors using the standard measurement method detailed in (ISO 9052-1, 1989). According to this method a material sample is loaded with > 0.4kPa in the case of wall insulation materials, or < 4kPa in the case of machinery foundation materials.

3.4.2.3.2 Experimental setup

The basic experimental setup is presented in Figure 3-19**.** The equipment requires a loading plate and a base plate. The shaker and top accelerometer are fixed to the loading plate. The base plate must be rigid and has a smooth, flat surface without any bending. The total mass which included the shaker and accelerometer must be $8kg \pm 0.5kg$. The top accelerometer is screwed to a small disk attached to the shaker armature. The other accelerometer was attached with a magnet to the loading plate as shown in Figure 3-19. The total weight of the plate, shaker, accelerometers, disk and the magnet used in this experiment was 7.9kg. The accelerometers were connected to the charge amplifiers and were

calibrated before the measurement. The frequency dependent transfer function for the two measured accelerations was determined from

$$T(\omega) = \frac{S_b(\omega)}{S_t(\omega)} \tag{3.9}$$

where is $S_b(\omega)$ the acceleration spectrum for the signal is detected using the accelerometer attached to the loading plate and $S_t(\omega)$ is the reference acceleration spectrum detected using the accelerometer attached to the top of the armature disk.

The dynamic stiffness per unit area, s' is the ratio of dynamic force to dynamic displacement and is given by the following equation:

$$s' = \frac{F/S}{\Delta d} \tag{3.10}$$

where S is the area of the test specimen (mm^2), F is the dynamic force acting perpendicularly on the test specimen (N), Δd is the resulting dynamic change in thickness of the resilient material.

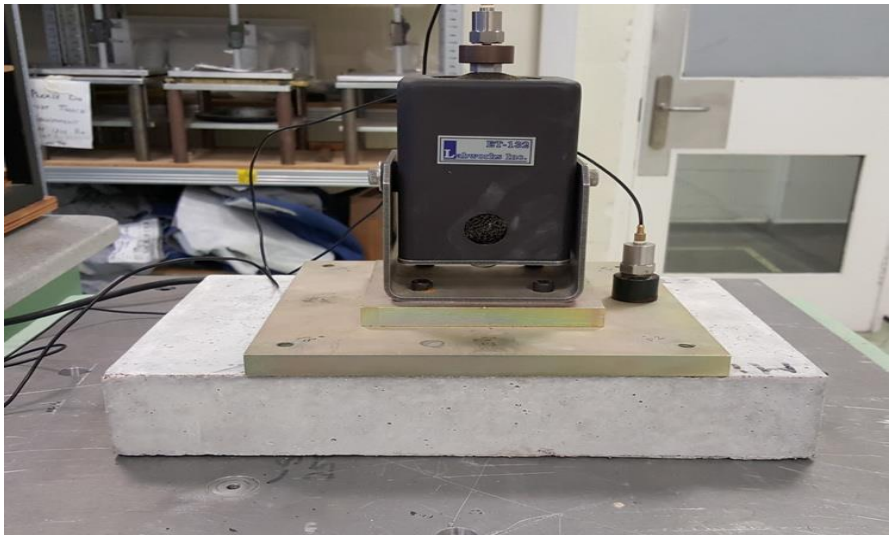

Figure 3-19 Experimental setup for BS29052 measurement

3.4.2.4 Damping performance

A common method of determining the damping at a resonance in a frequency domain is use the “3 dB method” also known as “half power method”. Fast Fourier transform (FFT) was used to convert the time domain signal presented in Figure 3-20 to the frequency domain.

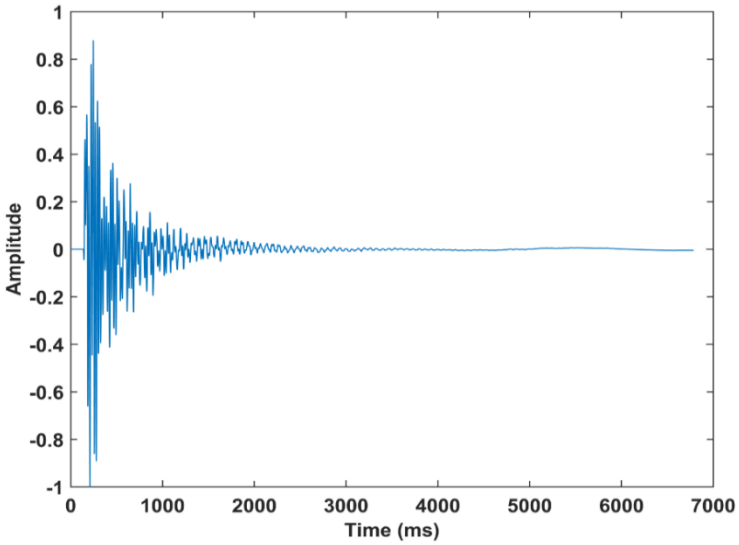

Figure 3-20 An accelerometer output of the recorded impact with WinMLS software.

The FFT spectrum shown in Figure 3-21 can be used to determine the natural frequencies, relative excitation amplitude, and damping of the specimen. The Fourier transform of a signal $u(t)$ is defined as

$$\bar{u}(\omega) = \int_0^T u(t)e^{-i\omega t}\,dt \tag{3.11}$$

where ω is the angular frequency and T is the duration of the recorded signal. Practically, it is implemented as

$$\bar{u}(\omega_k) = \sum_{m=0}^{M} u(t_m)\, e^{-i\omega_k t_m} \Delta t \qquad (3.12)$$

where ω_k=2πf_s; $\Delta t = \frac{1}{f_s}$; f_s= 4000Hz is the sampling frequency and $t_m = m\Delta_t$.

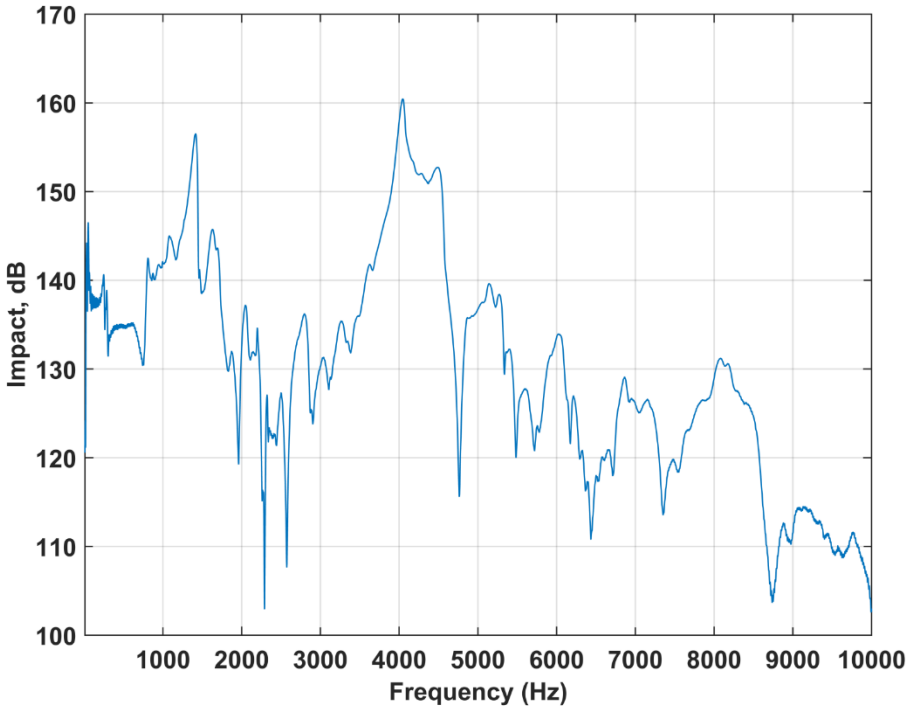

Figure 3-21 Frequency response of the recorded impact.

In the frequency response spectrum, the damping is proportional to the width of the resonant peak about the peak's centre frequency, by using the frequencies at the 3 dB down from the peak level, can determine the associated damping as shown in Figure 3-22.

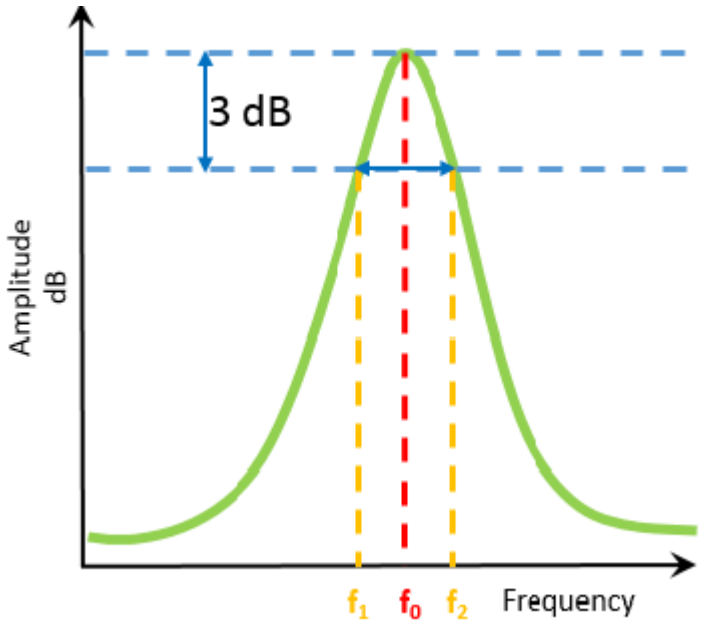

Figure 3-22 Amplitude of Vibration with Frequency

The damping factor also known as quality factor or "Q" is found by the equation:

$$Q = \frac{f_0}{f_2 - f_1} \tag{3.13}$$

where f_o is a frequency of resonant peak in Hertz; f_2 is a frequency value, in Hertz, 3 dB down from peak value, higher than f_0 and f_1 frequency value, in Hertz, 3 dB down from peak value, lower than f_0.

The width of the spectrum that is measured at $max\{(\omega)\}/\sqrt{2}$ gives the bandwidth of the resonance system. This quantity can be used to estimate the quality factor, i.e. the ratio of the energy stored in the resonator to the energy lost per cycle of oscillation, $Q = \frac{\omega_n}{\Delta\omega}$. A system with a high quality factor, e.g. $Q > 1$, is

underdamped. The damping ratio ζ or loss factor (LF) of an underdamped system can be calculated from the following expression:

$$\zeta = \frac{1}{2Q} \tag{3.14}$$

3.5 Concluding remarks

A series of laboratory tests were conducted on normal concrete mixes and rubberised concrete mixes in order to achieve the objectives of experimental part of the research. The procedures, specimen preparation, mixing, casting and testing set up were discussed in detail. Fresh, Mechanical, thermal and acoustic properties testing methods were discussed. Test results obtained from the experimental work will be discussed in details and presented in chapter four and chapter five of this research.

CHAPTER FOUR- WORKABILITY AND MECHANICAL PROPERTIES - RESULTS AND DISCUSSION

4.1 Introduction

Chapter four analyses the results from trial experimental testing and main experimental testing. The trial experimental tests focus on the influence of NS on workability and compressive strength of concrete. The main experimental stage comprised testing of slump, density, water absorption, compressive strength, flexural strength, splitting tensile strength. In addition, drying shrinkage strain and impact resistance under drop weight test are also discussed.

4.2 Trial experimental test results

The results from the trial experimental testing stage were used to determine the optimum size of nano silica particles and optimum replacement content of nano silica that worked best to enhance the compressive strength. The established optimum nano silica size and content were then used in main experimental stage to test its influence on mechanical, thermal, acoustic performance of rubberised concrete mixes.

4.2.1 Workability

The workability of fresh concrete generally decreased with the increase of the surface area and the content of nano silica in the mixture. Because of this, the reduction in workability was differed related to the change of nano silica surface area. The total water demand is involved a layer of absorbed water molecules around the particles and the amount of water required to fill the voids in the matrix (Bianchi, 2014).

This decrease in workability was compensated by adding the desired amount of superplasticisers (SP), based on the specific surface area and the quantity for each type of NS. Several trail mixes were conducted to adjust SP dosages for different NS amount and different surface area to keep the same level of workability. It should be mentioned that there is no need of SP for most mixes with NS-50 except those containing 3%, 5%, and 10% of NS because of the small surface area of this type. However, the addition of NS with a SSA of 250 and 500 m^2/g dramatically reduced the workability of mixes compared to the control mix, and it was vital to add SP for all percent of NS even for small dosages, especially for the finest particles (NS-500). Because there is a layer of adsorbed water molecules around these particles, this increases the need of water to fill the remaining void fraction. Moreover, it was difficult to mix concrete with more than 3% for NS-250 and NS-500 as it required a dosage of SP higher than the recommended dosage from the manufacturer (1.2%). The highly agglomerated state with the increase of those small particles caused the formation of silanol groups (Si-OH) with firmly-held clusters, may also explain the reason behind this remarkable reduction of workability (Hosseini et al., 2011).

4.2.2 Compressive strength

The variations of compressive strength at 7 and 28 days with different NS contents are presented in Figure. 4-1 (a) and (b). It can be observed that compressive strengths with NS at age of 7 days were higher than that of control concrete as shown in Figure. 4-1 (a). For this case, the addition of small dosages of nano silica (0, 25, 0.50 and 0.75%), NS-50 showed minor improvements in compressive strength compared to control mixture. However, the same dosages of NS-250 significantly enhanced the strength to recording over 16% enhancement at just 0.25%, then, it gradually improved with the increase of NS

content. This can be supported by the fact that with smaller silica particles, the rate of the early cement hydration can also be enhanced due to the increase of the heat release by C_3S-accelerated hydration rate (Land and Stephan, 2012). By varying the replacement ratios of NS to 1%, 1.25% and 1.5%, NS with specific surface area 50 m^2/g showed more improvements to reach the highest strength gain (18.02%) at 3%, then it slightly decreased to record 12.3% and 7.65% at 5% and 10% NS, respectively. This reduction in the performance may be attributed to the excess of NS particles, causing no further chemical reaction, and hence the particles only act as fillers without any more contribution to compressive strength (Givi et al., 2013).

On the other hand, nano silica with SSA 250 g/cm^2 exhibited distinct strength enhancements to attain the maximum strength of 56.22 MPa at 3% NS, representing approximately 37.79% compressive strength enhancement compared with the control mix, reflecting the ability of NS in refining the pores and enhancing hydration products distribution, particularly at interfacial transition zone (ITZ) as observed by Du et al., (2014). The findings recorded with NS-500 showed a considerable improvement even with very small dosages, reaching 16.67, 20.09 and 25 % strength gain for concrete having 0.25%, 0.50% and 0.75% NS, respectively, even higher than that obtained by NS-250. This is likely to be explained by the “filling gap materials” principle where smaller size particles were more effective in filling small voids when cement particles were replaced by a little amount of NS. However, less improvement was noted with the increase of NS-500 content in concrete, which may be justified by the agglomerated state of NS particles, preventing their reaction with cement grains. From Figure. 4-1 (b), it can be seen that the compressive strength at 28 days showed almost the same trend as that achieved at 7 days by exhibiting progressive improvements with the

particles having SSA (250 and 500 m^2/g). Nevertheless, the best performance of 31.8% compressive strength enhancement was found with 3% of NS-250. The improvement was slightly better for the smaller dosage of particles (5nm), then NS- 250 showed the best strength gain. This can be explained by the fact that the very small particles of NS-500 acted as a nucleus for C-S-H gel when cement particles were replaced by small amounts of NS, while the large quantities seemingly affected by agglomeration issues. This phenomenon may have led to the precipitation of C-S-H gel on the surface of agglomerated NS particles, preventing the particles from working individually, and hence a lesser effect is expected compared with that produced with those having smaller SSA (Berra et al., 2012; Kong et al., 2013).

Overall, nano silica with 250 m^2/g achieved the highest strength amongst the three types. The possible reason is the suitable size of its particles, which is very efficient in terms of packing ability, pozzolanic activity, and uniform dispersion, and hence the compressive strength apparently improved for all cases. Thus, it was decided that NS-50 and NS-500 were excluded from this study. Regarding the optimum dosage of nano silica, based on the obtained results, it can be probably said that the optimum ratio of NS in concrete may be ranged between 1 to 3%. Due to this results 0%, 1.5%, and 3% was chosen as a main dosage in this study.

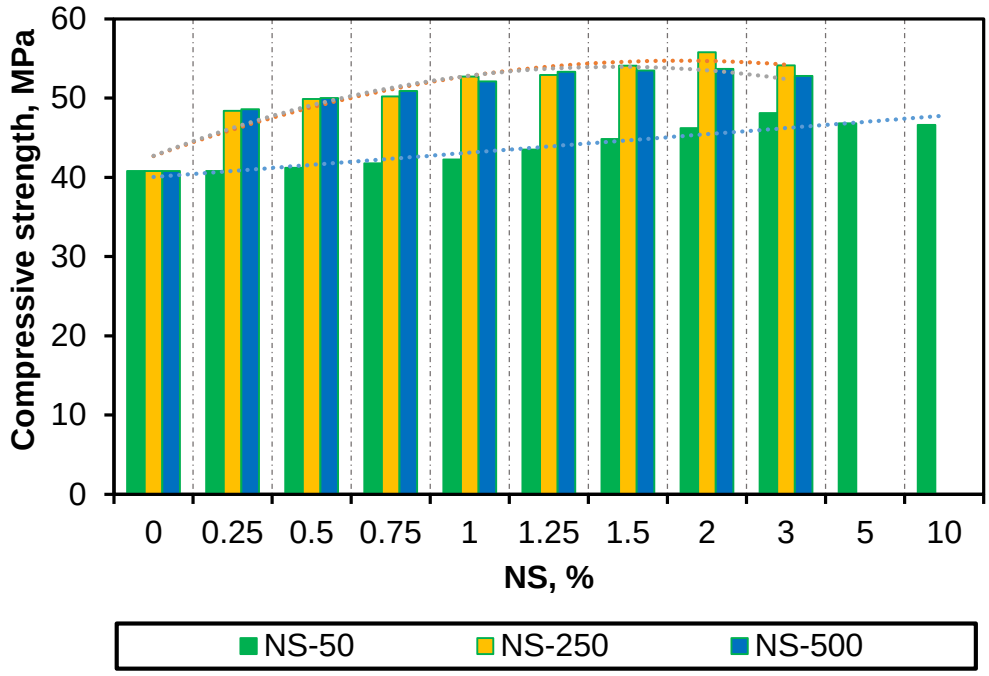

(a)

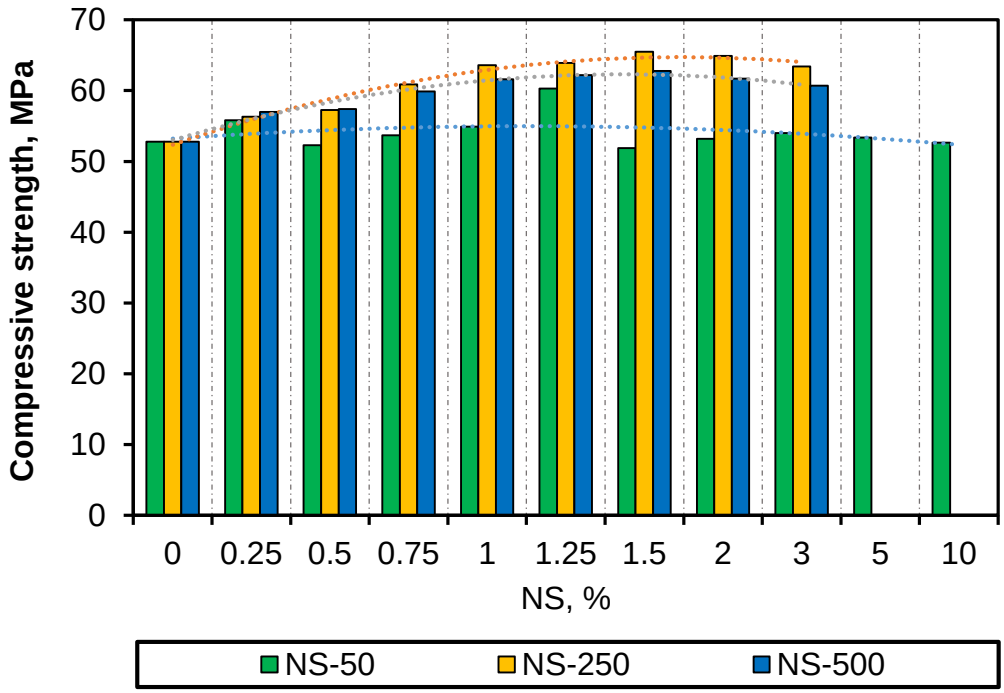

(b)

Figure 4-1 Effect of NS on the compressive strength of concrete (a) at 7 days and (b) at 28days.

4.3 Main experimental test results

4.3.1 Workability

The standard slump test according to ASTM C143/ C143-13 (ASTM/C143/C143M, 2015) was conducted to measure the workability of fresh concrete for all mixes. Figures 4-2 and 4-3 show the effect of increasing rubber content on the workability of concrete with and without nano silica for both sizes of rubber, R_A and R_B. Generally, increasing the percentage of rubber had a negative effect on the workability of the mixes, regardless of the rubber particle size. There is a decrease in the slump by 3.13%, 10% and 13.13% and about 15.63%, 21.3% and 28.13% for 10%, 20%, and 30% R_A and R_B, respectively in comparison to control mix. This reduction may attributed to the higher water absorption of rubber compared to fine aggregate, which decrease the free water, leading to less workable of all rubberised mixture. However, although the reduction in slump was noticed during mixing and casting, the increase of rubber still produced a workable mix compared to the control mix.

Moreover, it was found that the larger rubber particle size causes more reduction in slump values. The slump of mix with 30% R_B was recorded as 115 mm, while the slump of concrete with 30% R_A was 136 mm due to the higher water absorption of R_B compared to R_A. Thus, the saturated surface dry water absorption of R_B is 5.97%, which is higher than R_A (4.56%). This implies that the larger particles of rubber will absorb more water, during the mixing, than the finer particles of rubber to reach the saturated surface dry condition.

The addition of nano silica to rubberised concrete mixes resulted an increase in the water demand. This is principally due to the high specific surface area of the nano particles. Thus, the cement paste workability resulted to be significantly

lower than expected, due to the interactions between nano silica and the cement paste. To maintain a consistent level of workability for the rubberised concrete mixtures with nano silica, several trial batches were performed to adjust the dosages of superplasticizer. In general, rubberised concrete batches with and without nano silica exhibited reasonable workability in regards to simplicity of handling, placement, and finishing.

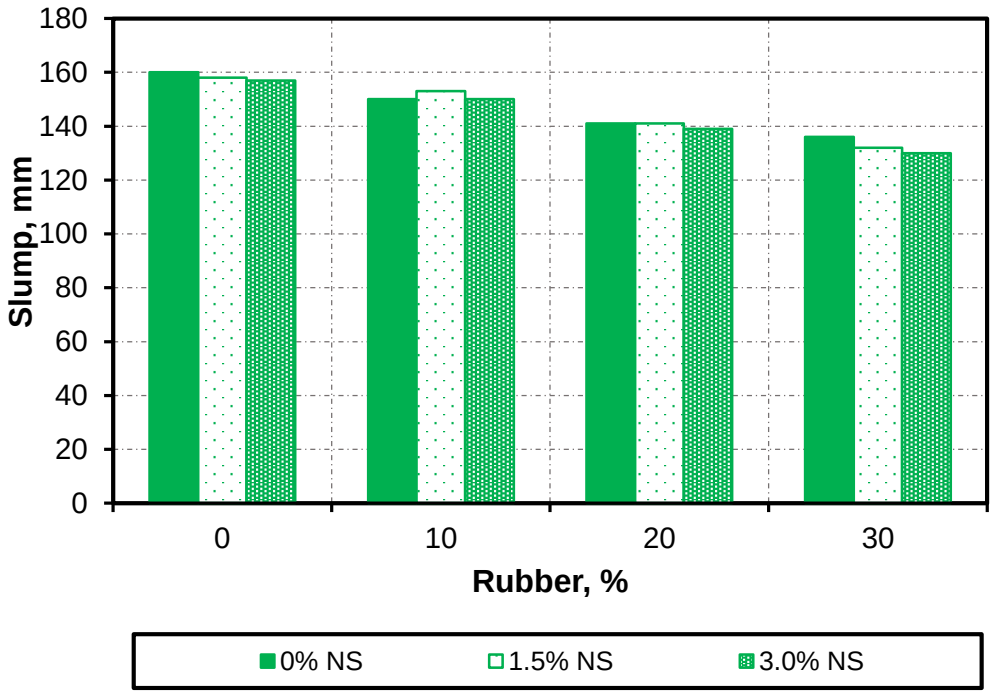

Figure 4-2 Slump of rubberised concrete with and without NS, R_A

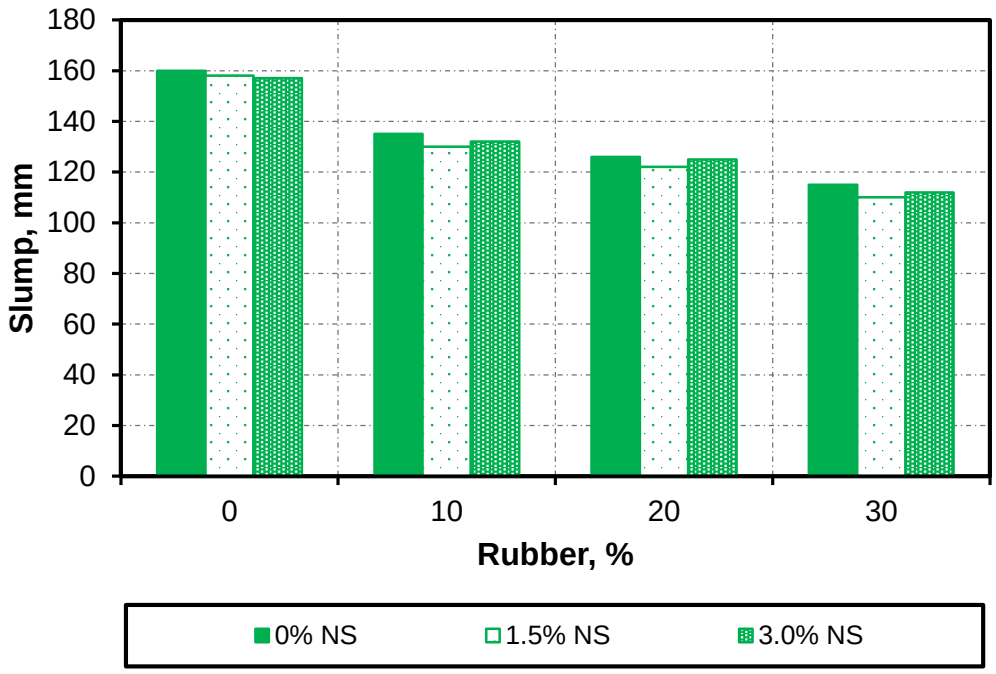

Figure 4-3 Slump of rubberised concrete with and without NS, R_B

4.3.2 Dry Density

The hardened concrete density was determined in accordance with BS 1881-114 (BS1881-114, 1983). The density of concrete mixtures was expected to reduce by the addition of rubber as the density of rubber is less than that of fine aggregate. Figure 4-4 shows that the inclusion of either R_A or R_B resulted in a decrease in concrete density. It can be seen that concrete with R_A exhibited a lower density than that with R_B, and as the rubber level increases in the mix the density decreases, in line with the original density values of the rubber particles, where R_B has a slightly higher density (776 kg/m^3) than R_A (726.5 kg/m^3). The density decreased from 2400 Kg/m^3 for control mix to 2179 kg/m^3 and 2197 kg/m^3 which is about 9.2% and 8.4% with respect to control mix when 30% of the sand was replaced by R_A and R_B, respectively. The density decreased by about 3% when the percentage of rubber inclusion increased from 10 to 20% and 20 to

30%. This trend was observed in all mixtures, similar to that observed in (Sukontasukkul, 2012, Su et al., 2015b).

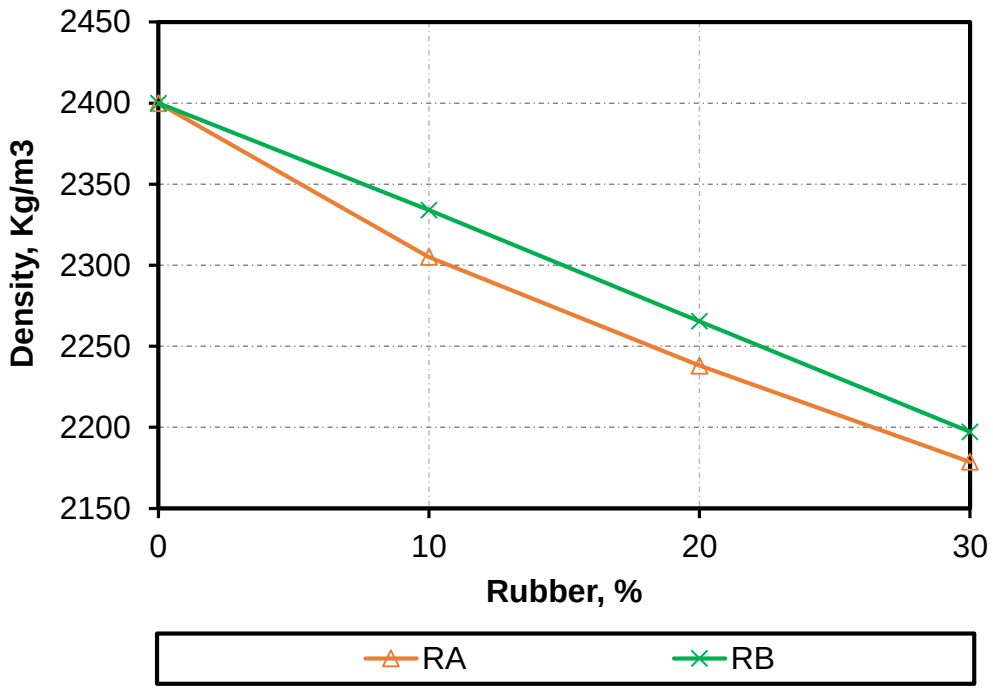

Figure 4-4 Density of rubberised concrete

Figure 4.5 shows that the addition of NS to rubberised concrete mixtures generally increased the density compared to rubberised concrete mixtures without NS owing to the ability of nano silica to fill the pore structure making the concrete mixtures more compact and denser. The density of RuC with 10%, 20% and 30% replacement of R_A increases by 0.11%, 0.42%, and 0.85 respectively, on 1.5% replacement of cement by nano silica. However, the density of rubberised concrete with 10%, 20% and 30% replacement of R_B increased by 0.22%, 0.58 and 0.68% respectively, on 1.5% replacement of cement by NS.

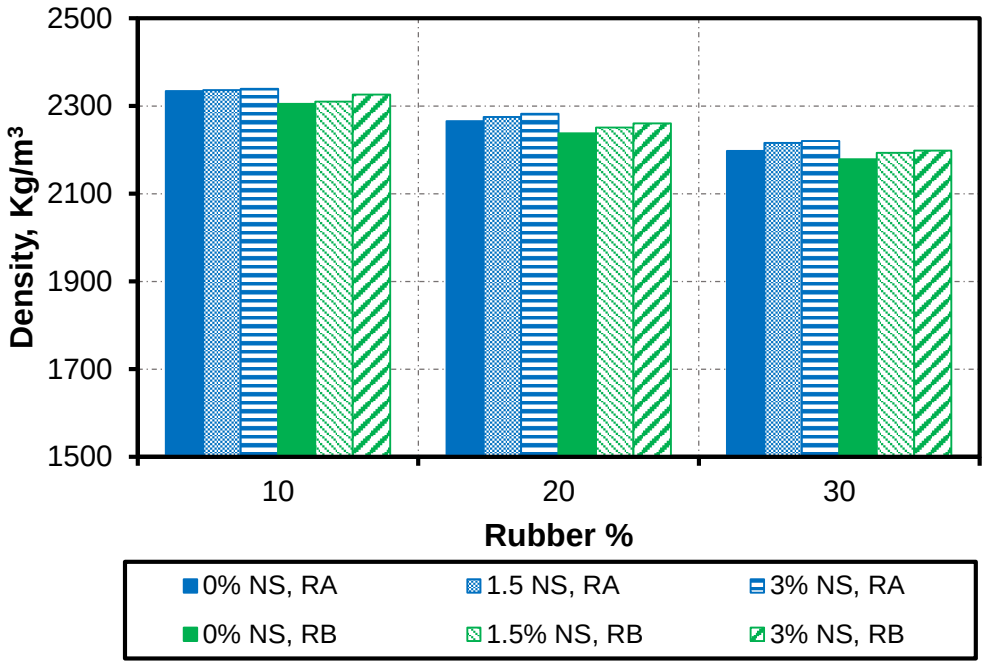

Figure 4-5 Density of rubberised concrete with different NS%

4.3.3 Water absorption

After 28 days of curing, three cubes of each mix were taken out from water tank for water absorption test according to BS 1881-122 (BS1881-122, 1983). Figure 4-6 shows the variation of water absorption results of concrete for two different size of rubber and NS. As expected, the increase in the rubber percentage leads to an increase in water absorption. However, the partial replacement of cement by nano silica leads to a decrease in water absorption. It was observed from Figure 4-6 that 10%, 20% and 30% rubber replacement increased the water absorption by 14%, 26%, and 37.6%, and around 19%, 26%, and 61.9%, for R_A and R_B respectively in comparison with the control mix.

It also was observed that the water absorption of rubberised concrete was decreased with increasing dosage of NS. This phenomenon was due to the denser packing of the particles present in the mix and also due to the pozzolanic

activity of the nano silica which filled the voids between cement grains, reducing the water absorption of mixtures.

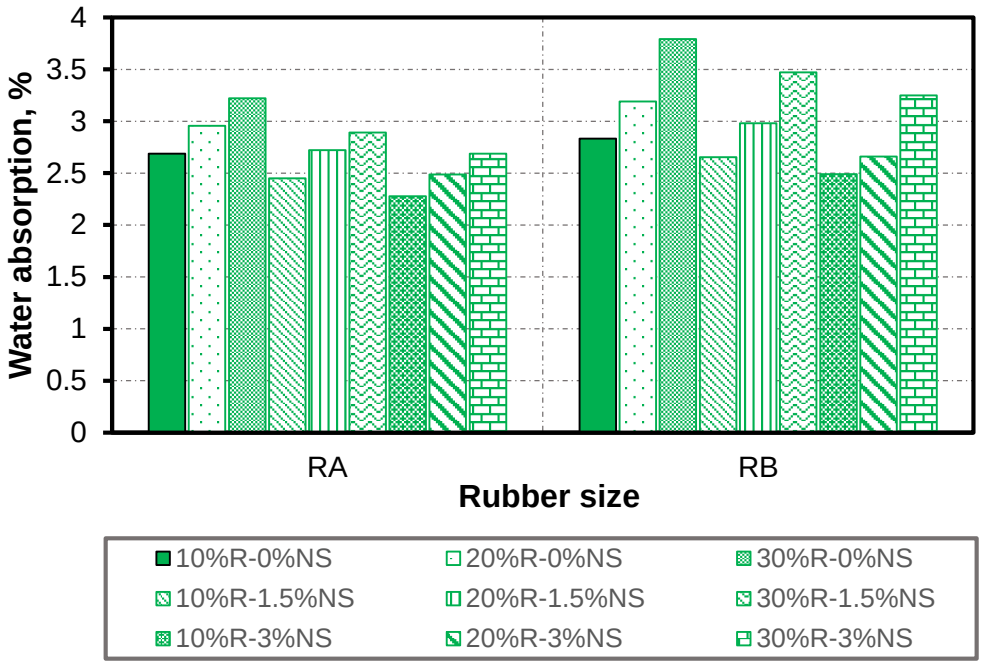

Figure 4-6 water absorption of concrete with two different size of rubber

4.3.4 Porosity

Porosity is defined as ratio of the volume of pores to the total volume of the sample. A simple method to measure the material porosity is the vacuum-saturation method. The test was carried out on three samples for each mix. Firstly, the samples were dried at 100 ±5°C for around 24 h, until constant weight was achieved, then their weight was recorded. The dried samples were submerged underwater in a vacuum vessel for 2 hours, and then these samples were kept in water for extra 24 hours to ensure full water saturation. After wiping out the wet surfaces of specimen by dry cloth, the weight of the sample is recorded. The ratio of weight difference before and after soaking in water divided by the concrete volume is considered as porosity.

The variation of porosity of concrete made with different mixes containing rubber and NS is shown in Figure 4-7**.** It can be seen that there was an increase in concrete porosity with the increase of rubber content for the two size of rubber. With 30% R_A the porosity is 7.05%, whereas samples with R_B had a porosity of 8.35% or almost 1.5 times higher compared to control concrete.

The increased void content of rubberised concrete is attributed to the tendency of rubber to float in mixtures, which made the compaction of rubberised concrete specimens difficult and ineffective. Thus, the voids percentage in rubberised concrete mixtures increased with increased rubber content and therefore retention of water in those voids during the period curing. However, the addition of NS reduces porosity.

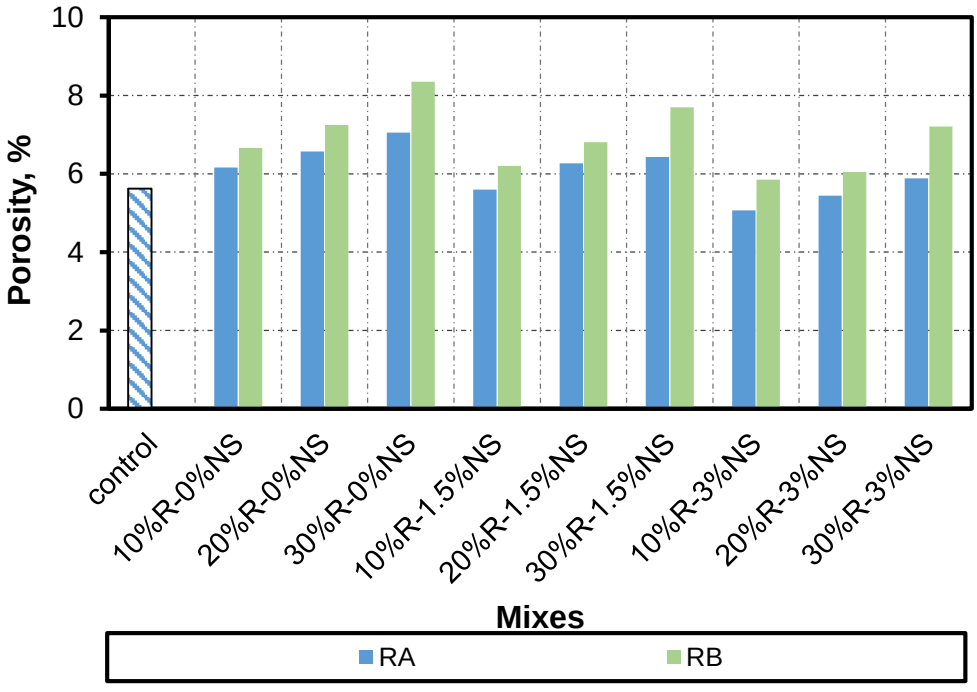

Figure 4-7 Porosity of different mixes of rubberised concrete mixes

4.3.5 Compressive strength

Compressive strength of each concrete mix was obtained at an age of 7, 28 and 90 days by testing three cubes of size 100×100×100 mm in accordance with BS EN12390-3:2009 BS-12390-3 (2009). The average of three samples results was taken as the final result of concrete compressive strength. The effect of various ingredients on concrete compressive strength is discussed below.

4.3.5.1 Effect of rubber content

Figure 4-8 shows the effect of replacing the fine aggregate with crumb rubber on of compressive strength at 7, 28 and 90 days: Figure 4-8 (a) for R_A and Figure 4-8 (b) for R_B. It can be seen that the R_B replacement causes a larger reduction in strength than R_A replacement for all mixes. The reduction in rubberised concrete mixes as compared to control mix was 25.3%, 37.6% and 36.8% for 30% replacement of fine aggregate by R_A, and 37.4%, 38.8% and 39.6% for 30%R_B replacement at 7, 28 and 90 days, respectively. These results indicate that rubberised concrete mixes with smaller size of rubber particles yields less reduction in compressive strength due to the voids-filling ability of finer rubber particles, causing low void space. Moreover, it can be obviously observed that the compressive strength reduces with higher replacement level of rubber regardless of the size of rubber.

This reduction in compressive strength can be referred to the low stiffness of rubber particles that caused weak bonding between rubber particles and cement paste, which leads to a decrease in the compressive strength. A similar trend of strength reduction with the use of various rubber sizes in concrete was reported by Haolin et.al, (2015).

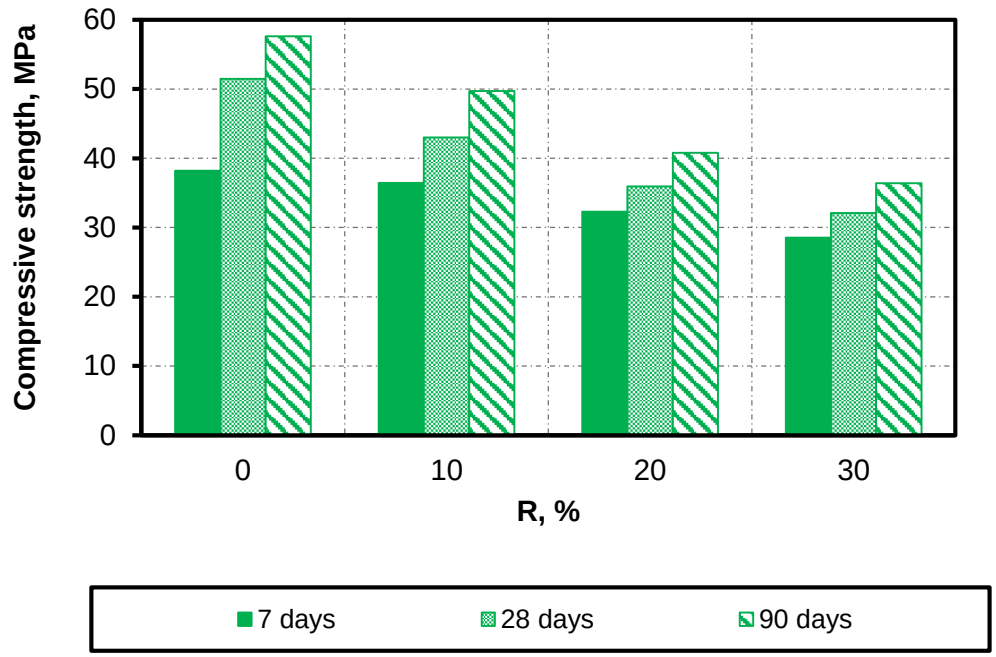

(a)

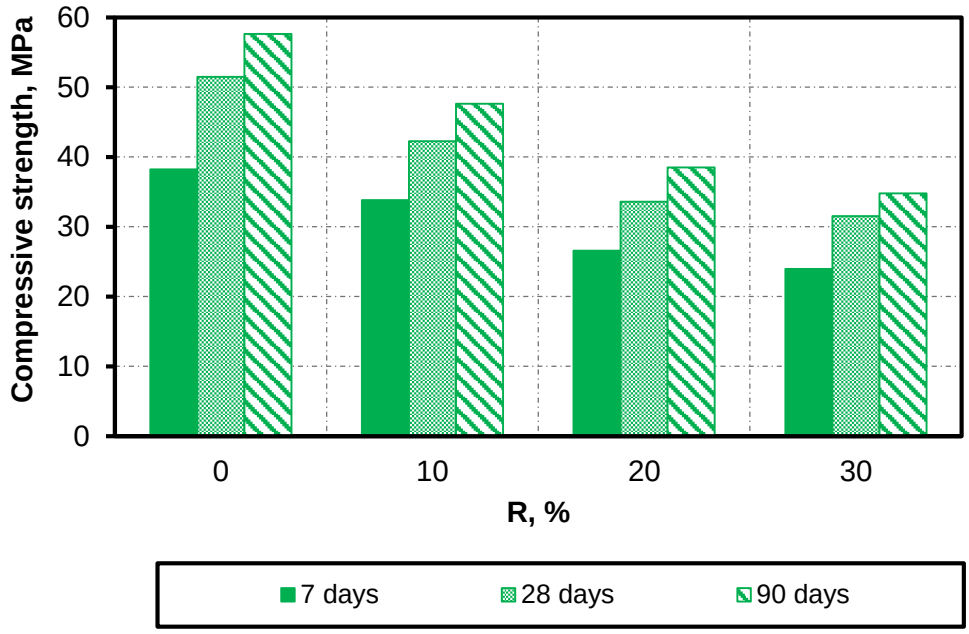

(b)

Figure 4-8 Effect of rubber replacement on compressive strength of the tested mixtures at 7 and 28 day (a) R_A, and (b) R_B

4.3.5.2 Effect of NS replacement

The effect of different NS contents on 7, 28 and 90 days compressive strength of rubberised concrete mixtures is shown in Figures 4-9, 4-10 and 4-11**,** respectively. It is observed that the partial replacement of cement with NS significantly improved the rubberised concrete performance. The addition of 1.5% NS was successful in achieving a higher compressive strength at 7, 28 and 90 days for mixes with 10% R_A as a fine aggregate replacement than the control mix For higher rubber content, nano silica partially alleviated the loss in strength. However, the addition of 3% NS compensates the strength loss for replacement percentage up to 20% for both sizes of rubber compred to control mix.

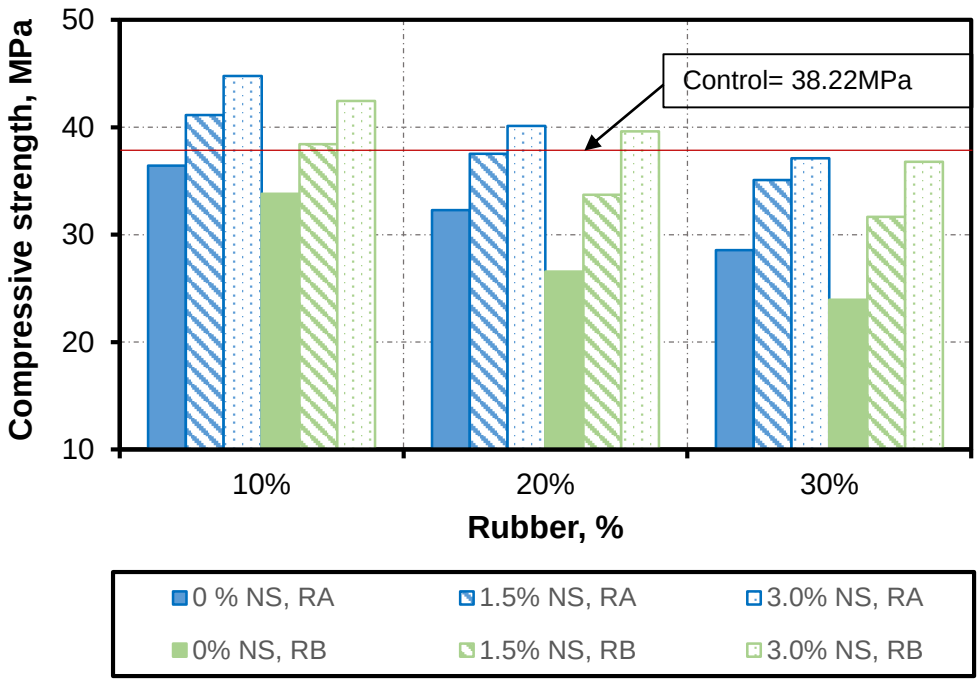

Figure 4-9 7days compressive strength of rubberised concrete

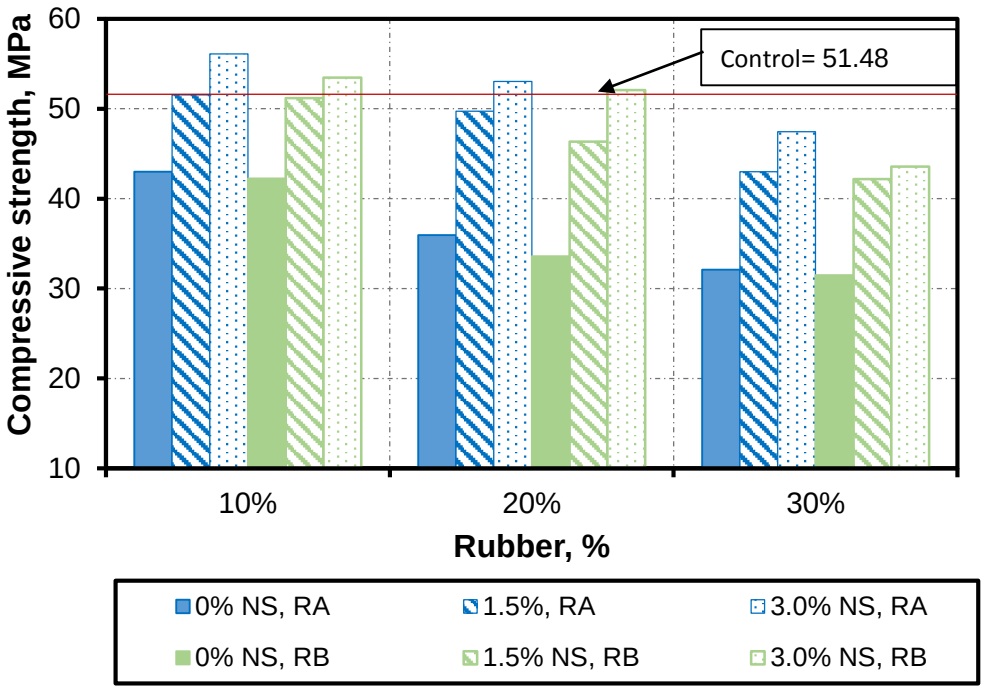

Figure 4-10 28 days compressive strength of rubberised concrete

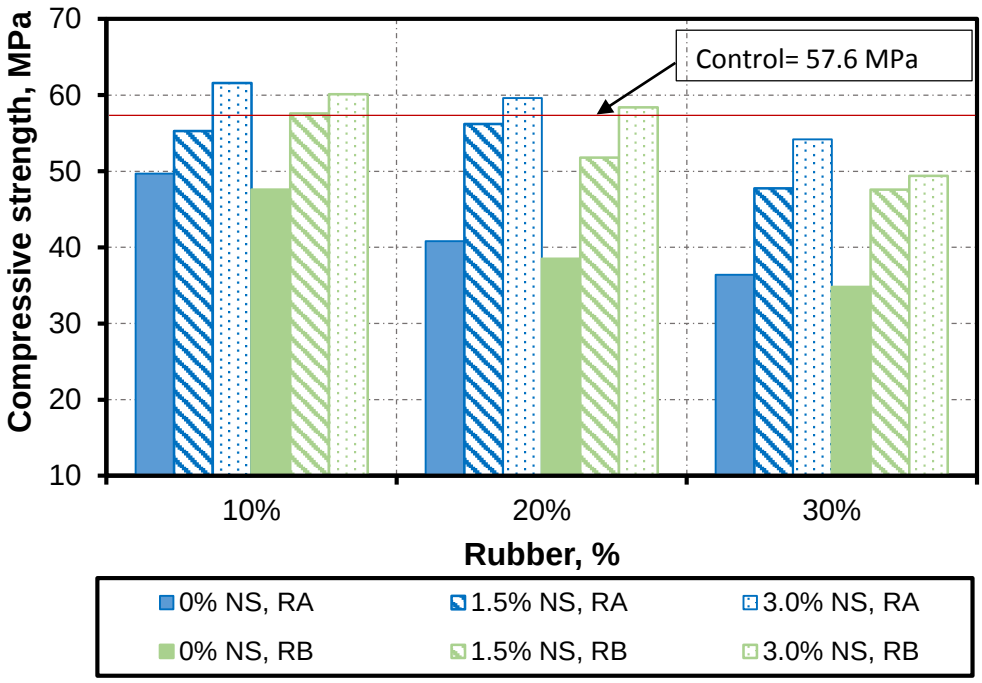

Figure 4-11 90 days compressive strength of rubberised concrete

This increase in compressive strength with nano silica might be due to the ability of nano silica in refining the pores and improving hydration products distribution, especially at interfacial transition zone (ITZ) leading to good adhesion between

rubber and cement matrix as observed in previous investigations (Du et al., 2014, Land and Stephan, 2012, Mohammed and Adamu, 2018).

Figure 4-12 presents the enhancement of compressive strength as nano silica level increasing from 0% to 3% while the percentage of rubber level was remained constant at 20% for all mixes. It can be observed that there is an increment in compressive strength of rubberised concrete as the amount of NS increases. Incorporating 1.5% of NS into the rubberised concrete mixture results in enhancing the compressive strength remarkably by 38.25% and 32.75% for R_A and R_B, respectively, compared to the control mix (NS 0%). This is mainly due to the advantages of NS in the rubberised concrete mixes as aforementioned. With the increase of nano silica level from 1.5% to 3.0%, a small improvement in compressive strength of rubberised concrete can be observed. Mohammed et al. (2016b) attributed this condition to inadequate amount of NS to fully react with the free portlandite.

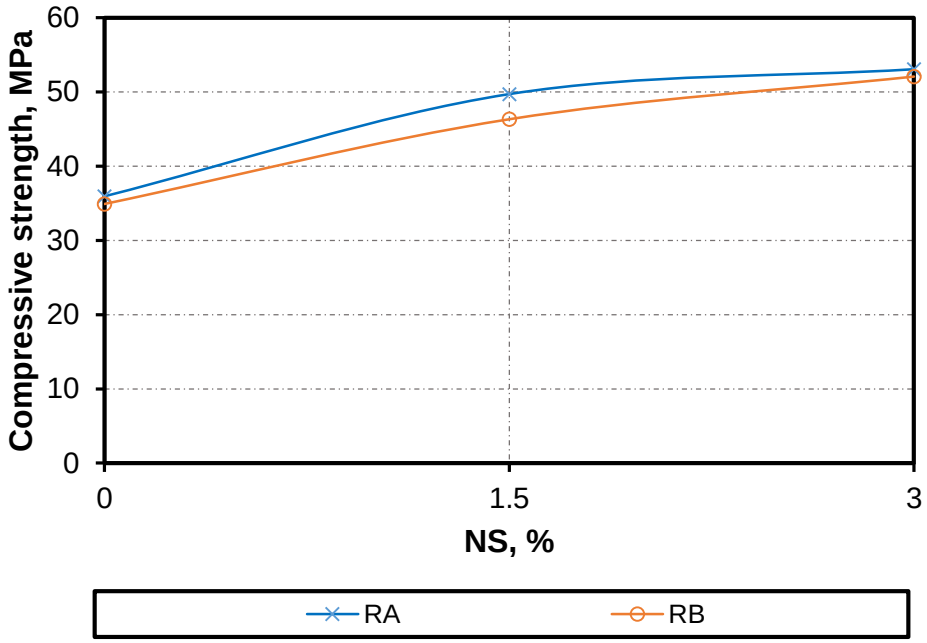

Figure 4-12 Compressive strength versus nano silica addition for rubberised concrete mixture with 20% of rubber.

Figures 4-13 and 4-14 seem to show a strong correlation between compressive strength and both density and porosity, respectively for all mixes. It can be clearly observed that the decrease in the density of concrete mixes is linked with the reduction of its compressive strength. Additionally, it should be mentioned that the increment of rubber content in concrete lowers its density, regardless of the size of rubber. However, the compressive strength has an inverse correlation with porosity, consistent with findings in (Sukontasukkul and Chaikaew, 2006, Najim and Hall, 2012, Raffoul et al., 2016).

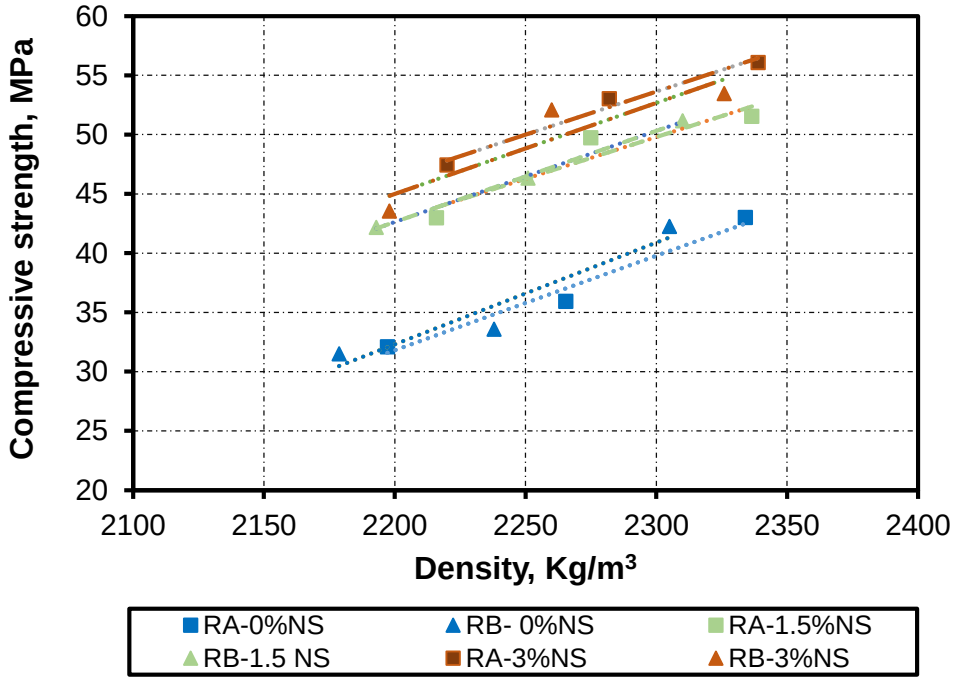

Figure 4-13 The relationship between Density and compressive strength of rubberised concrete

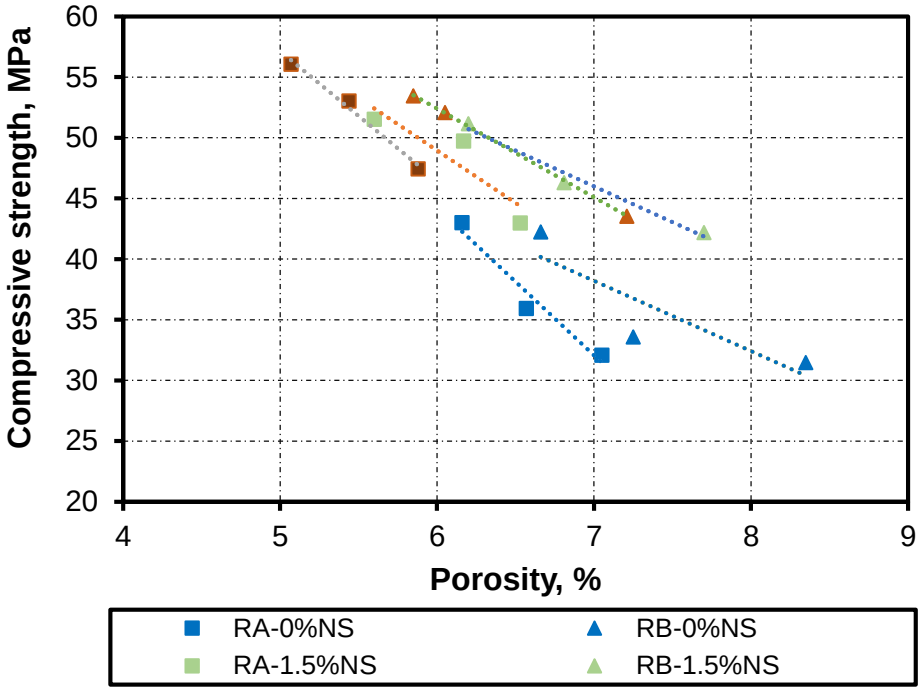

Figure 4-14 The relationship between porosity and compressive strength of rubberised concrete

4.3.6 Splitting tensile strength

The splitting tensile strength of various concrete mixes is obtained by testing 150 mm x 300 mm concrete cylinders in accordance with BS 1881-117 (BS-1881-117, 1983). The average of three samples results was taken as the final result of concrete splitting tensile strength. All the results of splitting tensile strength tests are presented in Figure 4-15. The strength reduction trend for the splitting tensile strength is similar to that observed in the compressive strength. Control concrete had initial splitting tensile strength of 3.7 MPa. Clearly, this initial strength value dropped to 2.35 MPa and 2.15 MPa when 30% of fine aggregate was replaced by R_A and R_B, respectively. However, the splitting tensile strength of rubberised concrete enhanced as the amount of nano silica increasing. Adding 3% of NS to rubberised concrete mixture with 20% rubber replacement leads to increasing the splitting tensile strength by 27.36% and 34.86% when using R_A and R_B,

respectively. This improvement in the splitting tensile strength is attributed to the high pozzolanic activity of the nano silica with cement.

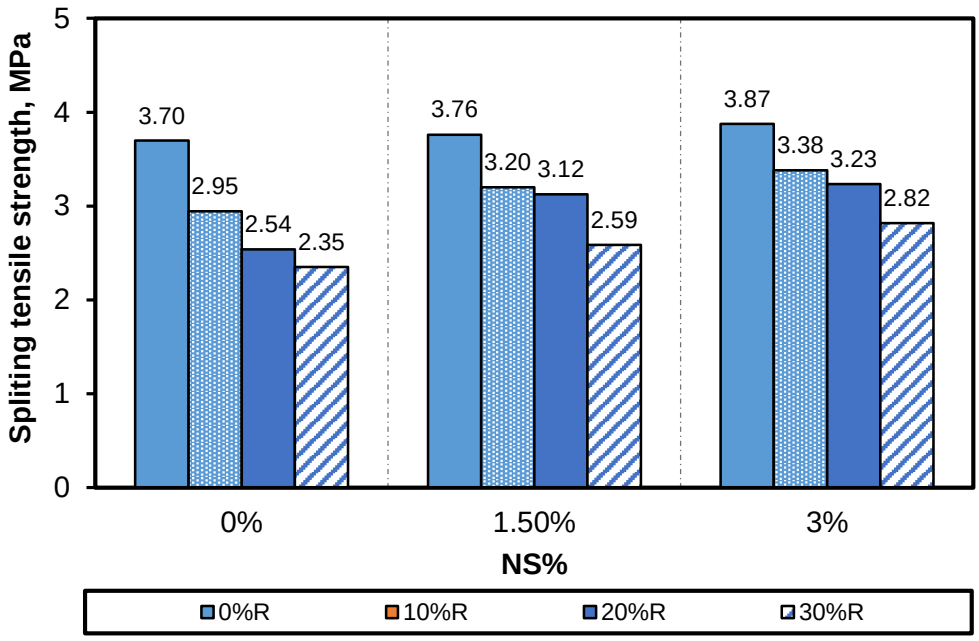

(a)

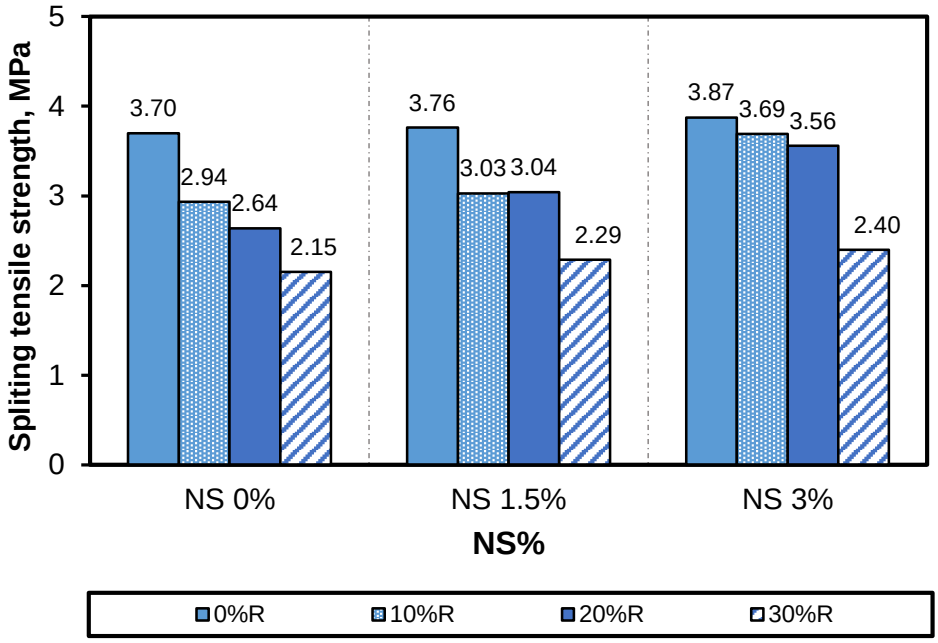

(b)

Figure 4-15 Variation in the splitting tensile strength of rubberised concrete with nano silica, (a) R_A and (b) R_B.

4.3.7 Flexural strength

Flexural strength test of hardened concrete was carried out at 28 days of curing using 100 × 100 × 500 mm prism sample in accordance with ASTM C78/78M-15 (ASTM/C78/C78M, 2015). The average value of two prisms for each mix was recorded. The results of flexural strength for rubberised concrete are shown in Figures 4-16 (a) for R_A and (b) for R_B. It can be seen that as in the case of compressive strength and splitting tensile strength, the addition of rubber aggregates decreases the flexural strength. This reduction was less than 14% for both sizes of 10% rubber replacement. However, when 20% and 30% of the fine aggregate was replaced with R_A, there was a decrease in flexural strength of approximately 17.7% and 28.9%, respectively. In similar trend, there was higher reduction around 23% and 33.9% when using R_B.

It can be concluded that the smaller the particle size of rubber, the higher the strength due to the higher filler ability of the smaller size rubber, increasing the denseness of concrete and reducing the probability of fracture. Decrease in flexural strength with the increase in rubber content was in agreement with the findings of previous study (Khatib and Bayomy, 1999, Su, 2015, Onuaguluchi and Panesar, 2014). However, others (Yilmaz and Degirmenci, 2009, Mohammed et al., 2016b) reported an increase in flexural strength.

The results of the addition of NS showed an enhancement in flexural strength compared to the mixes with 0% NS as presented in Figure 4-16 (a) and (b). This was expected due to the ability of nano silica to fill the voids, thus providing a good adherence between the rubber particles and the cement paste.

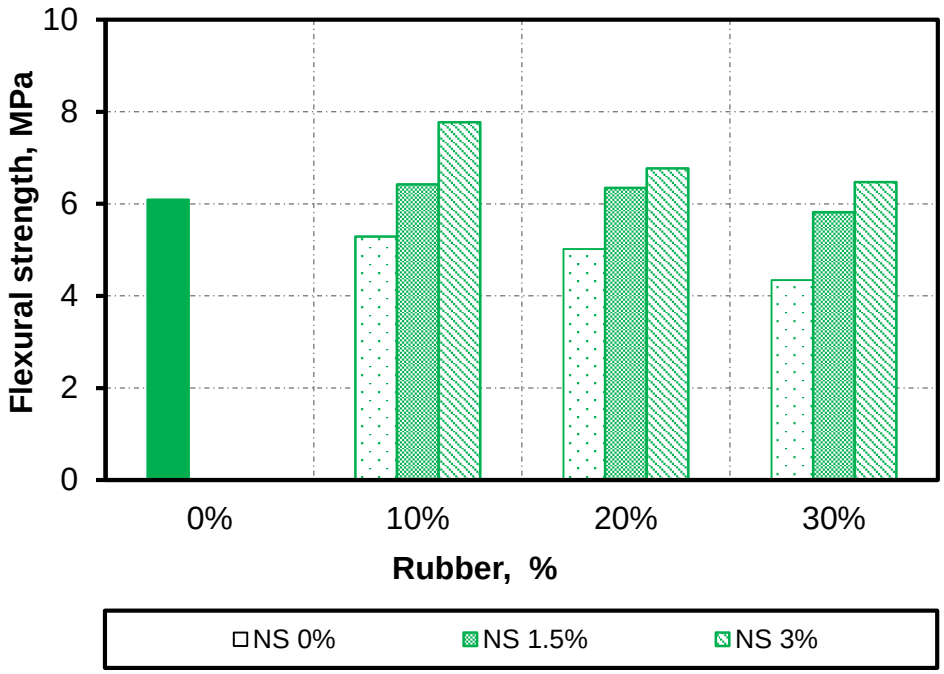

(a)

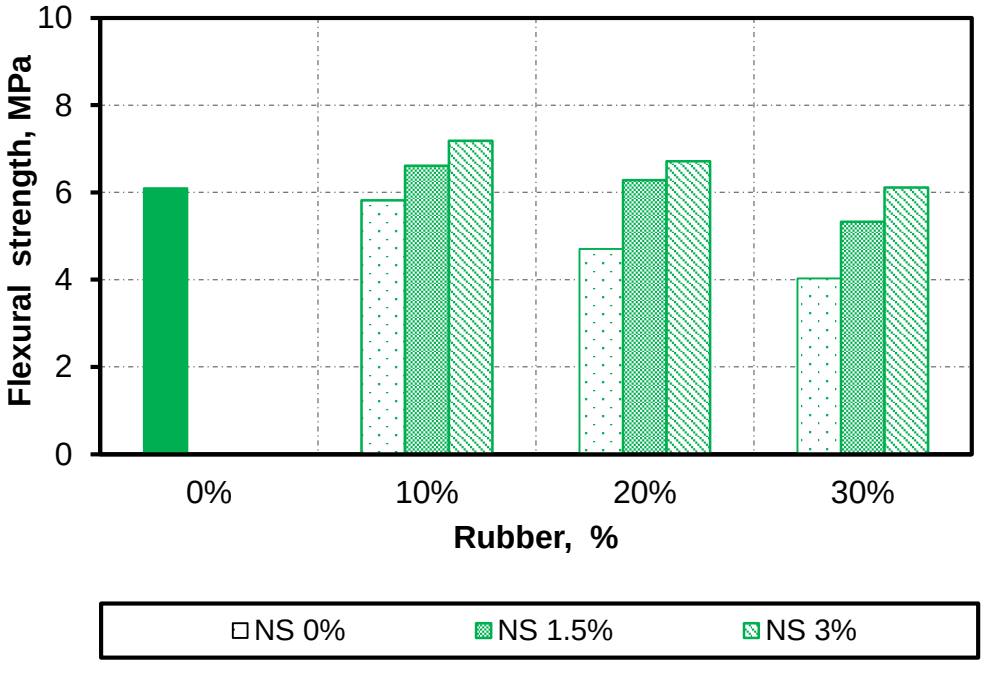

(b)

Figure 4-16 Flexural strength for varying percent of rubber, (a) R_A and (b) R_B.

4.3.8 Drying shrinkage strain.

Figures 4-17 and 4-18 illustrate the free drying shrinkage curves of concrete incorporating different dosage of rubber and NS. The drying shrinkage strains for control concrete and rubberised concrete at 90 days range between 520 and 684 micro strain. It can be seen that the addition of rubber into concrete increases the drying shrinkage strain in relation to the rubber replacement level and the control mix proportions. This increment of drying shrinkage can be attributed to the deformation property of rubber which decreases the internal restraints for drying stresses which lead to increase in the drying shrinkage and also may be due to an increase in porosity of rubberised concrete. It is observed that the drying shrinkage strain for concrete with R_A and R_B were nearly similar at the very early ages, whereas there was a considerable change after 28days.

A similar trend has been observed by (Sukontasukkul, 2012, Su, 2015, Mohammadi and Khabbaz, 2015). The effect of NS content on drying shrinkage strains and the variations with time for concrete with R_A and R_B are also presented in Figure 4-17 and Figure 4-18. It can be seen that the addition of NS caused reduction in drying shrinkage strain compared to rubberised concrete mixtures. This reduction is due to a decrease in porosity compared to rubberised concrete.

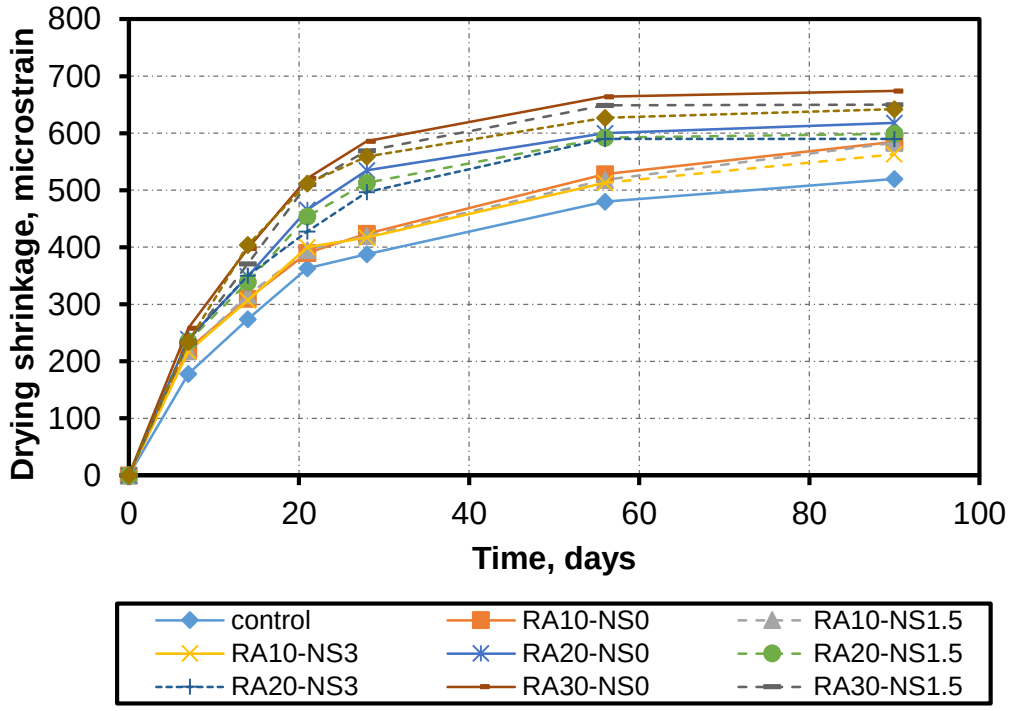

Figure 4-17 Effect of R_A content and NS addition on drying shrinkage of concrete

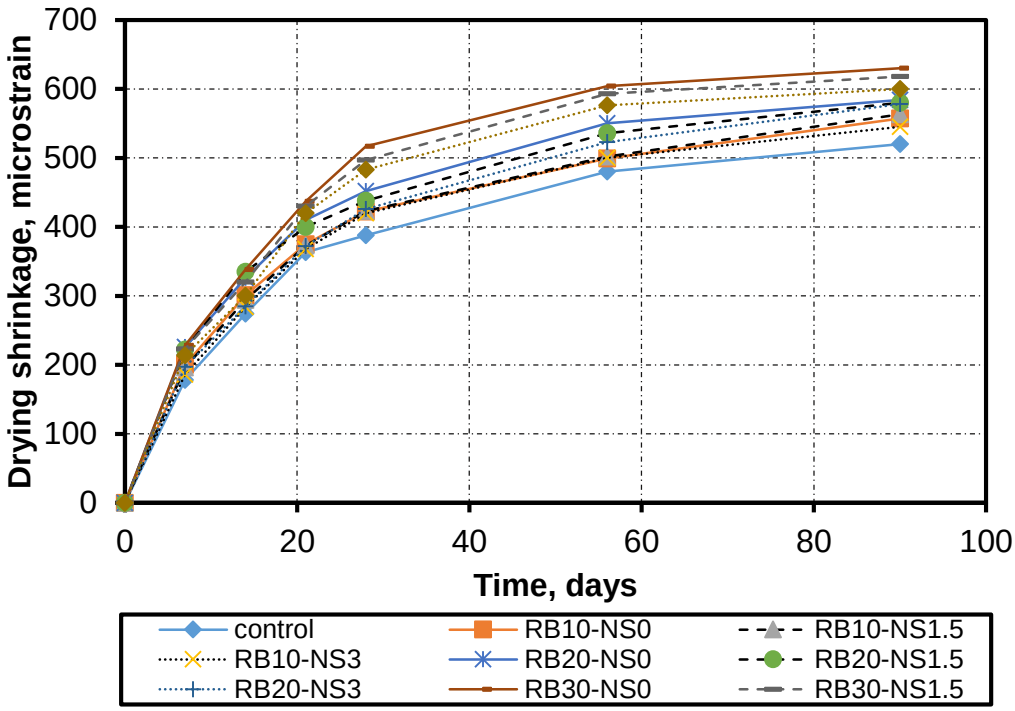

Figure 4-18 Effect of R_B content and NS addition on drying shrinkage of concrete

Figure 4-19 illustrates the relationship between rubber content and drying shrinkage strain. There is almost a linear relation between rubber content and drying shrinkage strain with R^2 = 0.9849 and 0.99903 for concrete with both different size R_A and R_B, respectively indicating a positive correlation for both sizes of rubber. However, Figure 4-20 shows an inverse correlation between drying shrinkage and nano silica content for both R_A and R_B concrete mixes, based on the experimental results of this study.

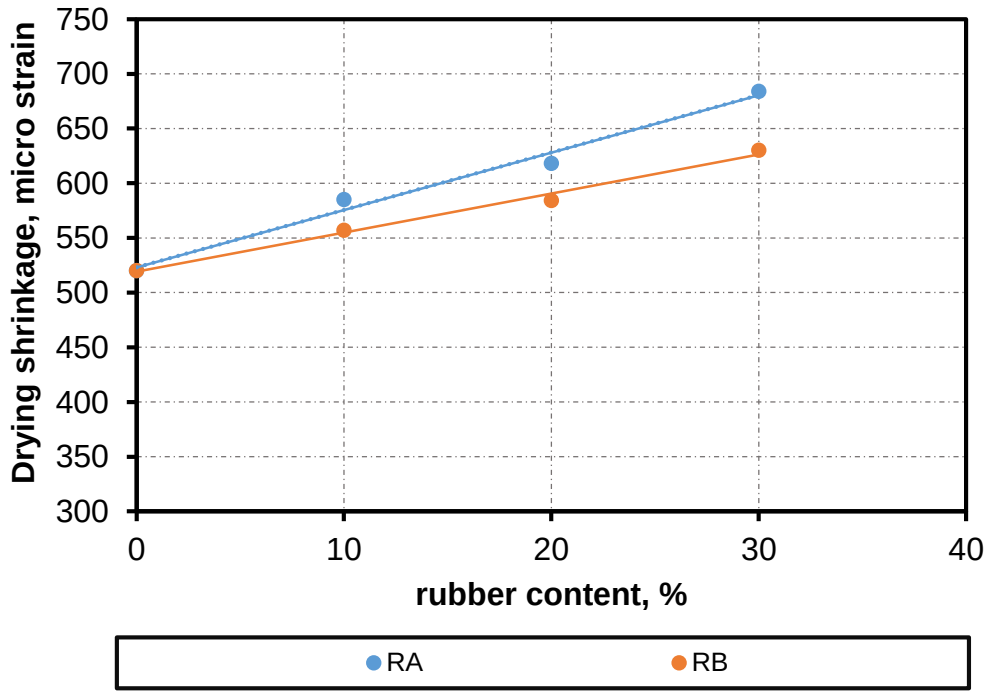

Figure 4-19 Relation between rubber content and drying shrinkage at 90 days for different two different size of rubber.

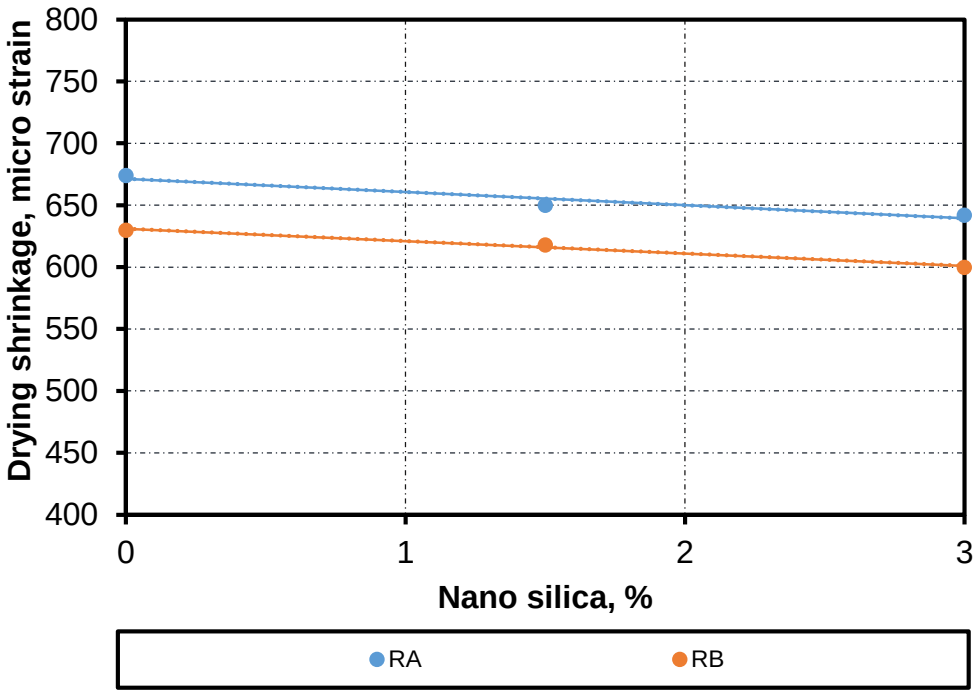

Figure 4-20 Relation between nano silica content and drying shrinkage at 90 days for different two different size of rubber.

4.3.9 Impact resistance under drop weight

The impact resistance of rubberised concrete with two different sizes of rubber (R_A and R_B) was recorded in terms of numbers of blows required for causing first visible crack (N_1) and ultimate failure (N_2) of the specimen. The numbers of blows for 0%-30% replacement of fine aggregate by rubber, with and without any replacement of cement by NS are listed in Table 4-1. It can be seen from the table that the number of blows, required for producing the first crack and ultimate failure, increase significantly with the increase of rubber content for both sizes of rubber, in which varying the percentage of rubber from 0 to 30% increased N_1 and N_2 by around four times compared to the control mixture.

Incorporating 1.5% NS with 30% R_B showed an increase in N_1 and N_2 reaching up to 4.4 and 4.2 times, respectively, higher than the control mixture. However,

the addition of 3%NS showed a slight enhancement compared to the mixture with 1.5%NS.

The difference between number of blows for ultimate failure and first crack (N_2-N_1) is also found to increase gradually with the increase of replacement level of rubber. This finding indicates a decrease in the brittleness of RuC mixtures with higher percentages of rubber. In contrast, as reported by (Reda Taha et al., 2008) who investigated the impact resistance of vibrated concrete containing crumb rubber and chipped rubber, using high level of rubber content can adversely affect both the ductility and the energy absorption of the mixture. High rubber content can weaken the rubber-cement paste as high strains are produced under loading, which limits the ability of the material to absorb energy. Furthermore, increasing the rubber replacement increased the volume of the rubber-cement interface (Ismail and Hassan, 2016).

Table 4-1 Impact resistance results for rubberised concrete with and without NS

	N_1	N_2	N_2-N_1	N_2/N_1	IE(J)	
	Mean (number of blows)	Mean (number of blows)			FC	UF
NC	21	25	4	1.17	424	497
RA10-NS0	39	45	6	1.16	775	901
RA20-NS0	63	70	8	1.12	1245	1397
RA30-NS0	81	93	12	1.15	1609	1847
RB10-NS0	46	53	7	1.14	920	1053
RB20-NS0	65	74	9	1.14	1285	1463
RB30-NS0	86	99	13	1.15	1708	1967
NC-NS1.5	23	28	5	1.22	457	556
RA10-NS1.5	42	49	7	1.16	834	967
RA20-NS1.5	65	75	10	1.15	1291	1483
RA30-NS1.5	90	101	11	1.13	1788	2013
RB10-NS1.5	49	57	8	1.16	973	1126
RB20-NS1.5	68	77	10	1.14	1344	1536
RB30-NS1.5	92	104	13	1.14	1821	2073
NC-NS3	27	35	9	1.33	530	702
RA10-NS3	45	54	9	1.19	901	1073
RA20-NS3	70	84	14	1.20	1523	1675
RA30-NS3	93	108	15	1.16	1854	2145
RB10-NS3	53	61	8	1.16	1053	1291
RB20-NS3	77	81	11	1.06	1397	1616
RB30-NS3	95	107	12	1.13	1887	1993

Note: N_1 Numbers of blows required for causing first visible crack, N_2 Numbers of blows required for causing ultimate failure, IE: Impact Energy

Figures 4-21 (a-c) show the number of blows till first crack occurs for the rubberised concrete specimen without and with 1.5% and 3% nano silica addition respectively. It is clear that, there is a wide variance in the results for all rubber replacement ratios. The statistical analysis of the results of first crack is made in

Table 4-1. The addition of nano silica has a slight effect on the impact resistance compared to rubberised concrete mixtures.

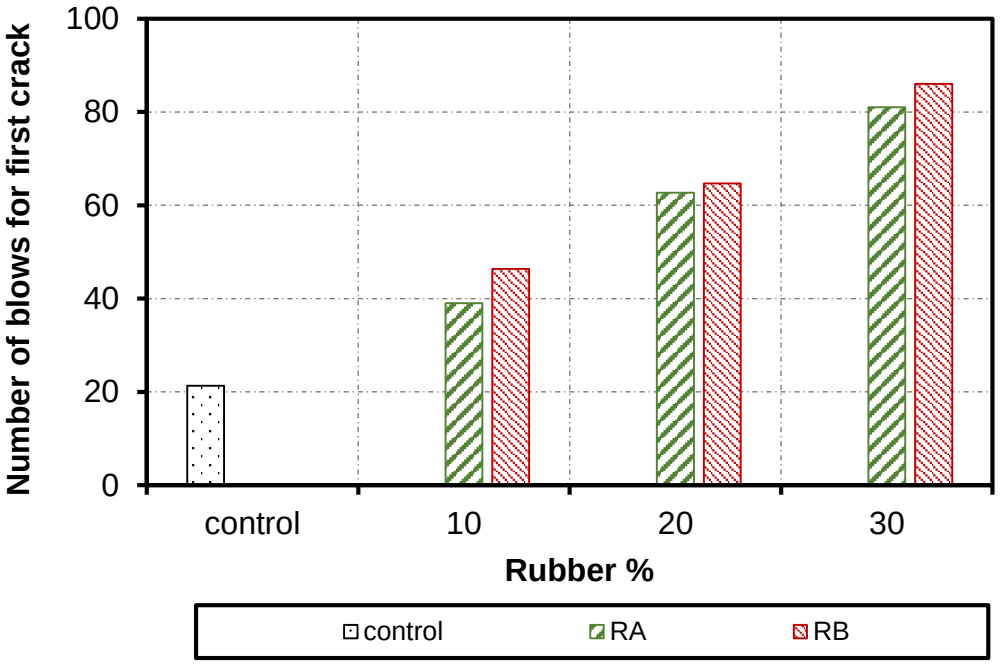

(a)

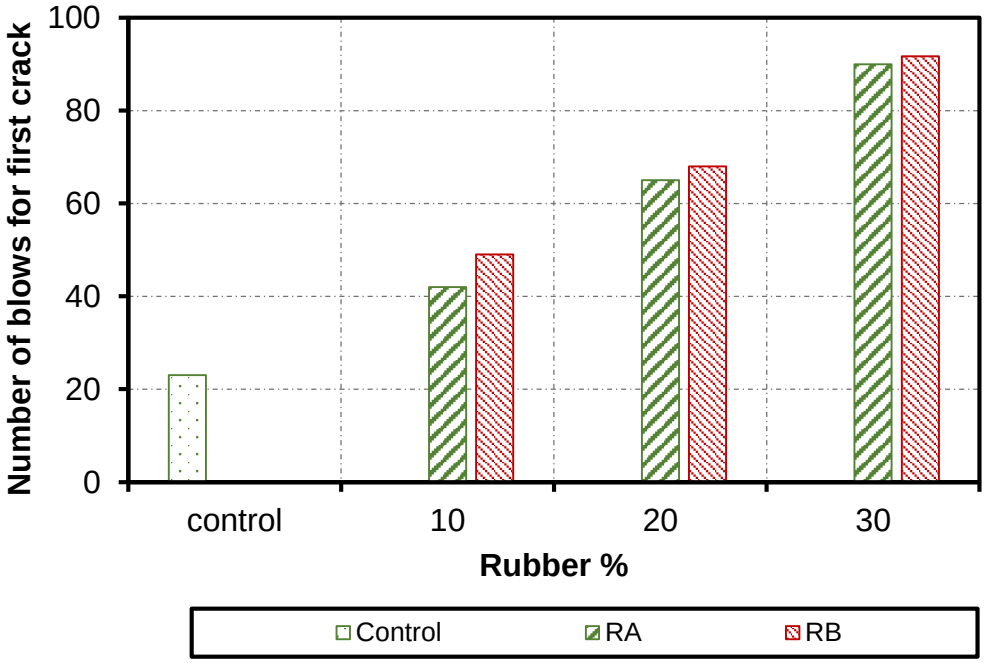

(b)

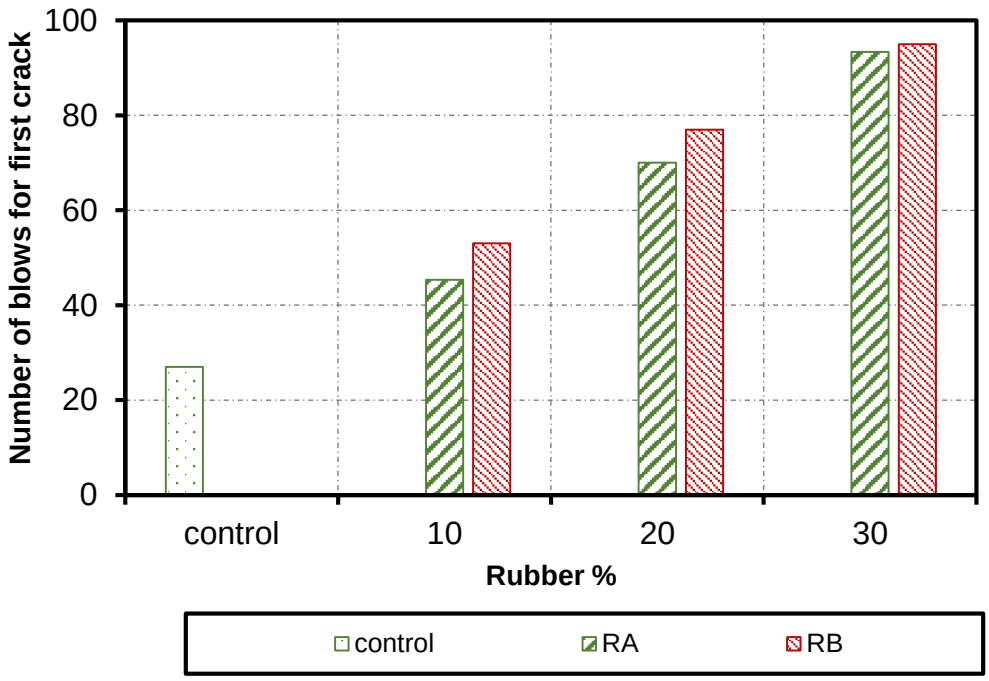

(c)

Figure 4-21 Number of blows for first crack (N1) (a) 0% NS, (b) 1.5% NS and (c) 3% NS

Figures 4-22 (a-c) show the number of blows cause the ultimate failure for the rubberised concrete specimen without and with 1.5% and 3% nano silica addition respectively. The same behaviour was found as in the first crack. Table 4-1 indicates that, the ratio of ultimate failure to the first crack (N_2/N_1) is slightly above one (ranged from 1.06 to 1.22), this indicates that the failure takes place rapidly in rubberised concrete.

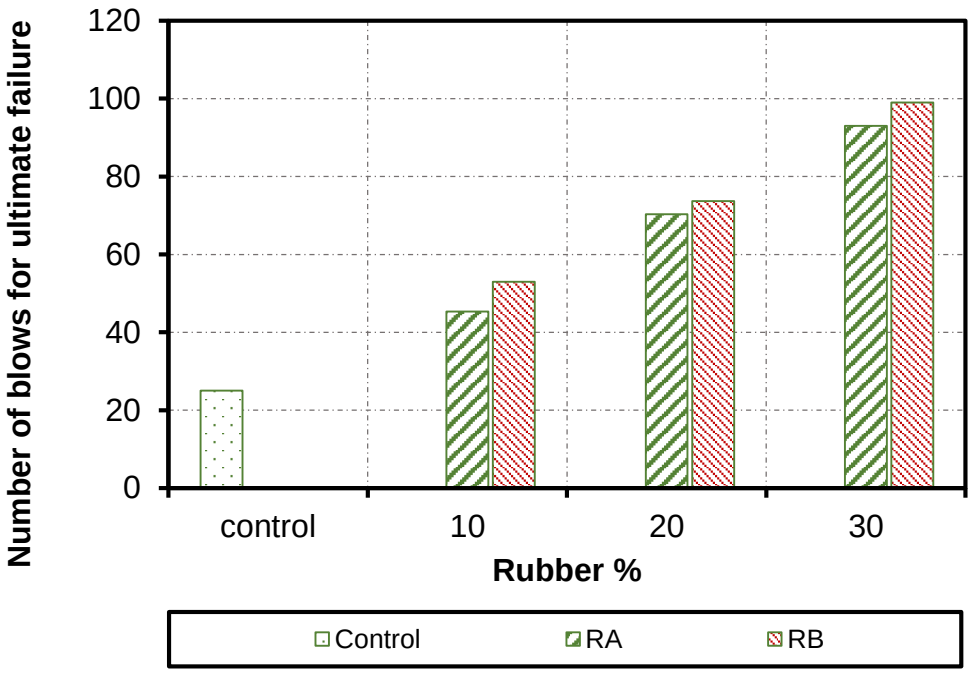
Number of blows for ultimate failure
120
100
80
60
40
20
0
control
10
20
30
Rubber %
Control
RA
RB

(a)

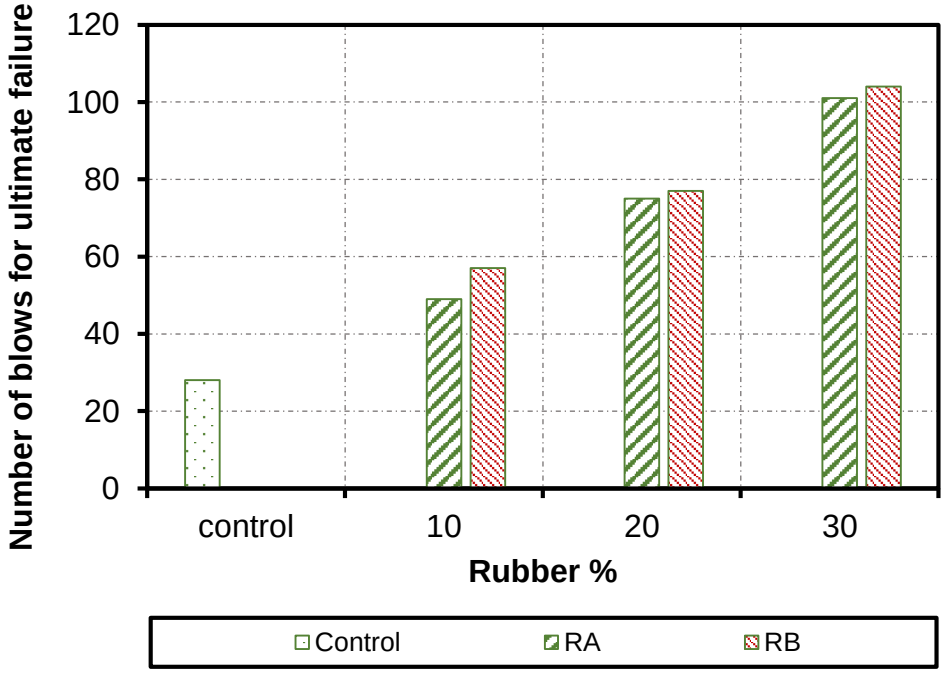
Number of blows for ultimate failure
120
100
80
60
40
20
0
control
10
20
30
Rubber %
Control
RA
RB

(b)

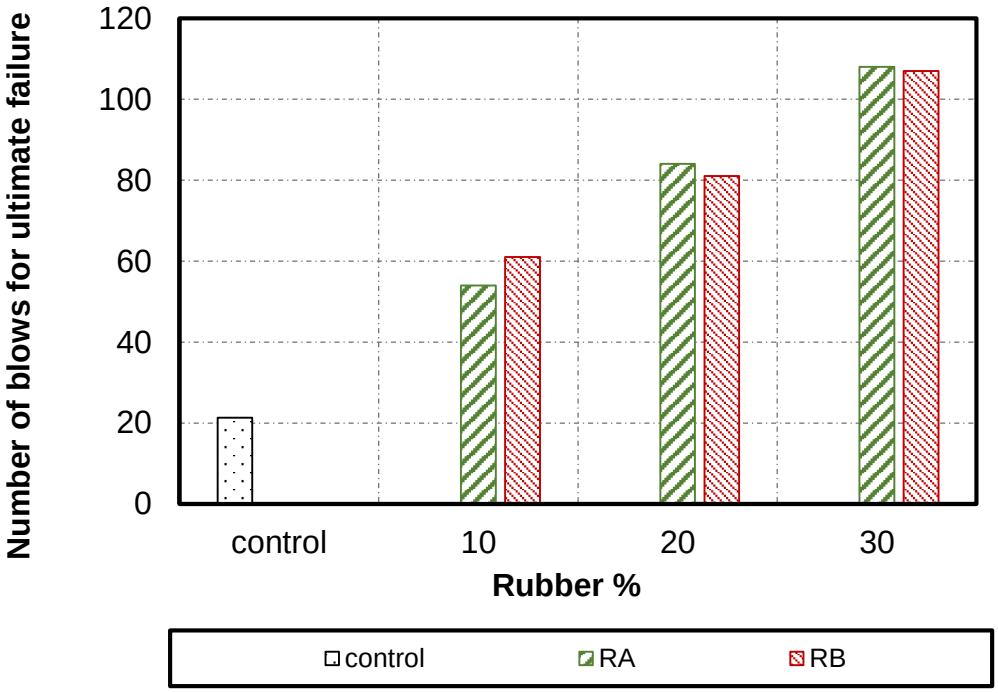

(c)

Figure 4-22 Number of blows for ultimate failure (N1) : (a) 0% NS, (b) 1.5% NS and (c) 3% Ns

4.3.9.1 Failure patterns under impact

Figure 4-23 shows the crack pattern of visible damage due to the impact force for either plain concrete or rubberised concrete. It is obvious that, all specimens are divided to separate parts under the effect of impact force. Therefore, the inclusion of rubber changed the failure pattern from one large crack to three small intersected cracks as shown in Figure 4-23(a) and (b). It can also be seen that combining nano silica with rubber in the mixture further increased the cracks widths (Figure 4-23 (c)).

(a) (b) (c)

Figure 4-23 Failure patterns: (a) plain specimen, (b) specimen with R and (c) specimen with R and NS

4.4 Conclusions

Series of tests were conducted on concrete mixes to evaluate the workability and mechanical properties of rubberised concrete incorporating colloidal nano silica. Based on the experimental test results of this study, the following conclusions can be summarised:

4.4.1 Trial experimental investigations

- The effect of NS on concrete workability is mainly governed by the specific surface area of NS. Therefore, the increase of specific surface area could hugely reduce the workability of concrete.
- The influence of NS on compressive strength of concrete was more apparent at the 7 days for all mixes compared with that at 28 days, which is consistent with the acceleration of hydration process due to the ultra-high surface area of these materials.

- The compressive strength of concrete is directly affected by the change of the specific surface area of NS. Amongst the three types of NS, NS with SSA of 250 m^2 /g showed a higher enhancement rate of compressive strength at 7 and 28 days, followed by NS with SSA of 500 m^2 /g, while using NS with SSA of 51.4 m^2 /g was less powerful for all mixes.
- The optimum replacement ratio for each type of NS is highly correlated with the particles reactivity and agglomeration state. Apparently, it becomes higher since the size of NS particles is larger, however, it is found to be ranging between 1% and 3%.

4.4.2 Main experimental investigations

- Utilisation of different particle sizes of rubber in concrete as a replacement of fine aggregates affects the workability. The reduction in slump values were observed as the rubber particle size was increased. This is due to the water absorption of the larger particle size of rubber is higher than the finer rubber particles.
- The addition of rubber aggregate significantly decreased the density whilst increasing the porosity and water absorption. The reduction in density is mainly due to the low specific gravity of rubber. Concrete mixes prepared with the smaller size of rubber particles show a higher increase in water absorption and porosity compared to those with larger ones. On the contrary, concrete with the larger rubber particles has a lower density values than those with the finer rubber particles.
- The compressive strength, splitting tensile strength and flexural strength decreased with the increase of both rubber content and rubber size.

However, the addition of variable dosages of NS showed a remarkable enhancement in the strength of rubberised concrete.

- Drying shrinkage test results revealed that adding rubber into concrete resulted in higher free drying shrinkage strain. However, incorporating NS to rubberised concrete decrease the drying shrinkage strain.
- The impact resistance under drop weight test showed that the impact resistance of concrete mixtures improved by replacing the fine aggregate with rubber particles.
- The variance between number of blows for ultimate failure and first crack increased as the rubber level increased, which indicates an increase in the ductility of rubberised concrete mixtures.

CHAPTER FIVE – THERMAL AND ACOUSTIC PROPERTIES OF RUBBERISED CONCRETE WITH AND WITHOUT NANO SILICA

5.1 Introduction

Chapter three described the measurement procedures which were used to characterise the rubberised concrete with and without nano-silica. In this chapter, the results of the measurements will be presented and discussed. In particular attention will be paid to the relations between the non-acoustic and acoustic characteristics, in an attempt to fully describe the acoustic performance of a particular material.

In this chapter, the thermal performance, sound absorption, transmission loss, and dynamic stiffness for the mixes are discussed.

5.2 Thermal Properties

5.2.1 Thermal Conductivity

The thermal performance study of concrete has become increasingly important with recent developments in engineering applications. Based on the literature review, it was expected that increasing rubber content would decrease the thermal conductivity (Fadiel et al., 2014). Figure 5-1 (a) and (b) show the thermal conductivity, (λ) of all rubberised concrete mixes with various sizes of rubber. In general there is a clear reduction in thermal conductivity with the increase in the percentage of rubber regardless of rubber particle size. A decrement of thermal conductivity can be attributed to several reasons a) the increase in porosity resulting from the incorporation of rubber particles, which reduces thermal conductivity, b) the insulating effect of rubber particle, which has lower thermal

conductivity compared to fine aggregate. Thermal conductivity of rubber ranged between 0.05-0.13 W/m.k for rubber particle size less than 12 mm (Benazzouk et al., 2008).

It was observed that the λ-values of rubberised concrete with R_A varied between 0.92 W/m.K to 0.59 W/m.K and within a range of 0.81 W/m.K and 0.51 W/m.K for rubberised concrete with RB compared to 1.15 W/m.K for the control concrete. It can be seen that a mix with R_A had higher values of thermal conductivity compared with R_B. This is around 20 to 49% and about 30 to 55% reduction in thermal conductivity of rubberised concrete with R_A and R_B, respectively. The lower thermal conductivity is observed in the mixes with a higher proportion of rubber particles. Moreover, Figure 5-2 shows that the presence of NS leads to a further reduction of thermal conductivity in rubberised concrete mixes, which was consistent with the studies conducted by Sikora et al. (2017) and (Jittabut, 2015).

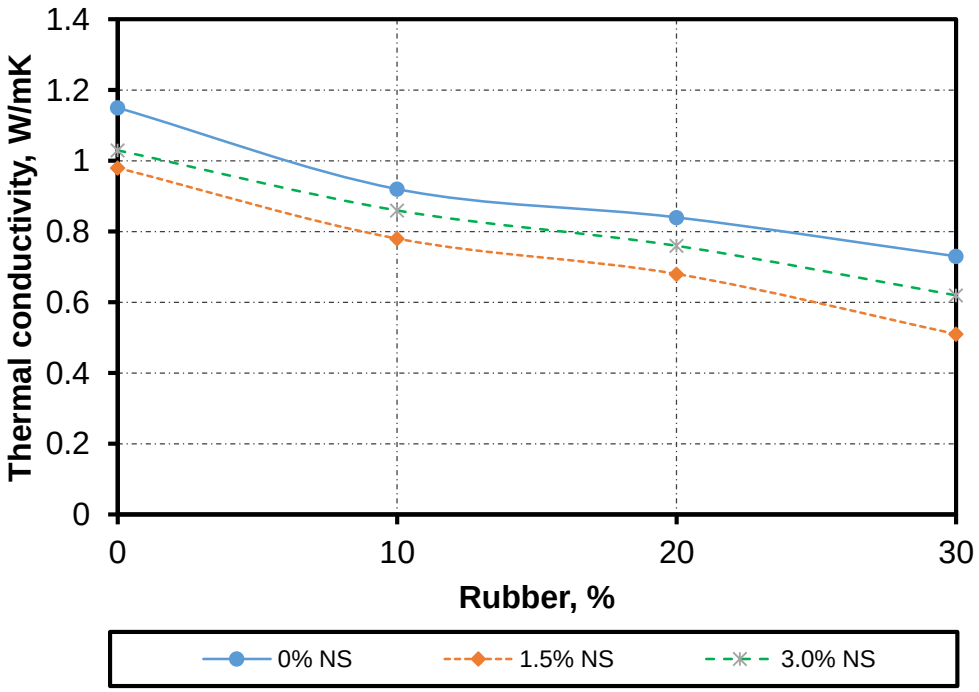

(a)

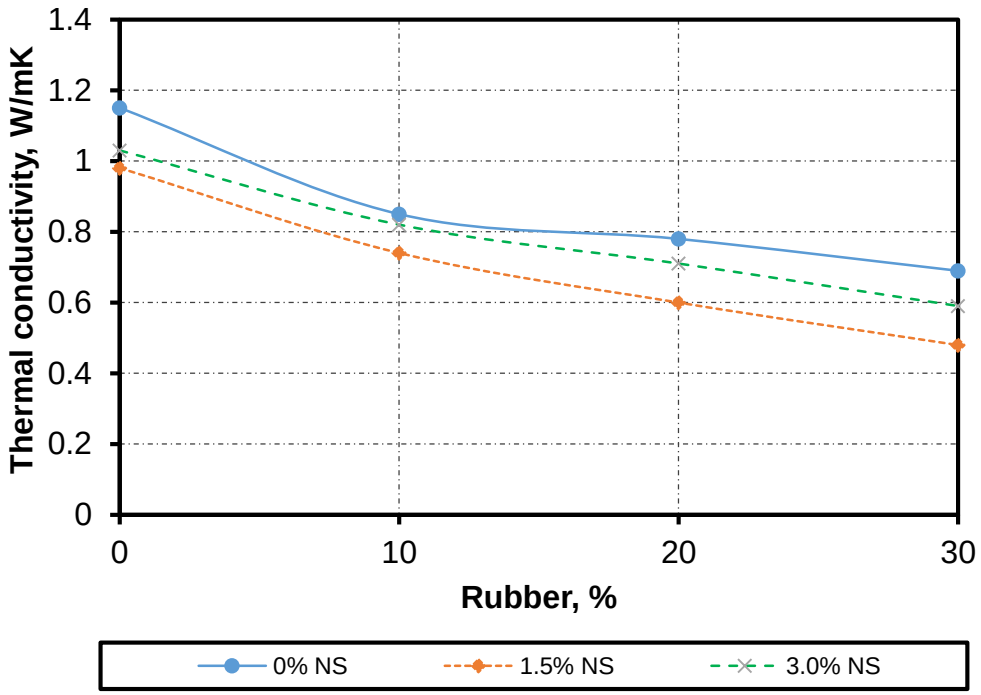

(b)

Figure 5-1 Thermal conductivity vs rubber % for different mixes with (a) R_A and (b) R_B

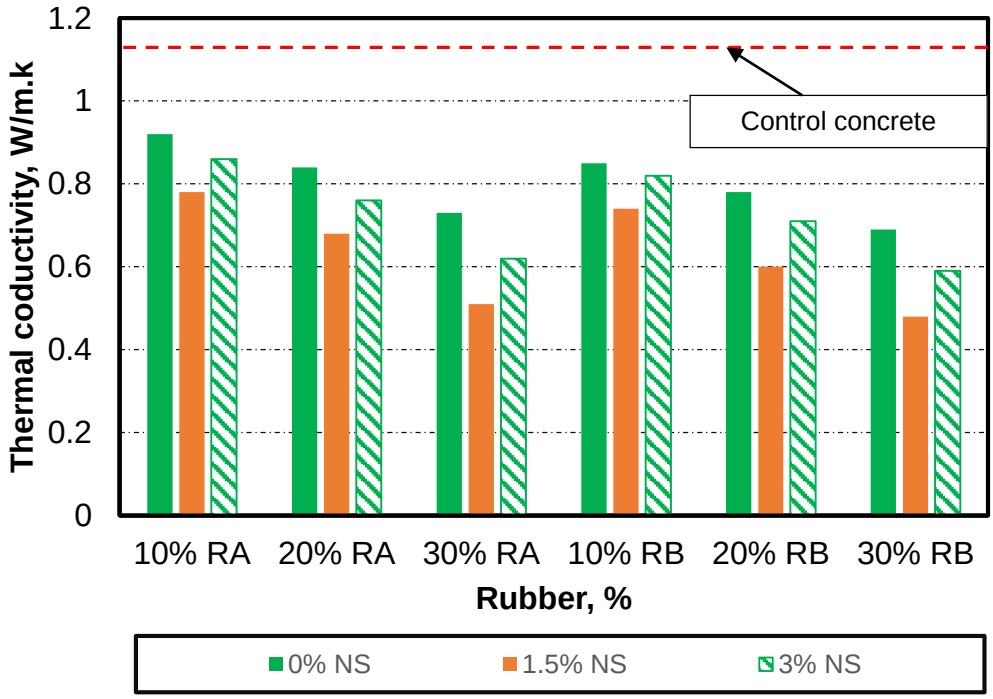

Figure 5-2 Thermal conductivity of rubberised concrete with various percentage of Ns compared with control concrete

5.2.2 The relationship between density and thermal conductivity of concrete

The relationship between thermal conductivity and density of specimens with two different size rubber granules is presented in Figure 5-3. The results demonstrate that in the range of the density of 2175 Kg/m^3 to 2425 Kg/m^3 the dependence is close to linear. The thermal conductivity performance in this range increases consistently with the increased value of density. In the case of specimens with a higher value of density, the thermal conductivity performance decreases fluctuating from 0.5 W/m.k to 1W/m.k. This can be explained by a more complex phenomenon related to material pore structure.

Several works found that the thermal conductivity is directly proportional to the material's density (Awang et al., 2012). Figure 5-3 illustrates the correlation between these properties for all rubberised concrete mixes. Rubberised concrete which have the lowest density tends to have the lowest thermal conductivity, this could be due to its low specific gravity and high porosity.

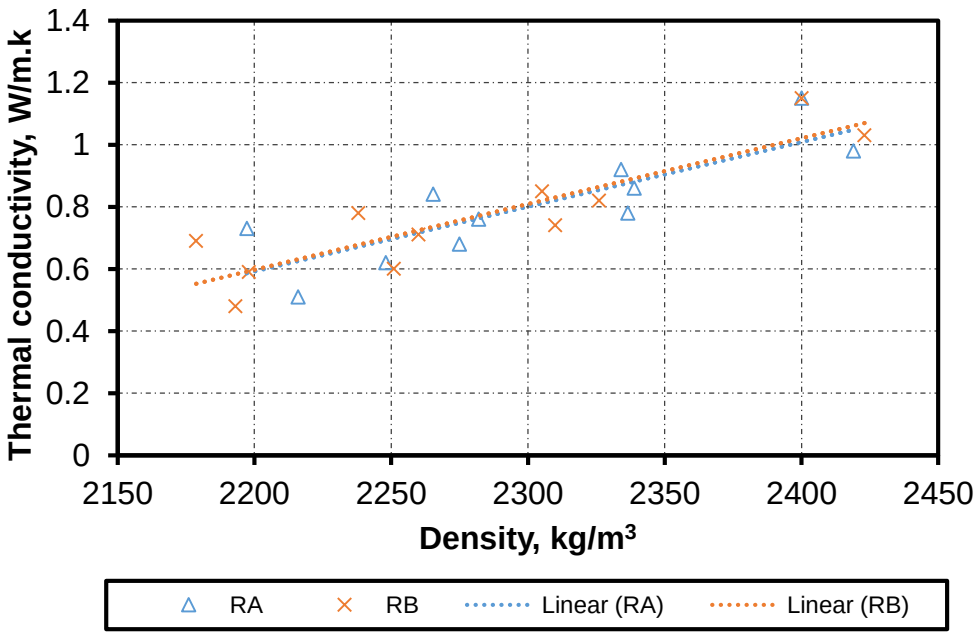

Figure 5-3 Variation of the thermal conductivity with the density

5.3 Acoustic Properties of Rubberised Concrete

5.3.1 Sound Absorption

Basically, two acoustic properties of a building material can be distinguished, the sound absorption and sound transmission. The former is of interest when the source of sound and the listener are in the same room. Energy of the sound waves, when they hit a wall are partially absorbed and partly reflected, and we can define a sound absorption coefficient as a measure of the proportion of the sound energy striking a surface which is absorbed by the surface. Sound transmission is of interest when the listener is in a room adjacent to that in which the source of sound is located.

The primary factor in sound absorption and transmission loss is the porosity of concrete by replacing some of the solid material in the mix by rubber / nano silica more voids are created thus reducing the specimen density. The addition of rubber/nano silica creates three possible locations of voids, (i) between the irregular grains of rubber particles, (ii) in the cement paste containing nano silica, and (iii) in the aggregate particles. Classification on the basis of density is sensible because density and strength are largely concomitant.

To assess the performance of sound absorption of R_uC, loss factor, LF, (damping ratio) and single number rating (SNR) were measured. The values of loss factor and SNR for various mixes are presented in Figures 5-4 (a) and (b). From Figure5-4 (a), it can be observed that the LF, in general, increases with the increase of rubber level in concrete. The LF for concrete made with 30% rubber and 1.5% NS are the highest, this indicates that any vibration set in motion in the specimen would fade faster due to the damping increment. Generally, R_uC mixtures with NS have high damping ratio compared with RuC without NS. Similar

trend was observed in Figure 5-4 (b) for single number rating (SNR), this is reflected in the higher frequency regions in the acoustic absorption spectra. Furthermore it is observed that the single number rating increases with increasing rubber and NS percentages, concrete with zero percentage of rubber and nano silica (control mix) has the lowest acoustic absorption. The improvement in damping characteristic might be attributed to that occurring at the interface between silica and the cement matrix during vibration (Chen and Chung, 2013) .

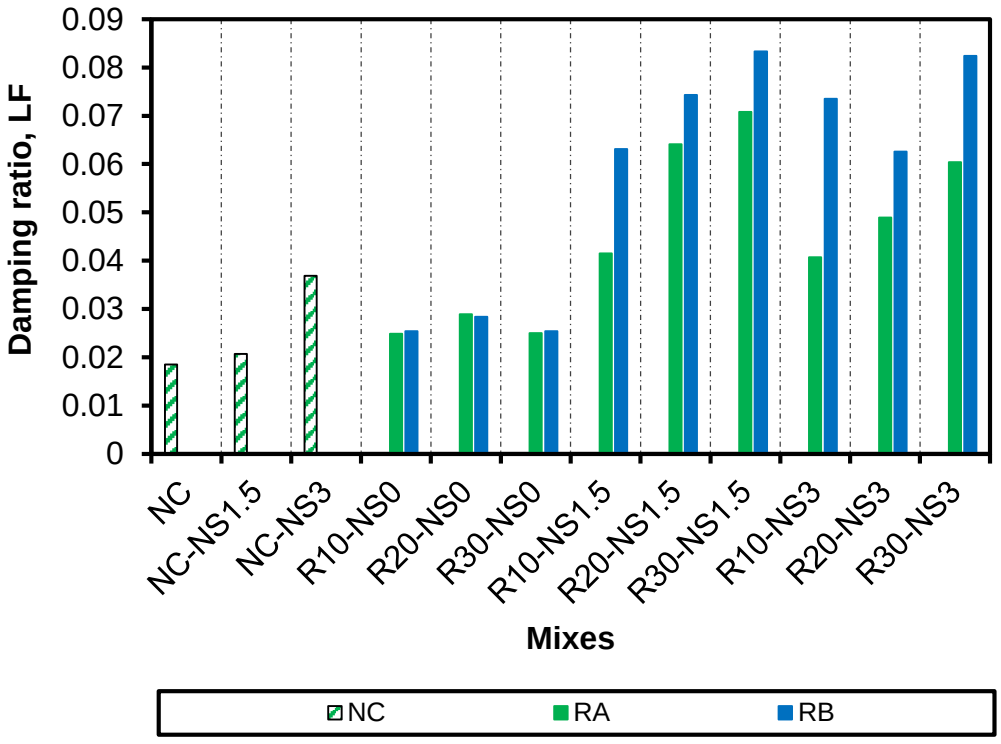

(a)

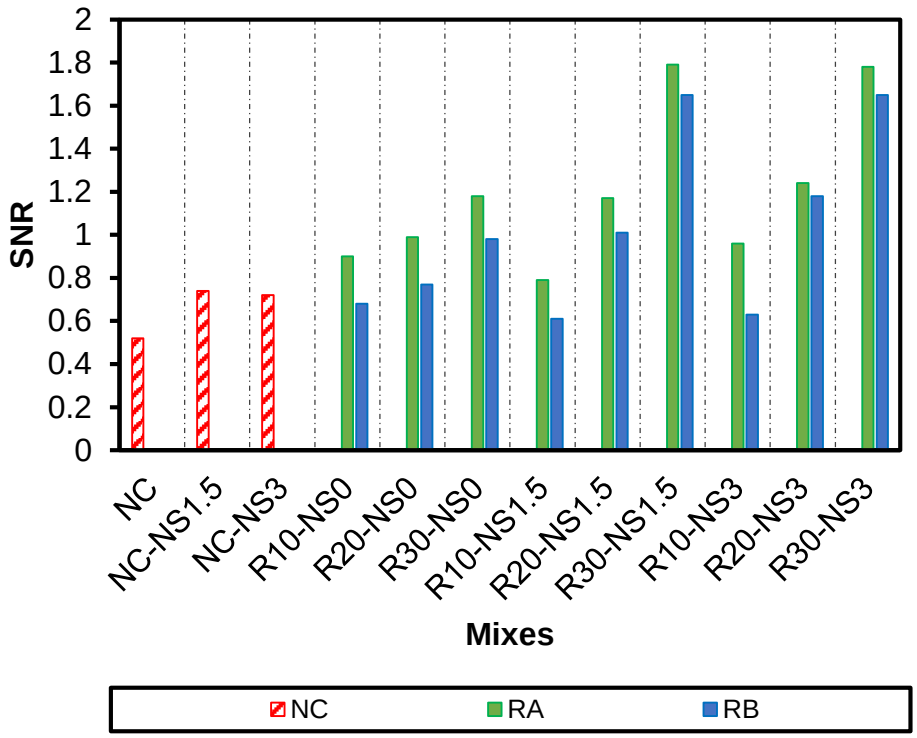

(b)

Figure 5-4 (a) damping ratio and (b) single number rating (SNR) for various mixes

In order to analyse the sound absorption characteristics of rubberised concrete according to the rubber content and rubber size as well as the NS content, the absorption coefficient was measured for each frequency using an impedance tube. The measurement results are shown in Figures 5-5 to 5-8. it can be clearly seen in Figures 5-5 (a) and (b) that the sound absorption of rubberised concrete especially at the higher frequencies is higher as the rubber content and rubber size increased. This is attributed to the porosity of RuC, as the rubber content increased the sound absorption coefficient also increases.. These findings are corroborated by (Sukontasukkul, 2009, Mohammed et al., 2012).

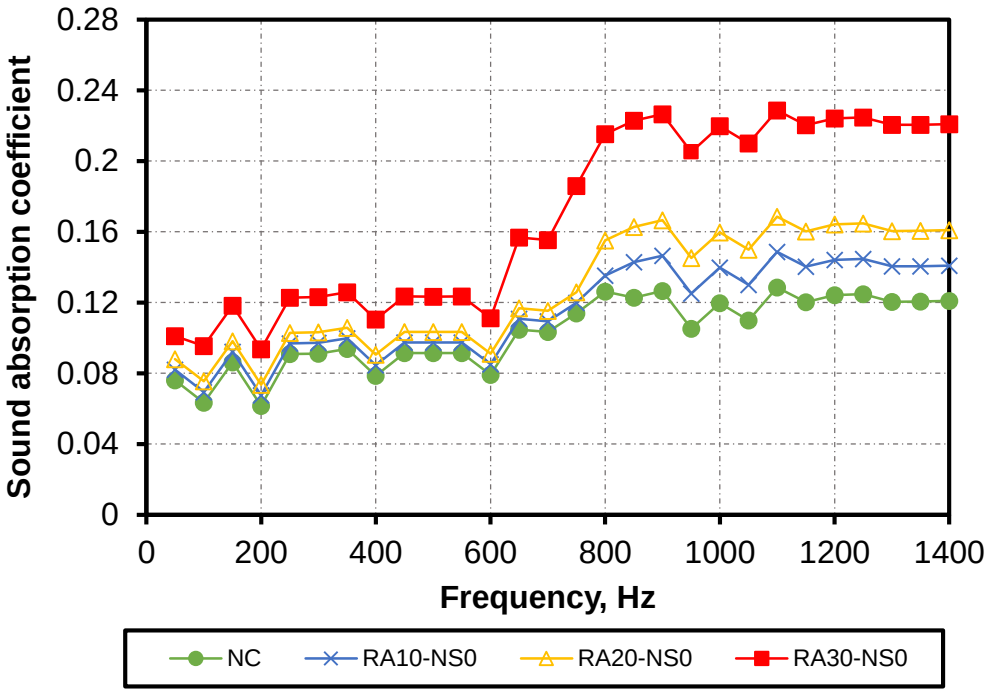

(a)

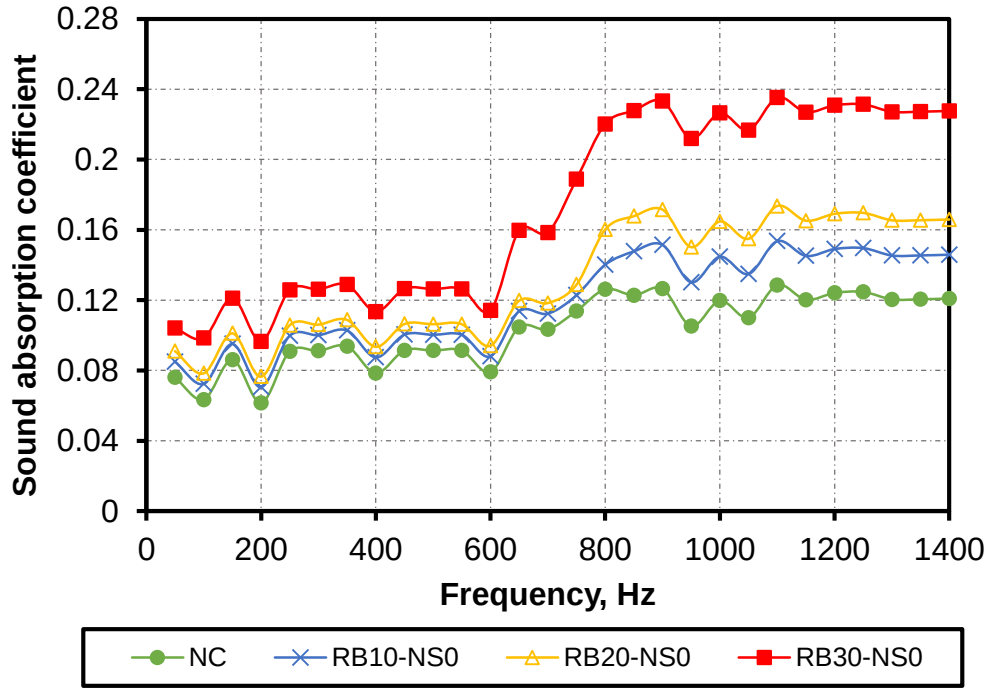

(b)

Figure 5-5 Acoustic absorption of RuC mixtures with (a) R_A, and (b) R_B

At frequencies lower than 600 Hz, there was marginal improvement in sound absorption coefficient compared to conventional concrete, whilst from 600 Hz up to 1.4kHz were significant enhancement regardless the size of rubber used. The control concrete sample had the smallest values for sound absorption coefficient along all frequencies not reaching above 0.2.

For R_uC mixtures, The mixes containing 30% of rubber particles show better sound absorption coefficient for larger particles of rubber on frequencies above 600 Hz. These findings corroborated by (Sukontasukkul, 2009, Mohammed et al., 2012). This improvement might be attributed to the ability of the sound to be absorbed by the entrapped air on the rubber surface. The mixture with R_A has a clearly lower absorption coefficient (0.3) than the mixtures with R_B. This can be explained by the fact that as the rubber size increases, the porosity tend to be higher coursed by the larger irregular rubber grains creating larger voids.

The influence of the addition of nano silica was studied on RuC made with R_A and R_B. The addition of NS is found to reduce the sound absorption coefficients as shown in Figure 5-6 and 5-7. This reduction in sound absorption can be described by the fact that the nano silica particles block the pores, resulting in an increase in sound reflection.

The addition of 1.5 and 3% NS (by weight of cement) resulted in no significant changes in acoustic absorption at the lower frequencies, as is seen in Figures 5-6 and 5-7 for RuC with R_A and R_B, respectively, however at higher frequencies there was an improvement in sound absorption by ~2% using 1.5% NS compared to 3%. This finding is similar to the influence of silica fume on sound absorption of crumb rubber hollow concrete block as obtained by Mohammed et al. (2012).

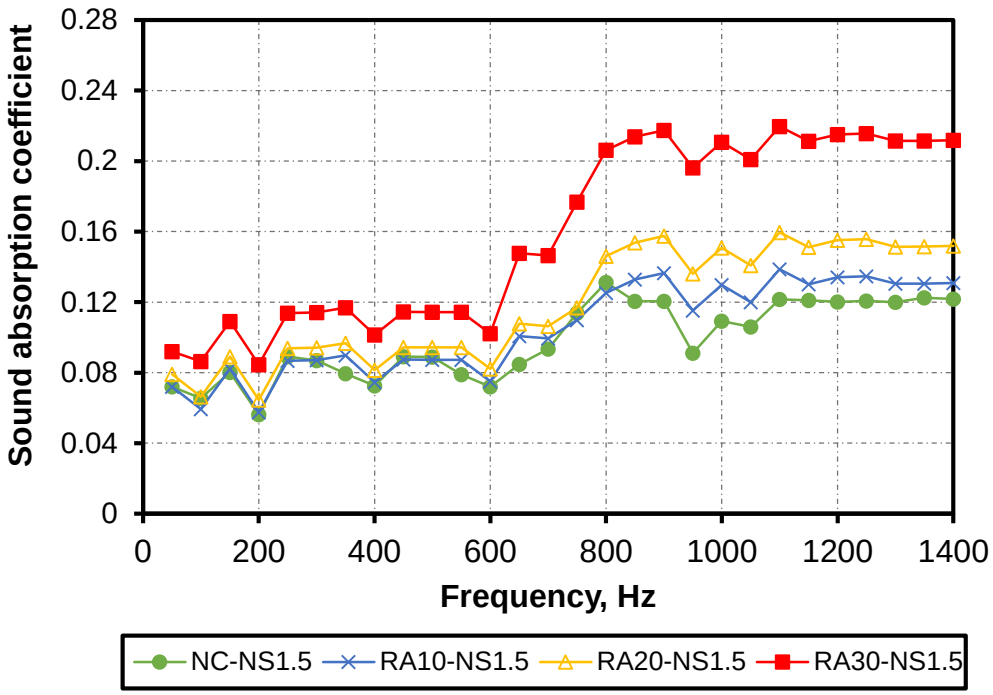

(a)

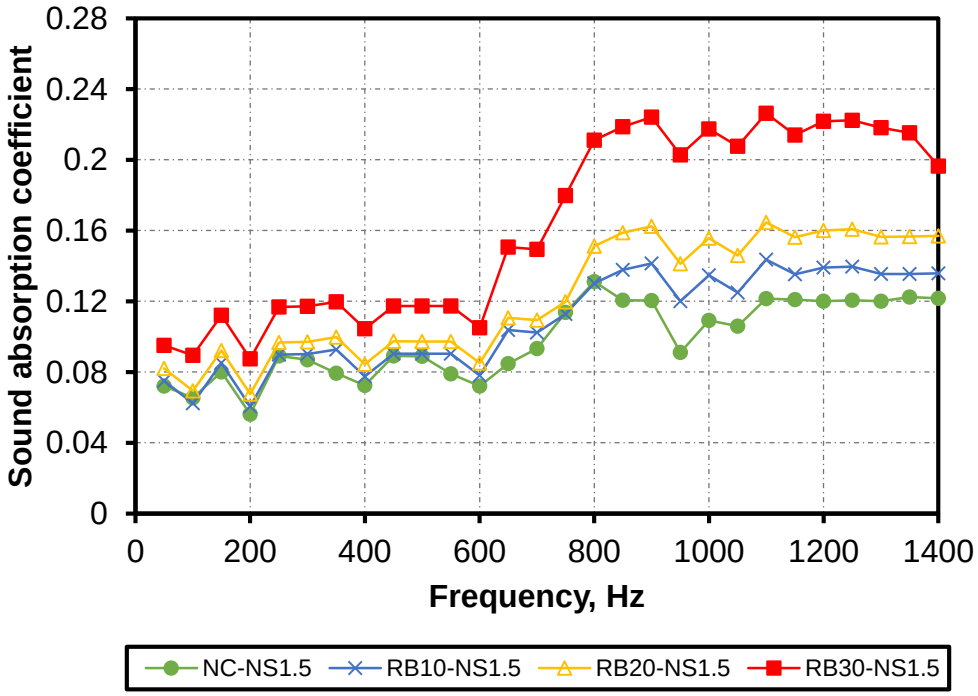

(b)

Figure 5-6 Acoustic absorption of RuC mixtures with 1.5 % NS for (a) R_A and (b) R_B

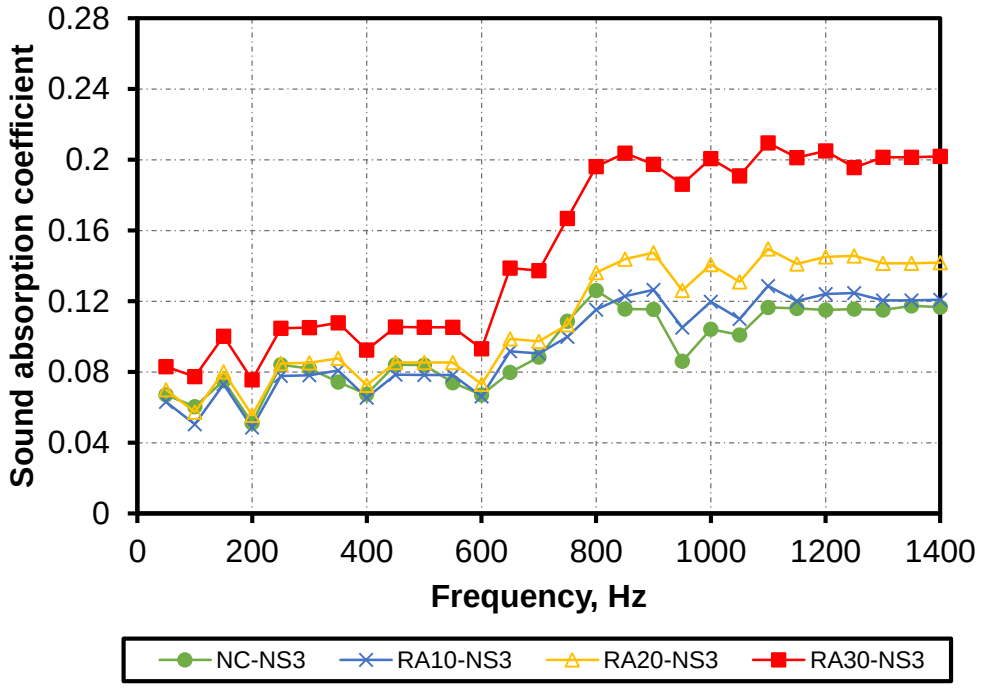

(a)

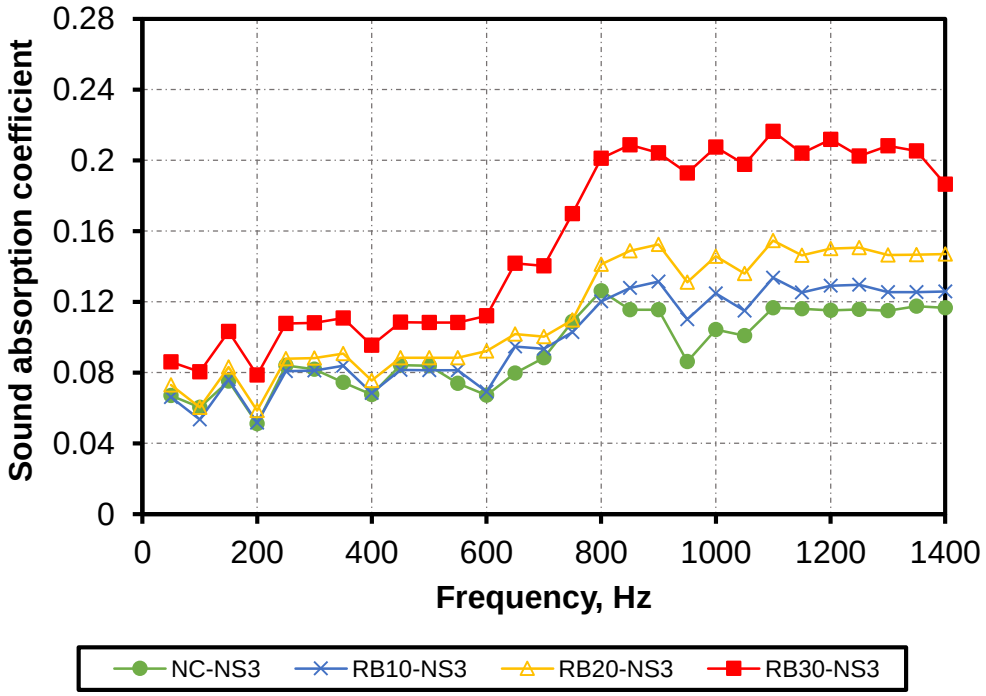

(b)

Figure 5-7 Acoustic absorption of RuC mixtures with 3 % NS for (a) R_A and (b) R_B

5.3.2 Dynamic modulus of elasticity

Dynamic modulus of elasticity (E_d) performance was determined by evaluating the effect of incorporating rubber and nano silica on damping properties of hardened concrete. The variation of dynamic modulus of elasticity of rubberised concrete with different proportion of NS for R_A and R_B is presented in Figure 5-8 (a) and (b), respectively. The results demonstrate that the dynamic modulus of elasticity values of the rubberised concrete decreased considerably with the increase of rubber content. For concrete with R_A, the decrease in dynamic modulus of elasticity was from 29.16% to 34.8% as the amount of rubber increased from 10% to 30%. However, the reduction was from 24.3% and 45.9% with the same increase in rubber level for the concrete with R_B. The utilisation of larger particles of rubber, R_B, in concrete showed more reduction on E_d than introducing smaller particles. Better vibration damping results from higher rubber content in concrete, for 30% rubber content in concrete samples.

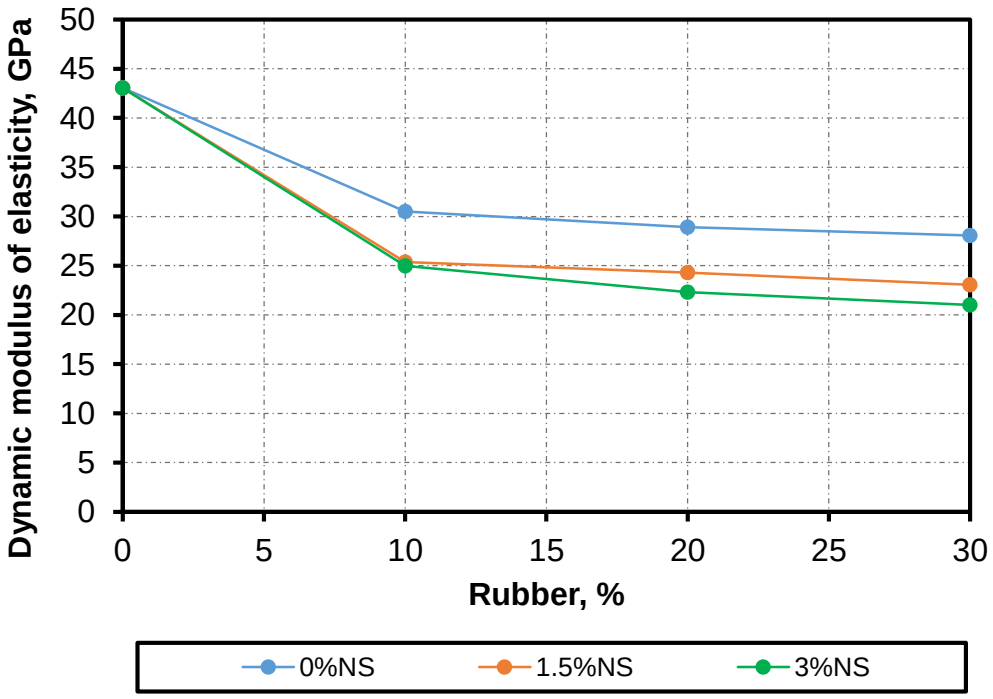

(a)

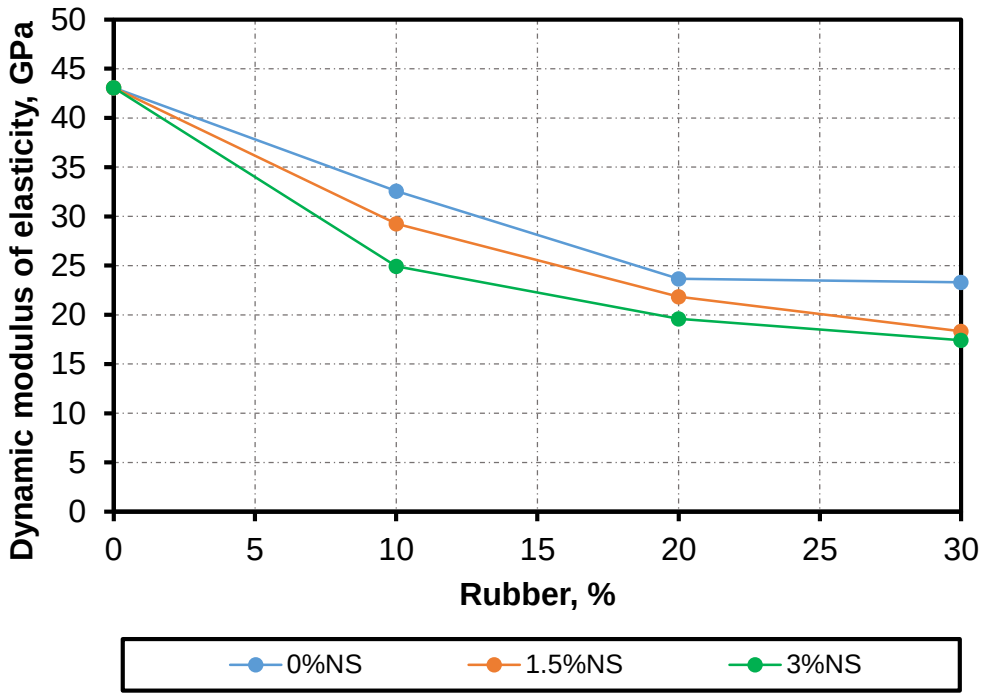

Figure 5-8 Relationship between dynamic modulus of elasticity and rubber content (a) R_A and (b) R_B

5.3.3 Acoustic Transmission Loss

Sound transmission is defined as the difference, measured in (dB) between the incident sound energy and the transmitted sound energy. The primary factor in transmission loss is the unit mass of the concrete, increasing with density of the material usually assessed over a range of frequencies. The relation between the transmission loss and density in general terms is related and is referred to as the mass law.

The sound transmission loss for rubberised concrete samples with various percentages of rubber for the two sizes of rubber R_A and R_B is presented in Figures 5-9 (a) and (B), respectively. It can be seen that as the percentage of rubber replacement increases in the concrete mixture the transmission decreased, this behaviour is related to the reduction in the density of the mixes.

The residual sound passing through the concrete was measured as loss of transmission.

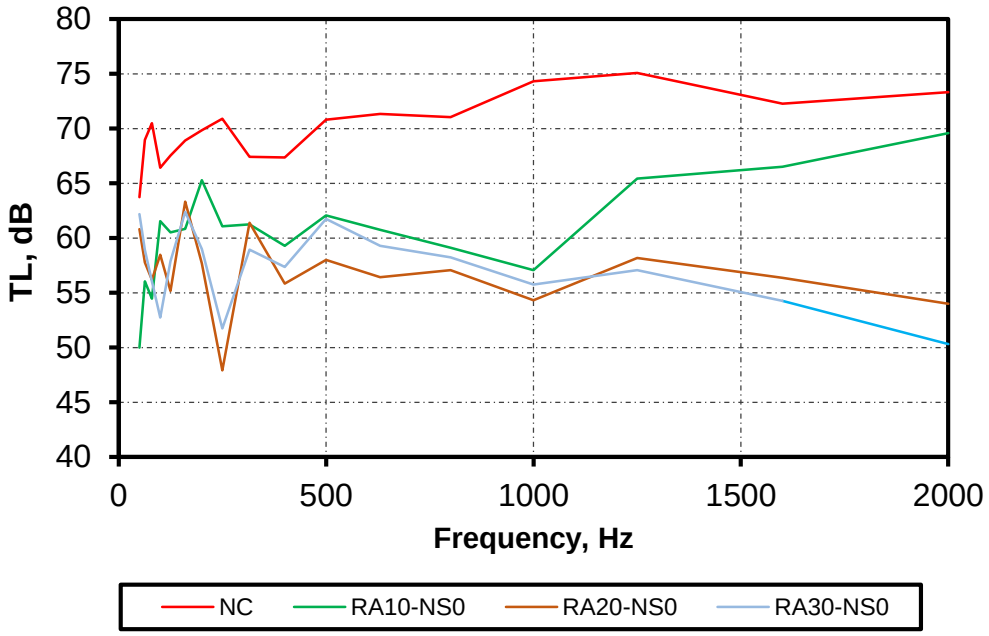

(a)

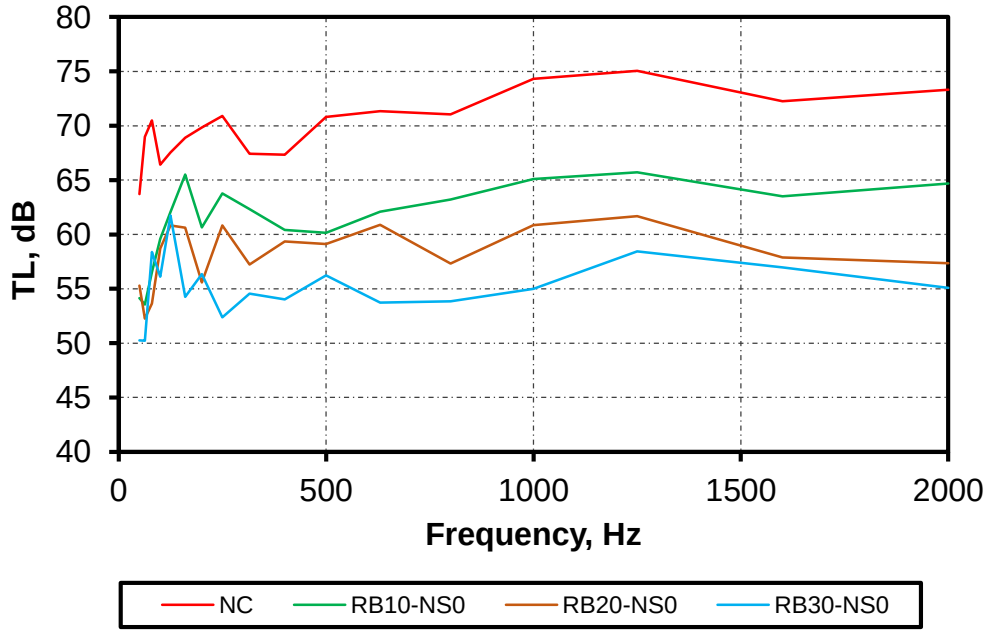

(b)

Figure 5-9 Transmission loss of rubberised concrete mixtures with (a) R_A, (b) and R_B

Overall, the transmission loss of the control mix is higher than the mixes with nano-silica and rubber especially at the lower frequencies this can be attributed due to the density and the porosity of the specimens. The effect of incorporating NS to the rubberised concrete sample helps by cementing the pores thus improving the transmission loss. Performance of mixes with R_A and R_B are presented in Figure 5-10 and figure 5-11, respectively. These figures show that there is a slight increase in TL for all rubberised concrete samples incorporating NS. This is due to the ability of NS to fill the pores in the matrix and hence, decrease the amount of air content in rubberised concrete mixture.

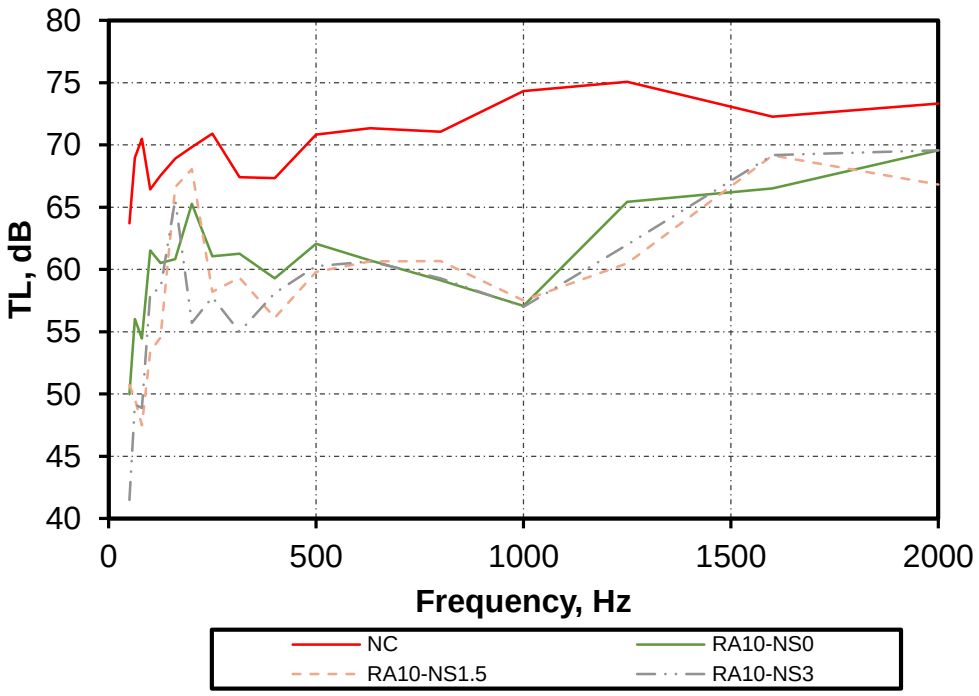

(a)

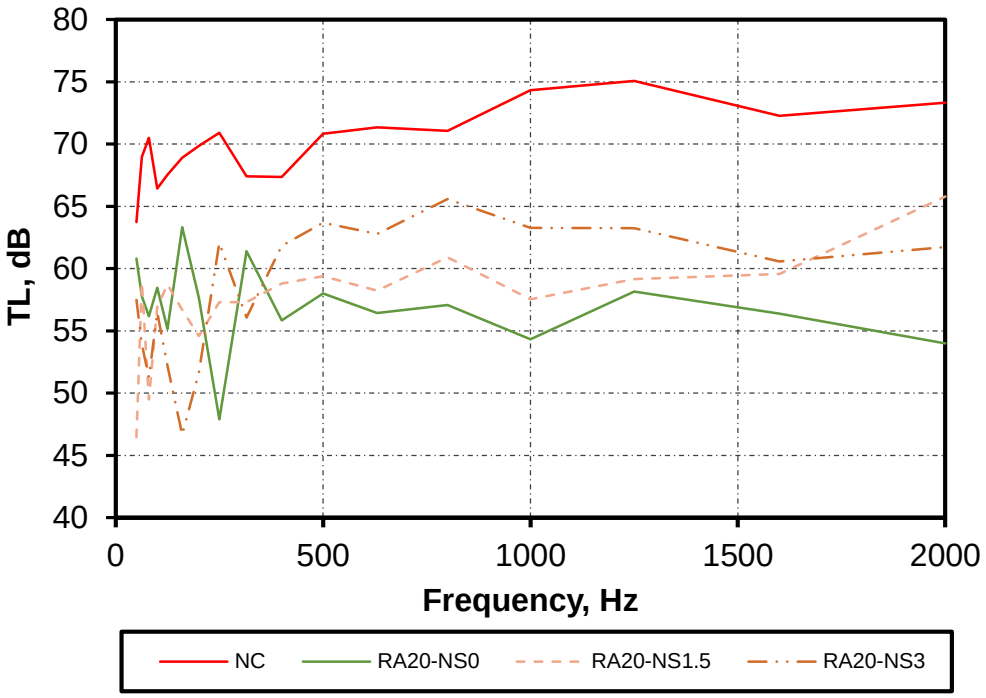

(b)

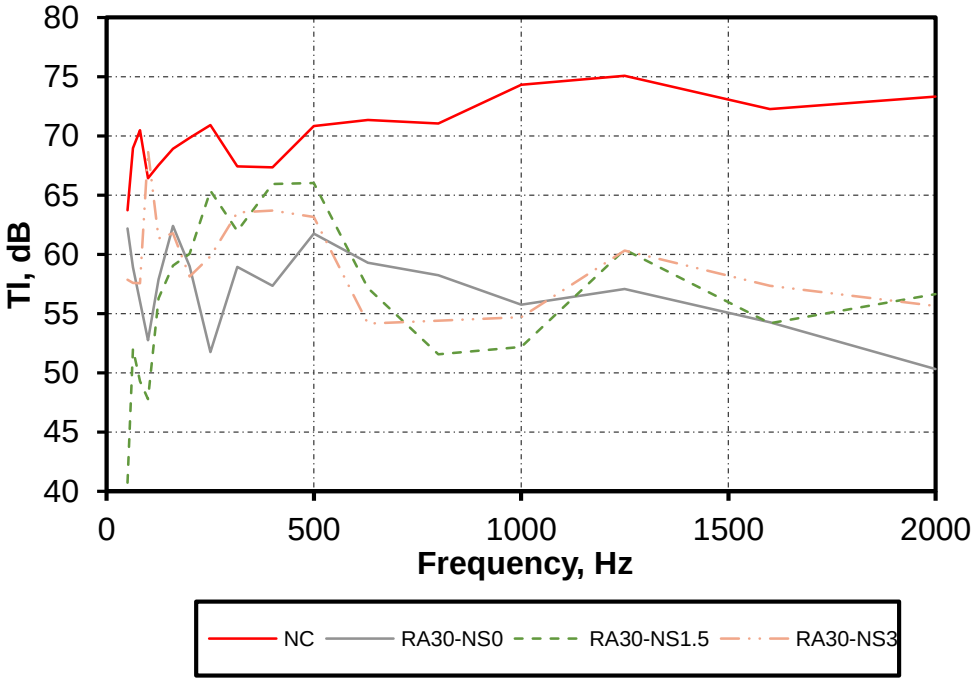

(c)

Figure 5-10 Transmission loss of rubberised concrete mixtures with (a) 10 %R_A, (b) 20% R_A and (c) 30%R_A

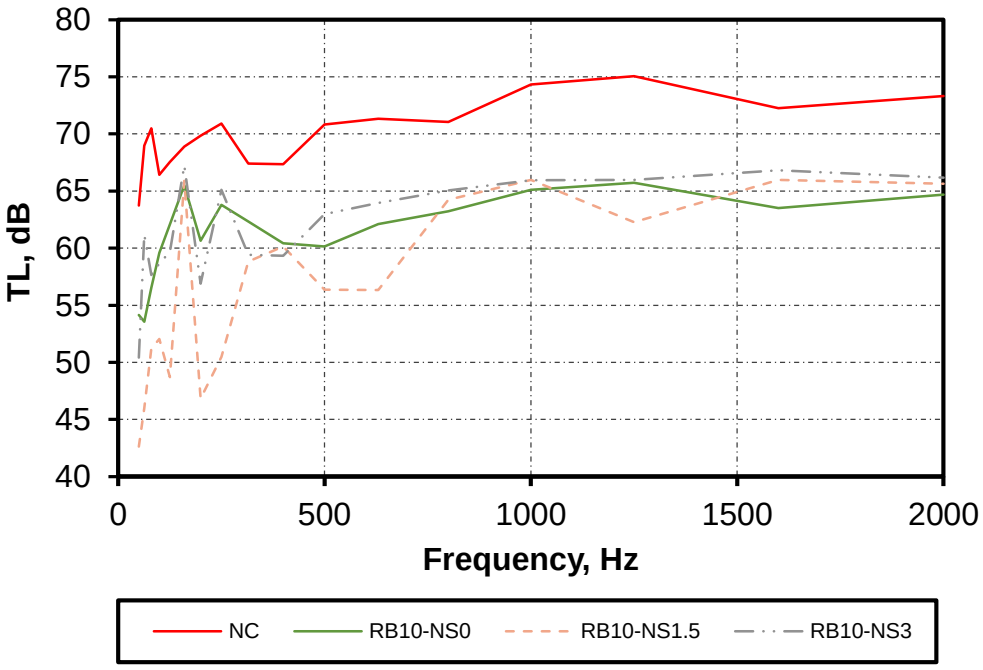
80
75
70
65
60
55
50
45
40
TL, dB
0
500
1000
1500
2000
Frequency, Hz
NC
RB10-NS0
RB10-NS1.5
RB10-NS3

(a)

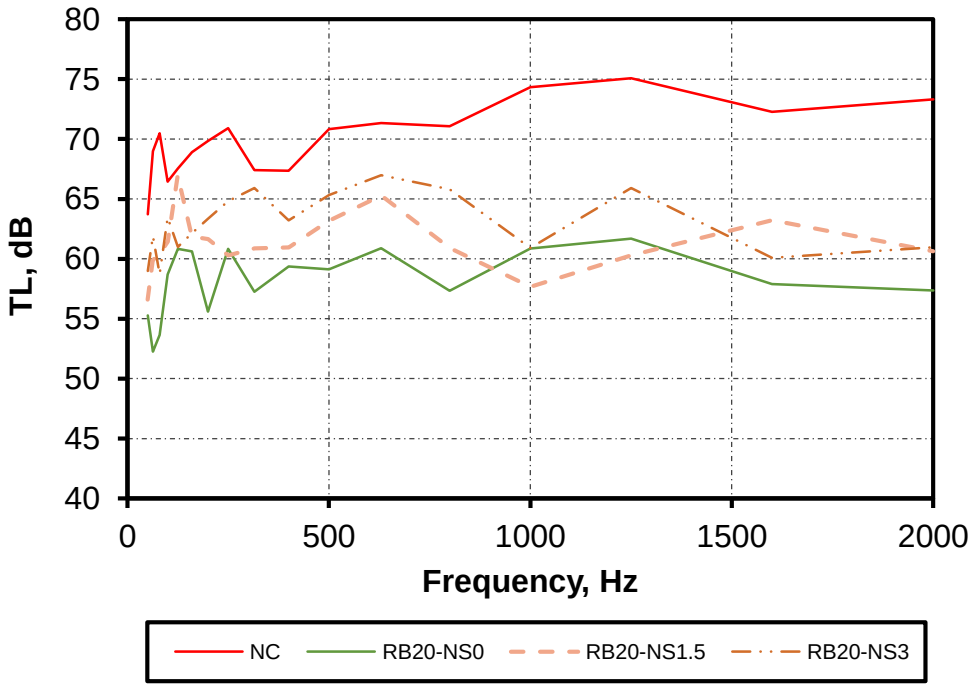
80
75
70
65
60
55
50
45
40
TL, dB
0
500
1000
1500
2000
Frequency, Hz
NC
RB20-NS0
RB20-NS1.5
RB20-NS3

(b)

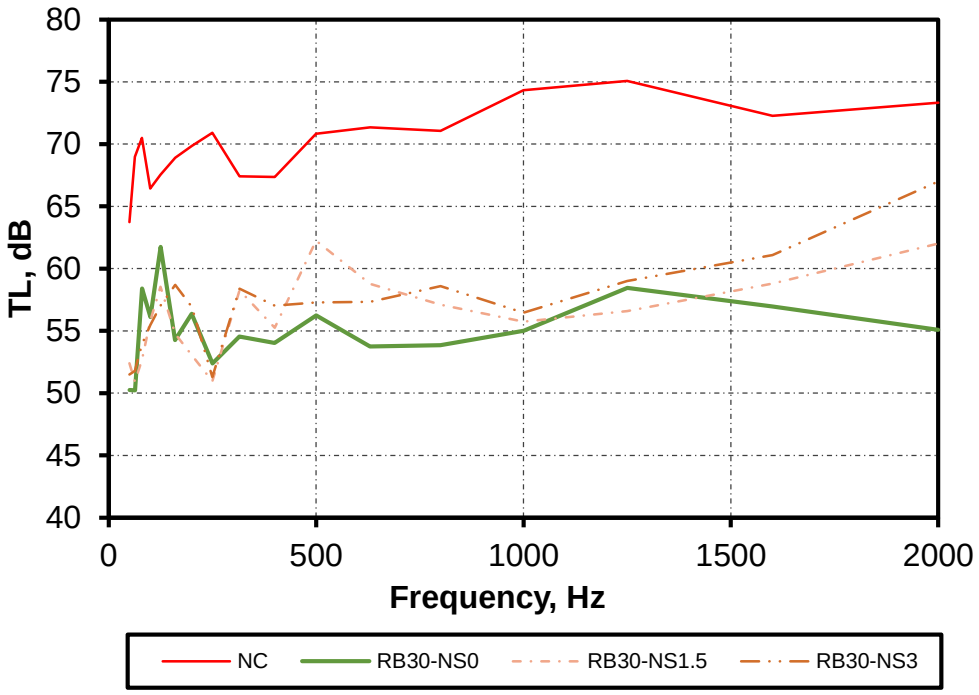

(c)

Figure 5-11 Transmission loss of rubberised concrete mixtures with (a) 10%R_B, (b) 20%R_B and (c) 30%R_B

5.4 Prediction of transmission loss

COMSOL Multiphysics software based on Finite Element Method (FEM) has been used to model the transmission loss performance of rubberised concrete. In this software solver, the mechanical module and the pressure acoustic module have been selected to develop a finite element model of a cylindrical disc section in combination with porous media module to model the transmission loss of concrete samples incorporating rubber and nano silica. This mathematical simulation has been built around the Nevair- Stokes equation as shown below (Multiphysics, 2008):

$$\rho\left(\frac{\partial u}{\partial t}+u.\nabla u\right)=-\nabla p+\nabla.\left[\mu(\nabla u+(\nabla u)^{T})-\frac{2}{3}\mu(\nabla.u)I\right] \quad (5.1)$$

where; u is the fluid velocity, p is the fluid pressure, ρ is the density of fluid, μ is the dynamic viscosity of fluid, $\rho\left(\frac{\partial u}{\partial t}+u.\nabla u\right)$ is the internal forces, $-\nabla p$ is the pressure forces, $\nabla.\left[\mu\left(\nabla u+(\nabla u)^T-\frac{2}{3}\mu(\nabla.u)I\right)\right]$ is the viscous forces and by applying the equation of motion:

$$\frac{\partial \rho}{\partial t}+\nabla.(\rho u)=0 \tag{5.2}$$

Hook's law has been applied, which is related to the stress tensor and the elastic strain tensor as shown in equation.

$$\sigma=\sigma_{ex}+C:\varepsilon_{el} \tag{5.3}$$

where C is the 4th order elasticity tensor, the 4th order elasticity tensor is used to capture the elasticity properties of the material more accurately over the whole frequency range, ":" stands for the double-dot tensor product (or double contraction). The elastic strain $\varepsilon_{el}$is the difference between the total strain and all inelastic strains.

There may be an additional stress contribution σ_{ex} with contributions from both initial and viscoelastic stresses. In case of geometric non-linearity, the second Piola Kirchhoff stress tensor and the Green-Lagrange strain tensor are used. The elastic strain energy density is

$$W_s=\frac{1}{2}\varepsilon_{el}:(C:\varepsilon_{el}+2\sigma_0)=\frac{1}{2}\varepsilon_{el}:(\sigma+\sigma_0) \tag{5.4}$$

In this expression initial stress contribution is assumed to be constant during the straining of the material.

Loss factor damping is only applicable in the frequency domain. When using loss factor damping, a complex constitutive matrix is used. With an isotropic loss factor $\eta_{s,}$ so that

$$D^c = (1 + j\eta_s)D \tag{5.5}$$

Where; D^c is the complex constitutive matrix used when computing the stresses, D is the constitutive matrix computed from the material data.

For a linear elastic material, this would be equivalent to multiplying Young's modulus by the factor$(1 + \eta_s)$. However, for a nonlinear elastic material, this applies to the tangential stiffness.

It is also possible to give individual loss factors for each entry in the constitutive matrix, this means that

$$D^c_{mn} = (1 + j\eta_s, mn)D_{mn} \tag{5.6}$$

In the case of an orthotropic material, but another option is available, where each individual component of Young's modulus and shear modulus can be given an individual loss coefficient:

$$E_m{}^c = \left(1 + j\eta_{E,m}\right)E_m \tag{5.7}$$

$$EG_m{}^c = \left(1 + j\eta_{E,m}\right)G_m \tag{5.8}$$

where, m = 1, 2, 3.

The complex moduli are then used to form the constitutive matrix. For hyper-elastic materials, the loss information appears as a multiplier in the strain energy density, and thus in the second Piola-Kirchhoff stress:

$$S = (1 + j\eta_s)\frac{\partial W_s}{E} \tag{5.9}$$

For loss factor damping, the following definition is used for the elastic part of the entropy:

$$S_{elast} = \alpha : (s - j\eta_s)(C : \varepsilon) \tag{5.10}$$

the S_{elast} here indicates the entropy contribution and not any stress. This is because the entropy is a function of state and thus independent of the strain rate, while the damping represents the rate-dependent effects in the material. The internal work of such inelastic forces averaged over the time period $2\frac{\pi}{\omega}$ can be computed as:

$$Q_h = \frac{1}{2}\omega\eta sReal\big(\varepsilon : Conj(C : \varepsilon)\big) \tag{5.11}$$

Q_h can be used as a heat source for modelling of the heat generation in vibrating structures, when coupled with the frequency-domain analysis for the stresses and strains.

The normal incidence transmission coefficient τ_∞ is determined from wave number and the characteristic impedance of acoustical material as

$$\tau_\infty = -2\frac{Z_c}{Z_o+2Z_c\cot(kd)+{Z_c^2}/{Z_o}}\frac{1}{\sin(kd)}e^{-k_o d} \quad (5.12)$$

where Z_o is the characteristic impedance of ambient air. Finally, the normal incidence sound transmission loss is obtained from

$$TL = -20log(|\tau_\infty|) \quad (5.13)$$

This set of equations have been implemented in COMSOL Multiphysics commercial package. The experimental results and COMSOL model predictions are compared in section 5.4.1.

The main parameters required for the simulation are density, loss factor, Modulus of elasticity and Poisson ratio for each mix. The range of these parameter values used in the model were listed in Table 5-1.

Table 5-1 Range of the input parameter values used in the model

Parameter	Range	
	Min	Max
Thickness (mm)	50	200
Density (kg/m^3	2178	2400
Modulus of elasticity (GPa)	17.4	43.1
Loss factor	0.0185	0.0833
Poisson ratio*	0.2	0.2

*kept constant for each mix

The sound pressure that is transmitted into the impedance tube is shown in Figure 5-12 (a), the model was developed using the frequency domain (1-2000Hz), with air inside the impedance tube described by the acoustics module and the concrete sample described by the solid mechanics module.

The structural mechanics module of commercial software COMSOL Multiphysics 4.2 was used to develop a finite element model (FEM) to predict the transmission loss of the concrete material. The concrete is characterised by the five parameters presented in Table 5-1., these parameters fully define the concrete samples using the mechanical module. Figure 5-12 (b) presents the acoustic pressure filed inside the impedance tube drawn in 2D to determine the transmission loss with the sound source at the top, sample in the middle of the impedance tube. Figure 5-12 (c) presents the finite element mesh composed of the whole impedance tube composed of rectangular elements, Figure 5-12 (d) presents the mesh of the specimen inside the impedance tube composed of finer elements.

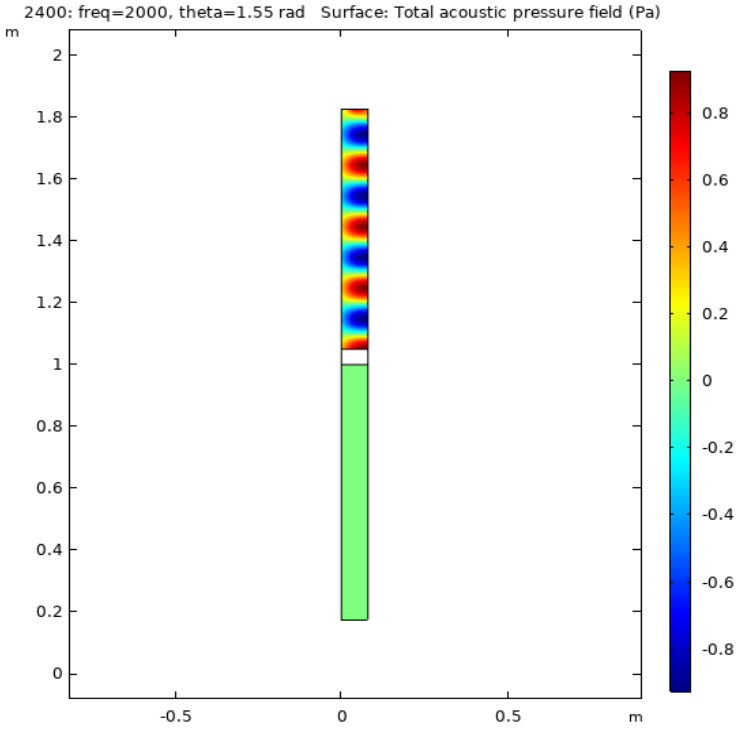
2400: freq=2000, theta=1.55 rad Surface: Total acoustic pressure field (Pa)
m
2
1.8
1.6
1.4
1.2
1
0.8
0.6
0.4
0.2
0
-0.5
0
0.5
m
0.8
0.6
0.4
0.2
0
-0.2
-0.4
-0.6
-0.8

(a)

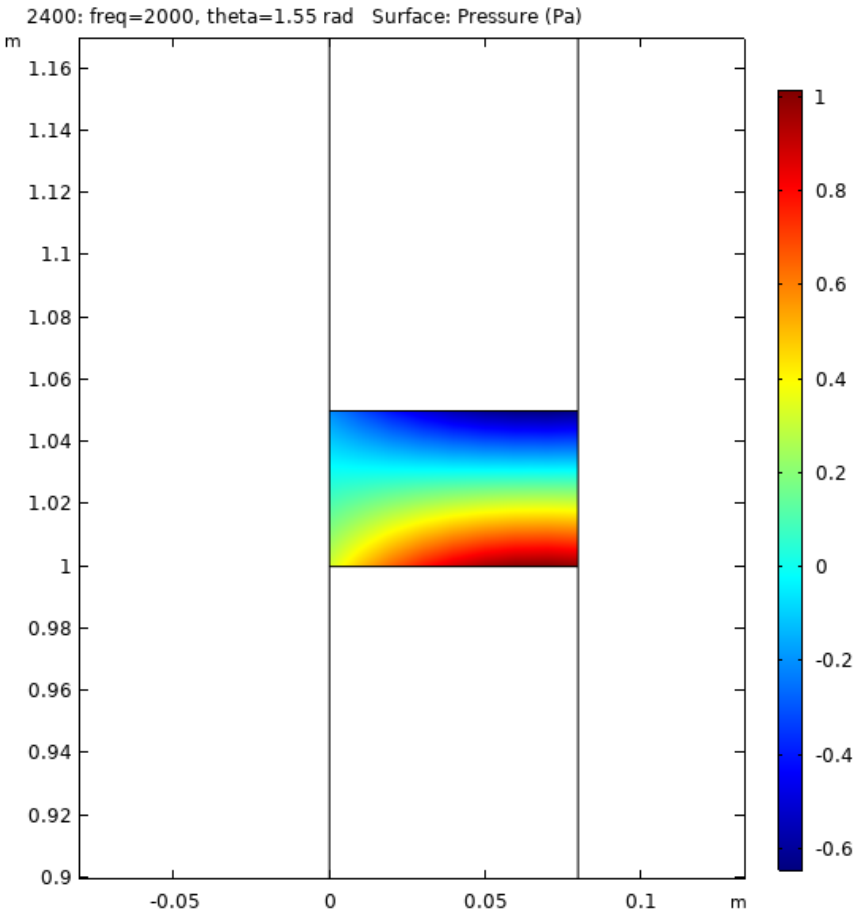
2400: freq=2000, theta=1.55 rad Surface: Pressure (Pa)
m
1.16
1.14
1.12
1.1
1.08
1.06
1.04
1.02
1
0.98
0.96
0.94
0.92
0.9
-0.05
0
0.05
0.1
m
1
0.8
0.6
0.4
0.2
0
-0.2
-0.4
-0.6

(b)

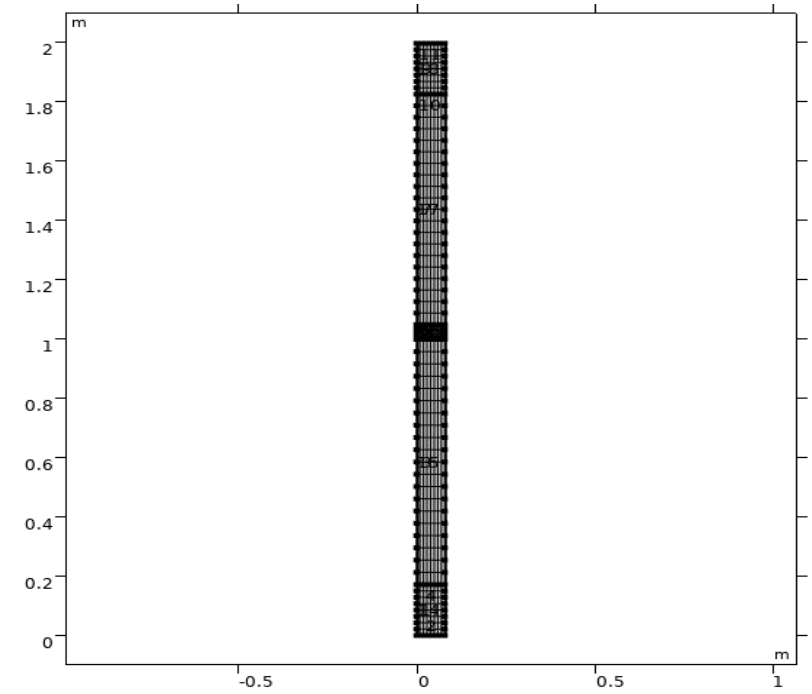

(c)

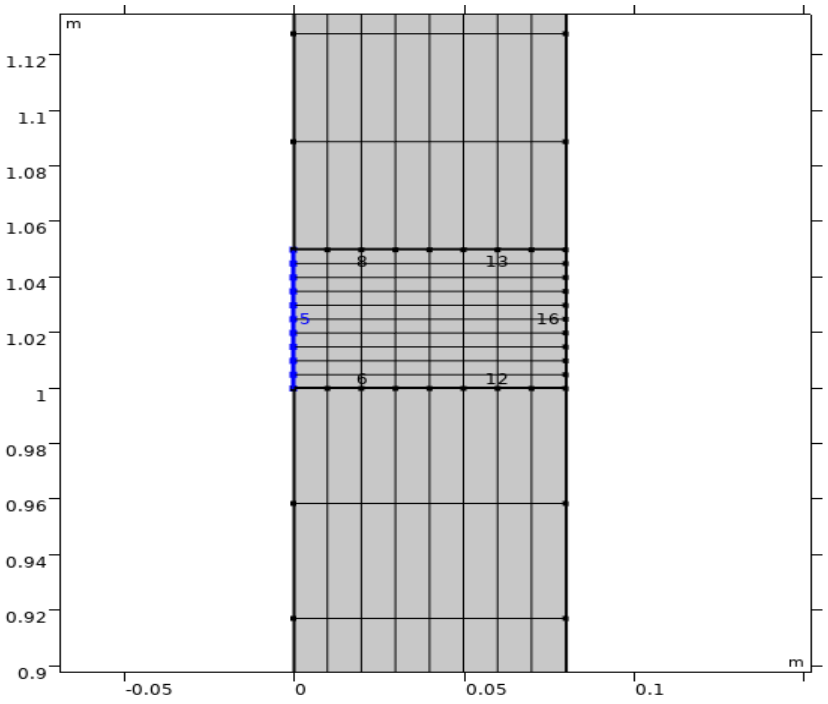

(d)

Figure 5-12 The model geometry adopted in COMSOL, (a) standing pressure waves in tube, (b) pressure profile in sample, (c) mesh of whole impedance tube, (d) finer mesh used for concrete specimens

The sound pressure that is transmitted into the impedance tube is shown in Figure 5-12 (a), the model was developed using the frequency domain (1-2000Hz), with air inside the impedance tube described by the acoustics module and the concrete sample described by the solid mechanics module.

5.4.1 Comparison with experimental measurement

In this section, the transmission loss values generated by FEM model are compared with the experimental values obtained from impedance tube for selected mixture as shown in Figure 5-13. The model overestimates by 10-25 dB the transmission loss in the frequency range below 300 Hz. Above this frequency, the agreement between the model and the measured data is within 0-15dB.

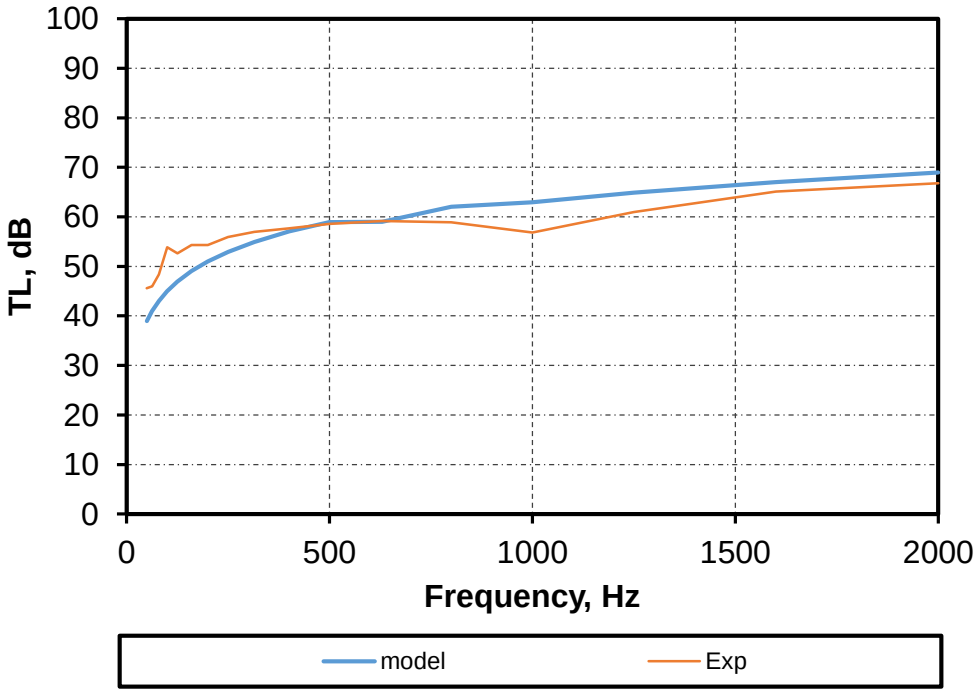

(a)

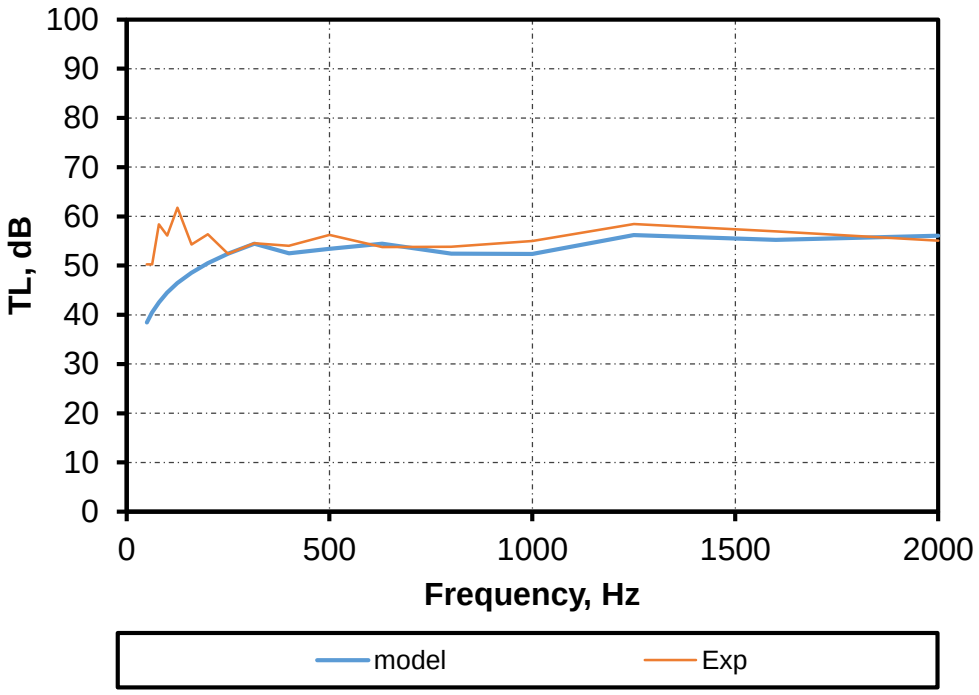
100
90
80
70
60
50
40
30
20
10
0
TL, dB
0
500
1000
1500
2000
Frequency, Hz
model
Exp

(b)

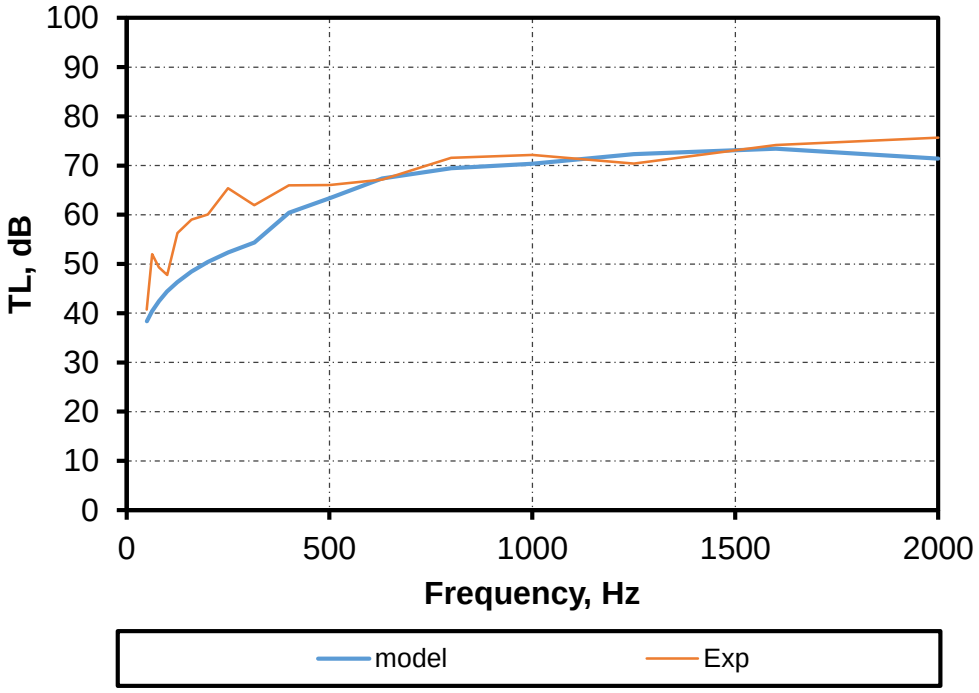
100
90
80
70
60
50
40
30
20
10
0
TL, dB
0
500
1000
1500
2000
Frequency, Hz
model
Exp

(c)

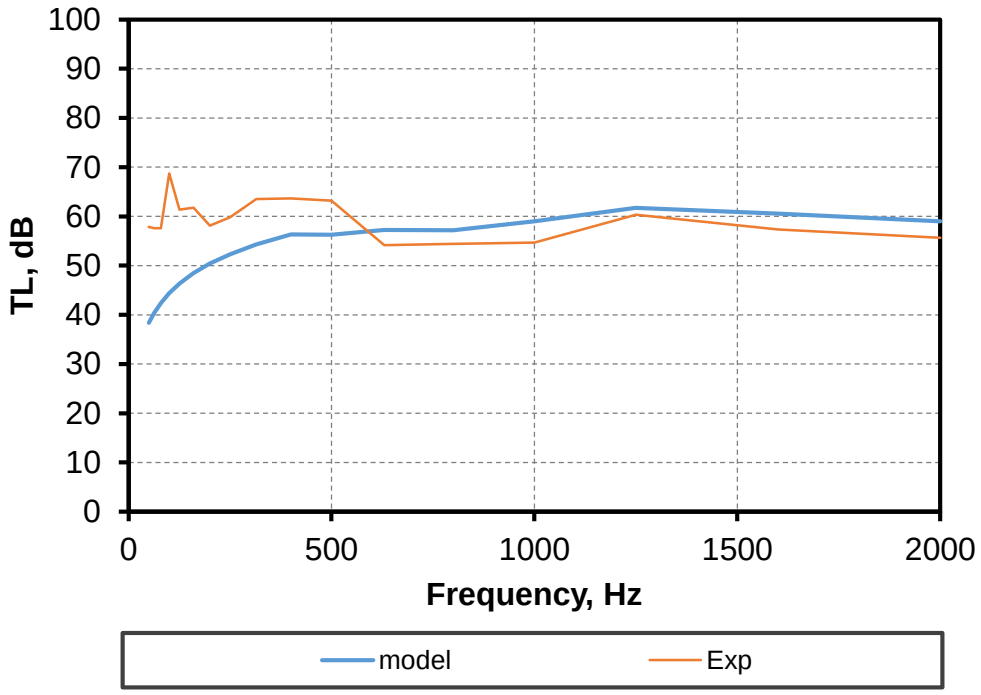

(d)

Figure 5-13 Comparison of experimental and predictive results of transmission loss (a) Control mix, (b) R30-0NS, (c) R30-1.5NS and (d) R30-3NS

5.4.2 Parametric study

This parametric study is mainly to determine the acoustic behaviour governed by four parameters (e.g. Thickness, Young's modulus, Density and Loss factor), the parameters are modelled based on the control specimen of concrete with one parameter changed and rest set to default values. The sensitivity of these parameters is crucial as it plays an important role in the design and development stages of predicting the TL of concrete. This prediction depends on the accuracy of the four parameters measurement.

In this study, it is found that the highest effect on transmission loss is from the thickness of concrete samples. As shown in Figure 5-14, thicker specimens gives higher TL this is in accordance with the empirical mass law. However, increasing

the thickness of concrete up to 200 mm shows a negative effect on the TL at a frequency higher than 1000 Hz, however for 200 mm sample the TL performance above 1600 Hz decreases this is due to the resonance phenomenon at higher density. From Figures 5-15 and 5-17, it can be observed that the effect of Young's modulus, density and loss factor on TL is negligible. In overall, the parametric study results show that the concrete samples can be developed to have an optimum TL performance, the outcomes of this study can be referred by noise control engineers on the selection of the sound insulation concrete materials for the noise insulation treatments.

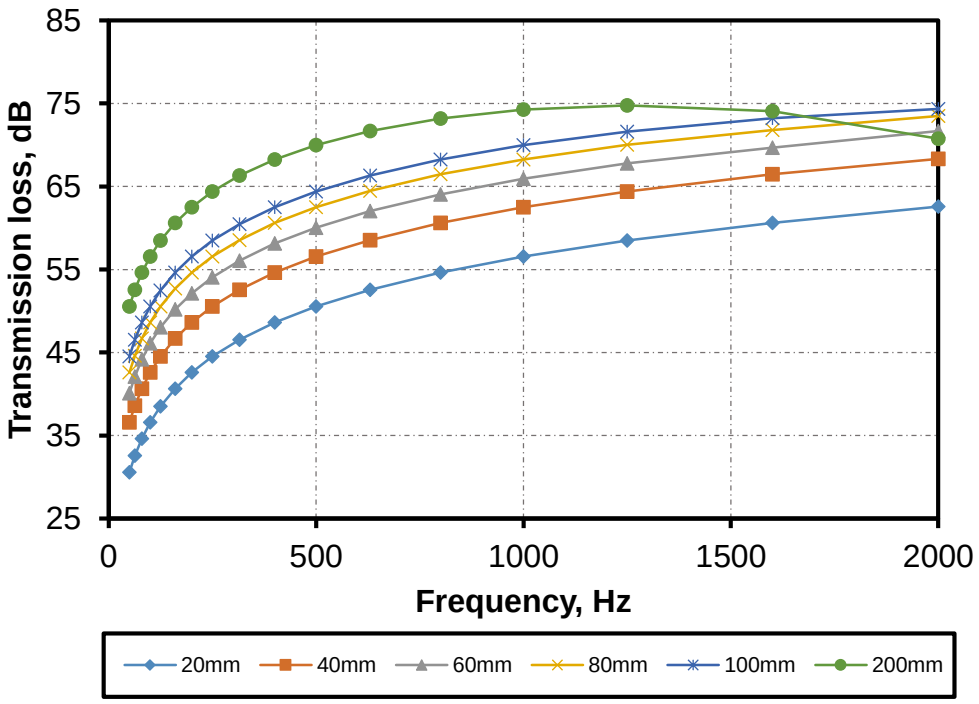

Figure 5-14 Effect of thickness on the transmission loss of concrete

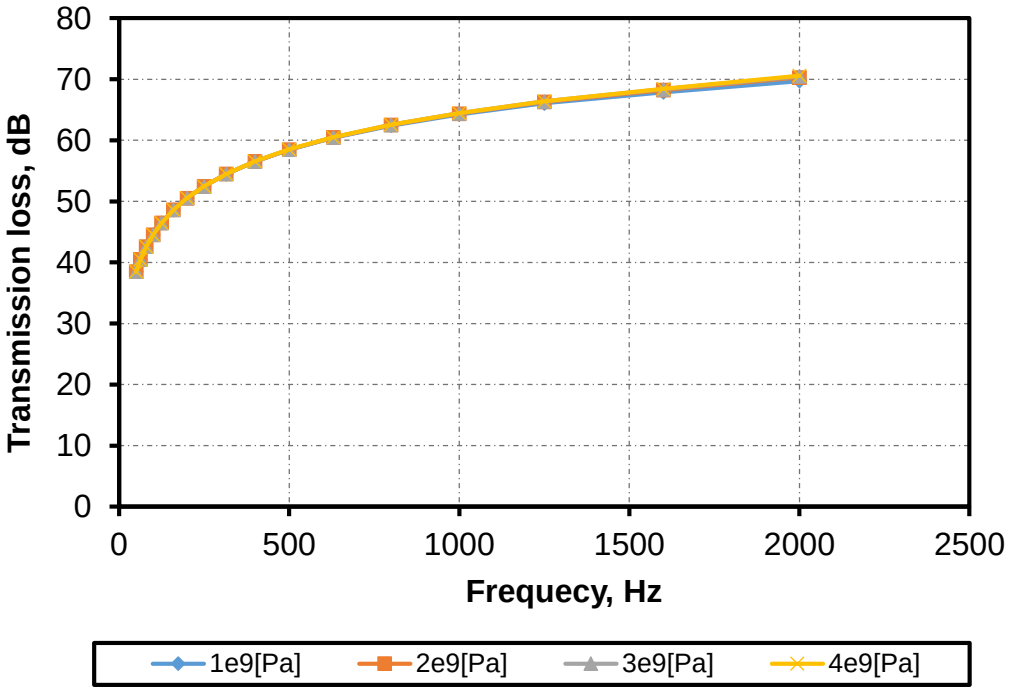

Figure 5-15 Effect of Young's modulus on the transmission loss

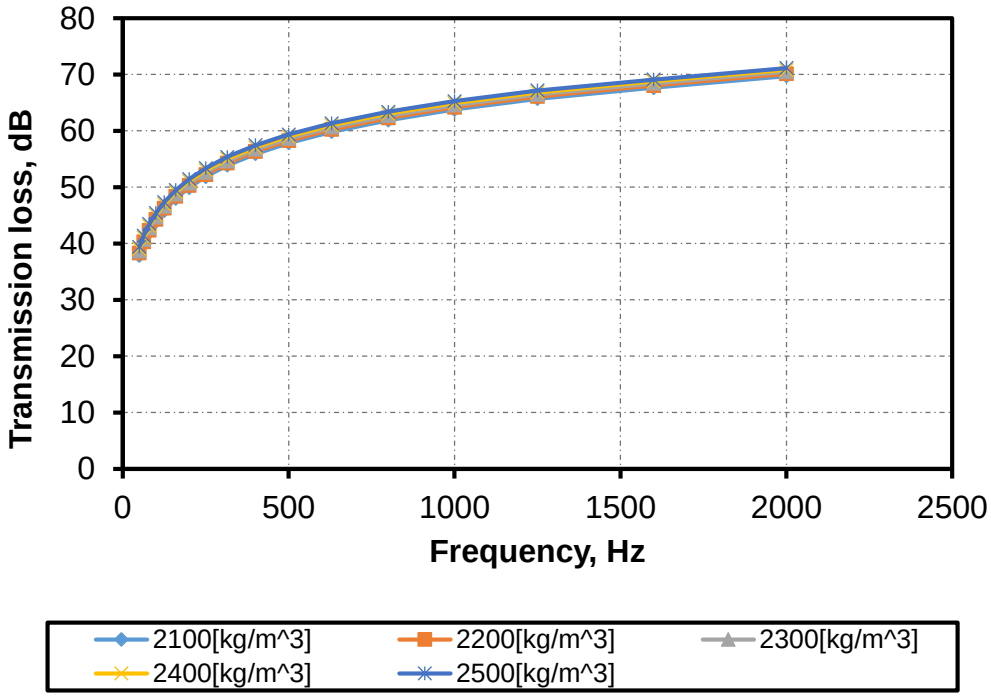

Figure 5-16 Effect of density of concrete on transmission loss

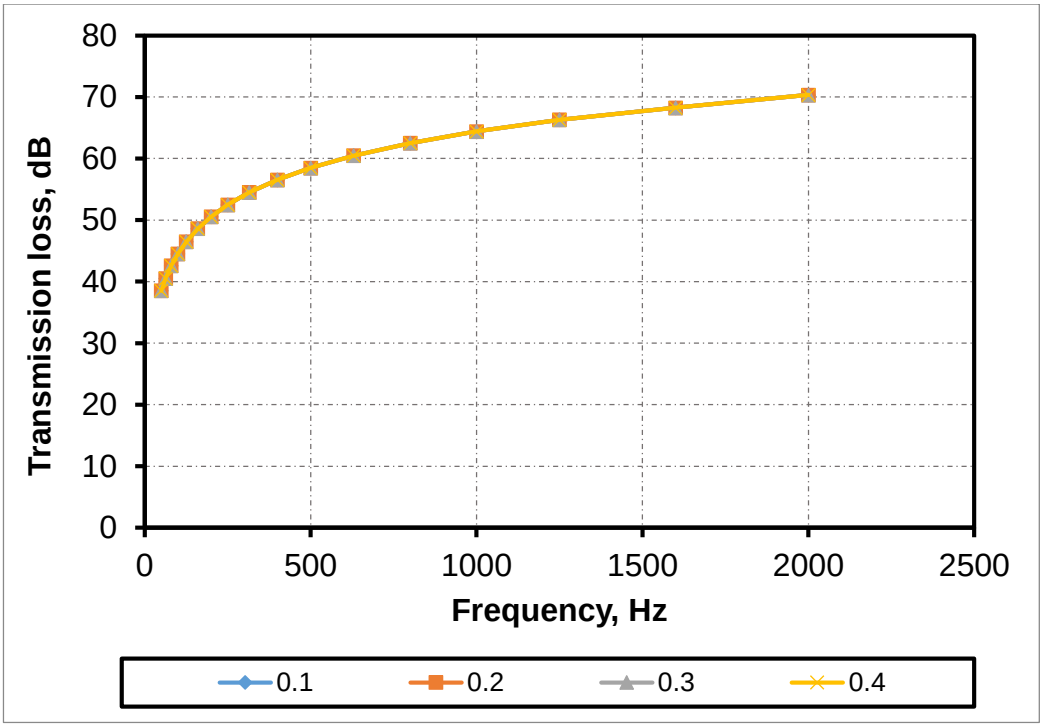

Figure 5-17 Effect of loss factor on the transmission loss

5.5 Impact sound insulation

Concrete designed for use for acoustic flooring must comply with Building Regulations Document E and be tested according to BS EN ISO 140 (1998).

This section discusses the sound insulation results of all rubberised concrete mixtures produced during the research investigation, following the impact sound insulation test procedure described in chapter three section 3.4.3.2.2. By comparing the 1/3 octave band spectra (dB) for each rubberised concrete sample between 32 and 2000 Hz. The lower the magnitude of the transmitted vibration, the better performing is the sample under test. Figures 5-14 (a) and (b) present the impact sound insulation data on rubberised concrete samples with R_A and R_B, respectively. A comparison is made on these figures with conventional concrete and this shows the remarkable utility of adding rubber particles to concrete on impact sound insulation at all frequencies. The performance improves as the

rubber content increase. At the frequency of 500 Hz, the impact sound insulation of RA30-NS0 is 48dB while the sound insulation reach 36dB for RB30-NS0. This indicates that the larger particle sizes of rubber increases the performance of rubberised concrete in sound insulation.

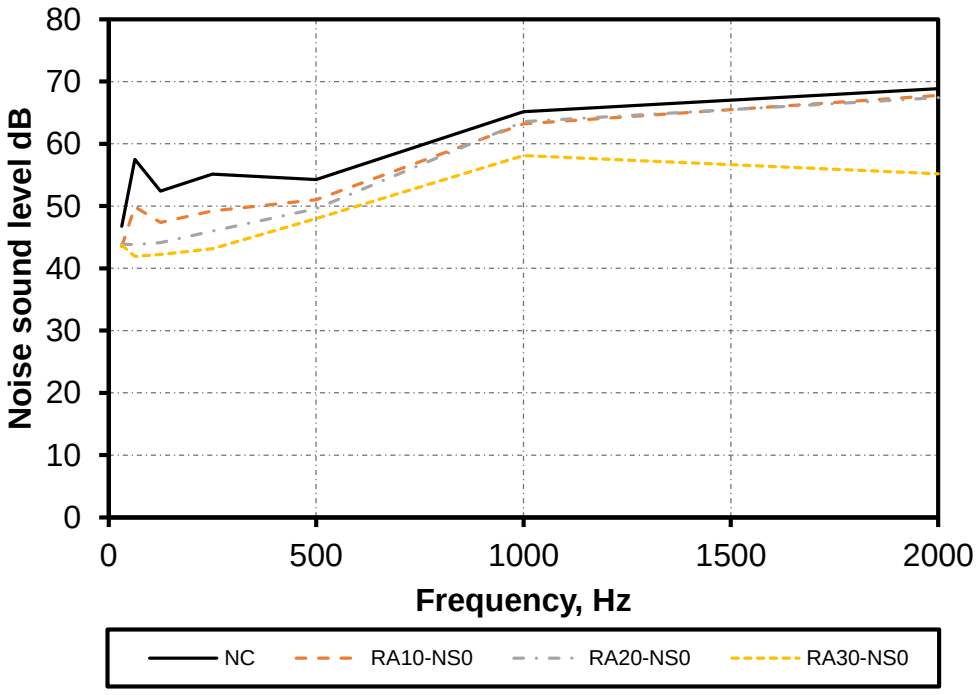

(a)

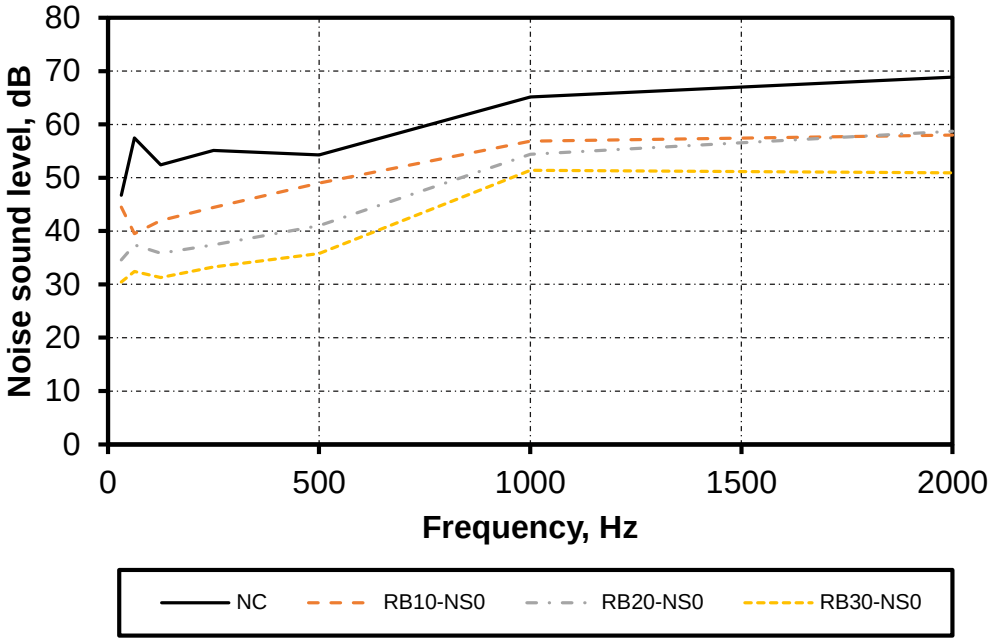

(b)

Figure 5-18 Acoustic insulation comparison between normal concrete and various rubberised concrete mixtures (a) With R_A and (b) with R_B

Figure 5-15 and Figure 5-16 show the effect of NS replacement on the impact sound insulation of rubberised concrete. With incorporating NS content, the sound insulation property slightly affected.

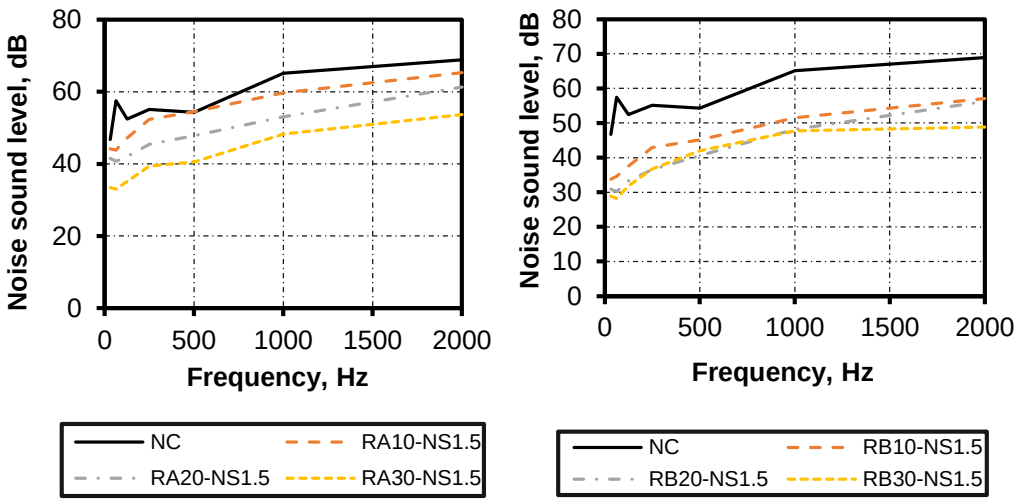

Figure 5.19 Effect of incorprating 1.5% NS on impact sound insulation of RuC

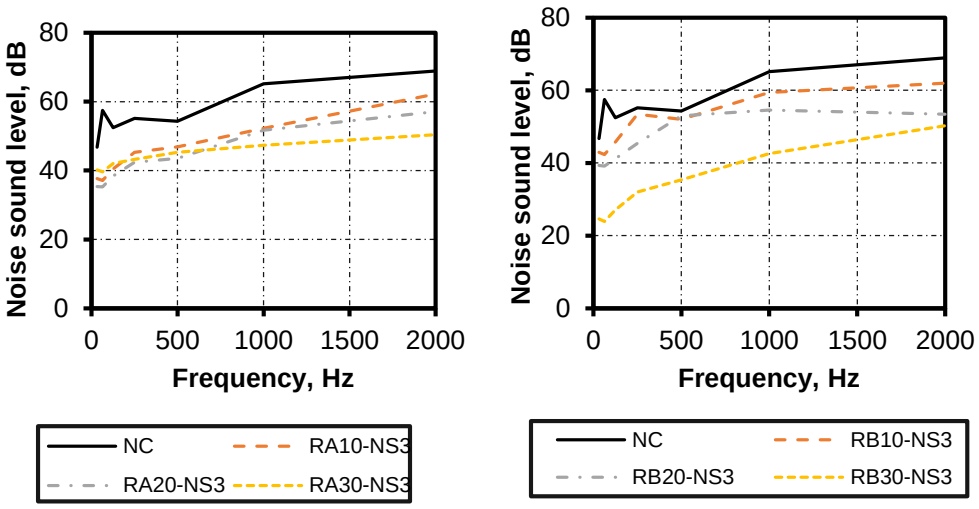

Figure 5-20 Effect of incorprating 3% NS on impact sound insulation of RuC

5.6 Conclusions

This chapter has investigated the influence of rubber content, rubber size, and nano silica content on the thermal conductivity, pore size, acoustic absorption, transmission loss and sound insulation of rubberised concrete. The conclusions from this study are summarized below:

- ✓ The rubberised concrete exhibits superior thermal and sound properties than normal concrete as measured by the reduction in thermal conductivity coefficient (k) and the increase in sound absorption coefficient (α), as well as transmission loss and sound insulation.
- ✓ The sound absorption coefficient of RuC with larger grain size of rubber is higher than that of smaller grain size.
- ✓ The dynamic modulus of elasticity of the rubberized concrete decreased substantially with the increasing of rubber content. Concrete mixtures with R_B caused a greater reduction on Ed than those with R_A.

- ✓ The transmission loss of rubberised concrete decreases as the percentage of rubber replacement increases due to an increase in the porosity of rubberised concrete and decrease in density.
- ✓ Rubberised concrete with 30% of rubber replacement has better sound absorption and lower transmission loss than conventional concrete.
- ✓ The addition of nano silica slightly effect the sound properties of rubberised concrete negatively due to the filling ability of nano silica resulting in reduction of concrete porosity.
- ✓ The FEM results showed that the models accurately reproduced the experimental behaviour of the transmission loss of rubberised concrete.
- ✓ The greatest effect on TL is from thickness of concrete sample. However, there is no significant effect of Young's modulus, density and loss factor on TL.

CHAPTER SIX - PREDICTION OF COMPRESSIVE STRENGTH OF RUBBERISED CONCRETE USING ARTIFICIAL NEURAL NETWORK

6.1 Introduction

In this chapter, artificial neural network model for predicting the compressive strength of rubberised concrete with and without nano silica have been developed. This chapter will cover the background and the principles of artificial neural networks (ANNs) as well as its advantages and disadvantages, training process of ANNs, experimental data, construction of the ANN model, parametric study and concluding remarks.

6.2 Background and Basic principle of ANN

In recent years, there has been a growing interest in applying artificial neural networks (ANNs) to predict and model various properties of concrete. ANN is defined as a soft computing technique that imitates the biological neural system of the human brain (Fischer and Igel, 2014). The first computational, trainable neural network was developed by (Rosenblatt, 1962) and (Rumelhart et al., 1986).

The ANN consists of at least three layers of neurons: An input layer, one or more hidden layers, and an output layer. All hidden layers are connected by weight, transport function and bias, while there is no link between nodes in the same layer (Fischer and Igel, 2014). A schematic representation of the neuron is shown in Figure 6-1.

A key aspect of ANN is that each input is multiplied by a weight and it is then given an independent term or bias. The result of the linear combination is applied

to a function that may be either linear or non-linear, which is called the activation function or transfer function that provides the neuron's output (Lippmann, 1987). Determining the number of hidden layers and the number of nodes in each hidden layer depends on the problem under investigation (Garzón-Roca et al., 2013). The difference between network output and the target is called an error function.

The error is propagated backward and both the biases and weights are fixed using specific optimisation methods that minimizes the error. The entire training process is repeated for a number of epochs. The training process can occur in a supervised or unsupervised manner. Supervised training means that the network is provided with sets of training data that include the expected output for each set of input. This means that the network is trained to learn specifics. However, in unsupervised learning, the learner has to learn from a set of inputs only, that is, to extract meaningful features from input data (Nehdi et al., 2001).

The validation step is used during the training of ANN to monitor the over-fitting of the NN and also act as an index to stop the training of the NN when validation error starts to rise (Londhe, 2009). This process can be expressed as a mathematical model in Figure 6-1:

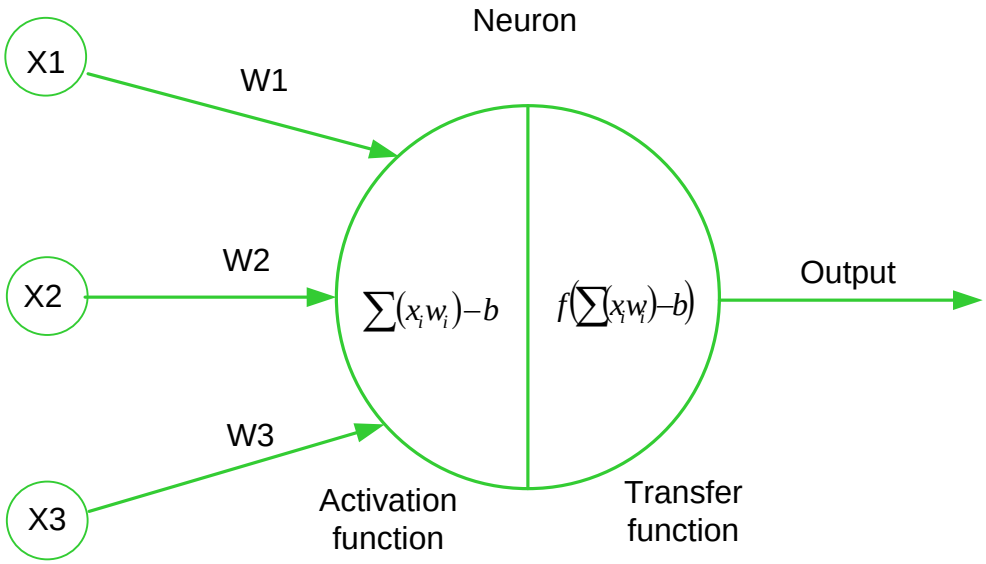

Figure 6-1 Artificial neuron model

$$Y = f(\sum_{i=0}^{n} w_i \; x_i \; - b \;), \; i = 1, 2, 3, \ldots\ldots\ldots n \qquad (6.1)$$

where; Y is the output, f is the transfer function, w_i is the weight of input and b is a bias.

6.3 Advantages and Disadvantages of ANN

ANN's strengths are due to their unique advantages that can be listed as follows(Gonzalez, 2000):

- Ability to automatically resolve non-linear complex relationships between inputs and output without the need for prior assumptions about the nature of these relations.
- High tolerance to noisy datasets.
- Ease of use
- adaptive to complex problems, by changing the network topology it would be able to handle different level of complexity

However, ANNs also have some weaknesses such as;

- Long training time
- Needs large number of data.
- Black box learning approach, it's hard to interpret and understand the relationship between input and output and cannot deal with uncertainties.
- Overfitting problem

6.4 Architecture of ANN

Previous studies have reported ANNs has a family of massively parallel architecture that can solve complex problems by collaborating with highly interconnected but simple computing. Most research is based on back-propagation neural networks (BPNNs) (Rumelhart, 1986, Haykin, 1999, Bal and Buyle-Bodin, 2013). Generally, the behaviour of the network depends on the way of interaction between the neurons. Besides the way of neurons' interaction, there are other elements, which build the ANN's architecture, and has direct impact on the behaviour of the network (Bandara et al., 2013). These components of ANN architecture are: the number of layers; the number of neurons in each layer; the transfer functions of each layer; the weights and biases; and the training algorithm.

6.4.1 Number of Layers and Neurons

It is important to mention that neurons are usually organised into layers for easier handling and mathematical describing of an ANN (Krenker et al., 2011). An optimum number of layers is generally depends on the number of training cases, the amount of noise in the target and on the complexity of the problem. In most practical problems, neural networks with three (input, hidden and output) layers or occasionally four (input, two hidden and output) layers are excessively used,

but five or more layers are rarely used (Jha, 2007). So far, there are no specific ways to determine the number of hidden layers.

To date, there is no specific formula for calculating the optimum number of neurons in each layer. (Wang, 1994, Boger, 1997) stated that the number of hidden layer neurons are 2/3 (or 70% to 90%) of the size of the input layer. Also, Blum and Rivest (1989) suggested that the size of the hidden layer neurons is between the input layer size and the output layer size. However, in order to select the best possible number of neurons in hidden layer, different trials of number of neuron in ANN are required. It has been found that NN may not be able to adequately represent the system if the number of neurons in the layer in the neural network is too small. On the contrary, it becomes over-trained if the network is too big (Yun and Bahng, 2000).

6.4.2 Transfer Function

The activation of each neuron is by the mathematical formula that predicts the output which is known by the transfer function (Meruane and Mahu, 2004). This function is another component of ANN architecture that also needs to be specified. Many forms of activation functions have been used to meet certain requirements according to the specific problem. In various ANN models, different activation functions have been used. These activation functions are formulated as follows: (a) Hyperbolic tangent sigmoid, (b) Logarithm sigmoid, (c) Linear, (d) Saturating linear and (e) Symmetric saturating linear. The most popular activation function used in the construction of ANNs is the sigmoid function, which illustrated in Equation 6.2.

$$f_{(Y)} = \frac{1}{1+e^{-Y}} \qquad (6.2)$$

6.4.3 Weights and Biases

The weights and biases are also other important factors of ANN architecture. The weights are utilised to scale the inputs which received from input neurons to the network or from neurons of the layer to neurons of the next layer. Weights are numerical parameters which show how strongly each of the neurons affects the other. However, bias is much like weight, except that it has a constant input of 1. Although the ANN can be created with or without the biases, the network with biases is more powerful than those without biases (Bandara, 2013). When ANN is trained according to a specified learning algorithm, a bias is only connected to neurons in the hidden and output layers with adjustable weighted connections (Caglar et al. 2008).

6.4.4 NN Learning

Supervised and unsupervised learning are two major learning methods to employ for neural networks. They can be used by any given type of neural network architectures (Krenker et al., 2011). The decision of utilising them is dependent on the existing data for training the network. Each of the learning method has many training algorithms. However, Back Propagation Neural Network (BPNN) and Learning Vector Quantisation (LVQ) are the most popular algorithm of supervised and unsupervised learning respectively (Abbas, 2013). The selection of learning algorithm has a vital impact on the performance of the ANN models.

6.5 Training and testing process of NNs

The ANN was developed using the popular MATLAB software package (MATLAB R 2018 a). There are several training algorithm provided in the MATLAB Toolbox namely;

- **Levenberg-Marquardt (LM), (trainlm);** this algorithm is suitable for training small- and medium-sized problems.
- **Scaled conjugate gradient (SCG), (trainscg);** this algorithm requires less memory. Training automatically stops when generalization stops improving.
- **Bayesian regularization (BR), (trainbr);** this algorithm requires more time, but can result in good generalization for difficult, small or noisy datasets.

To train the network, the weights of connections are modified according to the information it has learned. The difference between the output of the trained network and the target is called error. The error is propagated back and the weight and biases are adjusted to reduce the error. This process is repeated for a number of epochs until a desired accuracy in output is achieved.

To test the accuracy of a trained network, the correlation coefficient R is adopted. The coefficient is a measure of how well the independent variables considered account for the measured dependent variable. The higher the R value, the better the prediction relationship. Moreover, the mean squared error (MSE) was used to monitor the network performance for training the current neural networks. The closer the value of MSE to zero, the better the prediction is. MSE can be obtained by the following standard formula:

$$\mathrm{MSE} = \frac{\sum_{i=1}^{n}(T_i - A_i)^2}{n} \qquad (6.3)$$

where T_i and A_i are the target and actual network, respectively, and n is the total number of training dataset. The training process stops when any of the following conditions are satisfied:

- The maximum number of epochs is reached;
- The MSE of validation data set starts to increase for a specified number of epochs;
- The performance gradient falls below a minimum value.

6.6 Experimental database

The main purpose of this study is to develop an ANN model to predict the compressive strength of R_uC. The data were obtained from different sources available in the literature with experimental results obtained from this study.

To construct this model, a total number of 435 experimental data with partial or full replacement of fine aggregate with rubber were collected (Sukontasukkul, 2012, Al-Tayeb et al., 2013, Marie, 2016a, Daxini and Jaydevbhai, 2013a, Li et al., 2016a, Dong et al., 2013, Atahan and Sevim, 2008, Thomas et al., 2014, Batayneh et al., 2008b, Kumar et al., 2014, Reda Taha et al., 2008, Aiello and Leuzzi, 2010, Liu et al., 2016, Su, 2015, Grinys et al., 2012, Abusharar, 2015, Li et al., 2014b, Holmes et al., 2014, Mohammadi, 2014, Azevedo et al., 2012, Noaman et al., 2016, Balaha et al., 2007, Noor et al., 2016, Gupta et al., 2015, El-Gammal et al., 2010, Antil et al., 2014, Mohammed and Azmi, 2014, Hassanli et al., 2017, Youssf et al., 2014, Selvakumar and Venkatakrishnaiah, 2015, Mendis et al., 2017, Fan et al., 2017, Youssf et al., 2016, Mohammed and Adamu, 2018, Adamu et al., 2018b, Güneyisi et al., 2004). The details of data including their sources are presented in Appendix A. Table 6-1 shows the range of various input parameters used to train the ANN as well as the output.

Table 6-1Range of input and output parameters in database

	parameters	Range	
		minimum	maximum
Input	Water to Cement ratio,(W/C)	0.3	0.68
	Coarse aggregate, CA (kg/m^3)	233	1734
	Fine aggregate, FA (kg/m^3)	0	1256
	Crumb rubber , Cr (kg/m^3)	0	630
	Nano Silica, NS (kg/m^3)	0	15
Output	Compressive strength,f_c'(MPa)	2.5	80

The input data are divided randomly into three phases, namely; 70% for training phase, 25% for validation phase, and 5% for testing phase. The testing phase for assessing the network employs test specimens from the database, which should be used once only after training is complete. The main purpose of the validation phase is to arrest training when generalization stops improving. The frequency distribution of each variable element used in this study for training and testing are shown in Figure 6-2 to Figure 6-6.

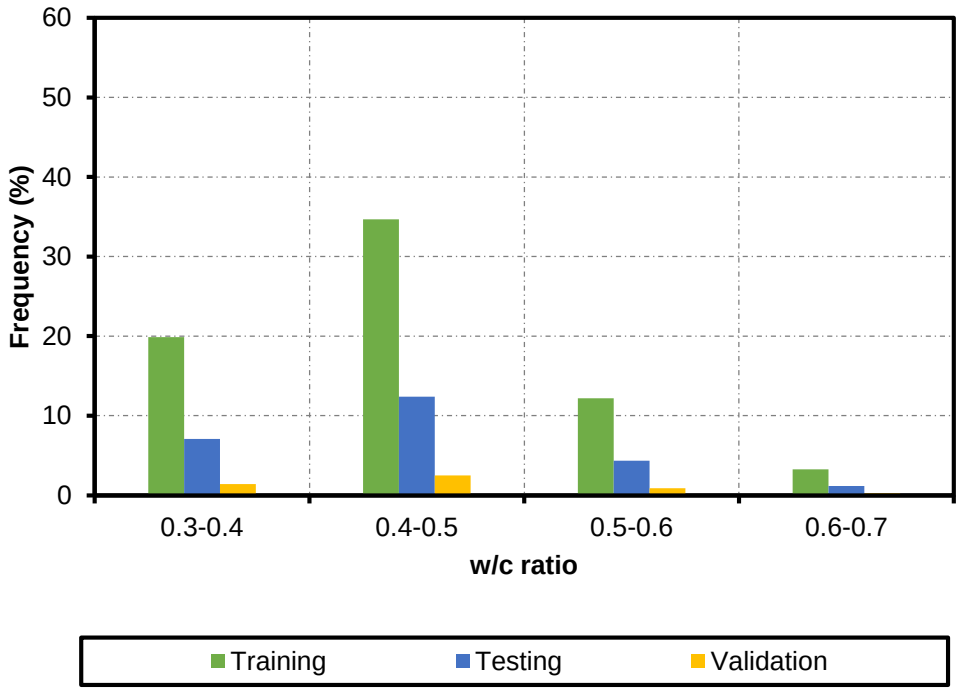

Figure 6-2 Frequency distribution of water/cement ratio

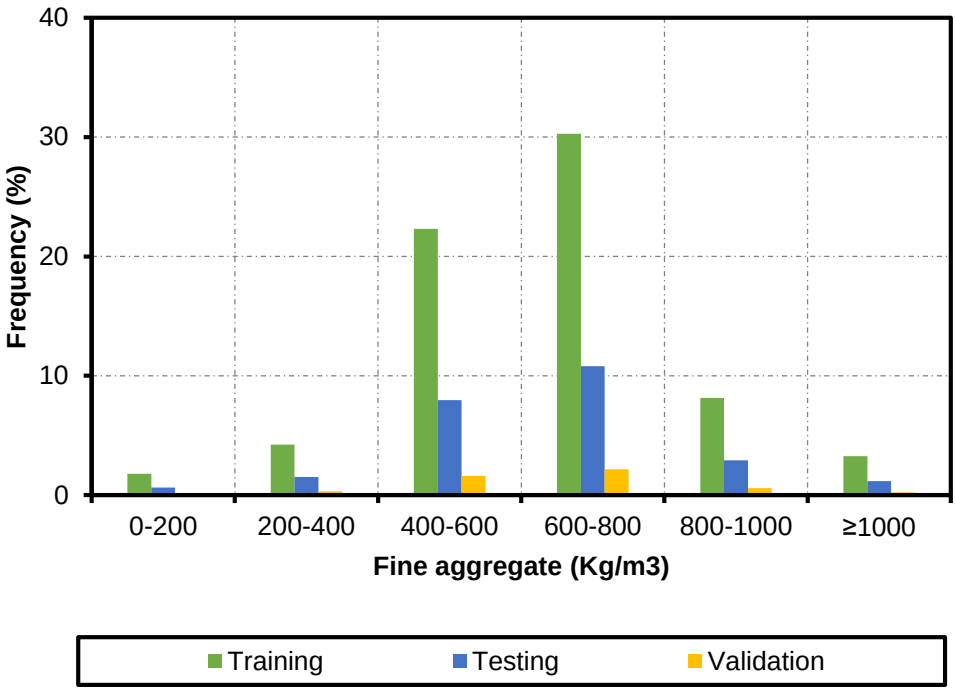

Figure 6-3 Frequency distribution of fine aggregate content

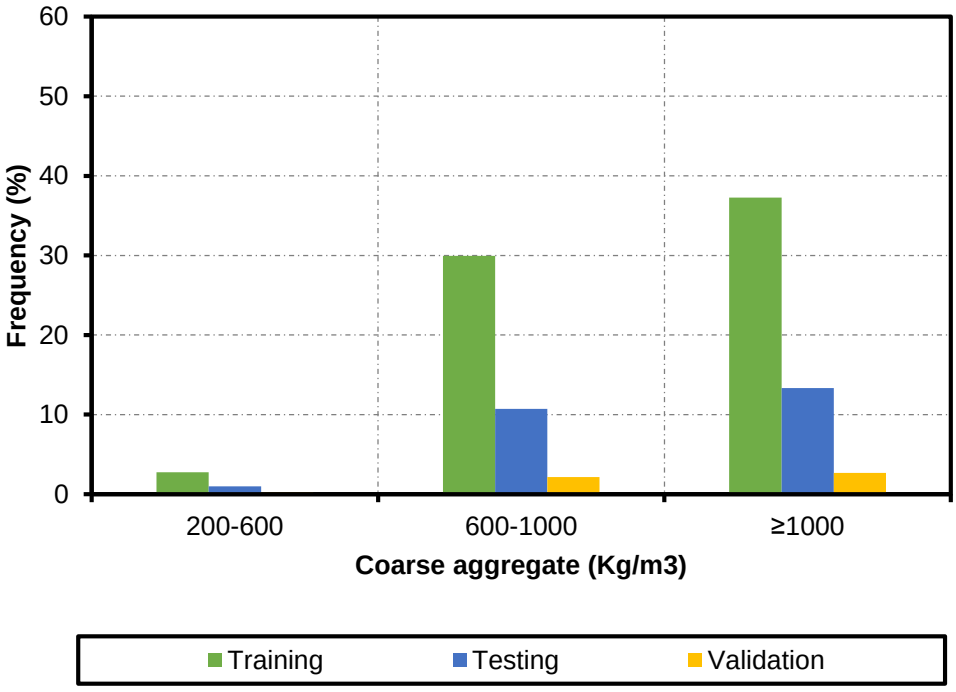

Figure 6-4 Frequency distribution of coarse aggregate content

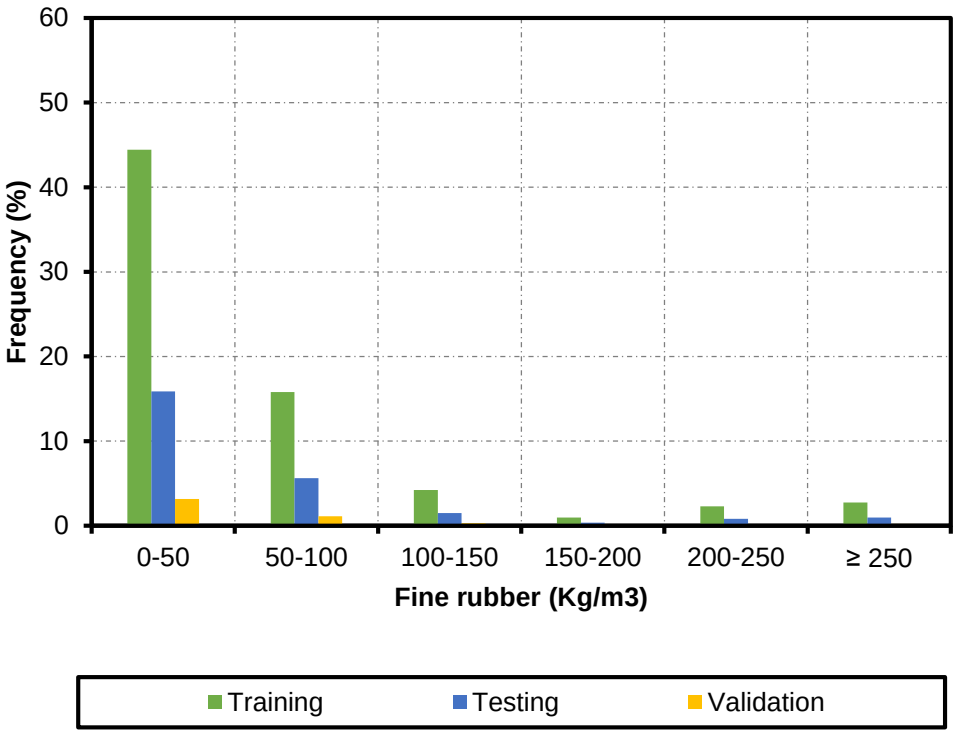

Figure 6-5 Frequency distribution of rubber aggregate content

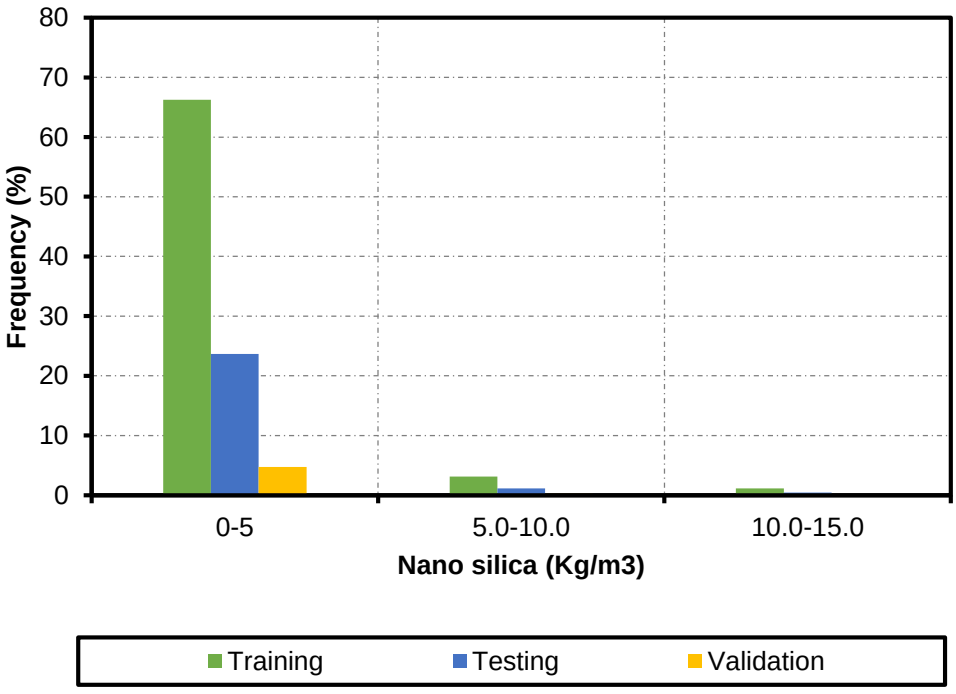

Figure 6-6 Frequency distribution of nano silica content

6.6.1 Data normalisation

Preprocessing steps can be made in the network input data and targets to enhance the efficiency of neural network training. Raw input data can be prepared to be suitable for the training when the normalisation process is used for such data. As reported by Bashir and Ashour (2012) and Bandara et al. (2013) normalising the input and output parameters prior they are used in training the artificial neural network model is important for many reasons, it will scale the data values to be at the same range to minimise bias within the neural network. Normalized data can also speed up training time by starting the training process for each feature within the same scale. The sigmoid transfer function is sensitive to input values in the range -1 to +1, thus the input data should be scaled to match this range. That was done according to (6.3):

$$\mathrm{I_{scaled}} = \frac{2\times(\mathrm{I}-\mathrm{I_{min}})}{\mathrm{I_{max}}-\mathrm{I_{min}}} - 1 \qquad (6.4)$$

where; $\mathrm{I_{scaled}}$ the normalised input variable, I is the value of the variable to be normalised, $\mathrm{I_{max}}$ is the maximum value of the variable used in the training set and $\mathrm{I_{min}}$ is the minimum input values.

6.7 Construction of ANN model

The neural network (NN) models are developed using neural network Toolbox in (MATLAB R2018a). Three ANN sets, namely ANN1, ANN2 and ANN3 have been constructed with one hidden layer with different number of neurones in the hidden layer. In the present study, a sigmoid transfer function and a linear transfer function were used in the hidden layer and output layer, respectively (Jadid and Fairbairn, 1996). The models were trained through multiple iterations. The

number of iteration is an indication of the number of times the weights have been recalculated until a satisfactory model with the highest correlation is obtained.

Table 6.2 shows the input parameters and the number of specimens used in each set to predict compressive strength of rubberised concrete. The database used in ANN1 and ANN2 are all experimental data with and without nano silica, whilst ANN3 only include data of rubberised concrete mixes with nano silica. The output neural network layer was the compressive strength f'_c in each set. The typical network architecture for ANN is shown in Figures 6-7.

Table 6-2 Artificial neural network selection

Model	No.of database	Input parameter
ANN1	435	Water/cement ratio, Coarse aggregate content (CA), Fine aggregate (FA), Fine rubber (Fr)
ANN2	435	Water/cement ratio, Coarse aggregate content (CA), Fine aggregate (FA), Fine rubber (Fr) and Nano silica (NS)
ANN3	58	Water/cement ratio, Coarse aggregate content (CA), Fine aggregate (FA), Fine rubber (Fr) and Nano silica (NS)

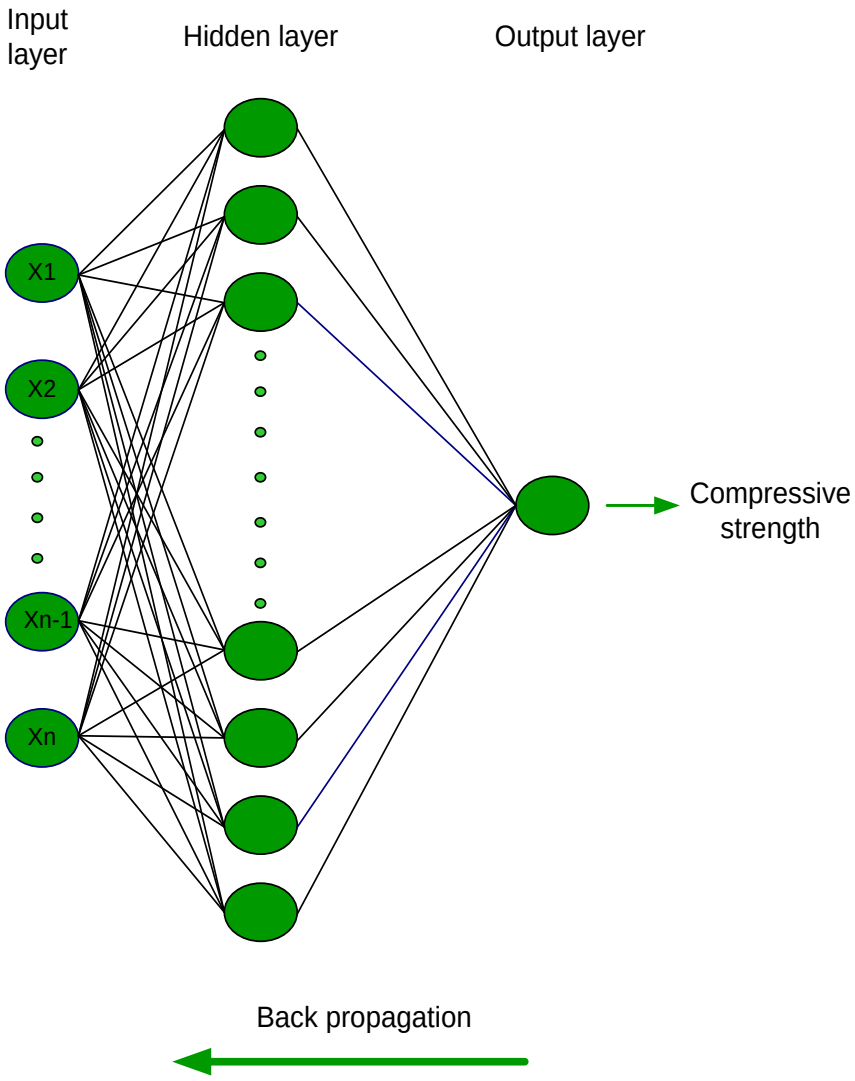

Figure 6-7 Typical artificial neural network model architecture

.

6.7.1 Performance of the developed neural network

Several architectures of neural network models were created and tested by varying the number of neurons in hidden layer using the three different training algorithms on each set of ANN**.** The best architecture network for each set was selected after a number of trials performed on different architecture of neurons. The Levenberg- Marquardt training algorithm (LM) was chosen as the best training algorithm due to lower number of iteration and higher performance for all

models (ANN1, ANN2 and ANN3) as shown in Table 6-3. To make a more accurate comparison, all learning algorithms were trained on the same number of iterations (1000 epochs).

The difference between the predicted values obtained from NN and the experimentally measured of compressive strength is referred as an error estimated for each point. The mean square error (MSE) was used to monitor the network performance for training the current NNs. The lesser the MSE, the better the estimates were. Table 6-4 shows different statistical parameters for the measurement of the performance of NN. It also shows the mean and standard deviation (SD) of the ratios of experimental values of compressive strength of RuC to the corresponding NN prediction values for different modelling techniques and the coefficient of correlation (R^2). The performance of the ANN1 4-12-1 and ANN2 5-10-1 were the best for all 435 results in the database and ANN3 5-10-1 was the best for the 58 results in the database using fly ash. These networks were selected for the prediction model for compressive strength of rubberised concrete.

All the neural network models (ANN1, ANN2 and ANN3) have the mean and correlation coefficient almost equal to 1. This shows that the NN models have high degree of conformity to the actual values. The average ratio of experimental compressive strength to predicted compressive strength of RuC (Mean) of ANN1, ANN2 and ANN3 were 1.009 1.004 and 1.019, respectively. The MSE values were 2.634, 2.211 and 18.56 for ANN1, ANN2 and ANN3, respectively. Both ANN1 and ANN2 models produced similar predictions for the compressive strength of RuC. However, the ANN3 model was less accurate with the highest MSE. The statistical values show small deviations between the experimental and

prediction values, it indicated that all ANN models are suitable and can be used to predict the compressive strength of RuC with reasonable precision. Model ANN2 had the highest correlation coefficient of 0.9859 for the overall data.

The performance of the developed models was monitored during the training process. The training process was stopped when any of the following conditions was archived:

- The maximum number of iterations (epochs) was reached.
- The Performance gradient of the LM algorithm was minimized to the required target.
- The validation set error starts to increase for a specified number of iterations.

A comparison between experimental and predicted values of compressive strength of the rubberised concrete for all ANNs models are shown in Figures 6-8 to 6-10 for training and testing data sets. It can be concluded from these figures that the ANN was successful in learning the relationship between the input and output values.

Table 6-3 Comparison of different training algorithms

Model	Training algorithm					
	LM		SCG		BR	
	Number of iteration	Performance	Number of iteration	Performance	Number of iteration	Performance
ANN1	10	0.000484	22	0.0150	214	0.000602
ANN2	17	0.000292	36	0.0247	207	0.000981
ANN3	12	0.0009237	14	0.0096	88	0.000580

Table 6-4 Performance of ANNMs models for different hidden layers neurones developed

ANN models	architecture	Mean	SD	COV (%)	MSE	R^2
ANN1	4-4-1	1.075	0.353	10.43	6.84	0.943
	4-6-1	1.037	0.264	9.51	7.09	0.951
	4-8-1	1.021	0.194	8.83	6.73	0.938
	4-10-1	1.018	0.128	7.64	5.07	0.970
	4-12-1	1.009	0.079	7.83	2.63	0.985
	4-14-1	1.012	0.137	8.05	4.83	0.969
ANN2	5-4-1	1.022	0.221	7.84	4.94	0.957
	5-8-1	1.028	0.141	9.45	3.09	0.937
	5-10-1	1.004	0.057	5.665	2.21	0.913
	5-12-1	1.008	0.073	6.31	3.95	0.972
	5-14-1	1.018	0.106	7.93	2.84	0.978
ANN3	5-4-1	1.026	0.371	20.72	20.64	0.891
	5-8-1	1.024	0.241	18.93	18.89	0.95
	5-10-1	1.019	0.164	16.09	18.56	0.971
	5-12-1	1.038	0.194	14.95	19.36	0.963
	5-15-1	1.061	0.264	16.94	20.04	0.961

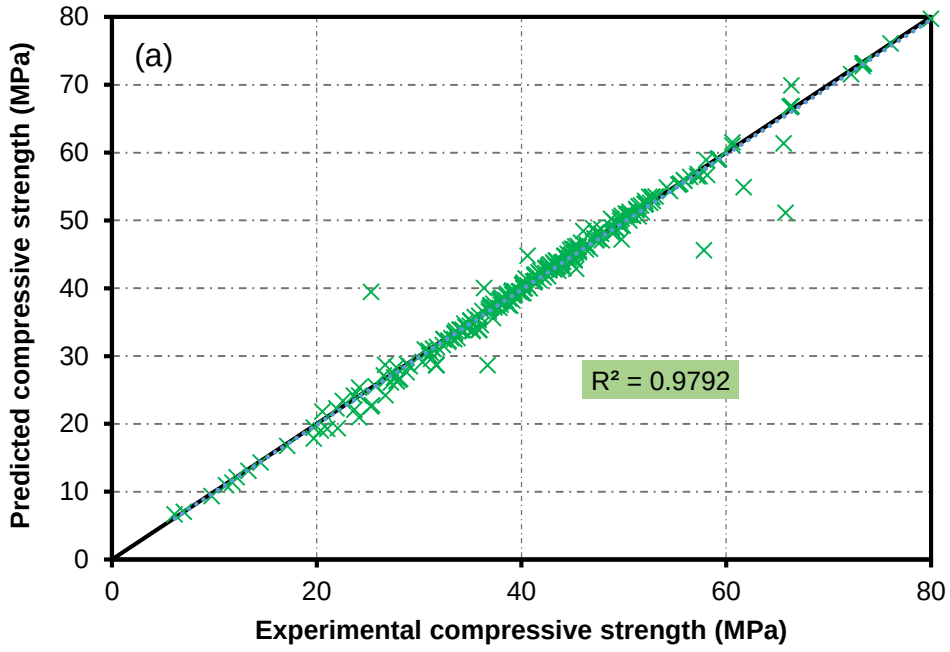

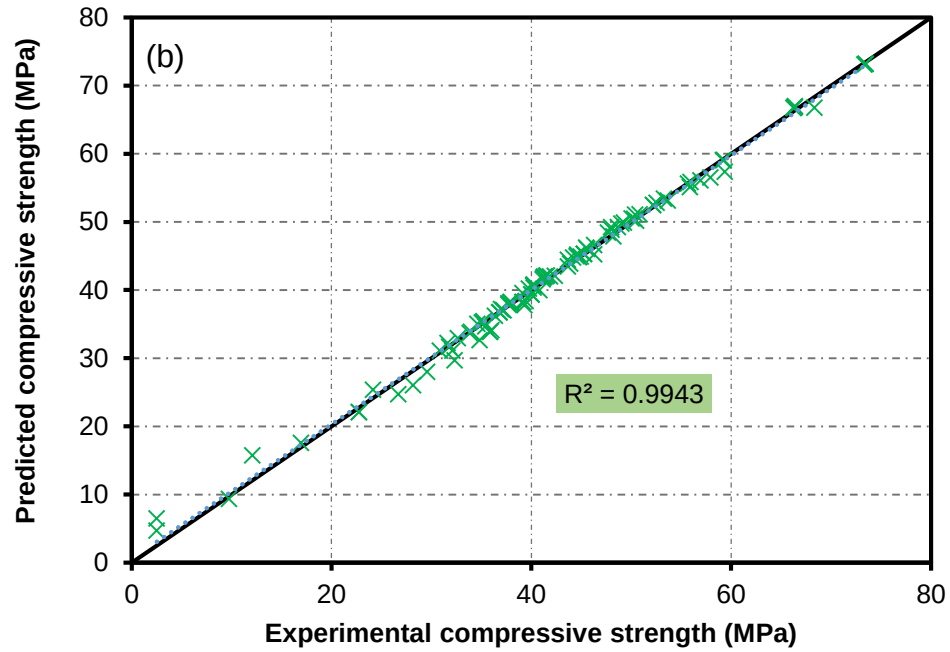

Figure 6-8 Comparison of experimental and predicted compressive strength for ANN1 (a) training data set and (b) testing data set.

.

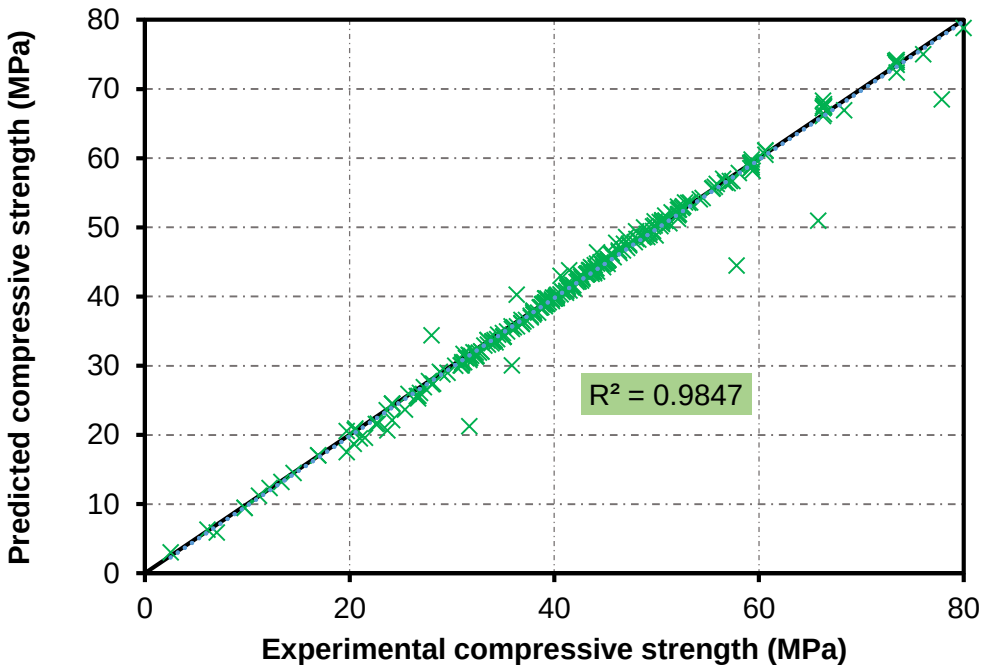

(a)

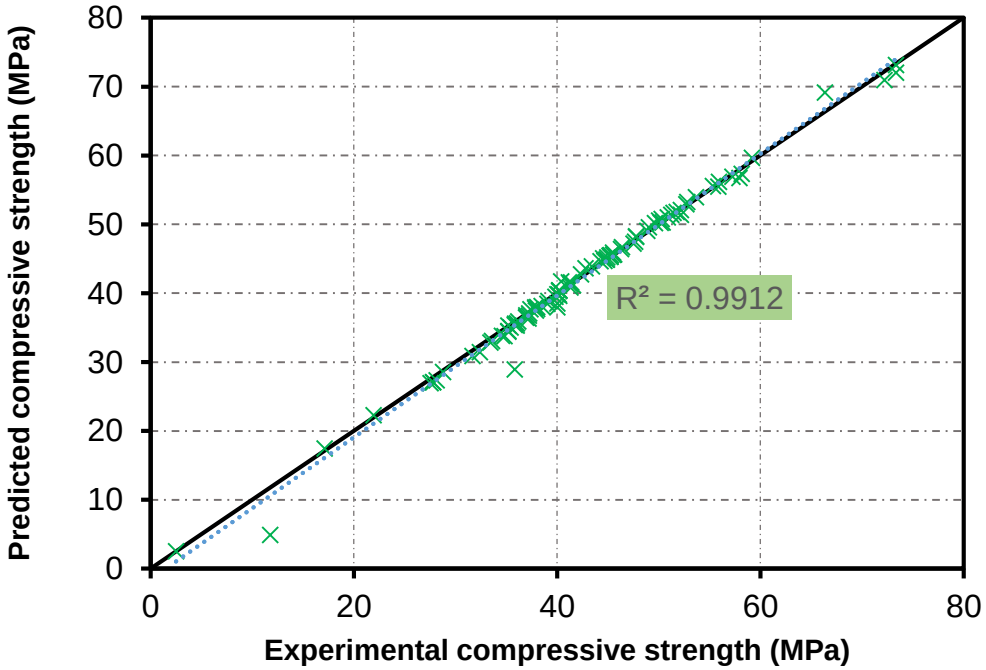

(b)

Figure 6-9 Comparison of experimental and predicted compressive strength for ANN2 (a) training data set and (b) testing data set.

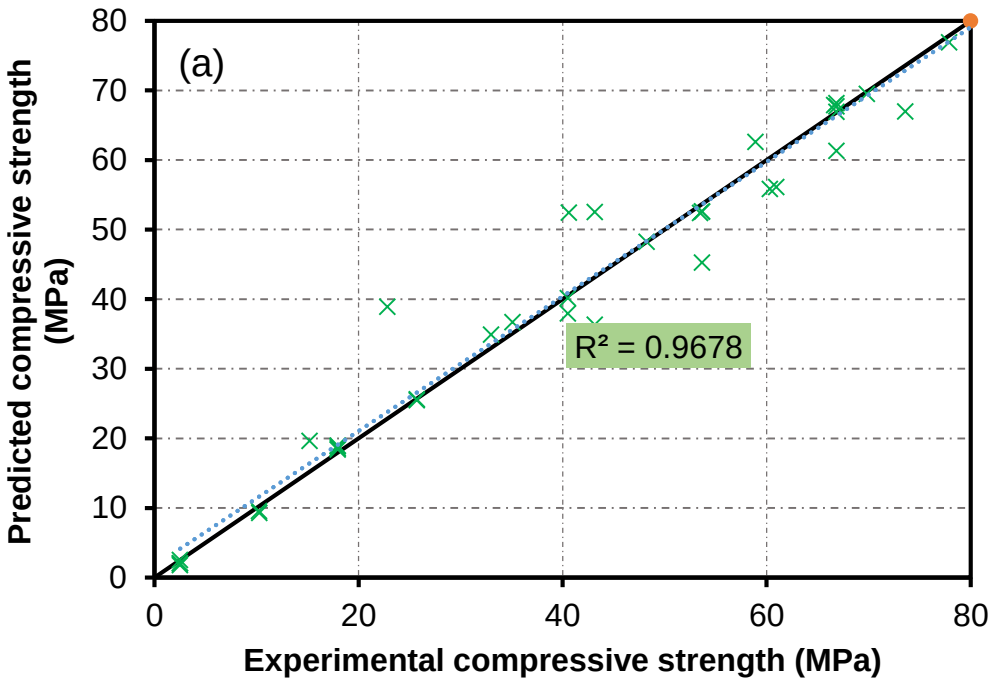

(a)

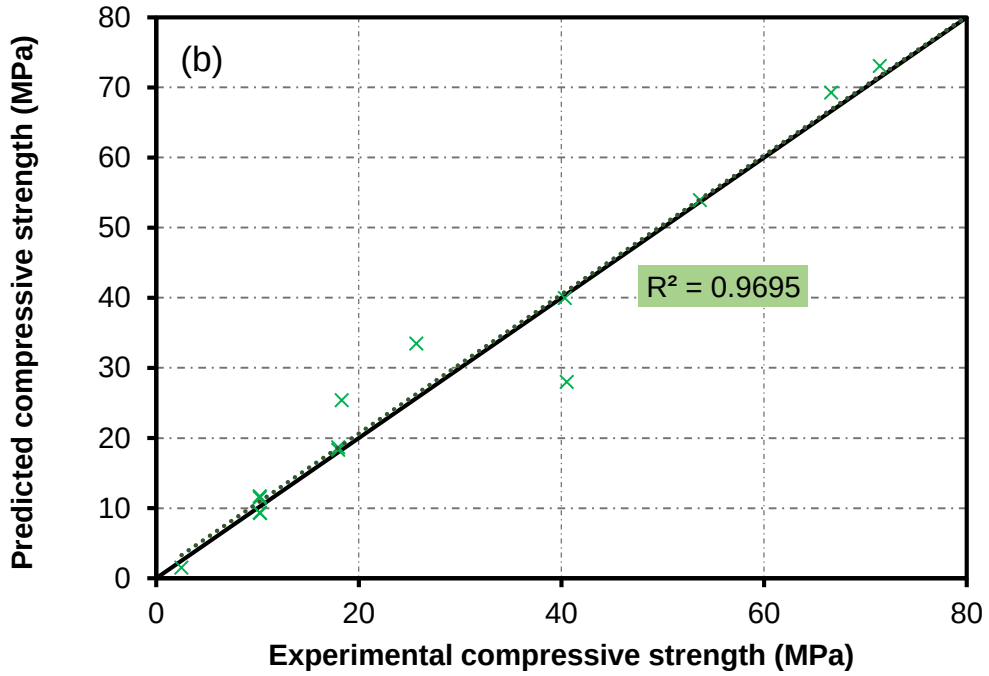

(b)

Figure 6-10 Comparison of experimental and predicted compressive strength for ANN3 (a) training data set and (b) testing data set.

6.8 Parametric study

The trained NN is used to simulate the effects of the input parameters on the compressive strength of rubberised concrete. The parametric study quantifies the effect of one parameter on compressive strength of RuC when all other parameters are kept constant by using the model of NN.

6.8.1 Influence of W/C Ratio

W/C was varied from 0.30 to 0.60 while all other parameters were held constant according to database frequency. Figure 6-11 illustrates the influence of W/C ratio on compressive strength of RuC. As shown in Figure 6-11 the increase in W/C ratio caused a decrease in the compressive strength. Results obtained from the current study and literature (Aiello and Leuzzi, 2010, Kumar et al., 2014) were plotted in Figure 6-11 to compare to the prediction values. From the figure it can be seen that the compressive strength predicted by ANN3 model was lower than those predicted by ANN1 and ANN2 it could be due to the small number of database used in the ANN3 model.

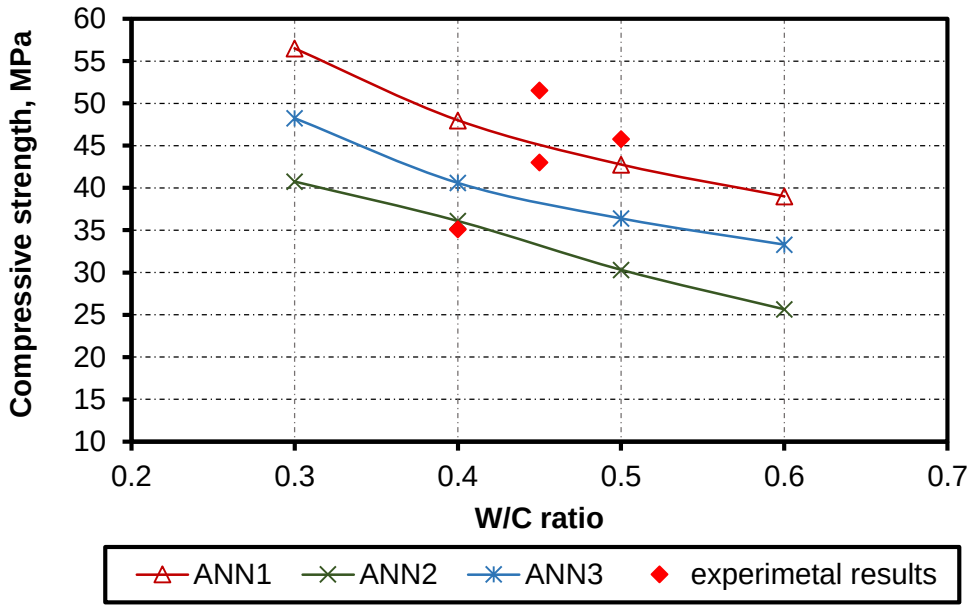

Figure 6-11 Effect of water- cement ratio on compressive strength using ANNs models

6.8.2 Influence of fine rubber content

Figure 6-12 shows the effect of fine rubber content on compressive strength of RuC using ANN1, ANN2 and ANN3 models. Fine rubber content changed from 0 to 630 kg/m^3 while all other parameters were held constant according to database frequency as shown in Table 6-1. As expected, it was observed that as the rubber content increases, the compressive strength clearly decreases for all models. Experimental data of compressive strength obtained from (Azevedo et al., 2012, Grinys et al., 2012, Mohammadi et al., 2014) were plotted in the same graph.

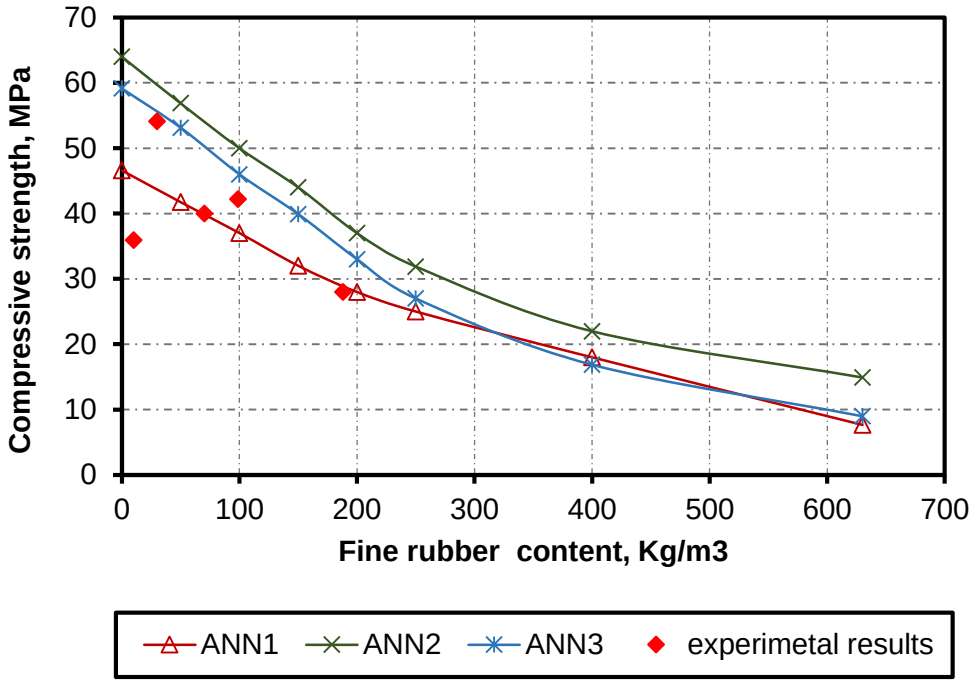

Figure 6-12 Effect of fine rubber content on compressive strength using ANNs models.

6.8.3 Effect of nano silica content on compressive strength

The relations between nano silica content and compressive strength predicted by ANN2 and ANN3 models are presented in Figure 6-13. The values of nano silica

were changed from 10 to 15 Kg/m^3 while all other input parameters values were held constant according to their frequency of occurrence in the database. It is obvious that the more the nano silica content increases, the higher the compressive strength predicted increases for both models ANN2 and ANN3. Experimental results of compressive strength obtained from the current study and (Mohammed et al., 2011, Mohammed and Adamu, 2018) were plotted to compare with the prediction results as shown in the same graph.

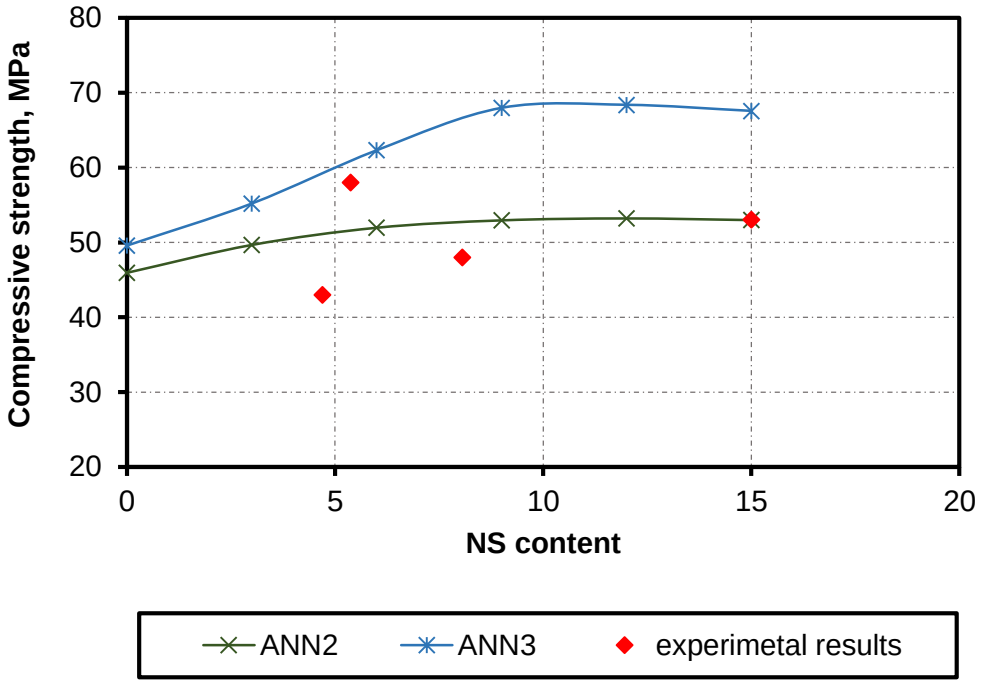

Figure 6-13 Effect of nano silica content on compressive strength using ANN2 and ANN3

6.9 Concluding remarks

In this chapter, three different models of artificial neural network were developed to predict the compressive strength of RuC. Both ANN1 and ANN2 were constructed using a database of 435 tests. However, ANN3 was built using a database of 58 tests which contained nano silica. The developed ANNs and

observations from the parametric analysis are valid for a range of data sets documented in Table 6-1.

Based on the above study, the following conclusions may be drawn:

- ✓ A back propagation neural network (BPNN) with a (LM) training algorithm has chosen in order to assess feasibility of ANN to predict the compressive strength of RuC.
- ✓ Experimental data collected from the thorough experimental investigations provided in the literature were used together with the experimental results obtained from this investigation to train the ANN1, ANN2 and ANN3.
- ✓ The most vital effect on the generalization of the neural network is the effect of the size of the architecture and the training set. After several trials of training, it is obvious that the selection of the training algorithm and the size of the training rate have an important impact on the circulation capacity of ANN.
- ✓ There is a clear reduction in predicted compressive strength with the increase in rubber content and W/C ratio using ANN1, ANN2 and ANN3 models. Experimental results of compressive strength obtained from this study and the literature were close to the predicted results.
- ✓ The influence of NS content results on compressive strength obtained from ANN2 and ANN3 was close to the experimental results.
- ✓ This investigation has contributed to understanding the role of ANNs in predicting compressive strength of rubberised concrete. Further, to study the main parameters effecting compressive strength of rubberised concrete.

- ✓ It was found from ANN2 and ANN3 that the greater the number of data collected, the more accurate prediction obtained.
- ✓ ANN method can be used as a quick and accurate tool to estimate the compressive strength of any rubberised concrete.

CHAPTER SEVEN – PREDICTION OF COMPRESSIVE STRENGTH OF RUBBERISED CONCRETE USING EXISTING MODELS

7.1 Introduction

This chapter begins by assessing the accuracy of the compressive strength prediction models proposed by several researchers. Then looks at compressive strength values determined by several models which are then compared against a large experimental database used in chapter six, the existing models are further compared with the ANN model obtained in the previous chapter.

7.2 Comparison of rubberised concrete compressive strength prediction models

Previous studies have shown that limited number of empirical models have been developed and introduced to improve the accuracy of compressive strength prediction of rubberised concrete (Youssf et al., 2013). Five prediction models are listed in Table 7-1. Khatib and Bayomy-99 Model (Khatib and Bayomy, 1999), Khaloo-08 Model (Khaloo et al., 2008b) and Guneyisi-04 Model (Güneyisi et al., 2004) proposed the same model but with different values for the functional parameters a, b and m. The main assumption in these models was that the control and rubberised concrete mixes must have the same constituents and volumetric contents. In the rubberised concrete mixes, rubber is replacing the total aggregate by an equal volume. However, Youssf et al-16. (Youssf et al., 2016)proposed a model in an exponential form. Bompa et al-17. (Bompa et al., 2017) presented a model to estimate the compressive strength of rubberised concrete based on the type of aggregate replaced. The number of database

considered to propose each model are summarised in Table 7.1 as well as the compressive strength of control mixes.

Table 7-1 Compressive strength prediction models of rubberised concrete

Model Name	Expression	Parameters	Number of data used	f_c' (MPa)
Khatib and Bayomy-99 Model	$f_{cr}' = f_c'[a + b(1 - R_t)^m]$, with a condition that $a = 1 - b$	$a = 0.1$ $b = 0.9$ $m = 7$	24	38
Khaloo-08 Model		$a = 0.02$ $b = 0.98$ $m = 12$	10	30
Guneyisi-04 Model		$a = 0.125$ $b = 0.875$ $m = 4.55$	70	54 - 86
Youssf et al.-16 Model	$f_{cr}' = f_c'[e^{-\alpha R_t}]$	$\alpha = 4.2$	148	23 - 90
Bompa et al.-17 Model	$f_{cr}' = f_c'\left[\frac{1}{1 + 2\left(\frac{3\lambda R_t}{2}\right)^{1.5}}\right]$	$\lambda = 2.43$	198	12.7 - 97.2
Parameters	f_{cr}'; $compressive\ strength\ of\ rubberised\ concrete\ (MPa)$; f_c'; $compressive\ strength\ of\ contol\ concrete\ (MPa)$, R_t; $rubber\ as\ a\ volumetric\ ratio\ by\ total\ aggregate\ volume$			

7.3 Assessment of rubberised concrete compressive strength prediction models

It is important to assess the quality of these predictive models presented in Table 7.1. In the models the effect of rubber content (R_t), as a volumetric ratio by total aggregate volume is directly related to the compressive strength of rubberised concrete which is predicted by the models in Table 7-1. A range of R_t was used in the models and the compressive strength of control mixes was fixed to 50 MPa.

7.3.1 Effect of rubber content on compressive strength using various models

As mentioned in the literature rubber content is one of the most important parameter related to the compressive strength of concrete. Figure 7-1 shows a clear reduction in compressive strength predicted with the increase of rubber content using all of the models. However, a significant reduction was observed in compressive strength predicted using Khaloo model with increased rubber ratio when compared to other models. Moreover, it can be seen that the prediction values from Guneyisi model are close to the values obtained from Youssf model.

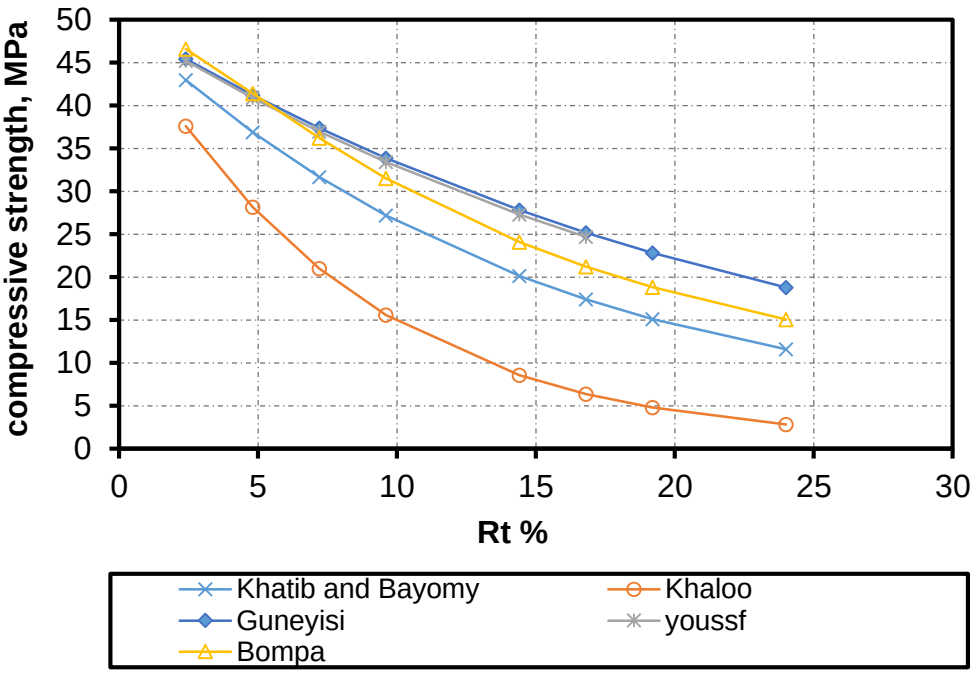

Figure 7-1 Effect of rubber content on predictive compressive strength with different models

7.4 Database for compressive strength

A total of 435 mixes with several proportions of rubber from various experimental investigations have been utilised in this study. The literature presented in section 6.5 with the experimental results of the current investigation were used to study the applicability of existing models of compressive strength. In particular, this thesis will examine the experimental data collected from 48 published papers. Table 7-2 summaries all the experimental database of rubberised concrete used in the models, moredetails about experimental database collected from different studies can be presented in Appendix A**.**

Table 7-2 Summary of rubberised concrete experimental database used in all models

Source	Number of mixes	Rt, %		Compressive strength of control mixes, (MPa)
		min	max	
This study	21	4.3	12.9	51.48
(Sukontasukkul, 2012)	6	5.7	17.1	38
(Al-Tayeb et al., 2013)	3	4.5	9	43.5
(Marie, 2016a)	12	2	35.1	27
(Daxini and Jaydevbhai, 2013b)	5	4.8	14.4	39.68
(Onuaguluchi and Panesar, 2014)	6	2.2	8.4	47.5
(Li et al., 2016a)	7	2	15	52
(Dong et al., 2013)	3	6.8	13.5	44.8
(Thomas et al., 2014)	27	1	7.6	36.5/42.5
(Batayneh et al., 2008b)	6	7.6	38	25.33
(Kumar et al., 2014)	9	3.8	11.4	43
(Reda Taha et al., 2008)	5	8	24	26
(Aiello and Leuzzi, 2010)	5	6.2	20.5	27.11
(Liu et al., 2016)	5	1.7	6.8	34.76
(Su et al., 2015b)	5	3.4	10.2	61.1
(Grinys et al., 2012)	12	2.4	14.4	64.3
(Abusharar, 2015)	4	3.4	3.4	33
(Li et al., 2014a)	3	3.4	4.8	51.3
(Holmes et al., 2014)	6	3.6	7.2	34
(Mohammadi et al., 2014)	14	3.8	15.2	55.6/63
(Azevedo et al., 2012)	4	2.6	7.8	80
(Noaman et al., 2016)	4	2.4	7.2	46.1
(Balaha et al., 2007)	15	2.4	9.6	37/52/58
(Noor et al., 2016)	10	4.8	9.6	46.18 / 68.8
(Gupta et al., 2016)	18	2.1	12	35/52/60
(El-Gammal et al., 2010)	3	24	48	26.9
(Antil et al., 2014)	5	2.4	9.6	36.2
(Mansoor et ai., 2014)	4	2.4	9.6	41.6
(Mohammed and Azmi, 2014)	45	4.8	7.2	23.4/29.56/30.12/34.2/35.5/ 36.5/40.1/44.3/48.1

(Hassanli et al., 2017)	4	2.9	8.6	55
(Youssf et al., 2014)	12	1.8	9.6	53.5 / 60.1 / 62.5
(Mendis et al., 2017)	18	2.6	10.1	10
(Fan et al., 2017)	4	4.8	14.4	36.7
(Fakhri and Saberi. K, 2016)	16	2.4	16.8	40 / 51
(Youssf et al., 2016)	8	9.8	9.8	47.7/50.6/53.5/55.4
(Mohammed et al., 2018)	16	4.8	14.4	45/47/52/58
(Mohammed and Adamu, 2018)	16	4.8	14.4	52
(Gerges et al., 2018)	20	1.9	7.6	30.42/37.19/43.42/51.54
(Mushunje et al., 2018)	4	4.2	4.2	43
(Bisht and Ramana, 2019)	5	1.68	2.31	34.3
(Haridharan et al., 2017)	6	2.35	11.75	54
(Zaoiai et al., 2016)	3	1.2	2.35	39
(Almaleeh et al., 2017)	4	21	22	19.03
(Selvakumar and Venkatakrishnaiah, 2015)	5	2.2	8.8	36.73
(Herrera-Sosa et al., 2015)	7	4.4	13.2	24
(Wang et al., 2014)	6	3.2	16	38.6
(Ristić et al., 2015)	4	4.8	14.4	62.89
(Adamu et al., 2018a)	5	4.3	4.3	50

7.5 Results and discussions

7.5.1 Experimental and predicted compressive strength comparison

Figures 7-2 to 7-7 present comparison results between experimental and predicted compressive strength of rubberised concrete using various prediction models. The experimental results of compressive strength obtained from this study with the collected database are used to assess the accuracy of the predictive models mentioned in Table 7-1. In order to evaluate the accuracy and quality of these models, three statistical indicators; standard deviation (SD),

mean and coefficient of variation (COV) were calculated as listed in Table 7-3. The standard deviation indicates the dispersion of dataset relative to its mean. As data spreads out, the standard deviation increases. It was noted that Khatib and Khaloo models have a tendency of underestimating the compressive strength values of rubberised concrete. Khaloo model showed a larger scatter compared with all other existing models, with the highest mean, standard deviation and COV of 2.51, 1.7 and 93.6, respectively. However, Guneyisi, Youssf and Bompa models had a tendency to overestimate compressive strength values with a mean experimental to predicted compressive strength ratios of 1.04, 1.06 and 1.1, respectively. A better prediction of compressive strength of rubberised concrete was provided by Guneyisi model, compared to Youssf and Bompa models with the mean, SD and COV of 1.04, 0.28 and 29.4, respectively.

Table 7-3 Statistical indicators for compressive strength predicted by the five models

Models	SD	Mean	COV, %
Khatib and Bayomy	0.4	1.27	35.6
Khaloo	1.7	2.51	93.6
Guneyisi	0.28	1.04	29.4
Youssf	0.29	1.06	29.6
Bompa	0.3	1.1	30.8

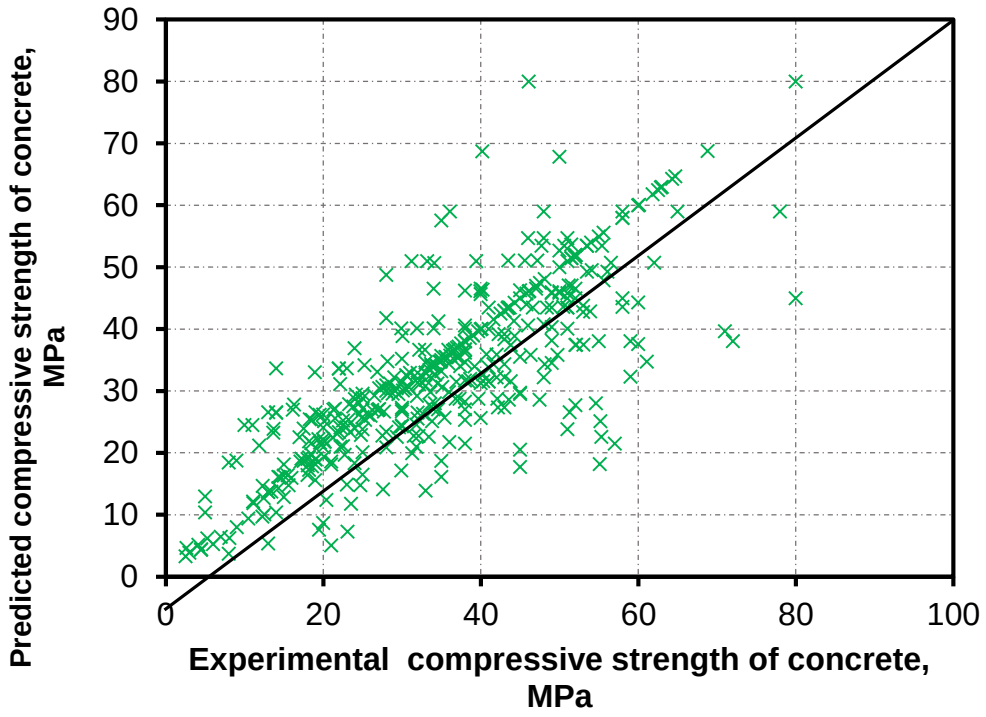
Predicted compressive strength of concrete, MPa
Experimental compressive strength of concrete, MPa
0
10
20
30
40
50
60
70
80
90
0
20
40
60
80
100

(a)

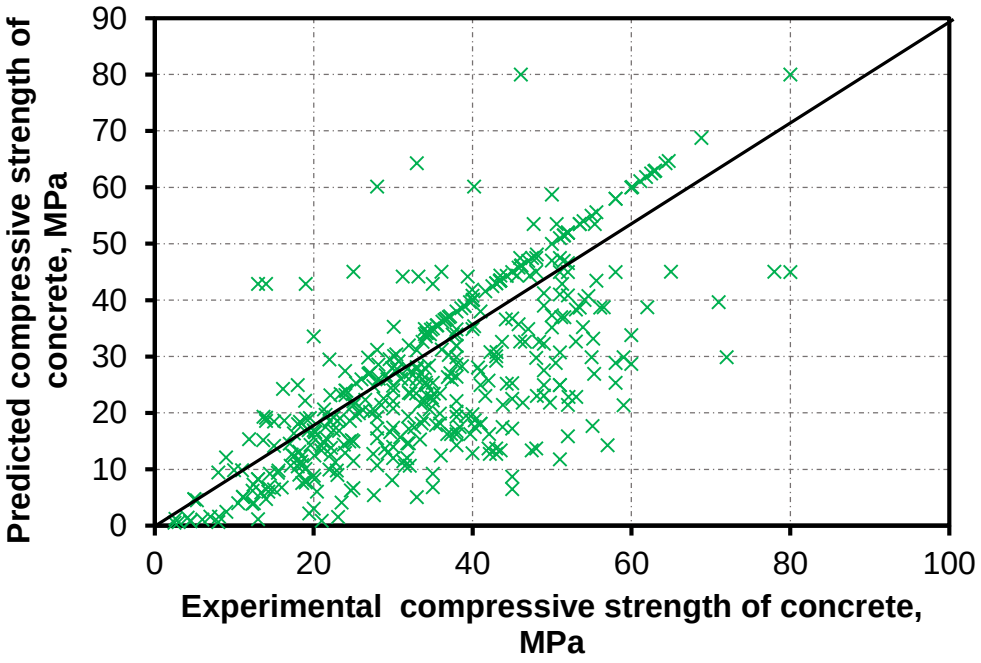
Predicted compressive strength of concrete, MPa
Experimental compressive strength of concrete, MPa
0
10
20
30
40
50
60
70
80
90
0
20
40
60
80
100

(b)

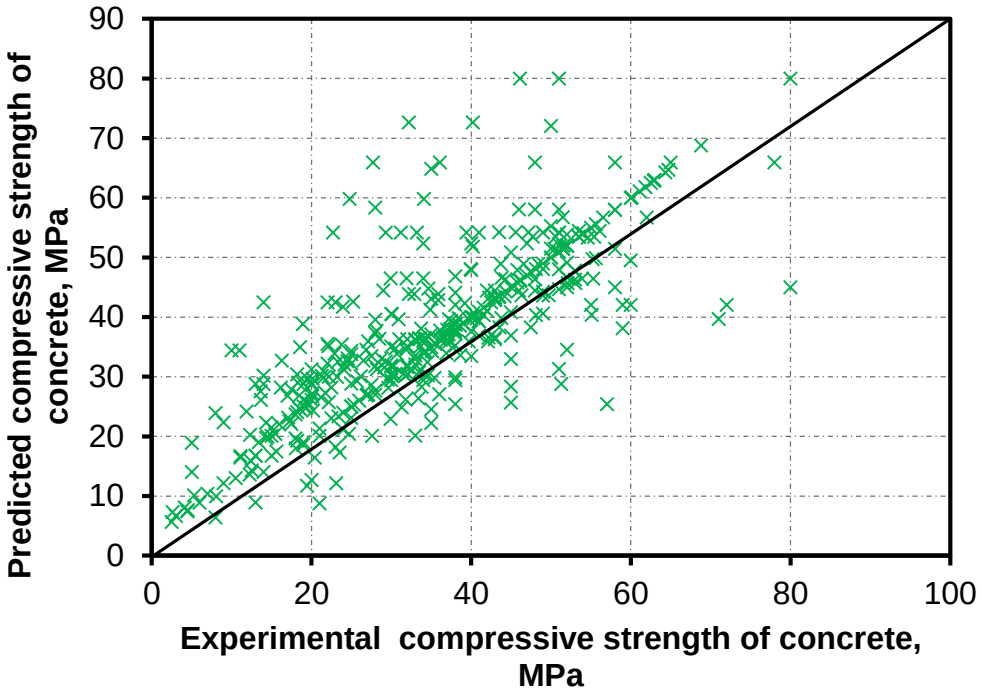
Predicted compressive strength of concrete, MPa
0
10
20
30
40
50
60
70
80
90
0
20
40
60
80
100
Experimental compressive strength of concrete, MPa

(c)

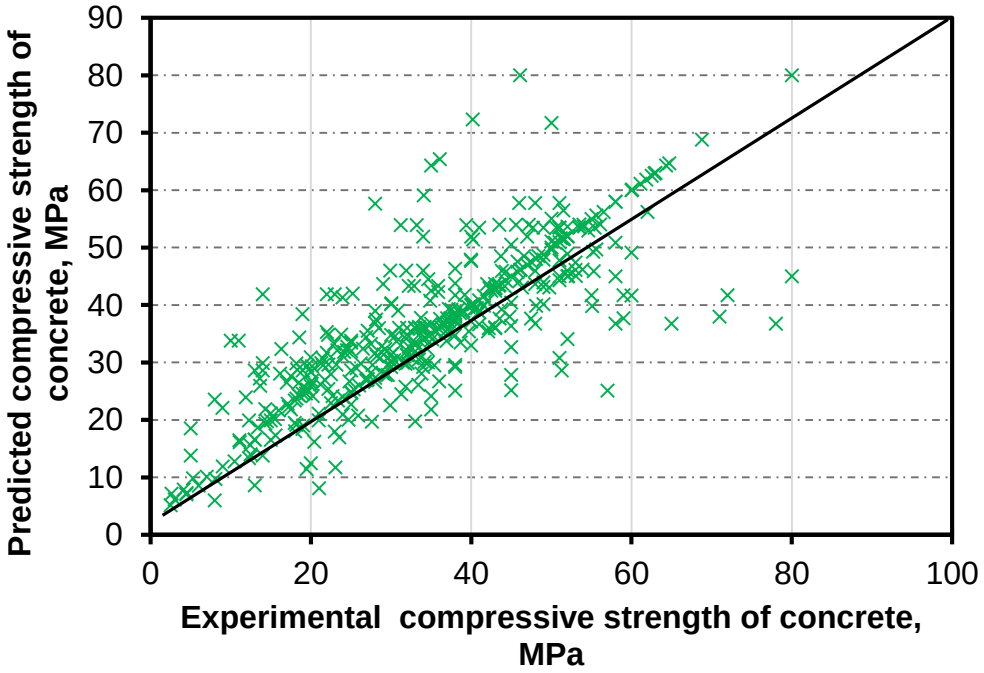
Predicted compressive strength of concrete, MPa
0
10
20
30
40
50
60
70
80
90
0
20
40
60
80
100
Experimental compressive strength of concrete, MPa

(d)

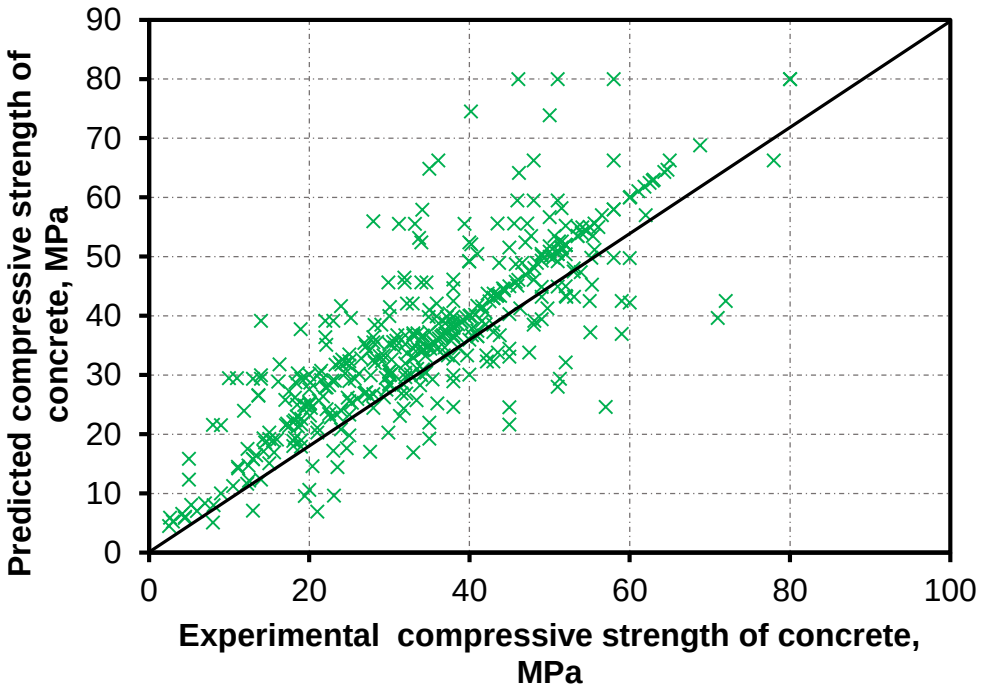

(e)

Figure 7-2 Comparison between experimental and predicted compressive strength of RuC using various prediction models: (a) Khatib and Bayomy model, (b) Khaloo model (c) Guneyisi model, (d) Youssf model and (e) Bompa model.

7.5.2 Evaluation of existing models to predict the compressive strength of rubberised concrete

The residual errors are the ratio of the prediction values of compressive strength obtained by the five existing models to the experimental results (P/E) and used to verify the adequacy of the models.

The residuals were plotted against the compressive strength for each model as shown in the Figures 7-3 to 7-7. Residual values over one denote that the model overestimates the compressive strength and residual values under one indicate that the model underestimates them. The residuals are randomly scattered around one which reveals that the models provide good representation of the

experimental data. It can be seen from Figures 7-3 to 7-7 that the Guneyisi, Youssf and Bompa models overestimated the compressive strength values with residual ratio of 65.5%, 61% and 63% respectively. However, Khatib and Bayomy model provided underestimation of 56.6% while Khaloo model showed underestimation with residual ratio of 87.5% and it also showed a large scatter compared to all other models.

Generally, it can be concluded that for all the existing models the prediction values of compressive strength between 40 and 60 MPa are less scattered compared to low compressive strength values.

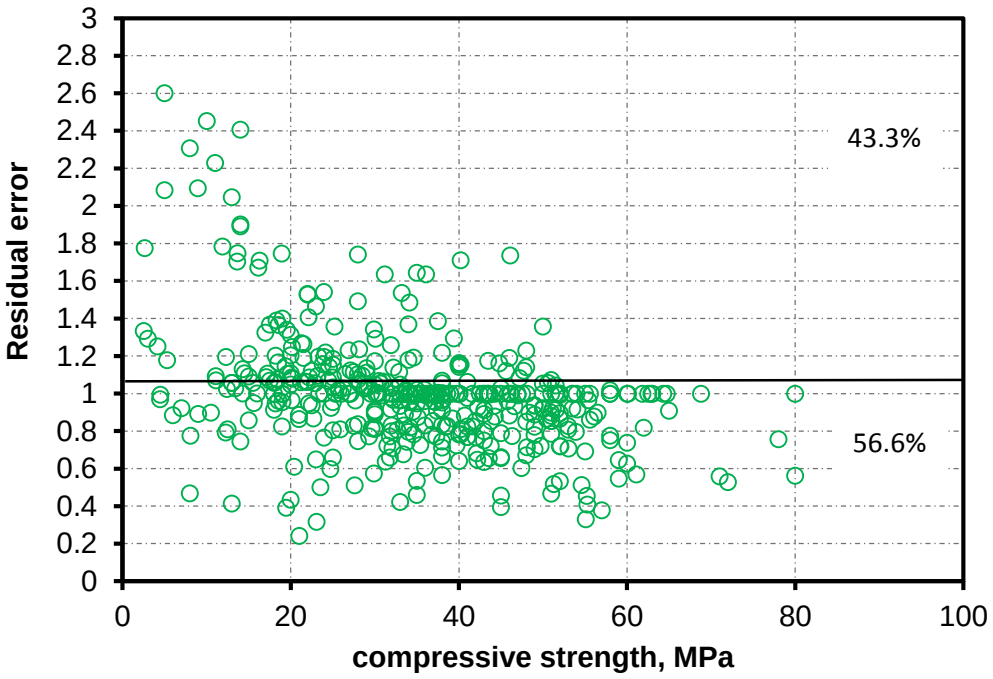

Figure 7-3 Residual error Versus Compressive Strength for Khatib and Bayommy model

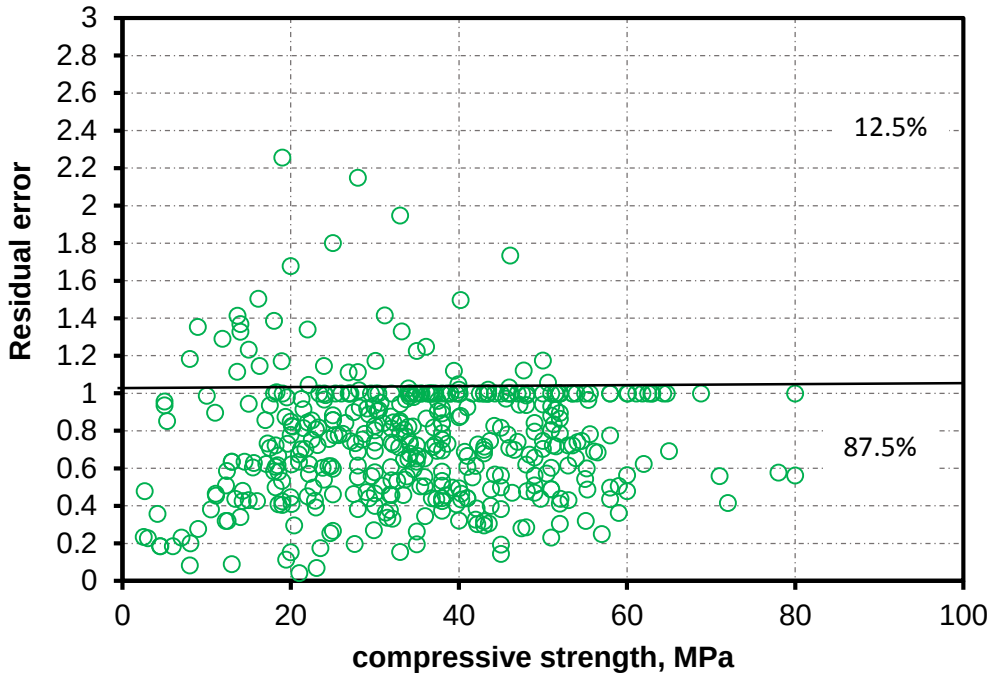

Figure 7-4 Residual error Versus Compressive Strength for Khaloo model

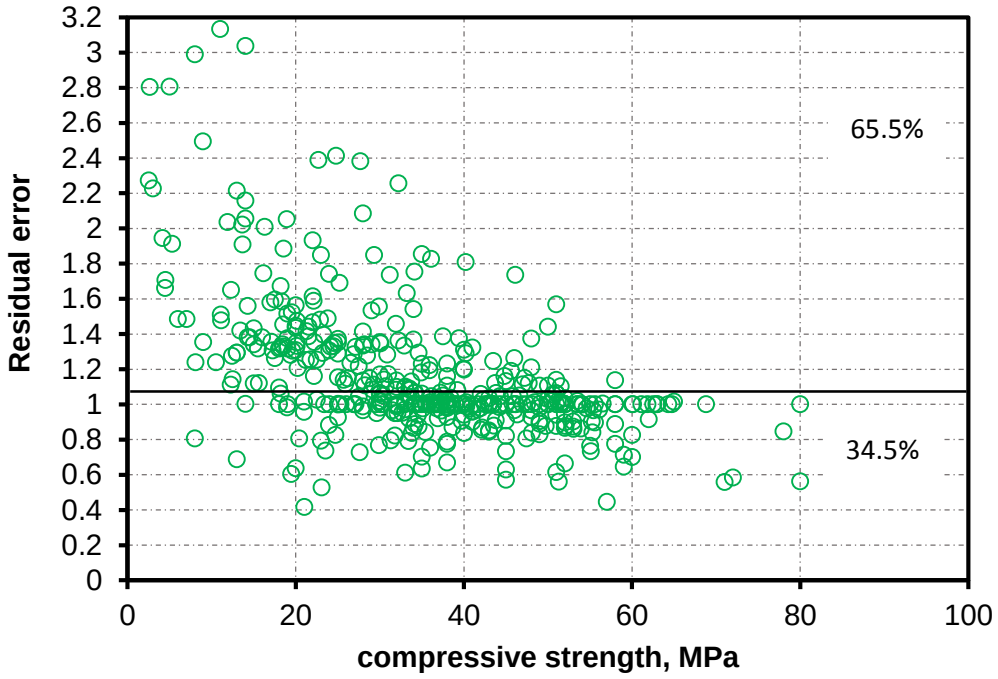

Figure 7-5 Residual error Versus Compressive Strength for Guneyisi model

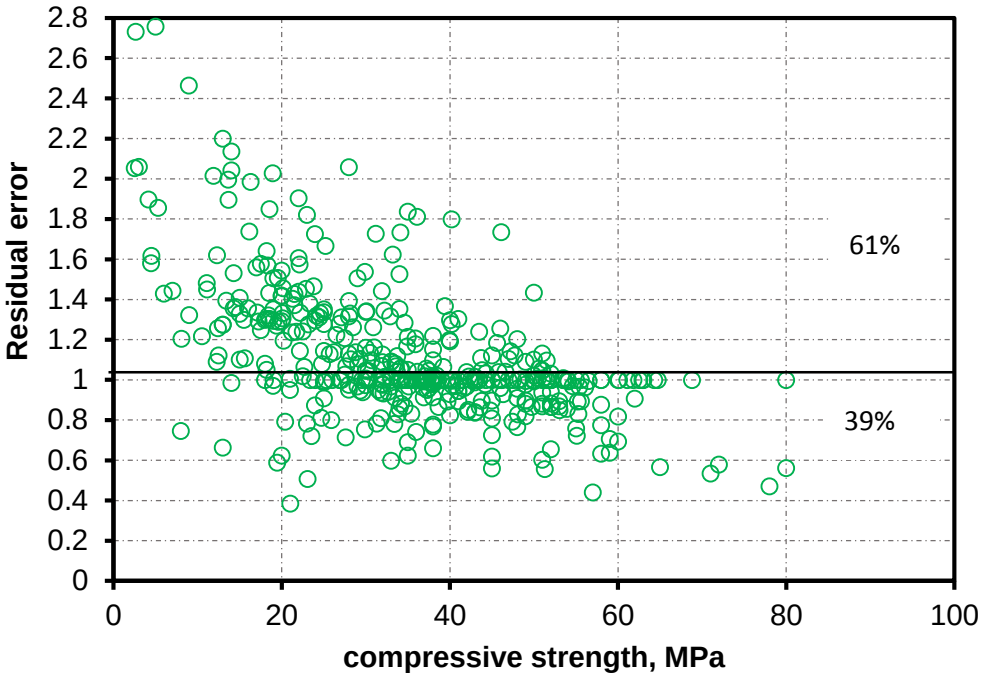

Figure 7-6 Residual error Versus Compressive Strength for Youssf model

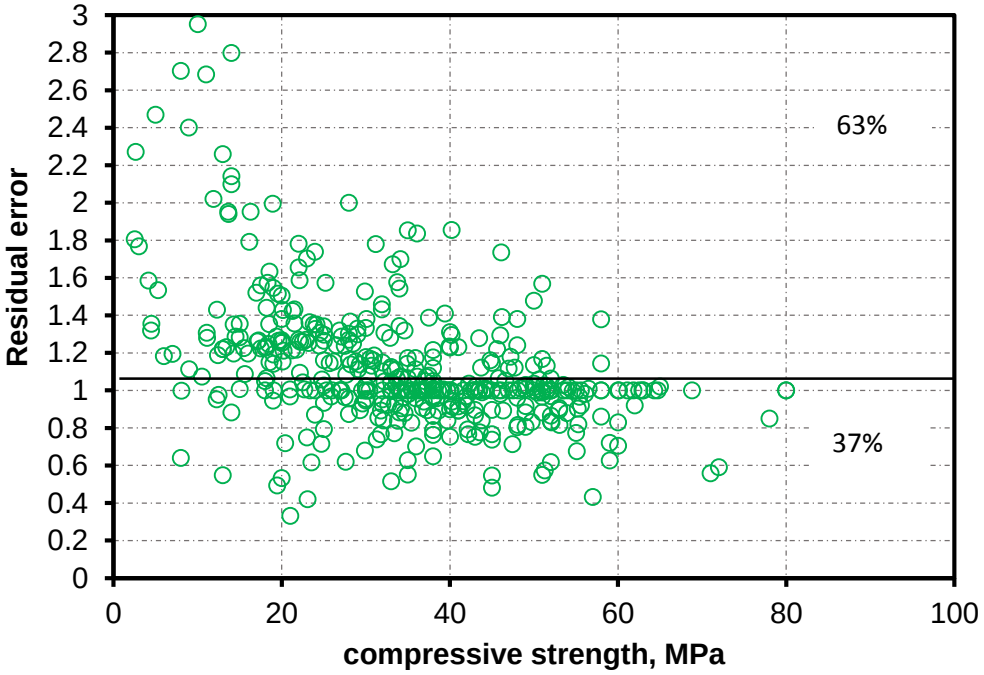

Figure 7-7 Residual error Versus Compressive Strength for Youssf model

7.5.3 Comparison between the prediction using different existing models and ANN model.

The prediction of compressive strength of RuC obtained by the existing predictive models in this chapter were compared with the selected ANN2 model presented in the previous chapter (Chapter six) of this study. Table 7-4 shows the statistical indicators of the compressive strength of rubberised concrete estimated by different models and ANN2 model. Theses statistical indicators have been used to determine which model fits best. It can be seen that the ANN2 model had a lowest values of standard deviation, mean and coefficient of variation compared to the values obtained by the existing models. This indicates that an extremely high predictive values was achieved when using ANN2 model.

Table 7-4 Comparison of statistical indicators between the predictions of compressive strength of rubberised concrete by different models and ANN model

Models	SD	Mean	COV, %
Khatib and Bayomy	0.4	1.27	35.6
Khaloo	1.7	2.51	93.6
Guneyisi	0.28	1.04	29.4
Youssf	0.29	1.06	29.6
Bompa	0.3	1.1	30.8
ANN2	0.057	1.009	5.665

A comparison between experimental and predicted values of compressive strength using the five existing models and ANN model are shown in Figure 7-3. This figure clearly show the high correlation for values obtained from ANN2. The potential reason of low accuracy of the existing models to predict the compressive strength of rubberised concrete that it did not take into account the

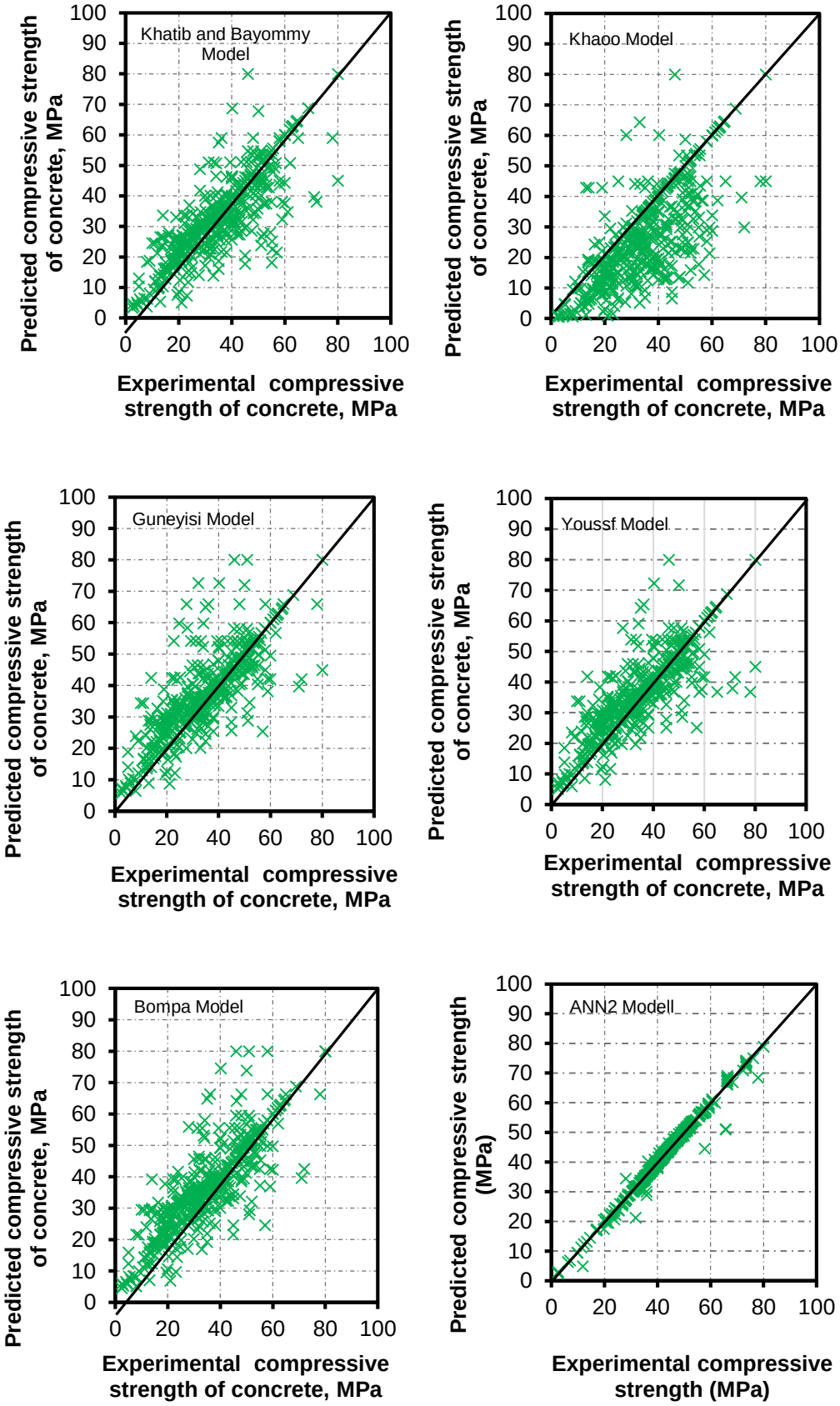

Figure 7-8 Comparison between experimental and predicted compressive strength of RuC using the existing models and the ANN2model.

effect of other parameters which also affect the strength such as w/c ratio and the constituent of concrete

7.6 Conclusions

Based on the comparison between the five existing models of compressive strength of rubberised concrete in this study, the following conclusions can be summarised as follows:

1. The performance of Guneyisi model in predicting the compressive strength of rubberised concrete showed a better prediction compared to the rest of other models based on the statistical indicators (SD=0.28, Mean=1.04 and COV%=29.4)
2. The prediction values obtained from Guneyisi model are close to the values obtained from Youssf model.
3. Khaloo model showed a larger scatter compared with all other existing models, with the highest mean, standard deviation and COV% of 2.51, 1.7 and 93.6, respectively.
4. Existing models (Guneyisi, Youssf and Bompa) were shown to overestimate compressive strength prediction values. However, Khatib and Bayomy model and Khaloo model were provded underestimation results.
5. All the existing models used in this study have focused on one main parameter which is the rubber (%), as a volumetric ratio by total aggregate volume. However, there are other important parameters such as w/c ratio and the constituents of concrete which should be included in predicting models since these parameters affect compressive strength considerably.

6. ANN2 model provides a higher accuracy for the prediction of the compressive strength of rubberised concrete with lower SD, mean and COV of 0.057, 1.009 and 5.665, respectively.

CHAPTER EIGHT – CONCUSIONS AND RECOMMENDATIONS FOR FUTUTRE RESEARCH

8.1 Summary

The behaviour of rubberised concrete with the addition of nano silica was investigated in this thesis. The research includes three phases. Firstly, the experimental investigation was presented in chapters three, four and five including properties of RuC materials used on this research as well as the behaviour of rubberised concrete incorporating nano silica compared to NC and RuC without nano silica. Secondly, an artificial neural network was developed to predict the compressive strength of rubberised concrete using a large experimental data base collected from the literature together with the experimental results obtained from the current study as presented in chapter six. Finally, the reliability of existing models for the prediction of compressive strength was evaluated using the same database that was used in the previous chapter six to study the applicability of the existing models as conducted in chapter seven.

The experimental part includes preparing, casting and testing of six RuC mixes and twelve RuC mixes with nano silica. All specimens were designed with one water-cement ratios and with cement replacement by three different percentage (0%, 1.5% and 3%) of nano silica as well as different level (10%, 20% and 30%) replacement of fine aggregate by two different sizes of rubber. The main experimental measurements in this study were mechanical properties of RuC with and without NS. In addition, thermal and acoustic properties of RuC were tested. The experimental observation focused on the effect of the addition of NS on different properties of RuC.

The analytical part of this thesis was carried out to assess the quality of the predictive empirical models of compressive strength (Khatib and Bayomy-99, Khaloo-08, Guneyisi-04, Youssf et al-16 and Bompa et al -17). Furthermore, compressive strength obtained in the experimental stage of this research together with the data collected from previous studies were compared with the values calculated by the existing models.

The final part of this research was to develop an ANN model to predict the compressive strength of RuC using the neural network toolbox available in MATLAB (R2018 b). A parametric study was conducted to investigate the effect of different input parameters on the compressive strength of RuC. Moreover, a comprehensive comparison was conducted on the ANN models with the five empirical models to evaluate the accuracy of the models.

The main aim of this chapter is to summarise the essential findings of the research carried out in this study and provide a number of recommendations for future work.

8.2 Conclusions

Conclusions of each phase of the work have been drawn and reported in full detail at the end of each chapter. A summary of the major overall view of the findings of this research is drawn briefly in the following sections followed by some general recommendations for future work. Based on the findings of this study the following conclusions can be drawn.

8.2.1 Experimental findings

- Utilisation of different size of rubber particles as a replacement of fine aggregates in concrete have a significant influence on the workability. The larger particle size of rubber, the more reduction in slump values.

- The overall addition of rubber particles resulted in a significant decrease in density, compressive strength, splitting tensile strength and flexural strength of concrete, whilst causes an increase in porosity and water absorption.
- RuC mixes prepared with the smaller size of rubber particles show a higher increase in water absorption and porosity compared to those with larger ones. On the contrary, concrete with the larger rubber particles has a lower density values than those with the finer rubber particles.
- The reduction in strength is affected by both the content and the size of rubber particles. This reduction is normally anticipated and is mostly due to the weakness bond between the rubber particles and the cement matrix. However, the addition of variable dosages of NS showed a remarkable improvement in the strength of rubberised concrete.
- The drying shrinkage results of RuC were slightly similar at the early ages, whereas there was a significant change in the long-term. A higher magnitude of drying shrinkage of RuC than that of NC was observed. However, NS has a positive effect on the drying shrinkage strain.
- The addition of rubber particles and NS lead to improved impact resistance and energy absorption capacity of concrete. The variance between number of blows for ultimate failure and first crack increased as the rubber level and NS increased, which indicates an increase in the ductility of rubberised concrete mixtures.
- The rubberised concrete shows superior thermal and sound properties compared to conventional concrete.
- RuC with larger grain size of rubber has higher sound absorption coefficient than that of smaller grain size.

- The dynamic modulus of elasticity of the rubberised concrete decreased significantly with the increasing of rubber content and size.
- As the percentage of rubber replacement increases, the transmission loss of rubberised concrete decreases due to an increase in the porosity of rubberised concrete and decrease in density.
- Generally, rubberised concrete with 30% of rubber replacement has better sound absorption and lower transmission loss than conventional concrete. However, the inclusion of NS has a slightly negative affect on the sound properties of rubberised concrete due to the filling ability of nano silica resulting in reduction of concrete porosity.

8.2.2 Analytical findings

- The predicted transmission loss of rubberised concrete samples obtained from FE model was very close to the experimental behaviour.
- The parametric study conducted using the proposed FE models revealed that the greatest effect on TL is from thickness of concrete sample. However, there is no significant effect of Young's modulus, density and loss factor on TL.
- The developed neural network models to predict the compressive strength of rubberised concrete with and without NS had good predictions and generalization ability with acceptable errors.
- A parametric study could allow quantification of the effect of some of these parameters by using the ANN model. In this study the influence of the main factors affecting compressive strength such as water to cement ratio, rubber content and NS content were studied and the relation between

compressive strength and those parameters agreed with the experimental results.

- ANN method can be used as a quick and accurate tool to estimate the compressive strength of any rubberised concrete.
- Despite the same parameters considered in the existing models used in this research, Guneyisi-04, Youssf et al.-16 and Bompa-17 models tend to have overestimating prediction values of compressive strength. However, Khatib and Bayomy-99 and Khaloo-08 models were provded underestimation results.
- Based on the statistical indicators, the performance of Guneyisi-04 model showed a good prediction of compressive strength of rubberised concrete compared to the rest of other models.
- The artificial neural network model gives the best prediction of the compressive strength of RuC compared to the five existing models. It requires less computing time and it is not limited by the number and the nature of the input parameters.

8.3 Recommendations for future research

Based on the work carried out for this investigation and the conclusions made in the previous section, the following potential future studies area are recommended:

- Since the present study was limited to crumb rubber replacement, it is suggested to study other types of rubber such as chip rubber and ash rubber as a replacement of coarse aggregate and cement, respectively, to better understand the effect of NS on various properties of concrete.

- It is recommended to investigate the influence of incorporation of nano silica on different structural members such as beams, columns and reinforced walls of rubberised concrete.
- Different reinforced concrete elements such as beams need to be experimentally examined in terms of dynamic behaviour under repeated loads in order to test the material behaviour of rubberised concrete with NS.
- Carry out a cost analysis on rubberised concrete including rubber cost and cost of other raw materials, and casting, placing and finishing cost.
- There is no available research in the literature on long-term durability of rubberised concrete incorporating NS such as freeze-thaw resistance, and carbonation, and therefore, more investigations are needed.
- Other artificial intelligence techniques such as hybrid modelling strategy are recommended to predict the compressive strength of RuC with NS.
- In order to check effect of NS on the impact resistance of rubberised concrete behaviour, failure pattern should be studied.
- It is highly recommended to develop the existing methods presented in this research considering NS as one of the main parameters to predict compressive strength.
- It would be recommended to propose a new predictive models for tensile and flexural strength of rubberised concrete incorporating nano silica.

REFERENCES

Abdollahzadeh, A., Masoudnia, R. and Aghababaei, S. 2011. Predict strength of rubberized concrete using atrificial neural network. *WSEAS Transactions on Computers,* 10**,** 31-40.

Abusharar, S. W. 2015. Effect of particle sizes on mechanical properties of concrete containing crumb rubber. *Innovative systems design and engineering,* 6**,** 114-125.

Adamu, M., Mohammed, B. S. and Liew, M. S. 2018a. Effect of crumb rubber and nano silica on the creep and drying shrinkage of roller compacted concrete pavement. *International Journal,* 15**,** 58-65.

Adamu, M., Mohammed, B. S. and Liew, M. S. 2018b. Mechanical properties and performance of high volume fly ash roller compacted concrete containing crumb rubber and nano silica. *Construction and Building Materials,* 171**,** 521-538.

Ahangar-Asr, A., Faramarzi, A. and Javadi, A. An evolutionary numerical approach to modelling the mechanical properties of rubber concrete. Computing in Civil and Building Engineering, Proceedings of the International Conference, 2010. 411.

Ahmed, B. S. and Neil, N. E. 1993. Observations on rubberized concrete behavior. *Cement, Concrete and Aggregates,* 15**,** 74-84.

Aiello, M. A. and Leuzzi, F. 2010. Waste tyre rubberized concrete: Properties at fresh and hardened state. *Waste Management,* 30**,** 1696-1704.

Al-Khamisi, D. 1999. Study of the material characteristics and structural behavior of lightweight chopped worn-out tires concrete masonary walls. *Building and construction, University of Technology, Baghdad*.

Al-Mashhadani, J. 2001. Physical properties and impact resistance of rubber tyre waste concrete. *Faculty of Civil Engineering–Military Collage of Engineering, Baghdad*.

Al-Mutairi, N., Al-Rukaibi, F. and Bufarsan, A. 2010. Effect of microsilica addition on compressive strength of rubberized concrete at elevated temperatures. *Journal of Material Cycles and Waste Management,* 12**,** 41-49.

Al-Sakini, J. 1998. Behavior and characteristics of chopped worn-out tires lightweight concrete. *Building and construction, University of Technology, Baghdad*.

Al-Tayeb, M. M., Abu Bakar, B. H., Ismail, H. and Akil, H. M. 2013. Effect of partial replacement of sand by recycled fine crumb rubber on the performance of hybrid rubberized-normal concrete under impact load: experiment and simulation. *Journal of Cleaner Production,* 59**,** 284-289.

Albano, C., Camacho, N., Reyes, J., Feliu, J. and Hernández, M. 2005. Influence of scrap rubber addition to Portland I concrete composites: destructive and non-destructive testing. *Composite Structures,* 71**,** 439-446.

Aleem, S. A. E., Heikal, M. and Morsi, W. 2014. Hydration characteristic, thermal expansion and microstructure of cement containing nano-silica. *Construction and Building Materials,* 59**,** 151-160.

Ali, N., Amos, A. and Roberts, M. Use of ground rubber tires in portland cement concrete. Proceedings of the international conference on concrete, 2000. London, United Kingdom: Thomas Telford Services Ltd.

Almaleeh, A. M., Shitote, S. M. and Nyomboi, T. 2017. Use of waste rubber tyres as aggregate in concrete. *Journal of Civil Engineering and Construction Technology,* 8**,** 11-19.

Antil, Y., Verma, V. and Singh, B. 2014. Rubberized concrete with crumb rubber. *Int. J. Sci. Res.(IJSR),* 3**,** 1481-1483.

Aslani, F., Ma, G., Wan, D. L. Y. and Le, V. X. T. 2018. Experimental investigation into rubber granules and their effects on the fresh and hardened properties of self-compacting concrete. *Journal of cleaner production,* 172**,** 1835-1847.

ASTM/C78/C78M 2015. Standard Test Method for Flexural Strength of Concrete (Using Simple Beam with Third-Point Loading). *American Society for Testing*

and Materials.

ASTM/C143/C143M 2015. Standard Test Method for Slump of Hydraulic-Cement Concrete. *American Society for Testing and Materials.*

ASTM/C157 2008. Standard Test Method for Length Change of Hardened Hydraulic- Cement Mortar and Concrete. *American Society for Testing and Materials.*

ASTM/C192/C192M 2015. Standard Practice for Making and Curing Concrete Test Specimens in the Laboratory. *American Society for Testing and Materials*.

Atahan, A. O. and Sevim, U. K. 2008. Testing and comparison of concrete barriers containing shredded waste tire chips. *Materials Letters,* 62**,** 3754-3757.

Atahan, A. O. and Yücel, A. Ö. 2012. Crumb rubber in concrete: static and dynamic evaluation. *Construction and Building Materials,* 36**,** 617-622.

Awang, H., Mydin, M. A. O. and Roslan, A. F. 2012. Effect of additives on mechanical and thermal properties of lightweight foamed concrete. *Advances in applied science research,* 3**,** 3326-3338.

Azevedo, F., Pacheco-Torgal, F., Jesus, C., de Aguiar, J. B. and Camões, A. 2012. Properties and durability of HPC with tyre rubber wastes. *Construction and building materials,* 34**,** 186-191.

Bal, L. and Buyle-Bodin, F. 2013. Artificial neural network for predicting drying shrinkage of concrete. *Construction and Building Materials,* 38**,** 248-254.

Balaha, M., Badawy, A. and Hashish, M. 2007. Effect of using ground waste tire rubber as fine aggregate on the behaviour of concrete mixes. *Indian Journal of Engineering and Materials Sciences,* 14**,** 427.

Bandara, R., Chan, T. and Thambiratnam, D. 2013. The three-stage artificial neural network method for damage assessment of building structures. *Australian Journal of Structural Engineering,* 14**,** 13-25.

Bashir, R. and Ashour, A. 2012. Neural network modelling for shear strength of concrete members reinforced with FRP bars. *Composites Part B: Engineering,* 43**,** 3198-3207.

Batayneh, M. K., Marie, I. and Asi, I. 2008a. Promoting the use of crumb rubber concrete in developing countries. *Waste Management,* 28**,** 2171-2176.

Batayneh, M. K., Marie, I. and Asi, I. 2008b. Promoting the use of crumb rubber concrete in developing countries. *Waste Manag,* 28**,** 2171-6.

Benazzouk, A., Douzane, O., Langlet, T., Mezreb, K., Roucoult, J. and Quéneudec, M. 2007. Physico-mechanical properties and water absorption of cement composite containing shredded rubber wastes. *Cement and Concrete Composites,* 29**,** 732-740.

Benazzouk, A., Douzane, O., Mezreb, K., Laidoudi, B. and Quéneudec, M. 2008. Thermal conductivity of cement composites containing rubber waste particles: Experimental study and modelling. *Construction and Building Materials,* 22**,** 573-579.

Benazzouk, A., Mezreb, K., Doyen, G., Goullieux, A. and Quéneudec, M. 2003. Effect of rubber aggregates on the physico-mechanical behaviour of cement–rubber composites-influence of the alveolar texture of rubber aggregates. *Cement and Concrete Composites,* 25**,** 711-720.

Bignozzi, M. and Sandrolini, F. 2006. Tyre rubber waste recycling in self-compacting concrete. *Cement and concrete research,* 36**,** 735-739.

Bisht, K. and Ramana, P. 2019. Waste to resource conversion of crumb rubber for production of sulphuric acid resistant concrete. *Construction and Building Materials,* 194**,** 276-286.

Björnström, J., Martinelli, A., Matic, A., Börjesson, L. and Panas, I. 2004. Accelerating effects of colloidal nano-silica for beneficial calcium–silicate–hydrate formation in cement. *Chemical Physics Letters,* 392**,** 242-248.

Blum, A. and Rivest, R. L. Training a 3-node neural network is NP-complete. Advances in neural information processing systems, 1989. 494-501.

Boger, Z. G., Hugo. Knowledge extraction from artificial neural network models. 1997. Computational Cybernetics and Simulation., 1997 IEEE International Conference on Systems, Man, and Cybernetics, 1997. 3030-3035.

Bompa, D., Elghazouli, A., Xu, B., Stafford, P. and Ruiz-Teran, A. 2017. Experimental assessment and constitutive modelling of rubberised concrete materials. *Construction and Building Materials,* 137**,** 246-260.

Bravo, M. and de Brito, J. 2012. Concrete made with used tyre aggregate: durability-related performance. *Journal of Cleaner Production,* 25**,** 42-50.

BS1881-114 1983. Testing Concrete: Methods for Determination of Density of Hardened Concrete. *British Standards Institution.*

BS1881-122 1983. Testing Concrete: Method for Determination of Water Absorption,. *British Standards Institution,.*

BS-1881-117 1983. Method for Determination of Tensile Splitting Strength. *British Standard Institution.*

BS-12390-3 2009. Testing Hardened Concrete: Compressive Strength of Test Specimens. *British Standards Institution.*

BS EN ISO 140, A. 1998. Measurement of sound insulation in buildings and of building elements. *Part 7: Field measurements of impact sound insulation of floors.* 7.

Cairns, R. and Kenny, M. 2004. The use of recycled rubber tyres in concrete. *Used/post-consumer Tyres,* 3**,** 135.

Chen, P.-H. and Chung, D. 2013. Mechanical Energy Dissipation Using Cement-Based Materials with Admixtures. *ACI Materials Journal,* 110.

Chou, L. H., Lu, C. K., Chang, J. R. and Lee, M. T. 2007. Use of waste rubber as concrete additive. *Waste Manag Res,* 25**,** 68-76.

Danko, M., Cano, E. and Pena, J. 2006. Use of Recycled Tires as Partial replacement of Coarse Aggregate in the Production of Concrete. *Purdue University Calumet*.

Daxini, B. K. and Jaydevbhai, J. 2013a. Research Paper Engineering A Study on Crumb Rubber: Opportunities for Development of Sustainable Concrete in the New Millennium. *Research Paper,* 2.

Daxini, B. K. and Jaydevbhai, J. 2013b. Research Paper Engineering A Study on Crumb Rubber: Opportunities for Development of Sustainable Concrete in the New Millennium. *Global research analysis,* 2.

Demir, F., Yesilata, B., Turgut, P., Bulut, H. and Isiker, Y. 2015. Investigation of the effects of pH, aging and scrap tire content on the dissolution behaviors of new scrap tire-concrete mixture structures. *Journal of Cleaner Production,* 93**,** 38-46.

Dong, Q., Huang, B. and Shu, X. 2013. Rubber modified concrete improved by chemically active coating and silane coupling agent. *Construction and Building Materials,* 48**,** 116-123.

Du, H., Du, S. and Liu, X. 2014. Durability performances of concrete with nano-silica. *Construction and Building Materials,* 73**,** 705-712.

El-Gammal, A., Abdel-Gawad, A., El-Sherbini, Y. and Shalaby, A. 2010. Compressive strength of concrete utilizing waste tire rubber. *Journal of Emerging Trends in Engineering and Applied Sciences,* 1**,** 96-99.

Elchalakani, M. High strength rubberized concrete containing silica fume for the construction of sustainable road side barriers. Structures, 2015. Elsevier, 20-38.

Eldin, N. N. and Senouci, A. B. 1993. Rubber-tire particles as concrete aggregate. *Journal of materials in civil engineering,* 5**,** 478-496.

Eldin, N. N. and Senouci, A. B. 1994. Measurement and prediction of the strength of rubberized concrete. *Cement and Concrete Composites,* 16**,** 287-298.

Fadiel, A., Al Rifaie, F., Abu-Lebdeh, T. and Fini, E. 2014. Use of crumb rubber to improve thermal efficiency of cement-based materials. *American Journal of Engineering and Applied Sciences,* 7**,** 1-11.

Fakhri, M. and Saberi. K, F. 2016. The effect of waste rubber particles and silica fume on the mechanical properties of Roller Compacted Concrete Pavement. *Journal of Cleaner Production,* 129**,** 521-530.

Fan, S., Liu, G., Liu, L. and Wang, K. 2017. Compressive Strength of Rubberized Concrete with Cement Paste Wrapping Rubber Aggregate. *DEStech Transactions on Engineering and Technology Research*.

Fattuhi, N. and Clark, L. 1996. Cement-based materials containing shredded scrap truck tyre rubber. *Construction and building materials,* 10**,** 229-236.

Fedroff, D., Ahmad, S. and Savas, B. 1996. Mechanical properties of concrete with ground waste tire rubber. *Transportation Research Record: Journal of the Transportation Research Board***,** 66-72.

Fischer, A. and Igel, C. 2014. Training restricted Boltzmann machines: An introduction. *Pattern Recognition,* 47**,** 25-39.

Ganesan, N., Raj, B. and Shashikala, A. 2013a. Behavior of self-consolidating rubberized concrete beam-column joints. *ACI Materials Journal,* 110**,** 697.

Ganesan, N., Raj, J. B. and Shashikala, A. 2013b. Flexural fatigue behavior of self compacting rubberized concrete. *Construction and Building Materials,* 44**,** 7-14.

Ganjian, E., Khorami, M. and Maghsoudi, A. A. 2009. Scrap-tyre-rubber replacement for aggregate and filler in concrete. *Construction and Building Materials,* 23**,** 1828-1836.

Garzón-Roca, J., Marco, C. O. and Adam, J. M. 2013. Compressive strength of masonry made of clay bricks and cement mortar: Estimation based on Neural Networks and Fuzzy Logic. *Engineering Structures,* 48**,** 21-27.

Gerges, N. N., Issa, C. A. and Fawaz, S. A. 2018. Rubber concrete: Mechanical and dynamical properties. *Case Studies in Construction Materials,* 9**,** e00184.

Gesoğlu, M. and Güneyisi, E. 2007. Strength development and chloride penetration in rubberized concretes with and without silica fume. *Materials and Structures,* 40**,** 953-964.

Gesoğlu, M., Güneyisi, E., Khoshnaw, G. and İpek, S. 2014a. Abrasion and freezing–thawing resistance of pervious concretes containing waste rubbers. *Construction and Building Materials,* 73**,** 19-24.

Gesoğlu, M., Güneyisi, E., Khoshnaw, G. and İpek, S. 2014b. Investigating properties of pervious concretes containing waste tire rubbers. *Construction and Building Materials,* 63**,** 206-213.

Gesoğlu, M., Güneyisi, E., Özturan, T. and Özbay, E. 2010. Modeling the mechanical properties of rubberized concretes by neural network and genetic programming. *Materials and structures,* 43**,** 31-45.

Gesoğlu, M. G., Erhan 2011. Permeability properties of self-compacting rubberized concretes. *Construction and building materials,* 25**,** 3319-3326.

Ghosal, M. and Chakraborty, A. K. 2015. A comparative study of nano embedments on different types of cements. *International Journal of Advances in Engineering & Technology,* 8**,** 92.

Givi, A. N., Rashid, S. A., Aziz, F. N. A. and Salleh, M. A. M. 2010. Experimental investigation of the size effects of SiO2 nano-particles on the mechanical properties of binary blended concrete. *Composites Part B: Engineering,* 41**,** 673-677.

Gonzalez, S. 2000. *Neural networks for macroeconomic forecasting: a complementary approach to linear regression models*, Department of Finance Canada.

Goulias, D. G. and Ali, A.-H. Non-destructive evaluation of rubber modified concrete. Infrastructure Condition Assessment: Art, Science, and Practice, 1997. ASCE, 111-120.

Grinys, A., Sivilevičius, H. and Daukšys, M. 2012. Tyre Rubber Additive Effect on Concrete Mixture Strength. *Journal of Civil Engineering and Management,* 18**,** 393.

Güneyisi, E. 2010. Fresh properties of self-compacting rubberized concrete incorporated with fly ash. *Materials and structures,* 43**,** 1037-1048.

Güneyisi, E., Gesoğlu, M. and Özturan, T. 2004. Properties of rubberized concretes containing silica fume. *Cement and Concrete Research,* 34**,** 2309-2317.

Guo, Y., Zhang, J., Chen, G., Chen, G. and Xie, Z. 2014. Fracture behaviors of a new steel fiber reinforced recycled aggregate concrete with crumb rubber. *Construction and Building Materials,* 53**,** 32-39.

Gupta, T., Chaudhary, S. and Sharma, R. K. 2014. Assessment of mechanical and durability properties of concrete containing waste rubber tire as fine aggregate. *Construction and Building Materials,* 73**,** 562-574.

Gupta, T., Chaudhary, S. and Sharma, R. K. 2016. Mechanical and durability properties of waste rubber fiber concrete with and without silica fume. *Journal of Cleaner Production,* 112**,** 702-711.

Gupta, T., Sharma, R. K. and Chaudhary, S. 2015. Impact resistance of concrete containing waste rubber fiber and silica fume. *International Journal of Impact Engineering,* 83**,** 76-87.

Hall, M. R. and Najim, K. B. 2014. Structural behaviour and durability of steel-reinforced structural Plain/Self-Compacting Rubberised Concrete (PRC/SCRC). *Construction and Building Materials,* 73**,** 490-497.

Haridharan, M., Murugan, R. B., Natarajan, C. and Muthukannan, M. Influence of Waste Tyre Crumb Rubber on Compressive Strength, Static Modulus of Elasticity and Flexural Strength of Concrete. IOP Conference Series: Earth and Environmental Science, 2017. IOP Publishing, 012014.

Hassanli, R., Youssf, O. and Mills, J. E. 2017. Experimental investigations of reinforced rubberized concrete structural members. *Journal of Building Engineering,* 10**,** 149-165.

Haykin, S. 1999. Self-organizing maps. *Neural networks-A comprehensive foundation, 2nd edition, Prentice-Hall*.

Hernández-Olivares, F. and Barluenga, G. 2004. Fire performance of recycled rubber-filled high-strength concrete. *Cement and concrete research,* 34**,** 109-117.

Hernandez-Olivares, F., Barluenga, G., Bollati, M. and Witoszek, B. 2002. Static and dynamic behaviour of recycled tyre rubber-filled concrete. *Cement and concrete research,* 32**,** 1587-1596.

Hernández-Olivares, F., Barluenga, G., Parga-Landa, B., Bollati, M. and Witoszek, B. 2007. Fatigue behaviour of recycled tyre rubber-filled concrete and its implications in the design of rigid pavements. *Construction and building materials,* 21**,** 1918-1927.

Herrera-Sosa, E. S., Martínez-Barrera, G., Barrera-Díaz, C., Cruz-Zaragoza, E. and Ureña-Núñez, F. 2015. Recovery and modification of waste tire particles and their use as reinforcements of concrete. *International Journal of Polymer Science,* 2015.

Ho, A. C., Turatsinze, A., Hameed, R. and Vu, D. C. 2012. Effects of rubber aggregates from grinded used tyres on the concrete resistance to cracking. *Journal of Cleaner Production,* 23**,** 209-215.

Holmes, N., Browne, A. and Montague, C. 2014. Acoustic properties of concrete panels with crumb rubber as a fine aggregate replacement. *Construction and Building Materials,* 73**,** 195-204.

Huang, B., Li, G., Pang, S.-S. and Eggers, J. 2004. Investigation into waste tire rubber-filled concrete. *Journal of Materials in Civil Engineering,* 16**,** 187-194.

Huang, B., Shu, X. and Cao, J. 2013. A two-staged surface treatment to improve properties of rubber modified cement composites. *Construction and Building Materials,* 40**,** 270-274.

Ismail, M. K. and Hassan, A. A. 2016. Impact Resistance and Acoustic Absorption Capacity of Self-Consolidating Rubberized Concrete. *ACI Materials Journal,* 113.

ISO 9052-1, A. 1989. Determination of Dynamic

Stiffness. *Part 1 :Materials used in floating floors in*

dwellings. I.

Issa, C. A. and Salem, G. 2013. Utilization of recycled crumb rubber as fine aggregates in concrete mix design. *Construction and Building Materials,* 42**,** 48-52.

Jadid, M. N. and Fairbairn, D. R. 1996. Neural-network applications in predicting moment-curvature parameters from experimental data. *Engineering Applications of Artificial Intelligence,* 9**,** 309-319.

Jal, P., Sudarshan, M., Saha, A., Patel, S. and Mishra, B. 2004. Synthesis and characterization of nanosilica prepared by precipitation method. *Colloids and Surfaces A: Physicochemical and Engineering Aspects,* 240**,** 173-178.

Jha, G. K. 2007. Artificial neural networks and its applications. *IARI, New Delhi, girish_iasri@ rediffmail. com*.

Jingfu, K., Chuncui, H. and Zhenli, Z. 2009. Strength and shrinkage behaviors of roller-compacted concrete with rubber additives. *Materials and structures,* 42**,** 1117-1124.

Jittabut, P. 2015. Effect of Nanosilica on Mechanical and Thermal Properties of Cement Composites for Thermal Energy Storage Materials. *Energy Procedia,* 79**,** 10-17.

Kaloush, K., Way, G. and Zhu, H. 2005. Properties of crumb rubber concrete. *Transportation Research Record: Journal of the Transportation Research Board***,** 8-14.

Karger-Kocsis, J., Mészáros, L. and Bárány, T. 2013. Ground tyre rubber (GTR) in thermoplastics, thermosets, and rubbers. *Journal of Materials Science,* 48**,** 1-38.

Khaloo, A. R., Dehestani, M. and Rahmatabadi, P. 2008a. Mechanical properties of concrete containing a high volume of tire-rubber particles. *Waste Manag,* 28**,** 2472-82.

Khaloo, A. R., Dehestani, M. and Rahmatabadi, P. 2008b. Mechanical properties of concrete containing a high volume of tire–rubber particles. *Waste Management,* 28**,** 2472-2482.

Khatib, Z. K. and Bayomy, F. M. 1999. Rubberized Portland cement concrete. *Journal of materials in civil engineering,* 11**,** 206-213.

Kumar, G. N., Sandeep, V. and Sudharani, C. 2014. Using tyres wastes as aggregates in concrete to form rubcrete–mix for engineering applications. *International Journal of Research in Engineering and Technology,* 3**,** 500-9.

Land, G. and Stephan, D. 2012. The influence of nano-silica on the hydration of ordinary Portland cement. *Journal of Materials Science,* 47**,** 1011-1017.

Lee, H. S., Lee, H., Moon, J. S. and Jung, H. W. 1998. Development of tire added latex concrete. *Materials Journal,* 95**,** 356-364.

Li, D., Mills, J., Benn, B. and Ma, X. 2014a. Abrasion and impact resistance investigation of crumbed rubber concrete (CRC).

Li, G., Garrick, G., Eggers, J., Abadie, C., Stubblefield, M. A. and Pang, S.-S. 2004a. Waste tire fiber modified concrete. *Composites Part B: Engineering,* 35**,** 305-312.

Li, G., Stubblefield, M. A., Garrick, G., Eggers, J., Abadie, C. and Huang, B. 2004b. Development of waste tire modified concrete. *Cement and Concrete Research,* 34**,** 2283-2289.

Li, G., Wang, Z., Leung, C. K., Tang, S., Pan, J., Huang, W. and Chen, E. 2016a. Properties of rubberized concrete modified by using silane coupling agent and carboxylated SBR. *Journal of Cleaner Production,* 112**,** 797-807.

Li, G., Wang, Z., Leung, C. K. Y., Tang, S., Pan, J., Huang, W. and Chen, E. 2016b. Properties of rubberized concrete modified by using silane coupling agent and carboxylated SBR. *Journal of Cleaner Production,* 112**,** 797-807.

Li, L.-J., Chen, Z.-Z., Xie, W.-F. and Liu, F. 2009. Experimental study of recycled rubber-filled high-strength concrete. *Magazine of Concrete Research,* 61**,** 549-556.

Li, L.-J., Xie, W.-F., Liu, F., Guo, Y.-C. and Deng, J. 2011. Fire performance of high-strength concrete reinforced with recycled rubber particles. *Magazine of Concrete Research,* 63**,** 187-195.

Li, L., Ruan, S. and Zeng, L. 2014b. Mechanical properties and constitutive equations of concrete containing a low volume of tire rubber particles. *Construction and Building Materials,* 70**,** 291-308.

Lin, Q., Xu, Z., Lan, X., Ni, Y. and Lu, C. 2011. The reactivity of nano silica with calcium hydroxide. *J Biomed Mater Res B Appl Biomater,* 99**,** 239-46.

Ling, T.-C. 2011. Prediction of density and compressive strength for rubberized concrete blocks. *Construction and Building Materials,* 25**,** 4303-4306.

Ling, T.-C. 2012. Effects of compaction method and rubber content on the properties of concrete paving blocks. *Construction and Building Materials,* 28**,** 164-175.

Lippmann, R. 1987. An introduction to computing with neural nets. *IEEE Assp magazine,* 4**,** 4-22.

Liu, F., Chen, G., Li, L. and Guo, Y. 2012. Study of impact performance of rubber reinforced concrete. *Construction and Building Materials,* 36**,** 604-616.

Liu, F., Zheng, W., Li, L., Feng, W. and Ning, G. 2013. Mechanical and fatigue performance of rubber concrete. *Construction and Building Materials,* 47**,** 711-719.

Liu, H., Wang, X., Jiao, Y. and Sha, T. 2016. Experimental Investigation of the Mechanical and Durability Properties of Crumb Rubber Concrete. *Materials (Basel),* 9.

Londhe, S. N. Towards predicting water levels using artificial neural networks. OCEANS 2009-EUROPE, 2009. IEEE, 1-6.

Marie, I. 2016a. Zones of weakness of rubberized concrete behavior using the UPV. *Journal of Cleaner Production,* 116**,** 217-222.

Marie, I. 2016b. Zones of weakness of rubberized concrete behavior using the UPV. *Journal of Cleaner Production*.

Mavroulidou, M. and Figueiredo, J. 2010. Discarded tyre rubber as concrete aggregate: a possible outlet for used tyres. *Global NEST Journal,* 12**,** 359-367.

Meddah, A., Beddar, M. and Bali, A. 2014. Use of shredded rubber tire aggregates for roller compacted concrete pavement. *Journal of Cleaner Production,* 72**,** 187-192.

Mendis, A. S., Al-Deen, S. and Ashraf, M. 2017. Behaviour of similar strength crumbed rubber concrete (CRC) mixes with different mix proportions. *Construction and Building Materials,* 137**,** 354-366.

Mohammadi, I. 2014. *Investigation on the Use of Crumb Rubber Concrete (CRC) for Rigid Pavements.* MSc, University of Technology Sydney.

Mohammadi, I. and Khabbaz, H. 2015. Shrinkage performance of Crumb Rubber Concrete (CRC) prepared by water-soaking treatment method for rigid pavements. *Cement and Concrete Composites,* 62**,** 106-116.

Mohammadi, I., Khabbaz, H. and Vessalas, K. 2014. In-depth assessment of Crumb Rubber Concrete (CRC) prepared by water-soaking treatment method for rigid pavements. *Construction and Building Materials,* 71**,** 456-471.

Mohammed, B. S. 2010. Structural behavior and m–k value of composite slab utilizing concrete containing crumb rubber. *Construction and Building Materials,* 24**,** 1214-1221.

Mohammed, B. S. and Adamu, M. 2018. Mechanical performance of roller compacted concrete pavement containing crumb rubber and nano silica. *Construction and Building Materials,* 159**,** 234-251.

Mohammed, B. S., Adamu, M. and Liew, M. S. 2018. Evaluating the effect of crumb rubber and nano silica on the properties of high volume fly ash roller compacted concrete pavement using non-destructive techniques. *Case studies in construction materials,* 8**,** 380-391.

Mohammed, B. S., Awang, A. B., San Wong, S. and Nhavene, C. P. 2016a. Properties of nano silica modified rubbercrete. *Journal of Cleaner Production,* 119**,** 66-75.

Mohammed, B. S., Awang, A. B., Wong, S. S. and Nhavene, C. P. 2016b. Properties of nano silica modified rubbercrete. *Journal of Cleaner Production,* 119**,** 66-75.

Mohammed, B. S. and Azmi, N. 2014. Strength reduction factors for structural rubbercrete. *Frontiers of Structural and Civil Engineering,* 8**,** 270-281.

Mohammed, B. S., Azmi, N. J. and Abdullahi, M. 2011. Evaluation of rubbercrete based on ultrasonic pulse velocity and rebound hammer tests. *Construction and Building Materials,* 25**,** 1388-1397.

Mohammed, B. S., Hossain, K. M. A., Swee, J. T. E., Wong, G. and Abdullahi, M. 2012. Properties of crumb rubber hollow concrete block. *Journal of Cleaner Production,* 23**,** 57-67.

Mukharjee, B. B. and Barai, S. V. 2014a. Influence of nano-silica on the properties of recycled aggregate concrete. *Construction and Building Materials,* 55**,** 29-37.

Mukharjee, B. B. and Barai, S. V. 2014b. Statistical techniques to analyze properties of nano-engineered concrete using Recycled Coarse Aggregates. *Journal of Cleaner Production,* 83**,** 273-285.

Multiphysics, C. 2008. Documentation for COMSOL Release 3.4. *COMSOL, Inc*.

Mushunje, K., Otieno, M. and Ballim, Y. Partial replacement of conventional fine aggregate with crumb tyre rubber in structural concrete–effect of particle size on compressive strength and time dependent deformations. MATEC Web of Conferences, 2018. EDP Sciences, 11002.

Najim, K. and Hall, M. 2010. A review of the fresh/hardened properties and applications for plain-(PRC) and self-compacting rubberised concrete (SCRC). *Construction and Building Materials,* 24**,** 2043-2051.

Najim, K. B. and Hall, M. R. 2012. Mechanical and dynamic properties of self-compacting crumb rubber modified concrete. *Construction and building materials,* 27**,** 521-530.

Najim, K. B. and Hall, M. R. 2013. Crumb rubber aggregate coatings/pre-treatments and their effects on interfacial bonding, air entrapment and fracture toughness in self-compacting rubberised concrete (SCRC). *Materials and structures,* 46**,** 2029-2043.

Nazari, A. and Riahi, S. 2011. The effects of SiO2 nanoparticles on physical and mechanical properties of high strength compacting concrete. *Composites Part B: Engineering,* 42**,** 570-578.

Nehdi, M., El Chabib, H. and El Naggar, M. H. 2001. Predicting performance of self-compacting concrete mixtures using artificial neural networks. *Materials Journal,* 98**,** 394-401.

Neville, A. M. and Brooks, J. J. 1987. *Concrete technology*, Longman Scientific & Technical England.

Nili, M. and Ehsani, A. 2015. Investigating the effect of the cement paste and transition zone on strength development of concrete containing nanosilica and silica fume. *Materials & Design,* 75**,** 174-183.

Noaman, A. T., Bakar, B. A. and Akil, H. M. 2016. Experimental investigation on compression toughness of rubberized steel fibre concrete. *Construction and Building Materials,* 115**,** 163-170.

Noor, N. M., Yamamoto, D., Hamada, H. and Sagawa, Y. Rubberized Concrete Durability Against Abrasion. MATEC Web of Conferences, 2016. EDP Sciences.

Onuaguluchi, O. and Panesar, D. K. 2014. Hardened properties of concrete mixtures containing pre-coated crumb rubber and silica fume. *Journal of Cleaner Production,* 82**,** 125-131.

Owen, K. C. 1998. Scrap tires: a pricing strategy for a recycling industry. *Corporate environmental strategy,* 5**,** 42-50.

Ozbay, E., Lachemi, M. and Sevim, U. K. 2011. Compressive strength, abrasion resistance and energy absorption capacity of rubberized concretes with and without slag. *Materials and structures,* 44**,** 1297-1307.

Pacheco-Torgal, F., Ding, Y. and Jalali, S. 2012. Properties and durability of concrete containing polymeric wastes (tyre rubber and polyethylene terephthalate bottles): An overview. *Construction and Building Materials,* 30**,** 714-724.

Pelisser, F., Zavarise, N., Longo, T. A. and Bernardin, A. M. 2011. Concrete made with recycled tire rubber: effect of alkaline activation and silica fume addition. *Journal of Cleaner Production,* 19**,** 757-763.

Pinto, P. R., Mendes, L. C., Dias, M. L. and Azuma, C. 2006. Synthesis of acrylic-modified sol–gel silica. *Colloid and Polymer Science,* 284**,** 529-535.

Raffoul, S., Garcia, R., Pilakoutas, K., Guadagnini, M. and Medina, N. F. 2016. Optimisation of rubberised concrete with high rubber content: An experimental investigation. *Construction and Building Materials,* 124**,** 391-404.

Rahman, I. A. and Padavettan, V. 2012. Synthesis of silica nanoparticles by sol-gel: size-dependent properties, surface modification, and applications in silica-polymer nanocomposites—a review. *Journal of Nanomaterials,* 2012**,** 8.

Rahman, M., Usman, M. and Al-Ghalib, A. A. 2012. Fundamental properties of rubber modified self-compacting concrete (RMSCC). *Construction and Building Materials,* 36**,** 630-637.

Reda Taha, M. M., El-Dieb, A., Abd El-Wahab, M. and Abdel-Hameed, M. 2008. Mechanical, fracture, and microstructural investigations of rubber concrete. *Journal of materials in civil engineering,* 20**,** 640-649.

Richardson, A. E., Coventry, K. A. and Ward, G. 2012. Freeze/thaw protection of concrete with optimum rubber crumb content. *Journal of Cleaner Production,* 23**,** 96-103.

Ristić, N., Topličić-Ćurčić, G. and Grdić, D. 2015. Abrasion resistance of concrete made with micro fibers and recycled granulated rubber. *Zaštita materijala,* 56**,** 435-445.

Rosenblatt, F. 1962. Principles of neurodynamics.

Rostami, H., Lepore, J., Silverstraim, T. and Zundi, I. Use of recycled rubber tires in concrete. Proceedings of the international conference on concrete, 2000. London, United Kingdom: Thomas Telford Services Ltd, 391-399.

Rumelhart, D. 1986. David E. Rumelhart, Geoffrey E. Hinton, and Ronald J. Williams. *Nature,* 323**,** 533-536.

Rumelhart, D. E., Hinton, G. E. and Williams, R. J. 1986. Learning Internal Representations by Error Propagation, Parallel Distributed Processing, Explorations in the Microstructure of Cognition, ed. DE Rumelhart and J. McClelland. Vol. 1. 1986. Cambridge, MA: MIT Press.

Rungrodnimitchai, S., Phokhanusai, W. and Sungkhaho, N. 2009. Preparation of silica gel from rice husk ash using microwave heating. *Journal of Metals, Materials and Minerals,* 19**,** 45-50.

Rupasinghe, M., San Nicolas, R., Mendis, P., Sofi, M. and Ngo, T. 2017. Investigation of strength and hydration characteristics in nano-silica incorporated cement paste. *Cement and Concrete Composites,* 80**,** 17-30.

Savas, B., Ahmad, S. and Fedroff, D. 1997. Freeze-thaw durability of concrete with ground waste tire rubber. *Transportation Research Record: Journal of the Transportation Research Board***,** 80-88.

Selvakumar, S. and Venkatakrishnaiah, R. 2015. Strength Properties of Concrete Using Crumb Rubber with Partial Replacement of Fine Aggregate. *International Journal of Innovative Research in Science Engineering and Technology***,** 1171-1175.

Shen, W., Shan, L., Zhang, T., Ma, H., Cai, Z. and Shi, H. 2013. Investigation on polymer–rubber aggregate modified porous concrete. *Construction and Building Materials,* 38**,** 667-674.

Shu, X. and Huang, B. 2014. Recycling of waste tire rubber in asphalt and Portland cement concrete: an overview. *Construction and Building Materials,* 67**,** 217-224.

Sikora, P., Horszczaruk, E., Skoczylas, K. and Rucinska, T. 2017. Thermal properties of cement mortars containing waste glass aggregate and nanosilica. *Procedia Engineering,* 196**,** 159-166.

Skripkiūnas, G., Grinys, A. and Černius, B. 2007. Deformation properties of concrete with rubber waste additives. *Materials science [Medžiagotyra],* 13**,** 219-223.

Skripkiūnas, G., Grinys, A. and Miškinis, K. 2009. Damping properties of concrete with rubber waste additives. *Materials Science (Medžiagotyra),* 15**,** 266-272.

Snelson, D., Kinuthia, J., Davies, P. and Chang, S.-R. 2009. Sustainable construction: composite use of tyres and ash in concrete. *Waste Management,* 29**,** 360-367.

Sobolev, K. and Ferrara, A. 2005. Application of Nanosilica (nS) in concrete mixtures. *America Ceramic Bulletin,* 84**,** 15-17.

Son, K. S., Hajirasouliha, I. and Pilakoutas, K. 2011. Strength and deformability of waste tyre rubber-filled reinforced concrete columns. *Construction and building materials,* 25**,** 218-226.

Su, H. 2015. *Properties of concrete with recycled aggregates as coarse aggregate and as-received/surface-modified rubber particles as fine aggregate.* University of Birmingham.

Su, H., Yang, J., Ghataora, G. S. and Dirar, S. 2015a. Surface modified used rubber tyre aggregates: effect on recycled concrete performance. *Magazine of Concrete Research,* 67**,** 680-691.

Su, H., Yang, J., Ling, T.-C., Ghataora, G. S. and Dirar, S. 2015b. Properties of concrete prepared with waste tyre rubber particles of uniform and varying sizes. *Journal of Cleaner Production,* 91**,** 288-296.

Sukontasukkul, P. 2009. Use of crumb rubber to improve thermal and sound properties of pre-cast concrete panel. *Construction and Building Materials,* 23**,** 1084-1092.

Sukontasukkul, P. and Chaikaew, C. 2006. Properties of concrete pedestrian block mixed with crumb rubber. *Construction and Building Materials,* 20**,** 450-457.

Sukontasukkul, P. T., Koshi 2012. Expansion under water and drying shrinkage of rubberized concrete mixed with crumb rubber with different size. *Construction and Building Materials,* 29**,** 520-526.

Thomas, B. S. and Gupta, R. C. 2015. Properties of high strength concrete containing scrap tire rubber. *Journal of Cleaner Production*.

Thomas, B. S., Gupta, R. C., Kalla, P. and Cseteneyi, L. 2014. Strength, abrasion and permeation characteristics of cement concrete containing discarded rubber fine aggregates. *Construction and Building Materials,* 59**,** 204-212.

Tomosawa, F., Noguchi, T. and Tamura, M. 2005. The way concrete recycling should be. *Journal of advanced concrete technology,* 3**,** 3-16.

Topcu, I. B. 1995. The properties of rubberized concretes. *Cement and concrete research,* 25**,** 304-310.

Topcu, İ. B. 1997. Assessment of the brittleness index of rubberized concretes. *Cement and Concrete Research,* 27**,** 177-183.

Topçu, İ. B. and Bilir, T. 2009. Experimental investigation of some fresh and hardened properties of rubberized self-compacting concrete. *Materials & Design,* 30**,** 3056-3065.

Topçu, İ. B. and Demir, A. 2007. Durability of rubberized mortar and concrete. *Journal of materials in Civil Engineering,* 19**,** 173-178.

Topcu, I. B. and Sarıdemir, M. 2008. Prediction of compressive strength of concrete containing fly ash using artificial neural networks and fuzzy logic. *Computational Materials Science,* 41**,** 305-311.

Toutanji, H. A. 1996. The use of rubber tire particles in concrete to replace mineral aggregates. *Cement and Concrete Composites,* 18**,** 135-139.

Turatsinze, A. and Garros, M. 2008. On the modulus of elasticity and strain capacity of self-compacting concrete incorporating rubber aggregates. *Resources, conservation and recycling,* 52**,** 1209-1215.

Turgut, P. and Yesilata, B. 2008. Physico-mechanical and thermal performances of newly developed rubber-added bricks. *Energy and Buildings,* 40**,** 679-688.

Wang, F. 1994. The use of artificial neural networks in a geographical information system for agricultural land-suitability assessment. *Environment and planning A,* 26**,** 265-284.

Wang, J., Sun, J., Li, Y. and Wang, F. 2014. Preparation, characterization and luminescent properties of dense nano-silica hybrids loaded with 1,8-naphthalic anhydride. *Luminescence,* 29**,** 188-94.

Wong, S.-F. and Ting, S.-K. 2009. Use of recycled rubber tires in normal-and high-strength concretes. *ACI materials journal,* 106**,** 325-332.

Wu, X., Tong, S., Liu, X., Bao, X., Jiang, S., Feng, D. and Siu, G. 1997. X-ray diffraction study of alternating nanocrystalline silicon/amorphous silicon multilayers. *Applied physics letters,* 70**,** 838-840.

Xu, F., Chen, J., Ruan, S. and Zhou, M. 2014. Influence of PP fiber and SBR latex on the mechanical properties of crumb rubber mortar. *Journal of Applied Polymer Science,* 131.

Yang, L.-h., Han, Z. and Li, C.-f. 2011. Strengths and flexural strain of CRC specimens at low temperature. *Construction and Building Materials,* 25**,** 906-910.

Yesilata, B., Isıker, Y. and Turgut, P. 2009. Thermal insulation enhancement in concretes by adding waste PET and rubber pieces. *Construction and Building Materials,* 23**,** 1878-1882.

Yilmaz, A. and Degirmenci, N. 2009. Possibility of using waste tire rubber and fly ash with Portland cement as construction materials. *Waste Management,* 29**,** 1541-1546.

Youssf, O., ElGawady, M., Mills, J. E. and Ma, X. 2013. Analytical Modeling of the Main Characteristics of Crumb Rubber Concrete.

Youssf, O., ElGawady, M. A., Mills, J. E. and Ma, X. 2014. An experimental investigation of crumb rubber concrete confined by fibre reinforced polymer tubes. *Construction and Building Materials,* 53**,** 522-532.

Youssf, O., Mills, J. E. and Hassanli, R. 2016. Assessment of the mechanical performance of crumb rubber concrete. *Construction and Building Materials,* 125**,** 175-183.

Yun, C.-B. and Bahng, E. Y. 2000. Substructural identification using neural networks. *Computers & Structures,* 77**,** 41-52.

Yung, W. H., Yung, L. C. and Hua, L. H. 2013. A study of the durability properties of waste tire rubber applied to self-compacting concrete. *Construction and Building Materials,* 41**,** 665-672.

Zaoiai, S., Makani, A., Tafraoui, A. and Benmerioul, F. 2016. Optimization and mechanical characterization of self-compacting concrete incorporating rubber aggregates.

Zheng, L., Huo, X. S. and Yuan, Y. 2008a. Experimental investigation on dynamic properties of rubberized concrete. *Construction and building materials,* 22**,** 939-947.

Zheng, L., Huo, X. S. and Yuan, Y. 2008b. Strength, modulus of elasticity, and brittleness index of rubberized concrete. *Journal of Materials in Civil Engineering,* 20**,** 692-699.

APPENDIX A- DATABASE OF RUBBERISED CONCRETE

Experimental database of 435 samples used in chapter six and seven to predict the compressive strength of rubberised concrete are shown in Table A-1 .

Table A-1 Details of database

References	Specimen No.	C (Kg/m^3)	CA (kg/m^3)	FA (kg/m^3)	W (kg/m^3)	w/c ratio	FR (kg/m^3)	compressive strength (MPa)
(Sukontasukkul, 2012)	1	479	695	838	225	0.47	0	38
	2	479	695	755	225	0.47	17	14
	3	479	695	671	225	0.47	35	8
	4	479	695	587	225	0.47	52	5
	5	479	695	755	225	0.47	9	16
	6	479	695	671	225	0.47	17	10
	7	479	695	587	225	0.47	26	6
(Al-Tayeb et al., 2013)	8	395	973	797	190	0.48	0	43.5
	9	395	973	758	190	0.48	10	34.12
	10	395	973	638	190	0.48	39.7	31.8
(Marie, 2016a)	11	446	961	585	252	0.56	0	27

	12	446	961	556	252	0.56	13.7	25
	13	446	961	526.5	252	0.56	32.3	22.5
	14	446	961	497	252	0.56	50.8	21
	15	446	961	468	252	0.56	67.5	18
	16	446	961	409.5	252	0.56	106.3	15
	17	446	961	351	252	0.56	135	12.5
	18	446	961	292.5	252	0.56	180.4	9
	19	446	961	234	252	0.56	202.5	7
	20	446	961	175.6	252	0.56	248	6
	21	446	961	117.2	252	0.56	270	4.5
	22	446	961	58.6	252	0.56	321	3
Bhavik K. Daxini et.al (2013)	23	592.68	673.35	775.96	243	0.4	0	39.68
	24	592.68	673.35	698.37	243	0.4	16.41	26.5
	25	592.68	673.35	659.56	243	0.4	24.62	20.13
	26	592.68	673.35	620.77	243	0.4	32.83	18.5
	27	592.68	673.35	343.18	243	0.4	49.24	15.98
(Onuaguluchi and Panesar, 2014)	28	375	1065	820	178	0.47	0	47.5
	29	375	1065	779	178	0.47	16.8	44.2
	30	375	1065	738	178	0.47	33.7	40.7
	31	375	1065	697	178	0.47	50.5	28.5

	32	375	1065	779	178	0.47	0	45.5
	33	375	1065	738	178	0.47	0	42.5
	34	375	1065	697	178	0.47	0	30
	35	375	1065	779	178	0.47	0	61.3
	36	375	1065	738	178	0.47	0	54
	37	375	1065	697	178	0.47	0	41
(Li et al., 2016)	38	360	1024	702	162	0.45	0	52
	39	360	1024	667	162	0.45	14.1	51
	40	360	1024	632	162	0.45	28.3	49
	41	360	1024	597	162	0.45	42.4	45
	42	360	1024	562	162	0.45	56.6	40
	43	360	1024	492	162	0.45	84.8	30
	44	360	1024	667	162	0.45	0	55
	45	360	1024	632	162	0.45	0	52
	46	360	1024	597	162	0.45	0	50
	47	360	1024	562	162	0.45	0	46
	48	360	1024	422	162	0.45	0	38
(Dong et al., 2013)	49	400	800	942	181	0.45	0	44.8
	50	400	680	942	181	0.45	46	29
	51	400	560	942	181	0.45	92	25.9

	52	400	680	942	181	0.45	0	38.8
	53	400	560	942	181	0.45	0	32.9
(Atahan and Sevim, 2008)	54	364	1734	150	200	0.55	0	43.5
	55	364	1650	150	200	0.55	0	32.9
	56	364	1567	150	200	0.55	0	28.2
	57	364	1484	150	200	0.55	0	22.4
	58	364	1400	150	200	0.55	0	14.1
	59	364	1316	150	200	0.55	0	12.9
(Thomas et al., 2014)	60	388	1202.8	698.4	155.2	0.4	0	42.5
	61	388	1202.8	680.94	155.2	0.4	7.37	41
	62	388	1202.8	663.48	155.2	0.4	14.73	37.5
	63	388	1202.8	646.02	155.2	0.4	22.11	37
	64	388	1202.8	628.56	155.2	0.4	29.47	33.5
	65	388	1202.8	611.1	155.2	0.4	36.84	30
	66	388	1202.8	593.64	155.2	0.4	44.22	25
	67	388	1202.8	576.18	155.2	0.4	51.58	23.3
	68	388	1202.8	558.72	155.2	0.4	58.95	20
	69	388	1202.8	698.4	174.6	0.45	0	39
	70	388	1202.8	680.94	174.6	0.45	7.37	38
	71	388	1202.8	663.48	174.6	0.45	14.73	33

	72	388	1202.8	646.02	174.6	0.45	22.11	30.5
	73	388	1202.8	628.56	174.6	0.45	29.47	27.5
	74	388	1202.8	611.1	174.6	0.45	36.84	25
	75	388	1202.8	593.64	174.6	0.45	44.22	21.5
	76	388	1202.8	576.18	174.6	0.45	51.58	21.5
	77	388	1202.8	558.72	174.6	0.45	58.95	20
	78	388	1202.8	698.4	194	0.5	0	36.5
	79	388	1202.8	680.94	194	0.5	7.37	33.7
	80	388	1202.8	663.48	194	0.5	14.73	30.7
	81	388	1202.8	646.02	194	0.5	22.11	29.3
	82	388	1202.8	628.56	194	0.5	29.47	24
	83	388	1202.8	611.1	194	0.5	36.84	21.3
	84	388	1202.8	593.64	194	0.5	44.22	18.3
	85	388	1202.8	576.18	194	0.5	51.58	17.5
	86	388	1202.8	558.72	194	0.5	58.95	17
(Batayneh et al., 2008)	87	446	961	585	250	0.56	0	25.33
	88	446	961	468	250	0.56	67.51	18.96
	89	446	961	351	250	0.56	135	12.27
	90	446	961	234	250	0.56	202.5	8.07
	91	446	961	117.2	250	0.56	270	4.47

(Kumar et al., 2014)	92	394	1206.82	717.99	157	0.4	0	43
	93	394	1206.82	646.2	157	0.4	14.9	41
	94	394	1206.82	574.39	157	0.4	29.8	32
	95	394	1206.82	502.59	157	0.4	44.7	28
	96	394	1206.82	430.79	157	0.4	59.6	25
	97	394	1176.65	682.09	157	0.4	37.62	38
	98	394	1176.65	646.19	157	0.4	45.07	32
	99	394	1176.65	610.29	157	0.4	52.52	30
	100	394	1176.65	574.39	157	0.4	59.97	27.5
(Reda Taha et al., 2008)	101	350	1160	630	200	0.57	0	26
	102	350	870	630	200	0.57	0	16
	103	350	580	630	200	0.57	0	14
	104	350	290	630	200	0.57	0	7
	105	350	1160	472	200	0.57	158	23
	106	350	1160	315	200	0.57	315	20
	107	350	1160	157	200	0.57	473	13
(Aiello and Leuzzi, 2010)	108	335	465	279	174	0.5	0	45.8
	109	335	350	279	174	0.5	0	23.9
	110	335	233	279	174	0.5	0	20.87
	111	335	115	279	174	0.5	0	17.42

	112	335	465	279	200	0.59	0	27.11
	113	335	465	237	200	0.59	42	23.97
	114	335	465	195	200	0.59	84	20.41
	115	335	465	140	200	0.59	139	19.45
	116	335	465	70	200	0.59	209	17.06
(Liu et al., 2016)	117	430	1197	593	180	0.42	0	34.76
	118	430	1197	563.4	180	0.42	13.4	34.52
	119	430	1197	533.7	180	0.42	26.8	34.19
	120	430	1197	504.1	180	0.42	40.2	33.82
	121	430	1197	474.4	180	0.42	56.3	33.41
(Su et al., 2015b)	122	632	1010	519	234	0.37	0	61.1
	123	627	1005	416	232	0.37	46	54.6
	124	621	996	410	230	0.37	37	55.2
	125	621	996	410	230	0.37	37	55.3
	126	627	1002	414	232	0.37	40	55.1
(Grinys et al., 2012)	127	451	949	875	160	0.35	0	64.3
	128	451	949	784	160	0.35	35.14	46.2
	129	451	949	693	160	0.35	70.28	33.8
	130	451	949	510	160	0.35	140.55	14
	131	451	949	328	160	0.35	210.83	10

	132	451	949	784	160	0.35	35.14	48
	133	451	949	693	160	0.35	70.28	40
	134	451	949	510	160	0.35	140.55	22
	135	451	949	328	160	0.35	210.83	11
	136	451	949	784	160	0.35	0	51
	137	451	949	693	160	0.35	0	47
	138	451	949	510	160	0.35	0	23
(Abusharar, 2015)	139	335	1220	660	190	0.57	0	33
	140	335	1220	594	190	0.57	66	14
	141	335	1220	594	190	0.57	66	13
	142	335	1220	594	190	0.57	66	19
(Li et al., 2014)	143	432	592	604	194	0.45	0	51.3
	144	432	592	543.6	194	0.45	18.8	46.1
	145	432	592	483.2	194	0.45	37.6	37.4
(Holmes et al., 2014)	146	475	1110	527.3	225.6	0.47	42.7	24
	147	475	1110	484.5	225.6	0.47	85.5	30
	148	475	1110	527.3	225.6	0.47	42.7	38
	149	475	1110	484.5	225.6	0.47	85.5	34
	150	475	1110	527.3	225.6	0.47	42.7	57
	151	475	1110	484.5	225.6	0.47	85.5	38

	152	475	1110	527.3	225.6	0.47	0	41
	153	475	1110	484.5	225.6	0.47	0	33
	154	475	1110	570	225.6	0.47	0	56
(Mohammadi et al., 2014)	155	370	1162	677	148	0.4	0	63
	156	370	1162	609	148	0.4	30	54.1
	157	370	1162	541	148	0.4	59	44.3
	158	370	1162	474	148	0.4	89	30.9
	159	370	1162	406	148	0.4	118	22.9
	160	370	1130	658	166	0.45	0	55.6
	161	370	1130	593	166	0.45	29	45.8
	162	370	1130	527	166	0.45	58	34.9
	163	370	1130	461	166	0.45	86	23.8
	164	370	1130	395	166	0.45	115	18.2
(Azevedo et al., 2012)	165	500	430	1256	174	0.35	0	80
	166	500	430	1192	174	0.35	63	50
	167	500	430	1130	174	0.35	126	35
	168	500	430	1067	174	0.35	188	28
(Noaman et al., 2016)	169	430	907	814	202	0.47	0	46.1
	170	430	907	773	202	0.47	11.1	40.2
	171	430	907	732	202	0.47	22.2	36.1

	172	430	907	692	202	0.47	33.3	34.1
(Balaha et al., 2007)	173	300	1073	768	200	0.66	0	37
	174	300	1073	729.6	200	0.66	13	33
	175	300	1073	691.2	200	0.66	26	30
	176	300	1073	652.8	200	0.66	39.1	28
	177	300	1073	614.4	200	0.66	52.16	25
	178	400	1073	686	200	0.5	0	52
	179	400	1073	651.7	200	0.5	11.65	49
	180	400	1073	617.4	200	0.5	23.3	46
	181	400	1073	583.1	200	0.5	4.95	42
	182	400	1073	548.8	200	0.5	46.6	38
	183	500	1073	604	200	0.4	0	58
	184	500	1073	573.8	200	0.4	10.25	52
	185	500	1073	543.6	200	0.4	20.51	50
	186	500	1073	513.4	200	0.4	30.76	48
	187	500	1073	483.2	200	0.4	41	41
(Noor et al., 2016)	188	330	965	790	165	0.5	0	46.18
	189	330	965	711	165	0.5	35	33.72
	190	330	965	671	165	0.5	53	31.89
	191	457	1013	741	160	0.35	0	68.8

	192	457	1013	667	160	0.35	34	56.52
	193	457	1013	629	160	0.35	50	50.46
	194	457	1013	594	160	0.35	67	43.81
(Gupta et al., 2015)	195	364	1124	764	127.4	0.35	0	60
	196	364	1124	726	127.4	0.35	16	50
	197	364	1124	688	127.4	0.35	32	45
	198	364	1124	650	127.4	0.35	48	38
	199	364	1124	611	127.4	0.35	64	35
	200	364	1124	573	127.4	0.35	80	28
	201	364	1124	764	163.8	0.45	0	52
	202	364	1124	726	163.8	0.45	16	40
	203	364	1124	688	163.8	0.45	32	38
	204	364	1124	650	163.8	0.45	48	30
	205	364	1124	611	163.8	0.45	64	28
	206	364	1124	573	163.8	0.45	80	25
	207	364	1124	764	200.2	0.55	0	35
	208	364	1124	726	200.2	0.55	16	28
	209	364	1124	688	200.2	0.55	32	25
	210	364	1124	650	200.2	0.55	48	20
	211	364	1124	611	200.2	0.55	64	18

	212	364	1124	573	200.2	0.55	80	15
(El-Gammal et al., 2010)	213	350	980	588	122.5	0.35	0	26.9
	214	350	980	300	122.5	0.35	175	5.29
(Antil, 2014)	215	425.73	1202.55	574.51	191.58	0.45	0	36.2
	216	425.73	1202.55	545.78	191.58	0.45	16	32.2
	217	425.73	1202.55	517.06	191.58	0.45	32	27.7
	218	425.73	1202.55	488.33	191.58	0.45	48	24.8
	219	425.73	1202.55	459.61	191.58	0.45	64	22.7
A Mansoor Ali et.al.(2014)	220	475.14	1115.23	637.8	192	0.42	0	41.6
	221	432.28	1110.18	634.92	192	0.42	13.06	36.14
	222	411.42	1106.82	632.96	192	0.42	26.05	35.11
	223	388.57	1100.09	629.14	192	0.42	38.48	32.66
	224	365.71	1095.04	626.26	192	0.42	51.54	29.33
(Mohammed and Azmi, 2014)	225	556.1	697.32	803.58	228	0.41	0	35.5
	226	556.1	697.32	723.22	228	0.41	17	25.7
	227	556.1	697.32	683.05	228	0.41	25.5	21.2
	228	556.1	697.32	642.87	228	0.41	34	18.2
	229	556.1	697.32	562.51	228	0.41	46.36	14.3
	230	400	769.84	887.16	228	0.57	0	29.56
	231	400	769.84	798.44	228	0.57	18.77	20.21

232	400	769.84	754.08	228	0.57	28.15	17.5
233	400	769.84	709.73	228	0.57	37.53	14.5
234	400	769.84	621.01	228	0.57	51.18	11.13
235	335.29	799.9	921.8	228	0.68	0	23.4
236	335.29	799.9	829.26	228	0.68	19.5	18.2
237	335.29	799.9	783.53	228	0.68	29.25	15.6
238	335.29	799.9	737.44	228	0.68	39	12.43
239	335.29	799.9	645.26	228	0.68	53.18	10.5
240	592.68	673.35	775.96	243	0.41	0	44.3
241	592.68	673.35	698.37	243	0.41	16.41	34.21
242	592.68	673.35	659.57	243	0.41	24.62	24.56
243	592.68	673.35	620.77	243	0.41	32.83	22.19
244	592.68	673.35	543.18	243	0.41	49.24	18.56
245	426.32	750.65	750.65	243	0.57	0	36.5
246	426.32	750.65	778.53	243	0.57	18.3	26.2
247	426.32	750.65	735.28	243	0.57	27.45	21.74
248	426.32	750.65	692.03	243	0.57	36.6	18.45
249	426.32	750.65	605.53	243	0.57	54.9	12.3
250	357.35	782.69	901.96	243	0.68	0	30.12
251	357.35	782.69	811.76	243	0.68	19.08	19.39
252	357.35	782.69	766.67	243	0.68	28.62	17.24

	253	357.35	782.69	721.57	243	0.68	38.16	15.5
	254	357.35	782.69	631.37	243	0.68	57.24	11.1
	255	629.27	649.39	748.35	258	0.41	0	48.1
	256	629.27	649.39	673.51	258	0.41	15.83	37.2
	257	629.27	649.39	636.09	258	0.41	23.75	27.1
	258	629.27	649.39	598.68	258	0.41	31.66	24.5
	259	629.27	649.39	523.84	258	0.41	47.49	20.1
	260	452.63	731.45	842.92	258	0.57	0	40.1
	261	452.63	731.45	758.63	258	0.57	17.83	28.8
	262	452.63	731.45	716.48	258	0.57	26.75	23.2
	263	452.63	731.45	674.33	258	0.57	35.66	20.1
	264	452.63	731.45	590.04	258	0.57	53.49	14.3
	265	379.41	765.47	882.12	258	0.68	0	34.2
	266	379.41	765.47	793.31	258	0.68	18.66	22.5
	267	379.41	765.47	749.8	258	0.68	27.99	19.6
	268	379.41	765.47	705.69	258	0.68	37.32	17.1
	269	379.41	765.47	617.48	258	0.68	55.98	13.4
(Hassanli et.al,2017)	270	400	1080	687	200	0.5	0	55
	271	400	1080	646	200	0.5	13.5	49
	272	400	1080	605	200	0.5	27	49

	273	400	1080	563	200	0.5	40.5	38
(youssf et.al., 2014)	274	425	1257	628	148.8	0.35	0	53.5
	275	425	1257	597	148.8	0.35	10.2	55.6
	276	425	1257	565	148.8	0.35	20.4	53.9
	277	425	1257	502	148.8	0.35	40.8	48.1
	278	425	1257	502	148.8	0.35	40.8	41.6
	279	350	1038	866	175	0.5	0	62.5
	280	350	1038	823	175	0.5	13.8	51.5
	281	350	1038	779	175	0.5	27.7	50
	282	350	1038	693	175	0.5	55.5	39.2
	283	315	1038	865	175	0.55	0	60.1
	284	315	1038	778	175	0.55	27.7	60
	285	315	1038	692	175	0.55	55.5	40.3
(Selvakumar and Venkatakrishnaiah,2015)	286	380.95	1169.72	696.71	160	0.42	0	36.73
	287	380.95	1169.72	661.87	160	0.42	23.49	38.66
	288	380.95	1169.72	627.4	160	0.42	46.99	33.47
	289	380.95	1169.72	592.20	160	0.42	70.48	29.63
	290	380.95	1169.72	557.37	160	0.42	93.98	22.17
mendis et.al (2017)	291	388	1202.8	663.48	194	0.50	14.33	47.2
	292	388	1202.8	663.48	194	0.50	14.33	45.6

	293	388	1202.8	663.48	194	0.50	14.33	43.5
	294	388	1202.8	628.56	174.6	0.45	29.47	48.4
	295	388	1202.8	628.56	174.6	0.45	29.47	43.7
	296	388	1202.8	628.56	174.6	0.45	29.47	46.6
	297	388	1202.8	558.72	155.2	0.40	58.95	43.8
	298	388	1202.8	558.72	155.2	0.40	58.95	38.4
	299	388	1202.8	558.72	155.2	0.40	58.95	40.3
	300	424	1105	556	209	0.49	42.44	32.9
	301	424	1105	556	209	0.49	42.44	32.2
	302	424	1105	556	209	0.49	42.44	35.9
	303	388	1202.8	611.1	194	0.50	36.84	31.9
	304	388	1202.8	611.1	194	0.50	36.84	34
	305	388	1202.8	611.1	194	0.50	36.84	29.9
	306	300	1107.2	885.85	167	0.56	20	39.4
	307	300	1107.2	885.85	167	0.56	20	33.2
	308	300	1107.2	885.85	167	0.56	20	31.2
Fan et.al (2017)	309	325	1160	710	155	0.48	0	36.7
	310	325	1160	660	155	0.48	16.3	34.6
	311	325	1160	610	155	0.48	32.5	31.3
	312	325	1160	560	155	0.48	48.7	24.7

(Youssf et.al., (2016)	313	350	1038	866	175	0.50	0	53.5
	314	350	1038	693	175	0.50	55.5	42.1
	315	333	1034	862	175	0.50	0	55.4
	316	333	1034	690	175	0.50	55.3	39.7
	317	315	1031	859	175	0.50	0	50.6
	318	315	1031	687	175	0.50	55.1	37.3
	319	298	1027	856	175	0.50	0	47.7
	320	298	1027	685	175	0.50	54.9	36.8
(Mohammed Basher and Adamul, 2018)	321	134.6	833.3	1150.1	96.9	0.37	0	47
	322	134.6	833.3	1035.1	96.9	0.37	115.1	38
	323	134.6	833.3	920.1	96.9	0.37	230.2	32
	324	134.6	833.3	805.1	96.9	0.37	345.3	19
	325	134.6	833.3	1150.1	96.9	0.37	0	58
	326	134.6	833.3	1035.1	96.9	0.37	115.1	53
	327	134.6	833.3	920.1	96.9	0.37	230.2	41
	328	134.6	833.3	805.1	96.9	0.37	345.3	22
	329	134.6	833.3	1150.1	96.9	0.37	0	52
	330	134.6	833.3	1035.1	96.9	0.37	115.1	43
	331	134.6	833.3	920.1	96.9	0.37	230.2	38
	332	134.6	833.3	805.1	96.9	0.37	345.3	20

	333	134.6	833.3	1150.1	96.9	0.37	0	45
	334	134.6	833.3	1035.1	96.9	0.37	115.1	35
	335	134.6	833.3	920.1	96.9	0.37	230.2	30
	336	134.6	833.3	805.1	96.9	0.37	345.3	19
(Adamu et al., 2018)	337	268.69	831.88	1148.05	98.24	0.37	0	52
	338	268.69	831.88	1033.25	98.24	0.37	114.89	58
	339	268.69	831.88	918.44	98.24	0.37	229.78	41
	340	268.69	831.88	803.64	98.24	0.37	344.67	42
	341	268.69	831.88	1148.05	98.24	0.37	0	80
	342	268.69	831.88	1033.25	98.24	0.37	114.89	78
	343	268.69	831.88	918.44	98.24	0.37	229.78	51
	344	268.69	831.88	803.64	98.24	0.37	344.67	48
	345	268.69	831.88	1148.05	98.24	0.37	0	58
	346	268.69	831.88	1033.25	98.24	0.37	114.89	65
	347	268.69	831.88	918.44	98.24	0.37	229.78	49
	348	268.69	831.88	803.64	98.24	0.37	344.67	43
	349	268.69	831.88	1148.05	98.24	0.37	0	51
	350	268.69	831.88	1033.25	98.24	0.37	114.89	48
	351	268.69	831.88	918.44	98.24	0.37	229.78	51
	352	268.69	831.88	803.64	98.24	0.37	344.67	29

Guneyisi et.al, (2004)	353	450	1062	688	180	0.4	0	75.8
	354	450	1062	670.5	180	0.4	17.5	70.4
	355	450	1062	653.6	180	0.4	34.4	62.8
	356	450	1062	619.2	180	0.4	68.8	50.7
	357	450	1062	584.8	180	0.4	103.2	40.3
	358	450	1062	516	180	0.4	172	26.4
	359	450	1062	344	180	0.4	344	10.5
	360	428	1062	670.5	180	0.4	17.5	72.5
	361	428	1062	653.6	180	0.4	34.4	67.8
	362	428	1062	619.2	180	0.4	68.8	55.3
	363	428	1062	584.8	180	0.4	103.2	44.5
	364	428	1062	516	180	0.4	172	29.6
	365	428	1062	344	180	0.4	344	11.2
	366	405	1062	670.5	180	0.4	17.5	75.4
	367	405	1062	653.6	180	0.4	34.4	68.2
	368	405	1062	619.2	180	0.4	68.8	56.3
	369	405	1062	584.8	180	0.4	103.2	45.1
	370	405	1062	516	180	0.4	172	30.5
	371	405	1062	344	180	0.4	344	11.6
	372	383	1062	670.5	180	0.4	17.5	78.3

373	383	1062	653.6	180	0.4	34.4	68	
374	383	1062	619.2	180	0.4	68.8	55.6	
375	383	1062	584.8	180	0.4	103.2	46.4	
376	383	1062	516	180	0.4	172	31.8	
377	383	1062	344	180	0.4	344	11.7	
378	360	1062	670.5	180	0.4	17.5	79.1	
379	360	1062	653.6	180	0.4	34.4	69.4	
380	360	1062	619.2	180	0.4	68.8	61.7	
381	360	1062	584.8	180	0.4	103.2	47	
382	360	1062	516	180	0.4	172	31.8	
383	360	1062	344	180	0.4	344	11.7	
384	350	1076	697	210	0.6	0	53.8	
385	350	1076	679.6	210	0.6	17.4	47	
386	350	1076	662.2	210	0.6	34.8	41.5	
387	350	1076	628.2	210	0.6	68.8	31.8	
388	350	1076	593.8	210	0.6	103.2	24.3	
389	350	1076	525	210	0.6	172	16.2	
390	350	1076	348.5	210	0.6	348.5	7.1	
391	333	1076	679.6	210	0.6	17.4	50.2	
392	333	1076	662.2	210	0.6	34.8	43.1	
393	333	1076	628.2	210	0.6	68.8	35.8	

394	333	1076	593.8	210	0.6	103.2	28.8
395	333	1076	525	210	0.6	172	18.2
396	333	1076	348.5	210	0.6	348.5	7.2
397	315	1076	679.6	210	0.6	17.4	52.5
398	315	1076	662.2	210	0.6	34.8	46.1
399	315	1076	628.2	210	0.6	68.8	37.6
400	315	1076	593.8	210	0.6	103.2	31.4
401	315	1076	525	210	0.6	172	20.1
402	315	1076	348.5	210	0.6	348.5	8.1
403	298	1076	679.6	210	0.6	17.4	55.4
404	298	1076	662.2	210	0.6	34.8	49.3
405	298	1076	628.2	210	0.6	68.8	41.3
406	298	1076	593.8	210	0.6	103.2	32.8
407	298	1076	525	210	0.6	172	21.2
408	298	1076	348.5	210	0.6	348.5	8.4
409	280	1076	679.6	210	0.6	17.4	56.4
410	280	1076	662.2	210	0.6	34.8	51.3
411	280	1076	628.2	210	0.6	68.8	41.2
412	280	1076	593.8	210	0.6	103.2	34.2
413	280	1076	525	210	0.6	172	23.1

	414	280	1076	348.5	210	0.6	348.5	8.6
Current study, (2018)	415	500	731.9	675.6	225	0.45	0	51.48
	416	500	731.9	608.04	225	0.45	30.81	43.01
	417	500	731.9	540.8	225	0.45	61.62	35.95
	418	500	731.9	472.92	225	0.45	92.42	32.1
	419	500	731.9	608.04	225	0.45	32.9	42.26
	420	500	731.9	540.8	225	0.45	65.8	33.6
	421	500	731.9	472.92	225	0.45	98.71	31.5
	422	492.5	731.9	675.6	225	0.45	0	61.83
	423	492.5	731.9	608.04	225	0.45	30.81	51.55
	424	492.5	731.9	540.48	225	0.45	61.62	49.74
	425	492.5	731.9	472.92	225	0.45	92.42	42.99
	426	492.5	731.9	608.04	225	0.45	32.9	51.17
	427	492.5	731.9	540.48	225	0.45	65.8	46.33
	428	492.5	731.9	472.92	225	0.45	98.71	42.19
	429	485	731.9	675.6	225	0.45	0	64.71
	430	485	731.9	608.04	225	0.45	30.81	56.09
	431	485	731.9	540.48	225	0.45	61.62	53.05
	432	485	731.9	472.92	225	0.45	92.42	47.46
	433	4485	731.9	608.04	225	0.45	32.9	53.48

	434	485	731.9	540.48	225	0.45	65.8	52.09
	435	485	731.9	472.92	225	0.45	98.71	43.56

APPENDIX B- STATISTICAL ANALYSIS OF ANN MODELS

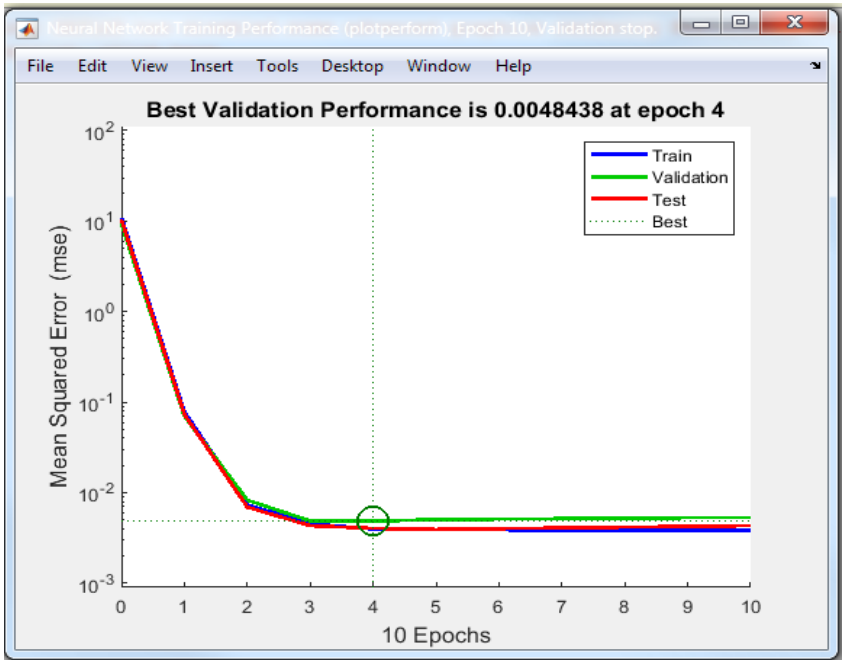

Figure B-1 Screenshot of best validation performance of ANN1

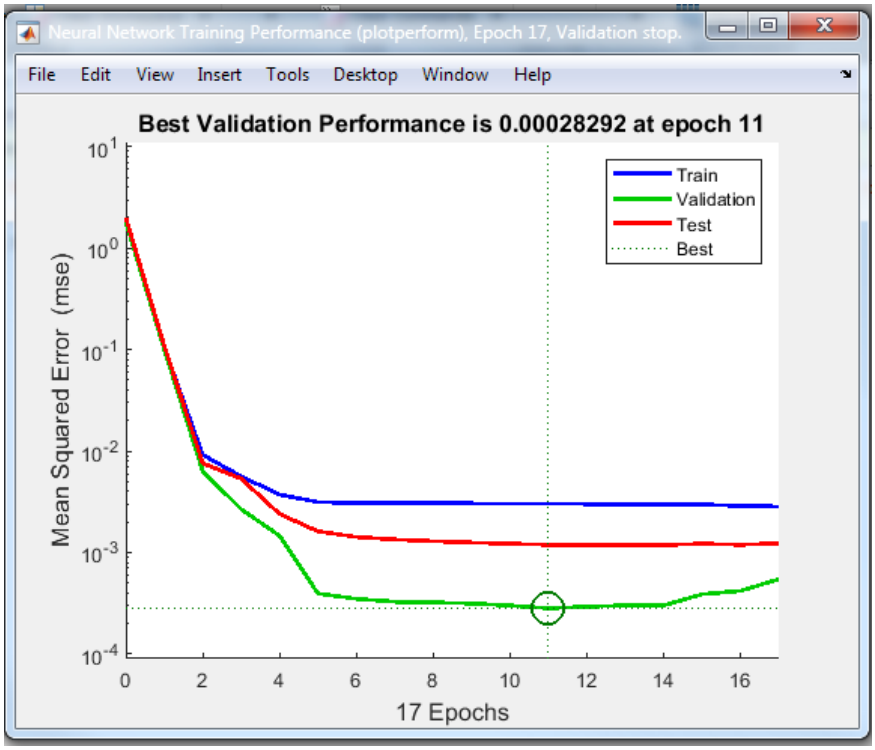

Figure B-2 Screenshot of best validation performance of ANN2

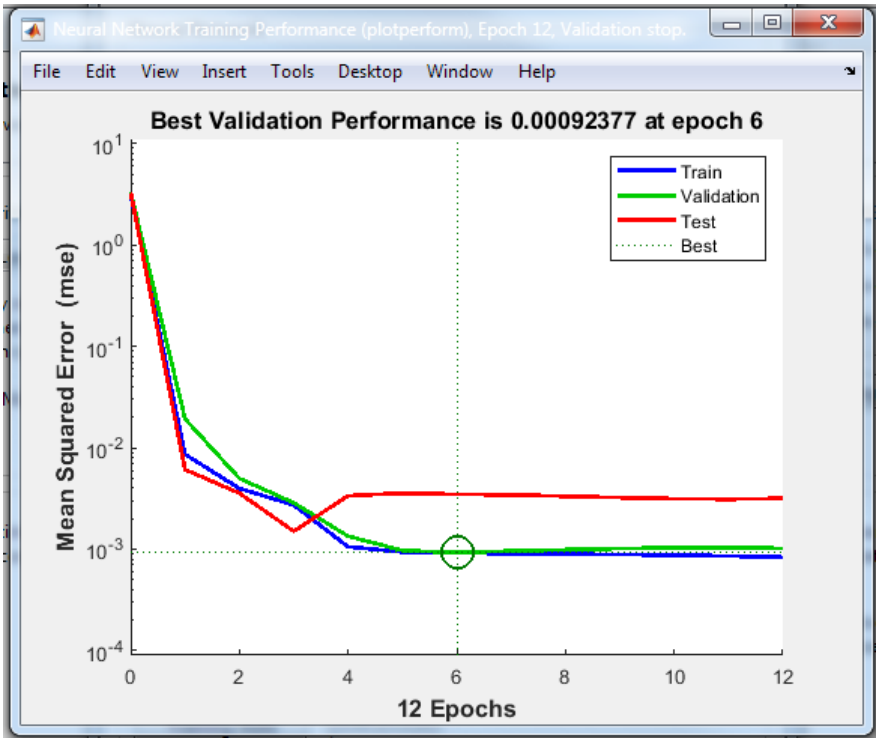

Figure B-3 Screenshot of best validation performance of ANN3

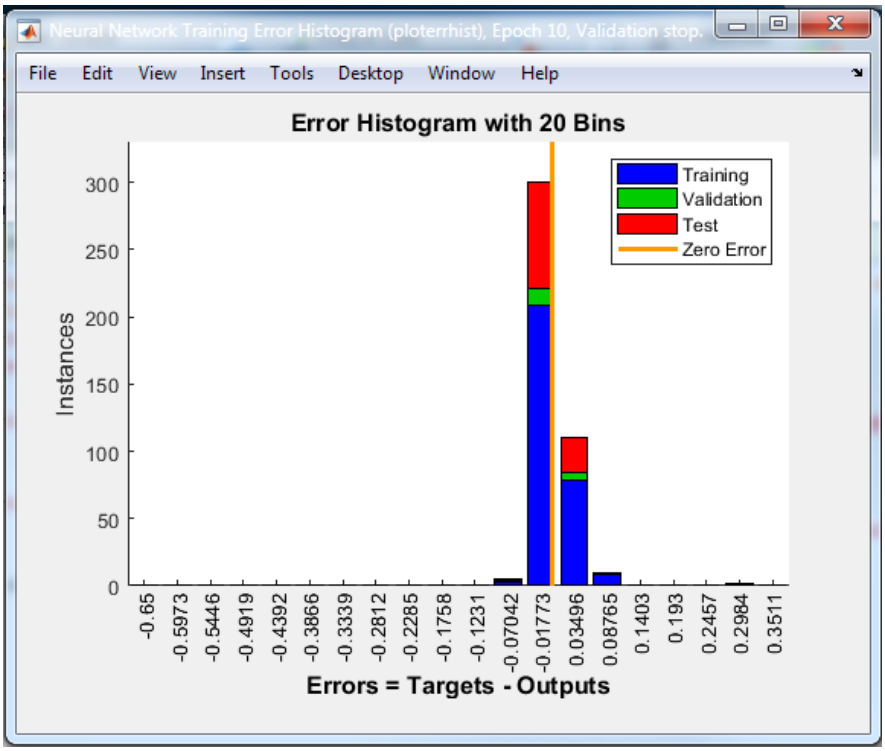

Figure B-4 Screenshot of error histogram of ANN1

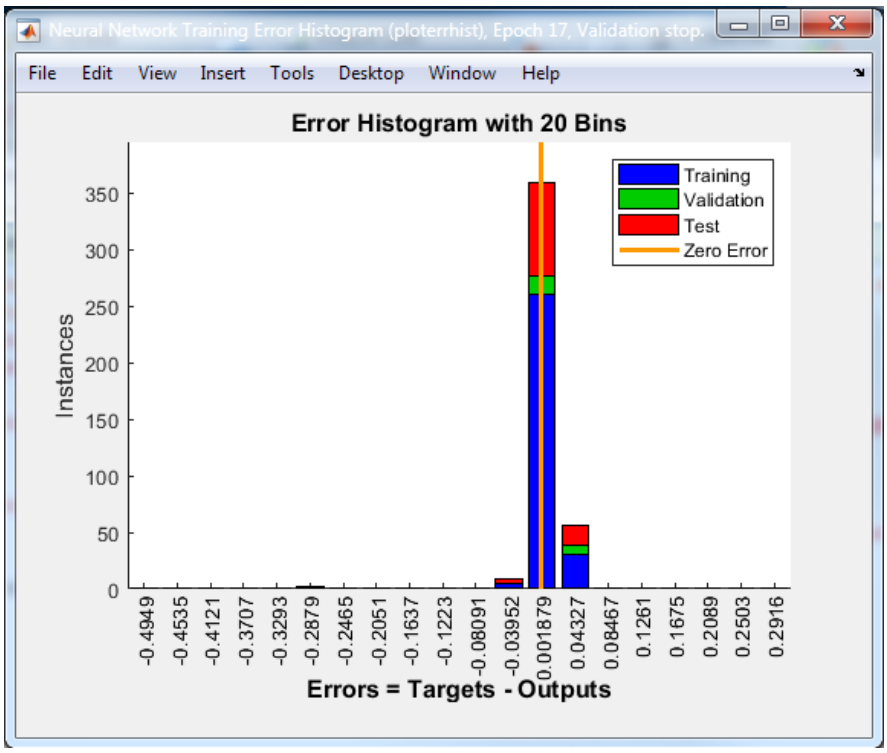

Figure B-5 Screenshot of error histogram of ANN2

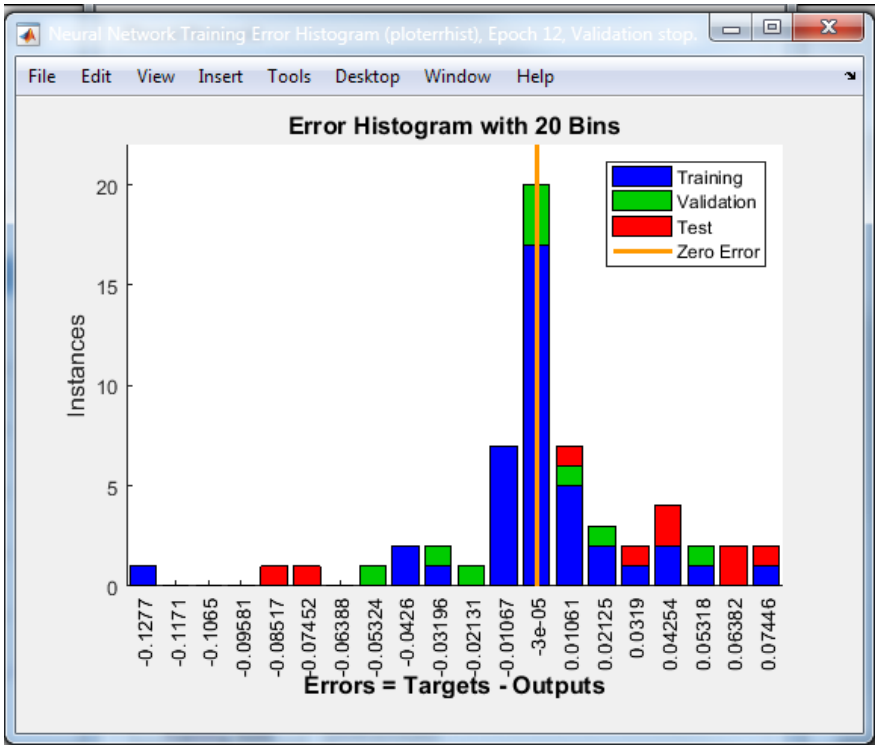

Figure B-6 Screenshot of error histogram of ANN3

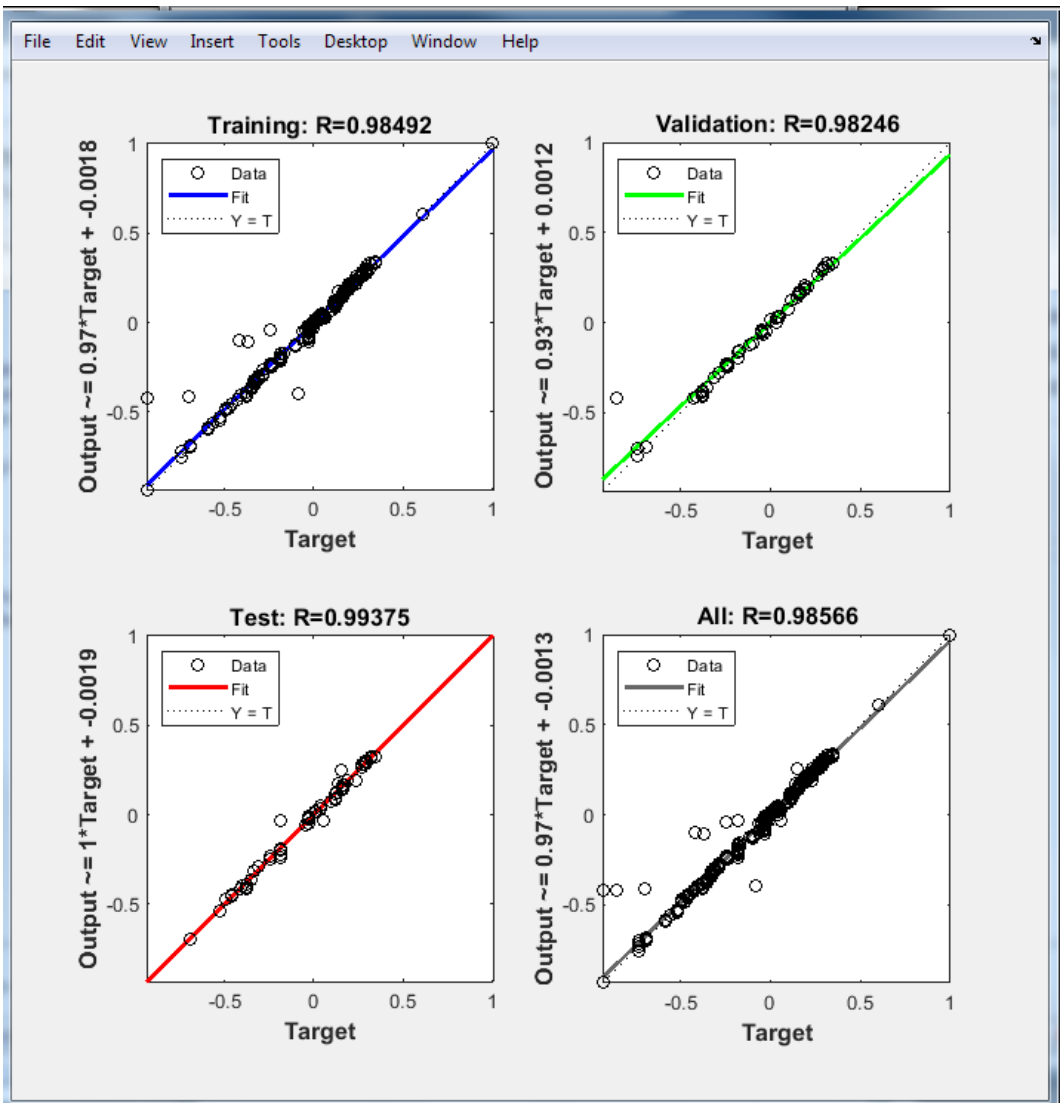

Figure B-7 Screenshot of Training Regression of ANN1

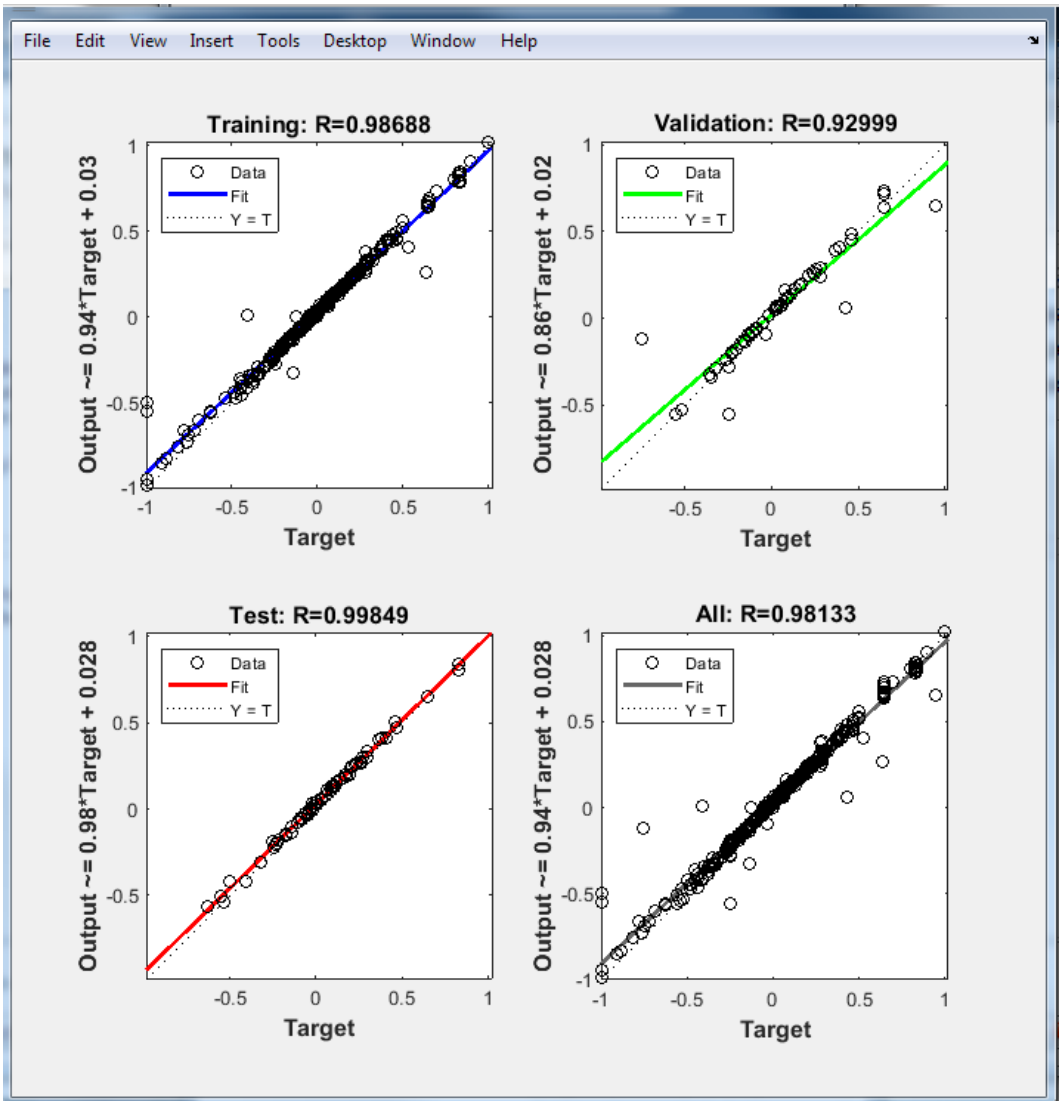

Figure B-8 Screenshot of Training Regression of ANN2

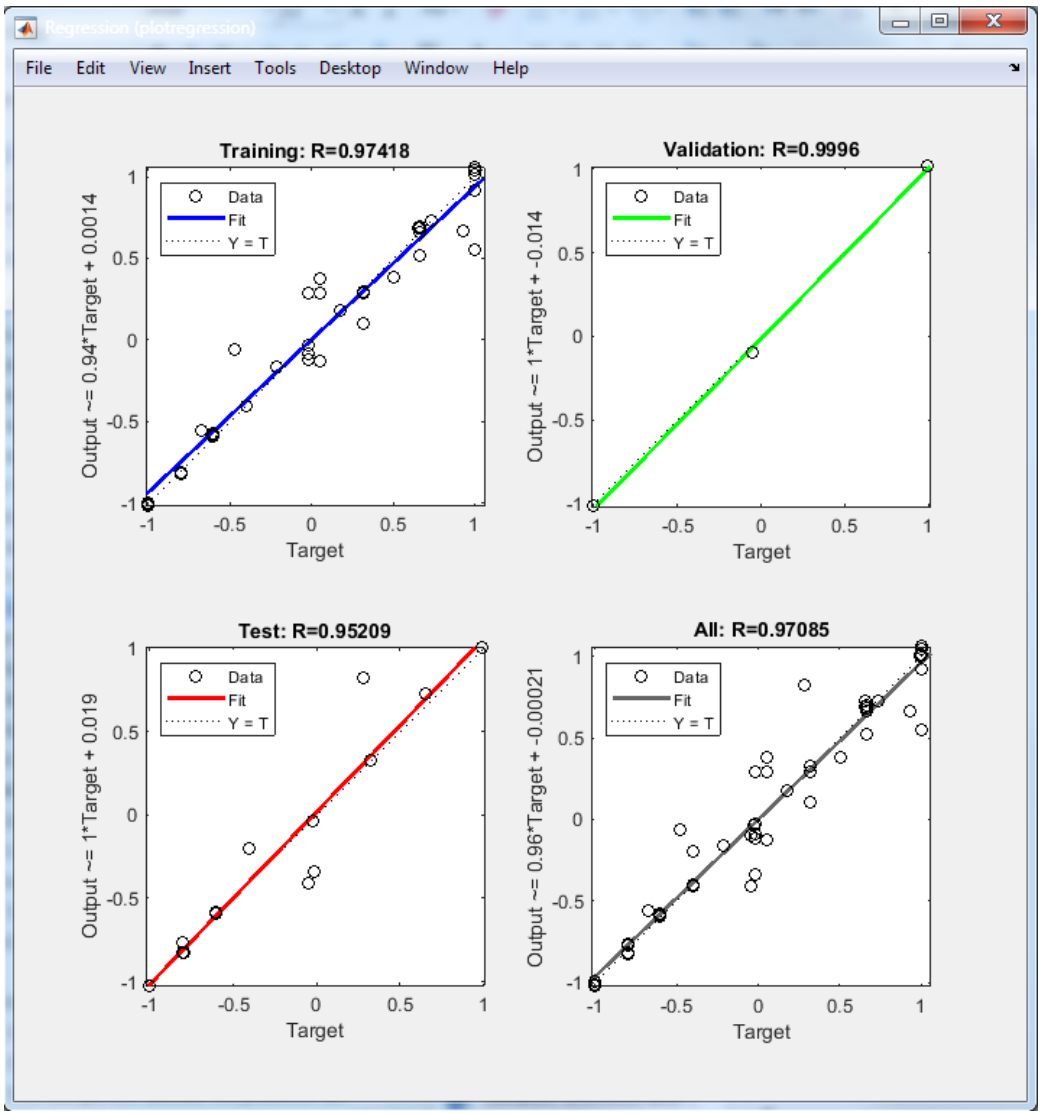

Figure B-9 Screenshot of Training Regression of ANN3